mpi

techinische universität
dortmund

Evaluation of the phage display protocol for target identification of small molecules. Identification and characterization of mitosis modulators.

Zur Erlangung des akademischen Grades eines
Doktors der Naturwissenschaften
(Dr. rer. nat.)
von der Fakultät für Chemie
der Technischen Universität Dortmund angenommene

Angefertigt am Max-Planck-Institut für molekulare Physiologie
in Dortmund

DISSERTATION

vorgelegt von

Master of Science

Tran, Thi Ngoc Tuyen

aus Vietnam

Dortmund, Januar 2014

Die vorliegende Arbeit wurde in der Zeit von August 2009 bis Januar 2014 am Max-Planck-Institut für molekulare Physiologie in Dortmund unter der Anleitung von Prof. Dr. Herbert Waldmann und Dr. Slava Ziegler durchgeführt.

Dekan: Prof. Dr. Roland Winter

1. Gutachter: Prof. Dr. Herbert Waldmann
2. Gutachter: Prof. Dr. Martin Engelhard
3. Wissenschaftliche Mitarbeiter: Dr. Tom Grossmann

Tag der mündlichen Prüfung: 19. Februar, 2014

Part of the results were published in the following journal:

- T. Voigt*, C. Gerding-Reimers*, **T. T. N. Tran***, S. Bergmann, H. Lachance, B. Schçlermann, A. Brockmeyer, P. Janning, S. Ziegler, and H. Waldmann. (2013). **A Natural Product Inspired Tetrahydropyran Collection Yields Mitosis Modulators that Synergistically Target CSE1L and Tubulin**, *Angew. Chem. Int. Ed,* 52, 410 –414**.** **equal contribution.*

- **T. T. N. Tran***, C. Gerding-Reimers*, B. Schölermann, B. Stanitzki, T. Henkel, H. Waldmann, S. Ziegler. (2014) **Podoverine A – a novel microtubule destabilizing natural product from the Podophyllum species**, *Bioorgan Med Chem*. (accepted). **equal contribution.*

Acknowledgements

First of all, I would like to thank my Ph.D. supervisor Prof. Dr. Herbert Waldmann for giving me an opportunity to join his research group, for his helpful discussions, and for excellent guidance as well as for his motivation for organizing the collaborations such as the project of the RIKEN-Max Plank Joint Research Centre, which gave me a great chance to participate in the Lab of Professor Hiroyuki Osada, RIKEN Advanced Science Institute in Wako, Japan. This research project could not have been finished without his kindness and wonderful support during my Ph.D. studies.

I would like to express my sincere gratitude to Dr. Slava Ziegler for her whole-hearted supervision, useful advice, valuable suggestions, motivating ideas as well as her careful reading, helpful comments and corrections for my thesis.

I am grateful to Max Planck Society for their financial support for my Ph.D. project, to the International Max Planck Research School in Chemical Biology Dortmund Team including Christa Hornemann, Dr. Waltraud Hofmann-Goody and Prof. Dr. Martin Engelhard for their help and great motivation.

My special thanks go to my friends and colleagues in my biology lab; we are not only friends but also worked together in a nice and friendly working environment, especially Beate Schölermann and Christine Nowak. I must say a big thank to Dr. Marion Rusch, who was not only my colleague but also a good friend helping me a lot, and to Dr. Gloria Vendrell-Navarro, Melanie Schwalfenberg, Andrei Ursu, Kirsten Tschapalda, Philipp Kuechler, Tim Foerster; Yasemin Akbulut, Dr. Maria Pascual-Lopez-Alberca, Dr. Trang Phan, Dr. Hoang Nguyen for their helpful comments and help regarding my thesis.

I am also grateful to the Analytical Team, especially to Dr. Petra Janning and the Compound Management and Screening Center team, especially Dr. Claude Ostermann, to Ms. Brigitte Rose for her official organization for the Chemical Biology Department, to all of my colleagues at this Department, and to all people from the Max Planck Institute of Molecular

Physiology in Dortmund, Germany, who kindly supported me during Ph.D. studies, especially for the cleaning team who worked from early mornings.

I had a happy time during my research period at RIKEN Advanced Science Institute in Wako, Japan, so I would like to express my sincere gratitude to Prof. Dr. Hiroyuki Osada for his supervision and for being a great host. I am very grateful to the Chemical Array Team, especially to Dr. Nobumoto Watanabe, Dr. Yasumitsu Kondoh, Motoko Uchida and Kaori Honda for their support and for giving me a friendly working environment. I would also like to thank the Collaboration Promotion Team Chemical Biology Core Facility RIKEN ASI, especially Dr. Tamio Saito, and Ms. Junko Abe for helping me and preparing all official documents for me. I would like to thank all the members there.

Finally, I would not forget to say thanks to our parents for their love for us forever. My work could not have been done well without support from my husband. My words are not enough to thank my husband Thanh Phong for taking care of our little son Anh Phi during my long working time. This thesis is certainly a nice present for my parents, my husband and especially Anh Phi, who always gave me motivation so that I could try my best to finish my work.

Dortmund, January 2014
Tran, Thi Ngoc Tuyen

To my family in Vietnamese

Con xin cảm ơn ba mẹ, anh chị em hai bên đã luôn yêu thương, ủng hộ, động viên và bên con trong mọi hoàn cảnh. Em xin cảm ơn tình yêu thương, sự hy sinh và những lo lắng của anh cho gia đình, cho em và cho con để em yên tâm hoàn thành ước mơ của mình! Con trai của mẹ Anh Phi, mẹ yêu con nhiều, mẹ yên tâm học vì con trai luôn ngoan và vui vẻ bên bố khi không có mẹ ở nhà!

Con, chị, em, vợ và mẹ: Ngọc Tuyền

Table of contents

Acknowledgements I

1 Introduction 1

1.1 Chemical genetics........ .1

  1.1.1 Classical genetics 1

  1.1.2 Chemical genetics 2

  1. 1.3 Natural products and compound collections 7

    1.1.3.1 Natural products 7

    1.1.3.2 Compound collections 9

  1.1.4 Screening for small molecules 10

    1.1.4.1 High-throughput screening 10

    1.1.4.2 Small molecule microarrays (chemical arrays) 16

1.2 Target identification and validation 19

  1.2.1 Target identification 19

    1.2.1.1 Microarray techniques 19

      1.2.1.1.1 DNA microarrays .... .19

      1.2.1.1.2 Protein microarrays........ 20

      1.2.1.1.3 “Reverse transfected” cell microarrays .... .21

    1.2.1.2 A useful method of chemical proteomics: Affinity chromatography 23

    1.2.1.3 Expression-cloning-based methods .... .29

      1.2.1.3.1 cDNA phage display........ .29

      1.2.1.3.2 Ribosome and mRNA display 31

      1.2.1.3.3 A yeast three–hybrid system 34

  1.2.2 Target validation........ 35

1. 3 The cytoskeleton, cell cycle and M-phase........ .36

  1.3.1 Cytoskeleton .... .36

    1.3.1.1 Microfilaments (actin filaments) 36

    1.3.1.2 Intermediate filaments 37

    1.3.1.3 Microtubules........ 37

  1.3.2 Cell cycle 40

  1.3.3 M-phase (mitosis and cytokinesis) 42

1.4 Cancer and cancer inhibitors........ 44

1.4.1 Cancer 44

1.4.2 Cancer inhibitors..... 46

1.4.2.1 Small molecules targeting microtubules 46

1.4.2.2 Inhibitors of mitosis and cell cycle signaling..... 48

1.5 CAS (CSE1L) and cancer..... 50

1.5.1 CAS (CSE1L) gene and protein 50

1.5.2 Studies related to CAS (CSE1L) 51

2 Objective 53

3 Materials 55

3.1 Instruments and laboratory devices 55

3.2 Chemicals and reagents 57

3.3 Buffers and solutions..... 59

3.4 DNA and protein ladders..... 63

3.5 Plasmids..... 63

3.6 Oligonucleotides for cloning and sequencing.....64

3.7 Enzymes and kits 65

3.8 Antibodies 65

3.8.1 Primary antibodies.....65

3.8.2 Secondary antibodies 66

3.9 Organisms and culture media 67

3.9.1 Bacterial strains 67

3.9.2 Mammalian cell lines..... 67

3.9.3 Cell Culture media 68

3.10. Proteins 69

4 Methods..... 70

4.1 General methods in molecular biology..... 70

4.1.1 Polymerase chain reaction (PCR) and colony PCR..... 70

4.1.2 DNA digestion 71

4.1.3 DNA dephosphorylation 71

4.1.4 DNA ligation..... 72

4.1.5 DNA purification 72

4.1.6 Transformation of *E. coli* with plasmid DNA 72

4.1.7 DNA electrophoresis..... 73

4.1.8 Cultivation and storage of *E. coli* 73

4.1.9 Biochemical methods 74

4.1.9.1 Determination of protein concentration 74

4.1.9.2 Protein gel electrophoresis 74

4.1.9.3 Staining of proteins 75

4.1.9.4 Semi-dry protein transfer 76

4.1.9.5 Detection of proteins on membrane supports 76

4.1.9.6 Stripping PVDF-membranes 77

4.2 General methods for phage display affinity selection and target validation 77

4.2.1 Growth of T7 lysates and liquid lysate amplification 77

4.2.2 Plaque assay 78

4.2.3 Biopanning 79

4.2.4 PCR-based analysis and *Hinf*I fingerprinting 79

4.3 Making phage display cDNA library and target validation 79

4.3.1 RNA extraction 79

4.3.2 Linker preparation 80

4.3.3 Generation of T7 phage display HeLa cDNA library 80

4.3.3.1 First and second cDNA strand synthesis 80

4.3.3.2 End modification of cDNA 81

4.3.3.3 Ligation to directional *Eco*RI/*Hind*III linkers 82

4.3.3.4 *Eco*RI and *Hind*III digestion 82

4.3.3.5 Size fractionation 83

4.3.3.6 Ligation of prepared-cDNA to vector arms 83

4.3.3.7 cDNA packaging in T7 packaging extracts 83

4.3.3.8 Phage enzyme-linked immunosorbent assay for validation 84

4.4 Expression and protein purification of CAS 84

4.4.1 Expression of CAS in *E. coli* 84

4.4.2 *E. coli*-lysate preparation and protein purification 85

4.5 RAN preparation 85

4.5.1 Expression and protein purification of RAN 85

4.5.2 Nucleotide exchange of RAN 86

4.6 Biochemical methods 86

4.6.1 Enzyme-linked immunosorbent assay for binding study 86

4.6.2 Tubulin polymerization *in vitro* assay 87

4.6.2.1 *In vitro tubulin* polymerization assay by measuring absorption 87

4.6.2.2 *In vitro* tubulin polymerization assay by measuring DAPI fluorescence 87

4.6.3 DNA binding studies based on fluorescence dyes 87

4.6.4 Affinity purification for target protein validation 88

4.6.5 Colchicine competition assay for binding site study 88

4.6.6 BODIPY FL-vinblastine competition assay for binding site study 89

4.6.7 Pulldown procedure based on immunoprecipitation (IP) 89

4.6.7.1 Preparing of G protein beads 89

4.6.7.2 Preparing complex of proteins and compound 89

4.6.7.3 Pulldown assay 89

4.6.8 Microscale thermophoresis (MST) 90

4.6.9 Circular dichroism for studying protein thermal stability shift 92

4.7 Cell biological methods 92

4.7.1 Mammalian cell culture 92

4.7.2 Thawing the cells 92

4.7.3 Freezing cells 92

4.7.4 Cell counts 93

4.7.5 DNA transfection to mammalian cells 93

4.7.5.1 DNA transfection to COS-7 cells 93

4.7.5.2 DNA transfection to HEK293T cells 93

4.7.6 Preparation cells lysate of mammalian cells 94

4.7.6.1 Preparation cells lysate of HeLa cells for affinity purification 94

4.7.6.2 Preparation cells lysate of HEK293T cells for chemical array 94

4.7.7 Determination of cell proliferation using WST-1 reagent 94

4.7.8 Time-lapsed images using Metamopth 95

4.7.8.1 Time-lapsed images using Metamopth for HeLa cells 95

4.7.8.2 Time-lapsed images using Metamopth for HeLa Fucci cells 95

4.7.9 Caspase-3/7 activation analysis 95

4.8 Immunofluorescence 96

4.8.1 General protocol for cell staining 96

4.8.2 Mitotic cells staining and cytoskeleton staining on coverslip 96

4.8.3 Phenotypic screening in HeLa cells 96

4.8.4 Importin alpha screening in HeLa cells 97
4.8.5 Importin alpha and RANBP1 staining on coverslip 97
4.8.6 Mitotic maker pHistone H3 analysis 97
4.8.7 Doulink II fluorescence 98
4.8.7.1 Cell preparation 98
4.8.7.2 Blocking and primary antibodies incubation 98
4.8.7.3 PLA probes 99
4.8.7.4 Ligation 99
4.8.7.5 Amplification 99
4.8.7.6 Extra step for tubulin staining to mark cells 99
4.9 Microarrays on glass slides 100
4.9.1 Screening of microarray slides 100
4.9.2 Data analysis for scanned arrays 100
5 Results 102
Development of a phage display protocol for target identification 101
5.1 Establishing a phage display protocol for target identification 101
5.1.1 Identification of proteins that bind to melophlin A 106
5.1.2 Identification of proteins that bind to CD 267 117
5.1.3 Phage display employing specific elution 120
5.1.3.1 Identification of glutathione binding proteins 120
5.1.3.2 Identification of proteins that bind to tubulexin A 121
5.1.4 Generation of a T7 phage display HeLa cDNA library 123
5.1.4.1 Strategy to make a T7 phage display HeLa cDNA library 123
5.1.4.2 Target identification of tubulexin A using a T7 phage display HeLa cDNA library 126
5.1.4.3 Validation of UCRBP as a target protein of tubulexin A 129
Evaluation of the mode of action of tubulexin A 131
5.2 Influence of tubulexin A on vinblastine-resistant KB-V1 cells 131
5.3 Time-course of the influence of tubulexin A on HeLa cells 133
5.4 Confirmation of CAS as target protein of tubulexin A 137
5.5 Pulldown of CAS using tubulexin A 140
5.6 Analysis of the binding affinity of CAS to tubulexin A 141

5.7 Mapping the binding site of tubulexin A in CAS 144

5.8 Influence of tubulexin A or/and CAS on tubulin polymerization *in vitro* 147

5.9 The effect of tubulexin A on nuclear export mediated by CAS 149

5.10 Influence of tubulexin A on the interaction of CAS, importin alpha and RAN 149

5.10.1 Optimization of the pulldown procedure based on immunoprecipitation (IP) 149

5.10.2 Influence of tubulexin A on the *in vitro* interaction of CAS, importin alpha and RAN 152

5.10.3 The influence of tubulexin A on the interaction of tubulin, importin alpha and RAN with CAS in HeLa cells 153

Evaluation of podoverine A as tubulin inhibitor 155

5.11 Influence of podoverine A on the *in vitro* tubulin polymerization 155

5.12 Evaluation of the binding site of podoverine A in tubulin 156

Investigation of CAS inhibitors by means of reverse chemical genetics 158

5.13 Chemical array for screening CAS inhibitors 158

5.13.1 Screening of NPDepo (RIKEN arrays) 158

5.13.1.1 Targeting purified CAS 158

5.13.1.2 Targeting CAS from DNA transfected-lysate 159

5.13.2 Screening of MPI compounds 160

5.13.2.1 Targeting purified CAS 160

5.13.2.2 Targeting CAS from DNA transfected-lysate 161

5.14 The influence of array-based potential hits on importin alpha localization 161

5.15 The influence of array-based potential hits on the phenotype of HeLa cells 161

5.16 The influence of array-based potential hits on the thermal stability of CAS 165

5.17 Determination of binding affinities of array-based potential hits and CAS 166

5.18 The influence of R89 on cell proliferation, cell cycle and cytoskeleton in HeLa cells 168

5.19 The influence of R89 on nuclear export of importin alpha and RANBP1 176

6 Discussion 179

6.1 Establishing a phage display for target identification protocol 179

6.2 The binding and influence of podoverine A on tubulin polymerization *in vitro* 179

6.3 Time-course of influence of tubulexin A on HeLa cells 180

6.4 CAS expression, purification and the binding of CAS to tubulexin A 180

6.5 Influence of tubulexin A or/and CAS on tubulin polymerization *in vitro* 182

6.6 Influence of tubulexin A on vinblastine-resistant KB-V1 cells 182
6.7 Influence of tubulexin A on function and protein interaction of CAS 183
6.8 Validation of array-based CAS inhibitors 183
6.9 Influence of R89 on HeLa cells 185
7 References 187
8 Summary .... .198
9 Zusammenfassung 200
10 Appendix 202
11 Abbreviations and symbols 220
12 Curriculum vitae 223

1 Introduction

1.1 Chemical genetics

1.1.1 Classical genetics

Charles Darwin contributed his theory based on natural selection “The Origin of Species” in 1859 without the mechanism of the inheritance, but in 1886 Gregor Mendel proved his theory based on the laws of inheritance and opposed to Darwin´s theory at the same time.[1] Genetics which was proposed by William Bateson in 1906 is a term of biological investigation for heredity and variation,[2] and in 1909 the word “gene” was first used by Wilhelm Johannsen.[3] With experiments of Frederick Griffith in 1928 and experiments of Oswald Avery in 1944, DNA was indicated as the carrier of genetic information and then other experiments of Alfred Hershey and Martha Chase in 1952 proved that DNA transmits genetic information.[4] The gene made by DNA which was clearly understood when Watson and Crick proposed the double helical structure of DNA in 1953.[5] Nowadays, the gene is defined by Gerstein *et al*. as “a union of genomic sequences encoding a coherent set of potentially overlapping function products”.[3] In eukaryotic gene, DNA contains the coding sequences “exons” and noncoding sequences “introns”.[6] In prokaryotes gene, DNA does not contain intron.[7] Currently, with the development of technical advances, the project of International Human Genome Sequencing Consortium (IHGSC) was finished and published (in 2001 as draft and completely in 2004) with the sequence of human genome encoding approximately 20,000–25,000 protein-coding genes.[8] This reported is valuable information for biomedical research.[9]

Classical genetics is based on detection of individuals with phenotypically apparent mutations.[10] Genetics is employed as forward and reverse approaches (**Figure 1A)**.

Forward genetics starts from phenotype (characteristic) to discover the genes that are responsible for the phenotype. It explores the changes of phenotype including morphology, behavior or growth that result from random genetic mutations or deletions. These genetic alterations are usually induced by radioactive or chemical mutagenesis. Forward genetics requires the introduction of random mutations into cells or organisms, the screening of -

mutant cells for a phenotype of interest and the identification of mutated genes in affected cells (**Figure 1A**).[11]

Reverse genetics starts with a given genotype or gene and investigates the phenotype (characteristic) to find the function or biological effect of that gene in cells or organisms. Reverse genetics require the introduction of a mutation into a specific gene of interest and the study of phenotypic changes in cells or organisms containing the mutant gene.[11] The process of mutation (or disruption or modification) can be either performed specifically by using gene silencing or homologous recombination or performed by using chemical mutagenesis or transposon mediated mutagenesis.[12]

With the development of molecular biology in the twentieth century, classical genetics has advanced to bring our understanding at molecular level. Nowadays scientists are able to investigate specific proteins by ´knocking out´ the corresponding gene, increasing the concentration of proteins of interest (for example by increasing the copy number of the corresponding gene or the usage of a strong promoter for gene expression) or by altering the function of proteins by specific mutation of the corresponding genes. Therefore, the great advantage of classical genetics is the specificity because each specific gene can be modified. The advent of new methodologies for genome manipulation and the availability of full genome sequences led to the success of classical genetic which can be applied to prokaryotes and to eukaryotes.[10]

This approach is a powerful tool to understand the biological system, but it bears some limitations. Although highly effective, reverse genetics (i.e. introducing gene mutations via homologous recombination) is hard to apply to mammals because of high cost, high complexity, and time costs. Recently an alternative method, transgenic RNAi, has been studied to silence genes and elicit phenotypes of gene dysfunction *in vivo* for reverse genetics in mammals.[13] However, a gene knockout might be lethal making it impossible to study this gene in cells or organisms. This problem can be overcome by chemical genetic approaches (see 1.1.2).[14]

1.1.2 Chemical genetics

Chemical biology is a new science as an intersection of chemistry and biology. It is contributed first by chemistry and extended by biophysics and biochemistry to investigate the biological system or phenomenon at the molecular level.[15] Sometime, there are confused points between the term of chemical biology, biochemistry, chemical genomics and chemical genetics. There terms would be shortly described as below.

Biochemistry is a field of study of biological macromolecules which are related to macromolecular assembles, structures and networks of molecular interaction.[16] Emil Fischer, who won the Nobel Prize in Chemistry for sugar and purine syntheses in 1902 and who is known as the 'Father of Biochemistry', proposed the term "lock and key metaphor" for the model of enzyme-substrate interaction in 1894.[17] This metaphor illuminated how specific enzymes work at the molecular level. His "lock and key metaphor" brought talent in chemistry and biochemistry in the twentieth century. Fischer postulated that for one specific enzyme (lock) there is a specific molecule that fit as his key.[17] Further, the "induced fit theory" which was proposed by Daniel E. Koshland in 1985 is a new model for enzyme-substrate/small molecules interaction and more accepted at currently.[18] This model includes Fischer´s idea and also the modified concepts as the flexible structures of enzyme which can be induced to be changed by substrate.[19] The "lock and key model" is retained in "induced fit model" only the case after the changes caused by substrate occurs.[18] The ideas proposed in the "induced fit theory" is that the correct orientation of catalytic group requires for enzyme action, so the change of active site on protein structure caused by substrate to bring the catalytic groups in suitable shape for binding of substrate.[19] Nowadays, development of the new technologies allows scientists to discover a large number of locks (proteins) and a wide range of keys (small molecules).[20]

Chemical genomics is a field of study of cell biology based on using small molecule as modulating ligand (positive or negative regulators) to investigate the function of gene-products, the cell pathway or cell cycle. This approach can be employed in chemical genetics for target identification. For this application, the loss-of-function mutants in genetic model organisms (yeast, worm, fly, or mammalian cells) are prepared by gene deletion or modification such as mutation, transposon insertion, RNA interference. The mutants which can be sensitive or resistant to small molecules are further examines to identified the target gene.[21]

The term “chemical genetics” was first used in the field of chemistry and biology in 1994. Chemical genetics is the investigation of the biological system using small molecules to perturb and control the cellular and physiological function of proteins.[22] By analogy to classical genetics, chemical genetics is also divided in forward and reverse approaches (**Figure 1B)**.

Forward chemical genetics (or called cell-based screening) is similar to forward genetics which explores the phenotypic changes in the biological system which can be a prokaryotic and eukaryotic single cell organism (bacteria, fungi). Instead of introducing genetic alterations to impair protein’s function, collection of small molecules is screened for changes phenotype. Then the targeted molecule which binds to a given biologically active compound needs to be identified. This method provides the link between the targets and the associated phenotype that is induced by the small molecule. It requires three components: a library of compounds, a phenotypic assay to screening for active compounds, and a suitable method for identification of target protein of the hit small molecule (**Figure 1B**). Different strategies are being developed to use for identification the targets of active compounds which include affinity-based proteomics, expression-cloning-based approaches. It should also be considered that one chemical molecule can target one or multiple proteins.[23] It should also be considered that one chemical molecule can target one or multiple proteins. (e.g. small molecule leptomycin B binds to only one target CRM1 and influences the function of this target.[24] Another compound centrocountin 1 binds to both target NPM and CRM1[25] or compound melophlin A also targets multiple proteins as human dynamin I-like protein, dynamin I, and dynamin II).[26]

An example of this approach is monastrol which was identified in a phenotypic–based screen. It is based on the information of the family of mitotic kinesin which involved in the assembly and maintenance of mitotic spindle and predicted candidate target, Mayer *et al.* identified a kinesin Eg5 as the target. Authors proved that monastrol arrested mammalian cells in mitosis by inducing monopolar mitotic spindles and through inhibition of the motility of the mitotic kinesin Eg5.[27] A monastrol derivative LaSOM 65 (dihydropyrimidinones) as an anticancer candidate was employed for pre-clinical pharmacokinetics investigation and toxicological evaluation on rat by either injecting to the lateral tail vein or oral and results showed that this monastrol analogue is a promising anticancer candidate.[28]

Reverse chemical genetics looks for small molecules which bind to and/or inhibit the function of a protein of interest. This approach requires overexpressing a protein of interest for a ligand screening and using active ligand to determine the phenotypic changes by altering the function of this target protein in cells.

An example of this is viagra (sildenafil citrate, with code: UK-92,480), that was developed by scientists at Pfizer in 1989 for the treatment of cardiovascular disease (heart and blood vessel disease, e.g. angina pectoris, hypertension) via selecting inhibitors of phosphodiesterase type 5 (PDE5, an enzyme catalyzed the breakdown of cyclin guanosine monophosphate (cGMP)). This compound inhibits specifically PDE5 and is related on the nitric oxide (NO)/cGMP pathway. Intracellular level of cGMP is controlled by stimulating cyclic nucleotide cyclases (NO-activated guanylyl cyclase) and breakdown by PDE.[29] cGMP plays an important function on smooth muscle relaxation by activating cGMP-dependent protein kinase (PKG).[30] Based on selection inhibitors targeting PDE5 for the therapy of cardiovascular disease, Terrett *et al.* found that viagra as a potent in improvement of erection by increasing relaxation of the corpus cavernosal smooth muscle mediated by NO. The efficacy of Viagra for oral therapy of male erectile dysfunction was assessed through clinical trials in 1996[31] and then viagra was considered as a new therapy for male erectile dysfunction in 1998.[32] Therefore Pfizer decided to market this compound as an anti-impotence drug rather than as a heart medication and this drug is as one of the fastest-selling drugs.[33]

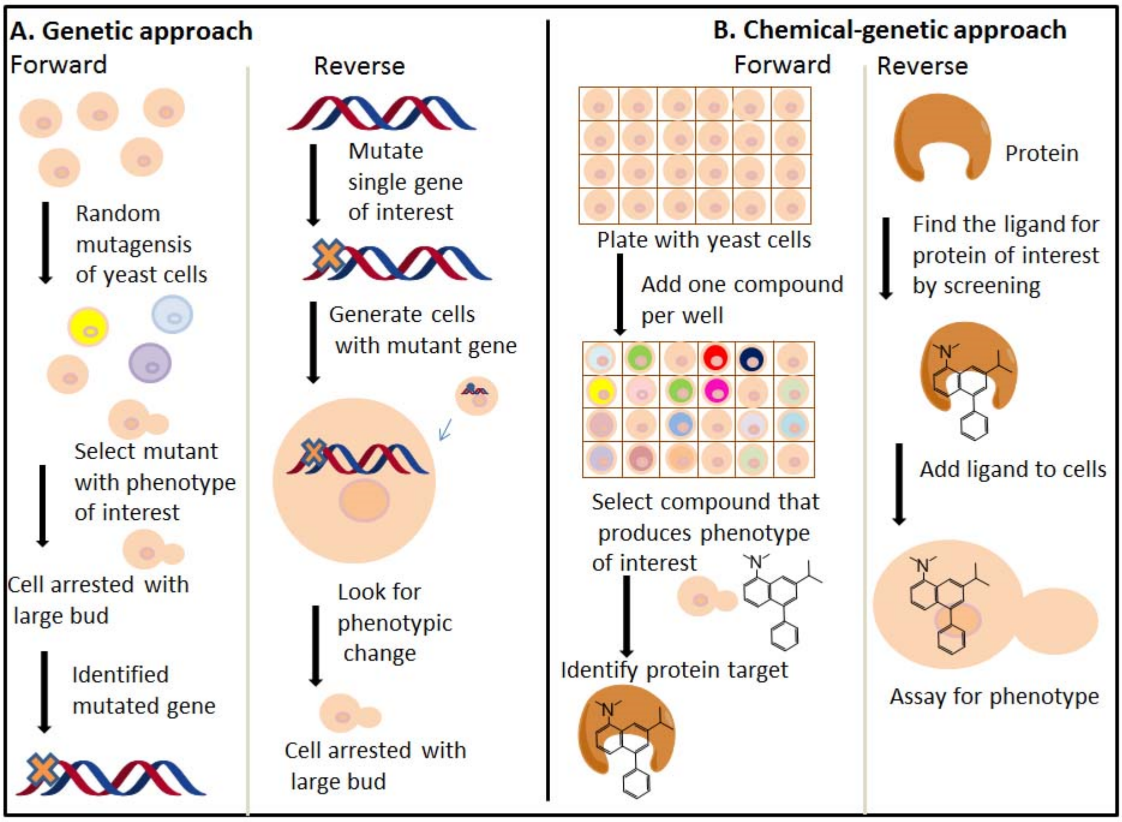
A. Genetic approach
Forward
Random mutagensis of yeast cells
Select mutant with phenotype of interest
Cell arrested with large bud
Identified mutated gene
Reverse
Mutate single gene of interest
Generate cells with mutant gene
Look for phenotypic change
Cell arrested with large bud
B. Chemical-genetic approach
Forward
Plate with yeast cells
Add one compound per well
Select compound that produces phenotype of interest
Identify protein target
Reverse
Protein
Find the ligand for protein of interest by screening
Add ligand to cells
Assay for phenotype

Figure 1: Classical and chemical genetics approaches (adapted from Stockwell *et al.)*.[11] **A**. Classical genetic approaches. Forward genetics: yeast cells are randomly mutated, cells showing a large-bud phenotype are selected, and genes mutated in these cells are identified. Reverse genetics: a single gene is mutated and introduced into yeast cells and a large-bud phenotype is observed. **B.** Chemical genetic approaches. Forward chemical genetics: compounds are screened on yeast cells, compound that induces a large-bud phenotype is selected and the protein target of this ligand is subsequently identified. Reverse chemical genetics: a protein of interest is purified and screening for ligands is performed. Hit compounds are subjected to phenotypic assay to identify ligands that induce a large-bud phenotype.

Chemical genetics can overcome some of the problems observed with classical genetics. Small molecules affect living organisms by perturbing proteins and other biomolecules instead of perturbing the function of gene through a gene knockout or RNA interference. Small molecules/compounds are easy to apply to the cells and organisms. They exert their effects rapidly and often reversibly, and can selectively disrupt only one of the functions of a multi-functional protein.[34] Tubacin, for example, inhibits the tubulin deacetylase activity of the multifunctional histone deacetylase 6 by binding to one of two catalytic domains.[35] Another advantage of small molecules is their capability to disrupt protein-protein interactions. A good example is Leptomycin B, which binds to CRM1 and inhibits the binding of the nuclear export signal (NES) cargo to CRM1 by binding covalently to cysteine 528 in the NES binding region of human CRM1 or cysteine 529 in *Schizosaccharomyces pombe* (fission yeast).[24] Other important benefits of chemical genetics are the easy applicability to cross-species studies and to study in living organisms for which standard genetic tools are not available, rudimentary or difficult. Chemical genetics can be employed to investigate the function of essential or recessive genes and can be applied in combination with classical genetics (e.g. multiple gene knock-outs or gene overexpression).[36]

However, chemical genetics has some drawbacks. The lack of specificity of small molecules can lead to unexpected toxicity at high concentration, where compound may bind to a wide range of proteins or non-specific killing of a wide-range of cell types. The small molecules with low solubility are not able to target each protein of interest in.[37,38] Polypharmacology as one challenge in drug discovery has been introduced for multi-targets drugs discovery.[39] Polypharmacology contains a single small molecule acting on multiple targets of unique disease pathway or multiple disease pathway.[39] For this issue, it is not easy to identify the complex of targets and complex system which responds to treatment with molecules.[40] However, there are some successful multi-target drugs as anticancer drug which are on the market (e.g. sunitinib, dasatinib and lapatinib).[41]

As the alternative approach, combination of classical and chemical genetics is a valuable strategy to understanding the biological systems better. In this sense, haploInsufficiency profiling (HIP) is employed in the method of yeast drug discovery.

1. 1.3 Natural products and compound collections

1.1.3.1 Natural products

Nature has been a source of drugs for thousands of years, and an impressive number have been isolated from plants.[42] Small molecules which are produced by plants or animals[43] or from microorganism[44] in nature as secondary metabolites are called natural products. Natural products are an interesting source for drug discovery as they can inhibit anti-tumor activity, and can be employed in the therapy of immunosuppressive[45] and neurodegenerative disorders such as Parkinson's[46] or Alzheimer's disease.[47] Bioactive natural products are identified and became candidates for drug discovery. Currently, there are more than 60% of marketed drug which are related to natural products.[48] In there, plants are considered as an important sources of compounds for discovery the new compound structure.[49] Plants-derived compounds have used for cancer treatment for long history and the some anticancer drug are known such as vinblastine isolated from *Madagascar* species and vincristine isolated from *Catharanthus* species (both compounds are belonged to vinca alkaloids) or paclitaxel (taxol) from *Taxus* species. Another source is microorganism which plays an important role in antibiotics discovery (such as penicillin from fungus *Penicillium* species, tetracyclines from *Streptomyces* species) and especially antitumor antibiotics (such as staurosprine from *Streptomyces* species).[44] Nowadays the advent of molecular biology allows modification the biosynthetic machineries in micro-organism (e.g. bacteria or yeasts) to produce the natural products and isolated them as secondary metabolites.

Compounds have been classified as original natural products, products derived semi-synthetically from natural products, or synthetic products based on natural product scaffolds.[50] In nature, the scaffolds of natural products are highly conserved and many of them contain the same scaffolds and just have different substituent patterns. Hence, the scaffolds of natural products are defined as an evolution-chosen.[51] Combinatorial approaches based on validated structures and scaffold of natural products as starting point for synthesis of natural product-based libraries with expected drug-like properties.[52] Molecular complexity and the prevalence of stereogenic centers are two important things which help to distinguish natural products from compounds of combinatorial chemistry libraries.[51] The natural products are valuable tool for chemical biology since their great chemical diversity of chemical structures, properties and capacity which can react on various biological targets.[53,52] Moreover natural products are dominant stereogenic centers and contain a part of chemical space which is not commonly occupied by synthetic molecules and drugs.[52,54] Natural product, Natural product-based compound libraries have contributed in the success of hit screening of chemical biology and biology.[51]

Natural products are able to specifically interact with targets, and the interaction between natural products and target need to be tight in case targets are proteins as well as the protein structure has to be correlated to the structure of natural products at the ligand-binding sites of proteins. The structure of protein fold formed by characteristic fold types of individual protein domains, which determine the size and shapes of their ligand-binding site, is conserved in nature better than the amino acid sequences since protein domains with low homologous sequences can form similar folds. Therefore, the conservation in the natural evolution of natural products and their protein targets are the scaffolds of natural products and the protein backbones. The result of interaction between natural product ligand and protein target is contributed by the substituents patterns in natural products and the diversity of amino acids side chain residues in proteins.[51]

1.1.3.2 Compound collections

Compound collection for screening, identification and validation hit compounds in the chemical libraries obtained from natural products libraries (biosynthetic machinery) or from combinatorial chemistry libraries is important part in drug discovery, chemical biology and chemistry. The properties of compound libraries are essential for the success of chemical genetic approaches to obtain a larger number of biologically active compounds. The drug-like “chemical space” is defined by all possible chemical compounds that can be created. It has been calculated that it contains around 10^{60} different molecules, but only limited number are bioactive compounds.[55,56]

Compound libraries for chemical genetic studies can be commercially available or are obtained synthetically. Although natural products are important for drug discovery, not many biologically active compounds which are available are natural products, thus chemical biologists and medicinal chemists need to synthesize new compound libraries for the further biological screening to develop new drug.

For the design of the synthetic libraries, some properties of the compounds are required, such as their ability to bind potently and specifically to target proteins, ability to cross biological membranes, chemical stability, and solubility in water and organic solvent (e.g. DMSO).[38] Two considered concepts in library design are “drug-likeness” which refers in combinatorial libraries having the approximately similar properties of drug molecules and “focus” which can be “target-focused” libraries or “ligand-focused” libraries.[57]

There are two successful approaches of compound library design, diversity-oriented synthesis (DOS) and biology-oriented synthesis (BIOS).[58] DOS has been introduced by Stuart L. Schreiber in 2000.[59] In contrast to target-oriented synthesis (traditional synthesis) which aims to prepare a specific target compound, DOS targets the facile preparation of collections of structurally complex and diverse compounds from simple starting materials.[59] DOS creates maximally diverse compound.[38,59] While DOS generates libraries based on the structurally diverse and complex compound libraries, BIOS generates libraries based on scaffolds of natural products.[58] An interesting example of BIOS-based approach was designed by Waldmann et al.[51,60-69] It combines two different concepts. The first concept is based on scaffolds from either natural products or from known drugs This brought Waldmann and colleagues to construct the hierarchical tree-like classification of scaffolds of natural products that could be used as a guide and hypothesis-generating tool in library design and development of natural products-inspired compounds for chemical biology and medicinal chemistry research as a result in the first Structure Classification of Natural Products (SCONP).[25,65,69-78] The second concept is based on Protein Structure Similarity Clustering (PSSC) of protein groups containing the similar structure of their ligand-binding site (or similar subfolds of ligand-binding site) since the ligands with similar scaffolds can bind to the proteins with similar subfolds. PSSC can be used to explore the promising type of ligand structure for known proteins or search the alternative targets for given ligands.[51] In this case, inhibitors should bind to related protein domains or subfolds. Hence, this concept is focused on target proteins, so it can be applied to reverse chemical genetics.[79,80] By combination of both concepts, Waldmann and colleagues have ready shown that the BIOS strategy is a promising approach to identify the biologically relevant compound classes in chemical space.[51]

1.1.4 Screening for small molecules

1.1.4.1 High-throughput screening

While natural products are still an important source of drug leads and research tools, chemists and biologists are increasingly employing chemical genetics to identify compounds from synthetic libraries. Compound screening is an important part for starting point of drug discovery as a technique which is used to find new hit compound. The requirement of screening the large number hit compounds for drug discovery has stimulated the technology development such as automation, miniaturization and detection methodologies (e.g. robotics, database and control software, liquid handling devices, and sensitive detectors).

High-throughput screening assay can be either solution-based biochemical or cell-based assays. Throughput was first used as 96-well plate for high-throughput screening and still used until today. At the same time, other format for high-throughput screening and ultra-high-throughput screening have been developed and moved to 384-wells plate and higher density plate formats such as 864-well plate, 1,536-well plate, 3, 456-well plate, and 9,600-well plate.[81] Therefore, recent development of high-throughput screening (HTS) allows researchers to rapidly identify active compounds or which modulate a particular protein or biological pathway.[34]

The principle of solution-based biochemical assay which is based on target-based approach is a screening of hit molecule which affects the biological activity of interested molecular target. The interested targets are normally recombinant expressed proteins (gene products which can be measured in the quantitative assays such as enzymes, receptor, channels and transporters).[82] There are several assays which can be employed for this approach and fluorescence-based techniques are the most common such as fluorescence polarization (FP), homogeneous time-resolved fluorescence and fluorescence lifetime.[82] Another biophysical method is surface plasmon resonance which permits identification of hit molecules in case of study the native target and/or unmodified substance.[82] The homogeneous "mix and measure" assays are suited for HTS since they can avoid time-consuming and they are convenient for biochemical assays such as enzyme inhibition and receptor-ligand assays.[81] The disadvantage of this approach is that the identified hits often affect the activity of purified target but does not response to the in more complex biological system, then the potent molecular inhibitors having no biological effect.[82] Moreover, this approach requires purified protein, active and soluble proteins.[83] In contrast, the cell-based approaches do not require purified protein.

Three categories (second message assays, reporter assays and cell proliferation assays) are usually employed in cell-based assays for HTS. Second message assays measure the signal transductions which are responsible for the activation of cell-surface receptors. These measurements are normally fast, transient fluorescent signal which occur for short time in measurement on the timescale of seconds. Reporter assays and cell proliferation assays require the incubations steps of several hours which are followed by colorimetric, fluorescent, or luminescent read-out. The reporter assays measure the activation of reporter genes which is resulted in the activation of target genes in the cell line of interest (**Figure 2A**). The reporter products may be enzymes or fluorescent proteins (e.g. luciferase, β-galactosidase or green fluorescent proteins).[81] Cell proliferation assays can be performed in microtiter plate for HTS by measurement the colorimetric formazan products produced after cleaving of tetrazolium salt WST-1 by cellular enzymes.[84] Recently, microscopy-mediated imaging techniques have developed with high resolution and drug screening approaches are employed on phenotypic screening which is one of cells-based screening approaches for HTS. This approach can analyse the cell shape of influent cells following the drug mediated perturbation of cytoskeleton. In this approach, the automated and high-sensitivity cellular imaging systems can be employed in research of functional genomics, target identification and entire proteome imaging.[82]

In forward chemical genetics, cellular changes can be determined by different methods in HTS. HTS can be carried out mostly using model organisms (yeast, plants, zebrafish, fruit flyand worms), mammalian cells or cell free systems. Yeast is suitable for screening assay because of high genetic conservation between yeast and human genome sequences[85] and their low cost of culture and flexible for robust assay.[83] Yeast-based HTS has the similar disadvantages of other cellular HTS which are related to insensitive due to drug pumps and membrane barriers and thick cell wall of yeast.[83] Plants are suited for screening because the entire genome is sequenced and compounds are easily taken up by the plant roots.[86] The fruit fly *Drosophila* is employed for screening as well because of its short life cycle and fully sequenced genome.[87] Zebrafish (Danio rerio) is a vertebrate and embryos and larvae can be studied, allowing easy visualization of developmental processes.[88] *The worm Caenorhabditis elegans* is also common model organism because of its short life span (as the time from birth until death),[89] low cost of culture, transparent appearance, known genome and RNA interference (RNAi).[90,91] Transparent appearance allows observation phenotype and the visible subcellular structure and scanning the cellular processes (such as meiosis, pronuclear appearance, cytokinesis and spindle) using DIC time-lapse imaging).[90] RNA interference (RNAi) is double-stranded RNA (dsRNA) which acts as gene silencing of sequence-specific target genes and two types of them such as short interfering RNAs (siRNAs) and microRNAs (miRNAs) which are depend on their origin (siRNAs are from exogenous RNA such as RNA transfection or virus infection and miRNAs are from endogenous RNA).[92] Mammalian cells can be performed in HTS with different methods (**Figure 2**). A reporter assay is widely used to monitor the cellular changes based on transduction signaling which stimulates the reporter gene expression. This assay is applied in study the signaling transduction which influence on regulation of gene expression. For doing this assay, promoter-reporter constructs are introduced into the cells and the activity of reporter gene in living cells are monitored after stimulating or inhibiting the transduction pathway, for example this assay can be used in HST for screening compounds having effect on gene expression (**Figure 2A**).[93] Multiplexed enzyme-linked immunosorbent assays (cytoblot) method can be used to explore the cellular change (amount of protein expression of total cells in well) and valuable for desired post-translational changes in a cell-based assay.[94] This assay is monitored as a normalizing value of well-to-well and can be used for detecting the intracellular localization of signal and the signal of cell-to-cell. For this assay, after compound incubation, cells are fixed and stained with specific antibody to proteins or peptides of interesting phenotype. Secondary antibody conjugated to horseradish peroxidase is put in to detect the signal as a luminescence (**Figure 2B**) or can use fluorescent antibodies and the signal can be detected by microarray scanner.[14] An example of application of cytoblot assay in drug discovery was monastrol (a mitotic inhibitor).[27]

High-throughput is based on automated imaging by fluorescence microscopy and quantitative image analysis and typically referred to as ‘‘high-content’’ screening (HCS) which allows screening small molecules influence on cells. Fluorescence microscopy-based screening is currently the best strategy of the cell-based screening and has great potential for identification of mitosis modulating substances. HCS can be used to study the subcellular localization of proteins, cell morphology and specific cellular changes such as the phosphorylation, translocation or abundance of a protein which can be determined on a per cell using highly sensitive fluorescence microscopy.[95] After compound incubation, cells are fixed and stained with specific antibodies that are conjugated to fluorophores (**Figure 2C**). Live cell imaging can be performed for HCS to study cell motility, the activation of receptor uptake. In addition, a combination of different fluorescent dyes (for multiplexing antibodies in three- and four-channel experiments) allows the analysis of multiple cellular parameters simultaneously.[95,96]

Flow cytometry (or fluorescence activated cell sorting, FACS) has been currently developed and considered as one great potential method of HTS for drug discovery. Flow cytometers can distinguish cell characteristics including surface markers, protein expression, intracellular ions and other biochemical species, such as DNA content, and cell functions such as apoptosis, cell cycle, and phosphorylation status.[97]

Additionally, the activities of reporter gene can be measured without any centrifugation, cell permeabilization, or lysis steps for example with β-galactosidase gene. β-galactosidase (product of the lacZ gene) activity is determined by simple addition of the fluorogenic substrate 4-methylumbelliferyl β-d-galactopyranoside to intact cells (bacteria, yeast and mammalian cells). This assay can be applied to HTS such as functional genomics, drug discovery, and diagnostic screens which are based on the differential expression of the lacZ gene.[98]

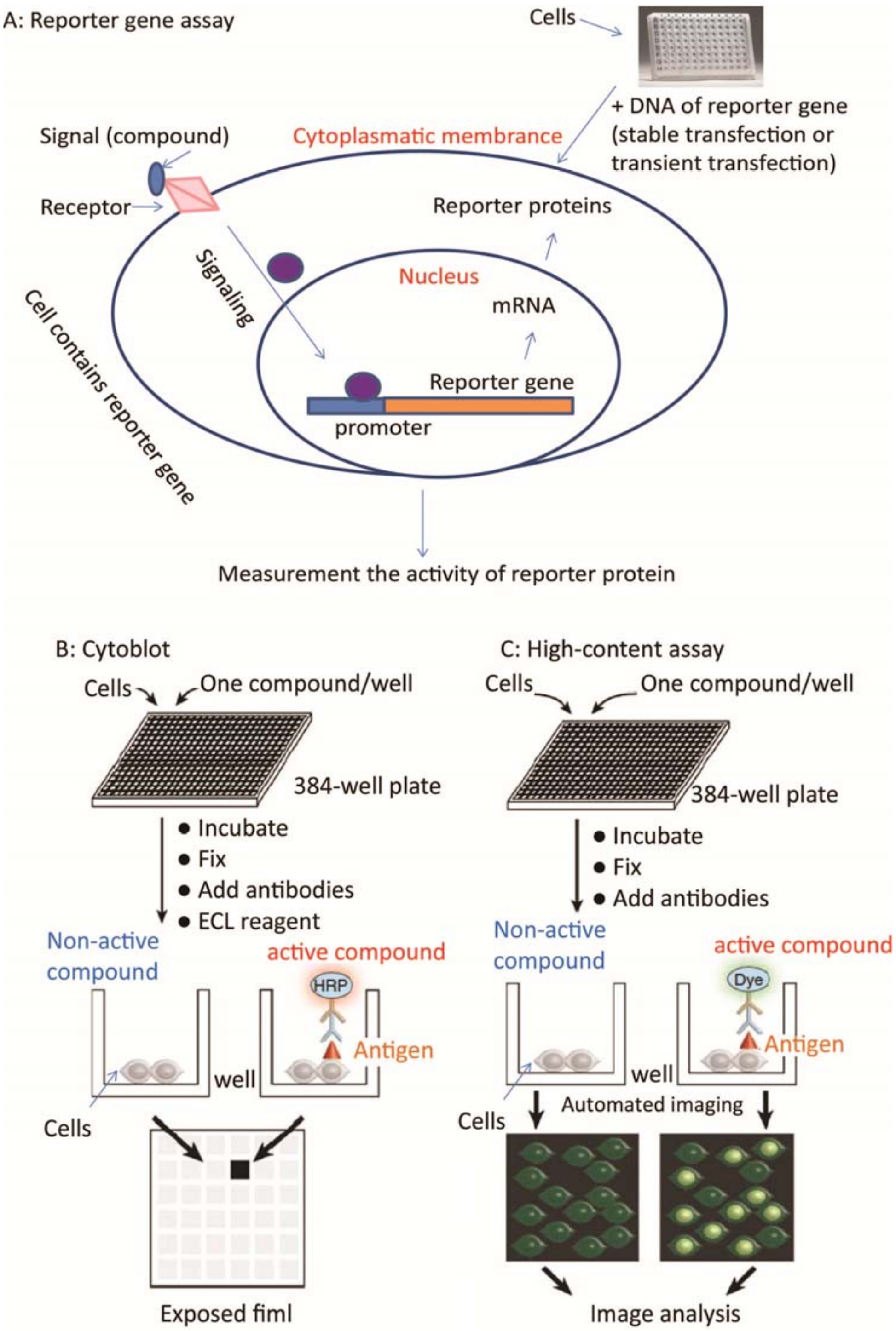
A: Reporter gene assay
Cells
+ DNA of reporter gene (stable transfection or transient transfection)
Signal (compound)
Cytoplasmatic membrance
Receptor
Reporter proteins
Signaling
Nucleus
mRNA
Reporter gene
promoter
Cell contains reporter gene
Measurement the activity of reporter protein
B: Cytoblot
Cells
One compound/well
384-well plate
Incubate
Fix
Add antibodies
ECL reagent
Non-active compound
active compound
HRP
Antigen
well
Cells
Exposed fiml
C: High-content assay
Cells
One compound/well
384-well plate
Incubate
Fix
Add antibodies
Non-active compound
active compound
Dye
Antigen
well
Cells
Automated imaging
Image analysis

Figure 2: Cell-based methods for screening. **A**. A reporter gene assay (adapted from Terstappen *et al.*).[93] Cells are seeded onto a multiwell plate and used for transient DNA transfection (or stable DNA cell line containing reporter gene). After compound incubation, cells are lysed and the followed by measurement of reporter activity. **B**. Cytoblot. Cells are seeded onto a multiwell plate and a single compound is added to each well. After incubation, cells are fixed and a primary antibody of desired specificity is added. Detection is done with a secondary antibody conjugated with horseradish peroxidase (HRP) and enhanced chemiluminescence (ECL) reagent. Light emission is visualized by exposing to autoradiography film or by using a chemiluminescence plate

reader. **C**. High-content assay (adapted from Kawasumi *et al.*).[14] Cells are seeded onto a multiwell plate and a single compound is added to each well. After incubation, cells are fixed and specific antibodies or and/or dyes are added. Fluorescence images of cells in each well are acquired using an automated fluorescence microscope. The acquired images are analyzed at the level of single cells.

1.1.4.2 Small molecule microarrays (chemical arrays)

Chemical arrays were first described by MacBeath *et al.* in 1999. In this approach, small molecules containing a carboxylic acid moiety were immobilized on maleimide-derivatized glass slides.[99] This method allows the screening of compounds that bind a protein of interest as high-throughput protein-binding assay. Chemical array was originally developed for identification of small molecule interacting purified protein and later improved for identification of small molecule interacting target protein in cell lysates. After incubation microarray with protein solution, compounds on a glass slide was monitored by fluorescent antibody using later scan.[14,100]

Osada and colleagues developed an approach to “non-selectively” and functional-group-independent immobilization of variety of small molecules on glass slides[101,102] or gold surfaces by using a photoinduced cross-linking reaction to anchor small molecules.[103,104] The immobilization depends on the reactivity of a generated carbene species of on photo-reactive group of trifluoromethyl aryldiazirine upon UV irradiation (**Figure 3A**).[103] Thousands of small molecules are covalently attached onto a glass slide in high density, called a small-molecule microarray (SMM) (**Figure 3B**).[14,100] This method does not require the incorporation of certain reactive groups in the library members. Therefore it is especially suited for natural product-derived compound libraries.[7] Osada and colleagues could demonstrate that the immobilized small molecules retained their ability to interact with their target proteins.[103,104] Moreover, they successfully identified triphenyl compound A (TPh A) as a pirin binder,[105] inhibitors of lysophospholipase-like 1 (LYPLAL1),[106] or inhibitors of acyl protein thioesterases (APT) 1 and 2[107] by using chemical array technique.

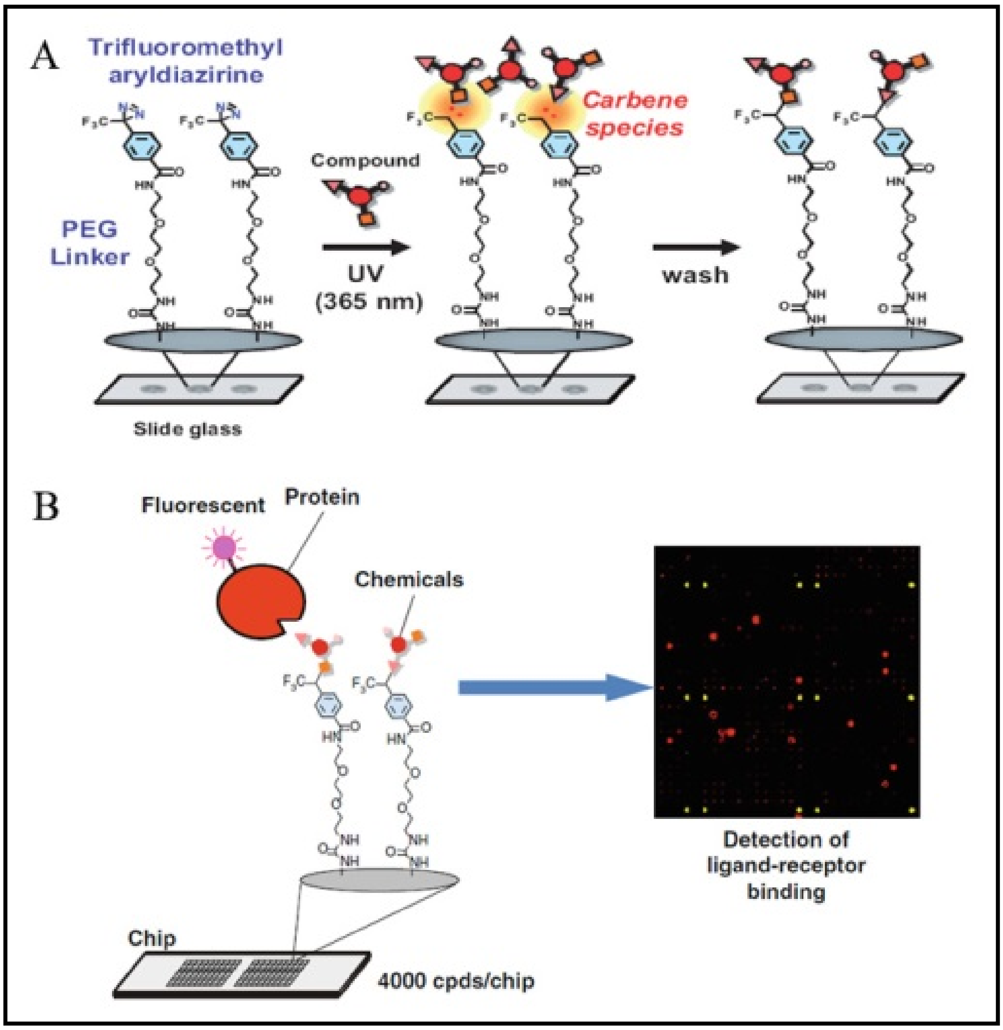
A
Trifluoromethyl aryldiazirine
PEG Linker
Slide glass
Compound
UV (365 nm)
Carbene species
wash
B
Fluorescent
Protein
Chemicals
Chip
4000 cpds/chip
Detection of ligand-receptor binding

Figure 3: Principle of the chemical array screening. **A**. Preparation of the chemical array. Trifluoromethyl aryldiazirine attached to a glass slide via Polyethylene glycol PEG linker. UV irradiation generates reactive carbene species of small molecules with attached trifluoromethyl aryldiazirine, resulting in “non selective” immobilization of compounds. **B**. Chemical array screening. Variety of small molecules which are introduced onto glass slides by photoaffinity reaction is incubated with target protein (protein with red-fluorescent tag or labelled antibodies anti-target proteins if target protein without red-fluorescent tag). After binding step, glass slides are washed and scanned on microarray scanner by laser scan. The results of two array slides (one for target protein and one for control) were painted green and red respectively using Photoshop 5.5 software. The color images were merged. After two slides are merged, true hit compounds are detected as red signals; false-positive signals are yellow.[100,103]

The chemical microarray can be incubated with either purified proteins or protein lysates of cells that express the protein of interest fused with red fluorescent protein (RFP) (**Figure 4**).[14,100] The target protein can be detected in a direct or indirect way. Proteins fused with red fluorescence tag are detected directly by means of the RFP fluorescence. Proteins without RFP fusion are detected using a specific primary antibody against the protein of interest (or protein tag) and a secondary antibody conjugated with a fluorescent dye (e.g. cy5). Upon binding, small molecule microarrays are washed and dried prior fluorescence detection using microarray scanner.[100]

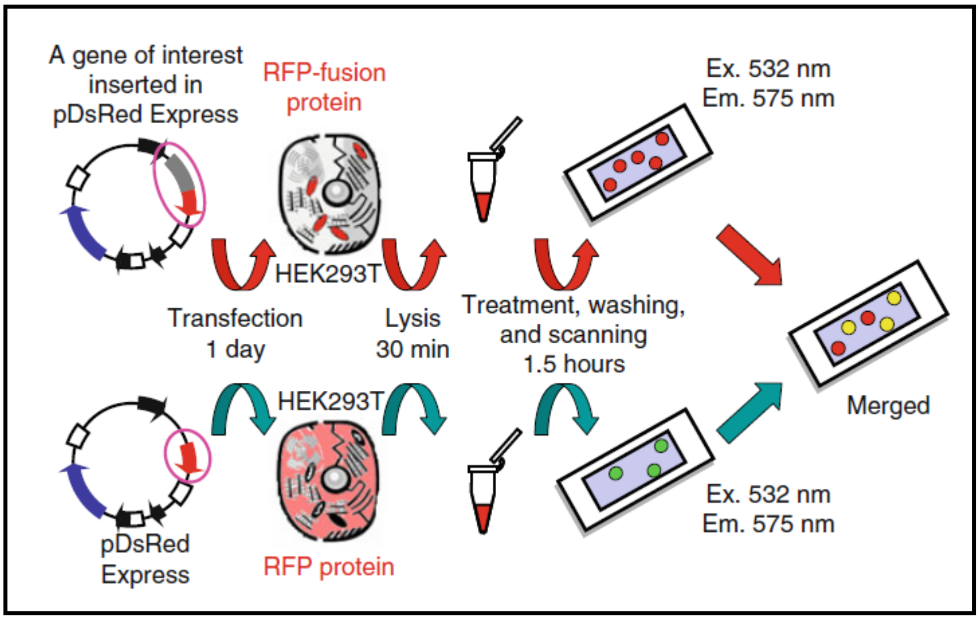
A gene of interest inserted in pDsRed Express
RFP-fusion protein
Ex. 532 nm
Em. 575 nm
HEK293T
Transfection
1 day
Lysis
30 min
Treatment, washing, and scanning
1.5 hours
Merged
HEK293T
Ex. 532 nm
Em. 575 nm
pDsRed Express
RFP protein

Figure 4: Overview of a chemical array screening method.[100] Genes of interest are cloned and can be expressed as RFP-fused proteins in the mammalian cell line HEK293T. After DNA transfection, cell lysates are prepared for incubation with glass slides. Hit compounds are detected via merged display analysis. Spots that interact with RFP or RFP-fused proteins are green and red. After two slides are merged, true hit compounds are detected as red signals; false-positive signals are yellow.

Chemical microarrays offer the advantages because thousands of compounds can be immobilized on one glass slide and could be used for detecting the interaction of small molecules and target proteins. This method could capture any type of small molecules on glass slide without depending on functional group of compounds. However, chemical microarrays restrict the orientation of the compounds and false negatives could occur when the interacting part of the hit compound is bound to the slide surface and is not available for protein binding.[100]

1.2 Target identification and validation

In contrast to previous chemical genetics approaches, a general effort is now focused on understanding the mechanisms of action of newly discovered small molecules in an early stage. In particular, target identification and validation, although time-consuming, are now widely considered as essential steps in the development of new drugs. In this context, several powerful target identification methods have been developed. The following chapters give an overview of the different techniques for target identification and target validation which have emerged in the last few years.

1.2.1 Target identification

Following cell-based screening, selected hit compounds are used to identify their binding partners therefore referred to as target proteins. To date, several approaches such as microarray techniques, or chemical proteomics, expression-cloning-based methods, genomics and genetics methods, and bioinformatics methods have been successfully developed. Among microarray techniques, some have revealed particularly useful such as DNA microarrays, protein microarrays and “reverse transfected” cell microarrays. In chemical proteomics, affinity purification methods are widely applied. More recently, expression-cloning-based methods have emerged as attractive methods for target identification such as, mRNA display, and yeast three-hybrid system and cDNA phage display.

1.2.1.1 Microarray techniques

1.2.1.1.1 DNA microarrays

The DNA microarray (also commonly known as DNA chip or biochip) was first introduced by Schena *et al.* in 1995[108] and later by Lockhart *et al.* in 1996.[109] DNA microarray allows the analysis of thousands of genes, enabling genome-scale transcriptional profiling of samples essentially in a single experiment. Microarrays have become tools in diagnostic applications and drug discovery. They can be used to identify disease-causing genes for new potential drug targets, to monitor the changes in gene expression in response to drug treatment and also to predict drug response for individual patients.[110-112] This method allows the measurement of the transcription of target gene in cells cellular changes which include their disease or their process of cell division or their response to a chemical and genetic disorder.

By comparing the expression profile of compound treated cells with the profile of control cells with known mutations, the potential target can be determined.[113]

DNA microarrays are based on probes, which are immobilized in an ordered two-dimensional pattern on a surface, such as nylon membranes or glass slides. Probes are either spotted cDNAs or oligonucleotides. They are designed to be specific for an organism, a gene, a genetic variant (mutation or polymorphism), or intergenic regions. Probe-target hybridization is usually detected and quantified by detection of fluorophore-, silver-, or chemiluminescence-labelled targets to determine the relative abundance of nucleic acid sequences in the target.[114]

1.2.1.1.2 Protein microarrays

Since most drug targets are proteins and mRNA transcript levels do not necessarily correlate with protein levels, then protein microarrays have been preferred to apply over DNA microarrays. Protein microarray (also known as a protein chip) was first described by MacBeath and Schreiber in 2000.[115] Protein arrays are not only useful for the screening of protein-protein interactions, but also for the identification of substrates for protein kinases, and for identifying protein targets of small molecules.[115] The principle of this method consists in the immobilization of proteins, peptides or antibodies on a surface which can be probed by a ligand. The array is then incubated with a labelled small molecule, and after stringent washing, labelled proteins are identified given their specific position on the array (**Figure 5**).[116] Bound small molecules can be either labelled with a fluorescent or radioisotope group allowing a direct readout or with a chemical group easily detectable using a fluorescently labelled detection system (e.g. biotin-functionalized molecule recognized by a streptavidin-fluorescent conjugate). As an alternative, the detection can also be performed by means of an enzyme-linked immunosorbent assay (ELISA), mass spectrometry, atomic force microscopy or radioactivity.[117] Fang *et al.* have successfully applied this method for compounds that bind to G protein coupled receptors.[118] Currently, there are available commercially protein microarray composed of approximately 3,000 individual human proteins.[119]

The advantage of this approach is the possibility to quickly analyze the binding profile of a small molecule with immobilization of thousands of different proteins at a high-density solid surface, and to identify target proteins which are expressed at low levels. In addition, this approach is developed not only application for purified protein but also for tissue or cell lysates which are directly spotted on a slide and called “reverse-phase” protein microarray.[119] However, there are also some limitations related to the attachment of the protein on the chip. Indeed, steric repulsion with the surface might not allow an optimal binding of the small molecule or ligand to the surface. In addition, the natural surroundings of target proteins (e.g. their involvement in complex formation with other proteins and their subcellular localization) might be essential for their affinity for their ligands and therefore some small-molecule target proteins might not be identified.[116]

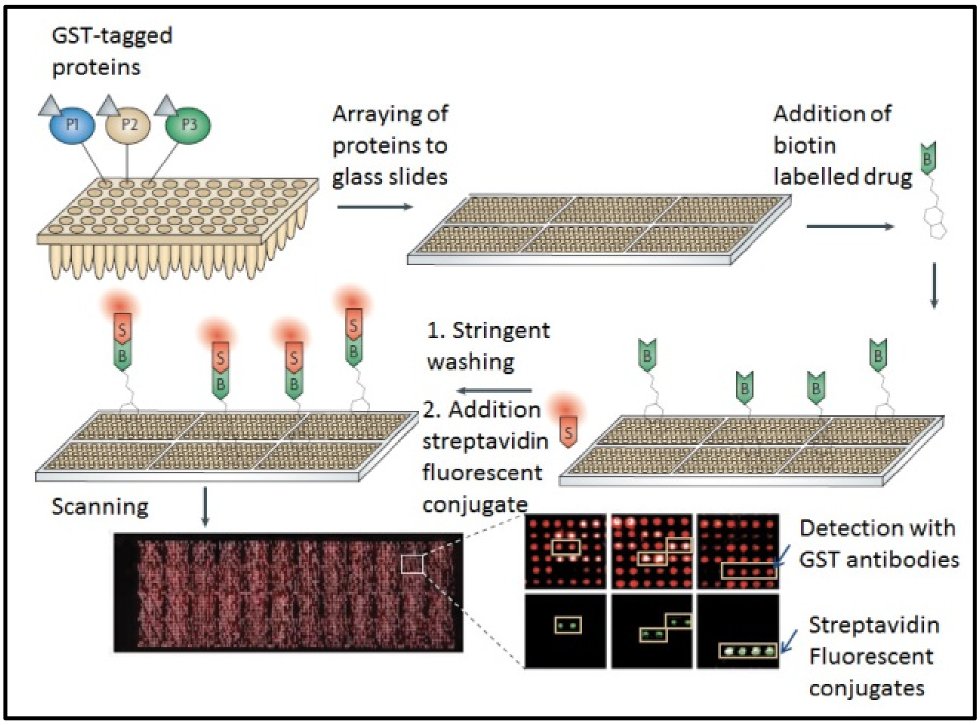
GST-tagged proteins
P1
P2
P3
Arraying of proteins to glass slides
Addition of biotin labelled drug
B
S
1. Stringent washing
2. Addition streptavidin fluorescent conjugate
Scanning
Detection with GST antibodies
Streptavidin Fluorescent conjugates

Figure 5: Principle of protein microarray for target identification. In this example, GST-tagged proteins (exemplified by P1, P2 and P3) are immobilized on a glass surface which is then exposed to a biotinylated small molecule. Bound target proteins are visualized by adding a fluorescently labelled streptavidin (S) conjugate. As a ‘loading’ control, the array is probed with GST-specific antibodies.[116]

1.2.1.1.3 “Reverse transfected” cell microarrays

This technology has been descried by Ziauddin and Sabatini in 2001.[120] By printing sets of complementary DNAs cloned in expression vectors, microarrays were developed whose features are clusters of live cells that express a defined cDNA at each location. Ziauddin and

Sabatini used a combination of two methods in their approach: as an alternative to protein microarrays for the identification of drug targets, and as an expression-cloning system for the discovery of gene products that alter cellular physiology (**Figure 6**).[120] In this approach, each transfected cell will express defined cDNAs at a defined location on the chip with each cluster overexpressing a specific protein. Incubation of the array with radioisotope-labelled small molecule, followed autoradiography readout (film autoradiography), allows the detection of the labelled small molecules which interacts with the cell cluster containing target proteins. For detecting expression of target gene in cell cluster, the plasmids containing an internal ribosome entry site-green fluorescent proteins (IRES-GFP) cassette downstream of the cDNA which can express the GFP-used target proteins are designed. Cell clusters are transfected with plasmids expressed either only GFP or GFP-fused target proteins can be detected by laser fluorescence scanner.[120]

The advantage of this approach is its applicability for a high-throughput screening and also for loss-of-function studies by monitoring the consequences of gene silencing. This technology was applied for target deconvolution using HEK293T cells allowing the identification of cells expressing FKBP12 when treated with radiolabelled FK506.[120] However, this technique also have some limitations given that cDNAs are only converted into proteins when needed and the expressed proteins remains concentrated on a small area of the transfected-cell cluster. cDNAs generating only small increase in signal intensity over the background can be identified. On the other hand, due to variation of transfection efficiencies, some cell types can be relatively low transfected DNA leading to low amount of target proteins, so that sensitivity of detection might be compromised. Moreover, differences in protein-expressions level might also complicate the interpretation of the results.[116]

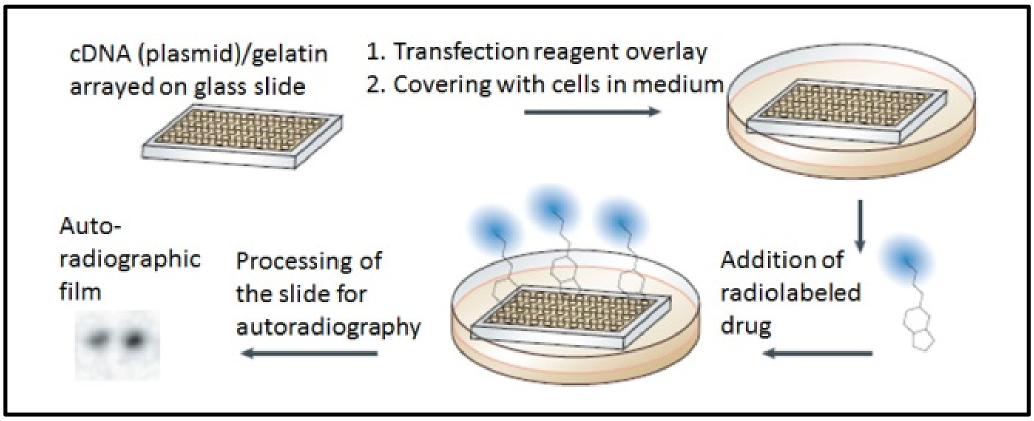
cDNA (plasmid)/gelatin arrayed on glass slide
1. Transfection reagent overlay
2. Covering with cells in medium
Addition of radiolabeled drug
Processing of the slide for autoradiography
Auto-radiographic film

Figure 6: “**reverse transfected” cell microarrays.** cDNAs are arrayed on a glass slide. Cells are transfected with arrayed cDNAs to generate a ‘living’ microarray. A radiolabelled small molecule is added to the chip and target proteins binding to the molecule are detected by autoradiography.[116]

1.2.1.2 A useful method of chemical proteomics: Affinity chromatography

Affinity chromatography is a classical method for identification of target protein. With the recent development of modern high-resolution mass spectrometry (MS) and liquid chromatography–tandem mass spectrometry (LC-MS/MS) analyses, affinity chromatography has become a powerful tool for target identification.[121] Several successful identifications of proteins that are targeted by small molecules are based on this technique.[25,26,122-127] In this approach, the small-molecule ligand is modified to be immobilized on solid support (or matrix) by an appropriate functional group (anchoring group). Once the small molecule is immobilized on the surface, the matrix is incubated with protein extracts, allowing the binding of proteins on the surface. Unbound proteins are subsequently washed out by successive washing steps. The matrix is then treated with either the unmodified (free) compound (which can be used for distinguishing between specific and nonspecific binding), or is boiled in buffer containing SDS to elute proteins that specifically bind to immobilized compound. Finally, the collected proteins can be identified by immunoblotting[128] or mass spectrometry.[129,130] Proteins that bind unspecifically to the surface can also be eluted by an inactive analogue (comparison variant) first and followed by elution with the free small molecule (competition ligand) that allow the collection of target proteins which can be identified by mass spectrometry (**Figure 7**).[116] Affinity chromatography is widely used given that it can be applied to any small molecule as long as its modification for immobilization does not impair its biological activity.

Affinity chromatography has the advantage that target proteins maintain their three-dimensional structure and their post-translational modifications. However, this technology also has some limitations which might be either due to the creation of an hydrophobic environment[131] or due to steric hindrance,[132] both resulting in nonspecific binding to the surface. Also, the binding affinity of the small molecule for its targets plays an essential role. A high-affinity interaction between a compound and the target, typically a low-abundance protein, will be the most physiologically relevant interaction identified as poor binding interaction are likely to be fully lost during washing steps. Another important factor is the amount of the target proteins in the extract, e.g. a low-affinity interaction between the small molecule and highly abundant proteins often creates significant noise during purification. In general, the higher affinity of the compound for its target is, and the easier target identification for its target will be. In practice, compounds with EC_{50} (the half maximal effective concentration of drug where 50% of its maximal effect is observed) or IC_{50} (inhibitory concentrations at 50% inhibition) values in the nanomolar or low-micromolar range are useful for affinity purification.[116,121] One option using this method is to consider proteins that are isolated by the active compound but not by the inactive control compound as candidate targets. However, apparently inactive molecules that does not show cellular activity, e.g. due to poor permeability or solubility, might still bind to the target proteins. These binding proteins are then considered as non-specific binders, resulting in false negative.[121]

Different methods have been used for the immobilization of a small molecule to a solid support. Given their availability, and the possibility to be easily modified, agarose beads are among the most frequently used matrix.[124-126] The attachment to the surface can be done covalently, for example through reaction of free amine group that has been incorporated in the active small molecule, with NHS-activated sepharose beads.[25] Alternatively, the strong affinity of biotin for avidin can be used, which allows the immobilization of biotinylated small molecule to avidin-sepharose beads.[26] Hydrophilic spacers such as tartaric acid–based spacers[133] and polyethylene glycol-based spacers (PEG-spacers)[122] should be incorporated between the functional group and the small molecule in order to minimize nonspecific binding to the surface.

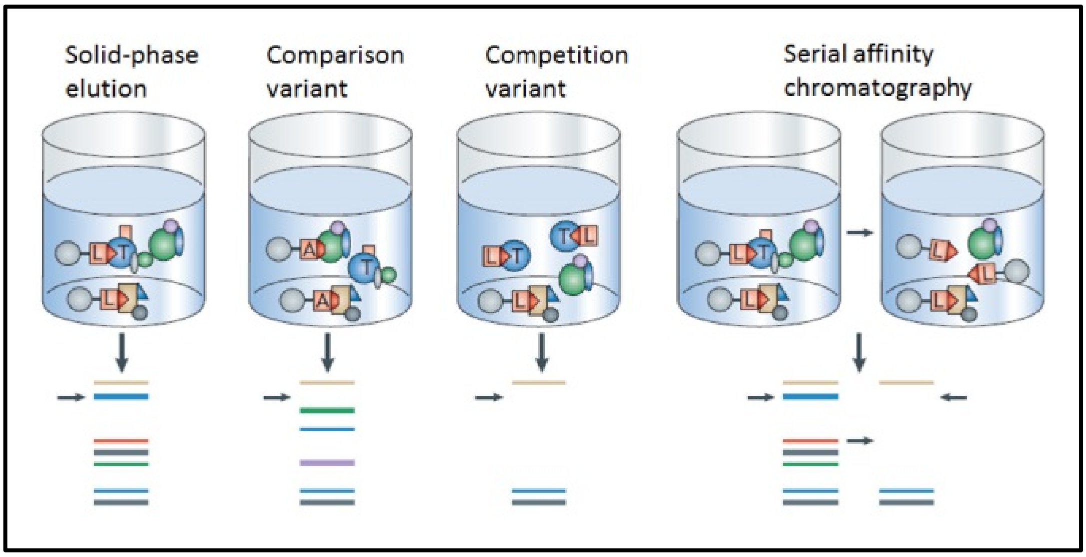

Figure 7: Affinity chromatography for target identification. The small molecule ligand (L) is attached to a matrix (shown in gray) and incubated with a protein extract that includes the target protein (T). All unbound proteins are washed out and ligand-bound proteins are eluted (solid-phase elution). To distinguish between specific and nonspecific binding, binding proteins which eluted from an inactive ligand (A) and active ligand (L) are compared (the 'comparison variant'). In the 'competition variant', protein elution is performed by an excess of free ligand. In the 'serial affinity chromatography', the ligand-attached matrix is incubated with protein extract which is then incubated with fresh ligand-attached matrix. Most of the proteins that bind specifically are captured by the first matrix, whereas the amounts of nonspecific binding proteins are similar for both matrices.[116]

The elution with free active small molecule constitutes a very efficient way to reduce non-specific bindings,[124] given that the free compound is soluble enough at high concentration. In case of low solubility, the elution of target proteins from the surface will have only low efficiency. To avoid collecting non-specific binders, the list of a "frequent hitter" which contains from a large number of target identification experiments as non-specific proteins can be generated.[134] However, the use of such a list is not always suitable, in particular if the target of the small molecule is a high-abundant protein. For instance, geldanamycin targets the high-abundant protein HSP90, a highly relevant cancer target.[121,135]

Recent development of quantitative mass spectrometry (MS) methods allows distinguishing specific and nonspecific binders. MS-based methods for protein quantification have become especially popular in recent years. Among them, one method has been developed which is based on the new chemical reagent termed the isotope-coded affinity tag (ICAT) and MS.[136] ICAT reagents consist of three functional elements: a specific activity (e.g. iodoacetamide group, which reacts specifically with cysteine thiol functional groups of proteins or peptides), and isotopically coded linker (e.g. linker with nine of ^{13}C or nine of ^{12}C) and an affinity tag (e.g. biotin). The biotin group of ICAT reagent allows for the binding of ICAT-labelled peptides to avidin bead.[136,137] Further, the ICAT reagent is developed with an acid-cleavable linker which is localized between biotin and affinity coded tag), so that the biotin can then be removed by treating the labelled peptides with trifluoroacetic acid.

ICAT as it permits the fast comparison of proteins obtained from pulldown experiments with active compounds (positive matrix) with proteins obtained from experiments employing the inactive compound (negative matrix) (**Figure 8A**). The chemical labeling of accessible cysteine moieties of proteins contained in both sample with different encoded linkers (heavy or light chain), allows the clear detection of differentially enriched proteins, which can subsequently be identified by mass spectrometry. The use of this approach has permitted to discovery malate dehydrogenase (MDH) as the specific target of the anti-cancer agent E7070.[127,138] The disadvantage of this method is the ability of target identification since only cysteine-containing proteins can be identified and missed cysteine-lacking proteins.

Another widely used target identification approach consists in the stable isotope labelling by amino acids in cell culture (SILAC), which has been described by Ong *et al.* in 2002.[139] To date, SILAC is the most commonly used quantitative MS method. Two similar cell populations are cultured with either heavy or light stably isotope-labelled amino acids (arginine or lysine). During cells growing, cells use labelled amino acids which are contained in media and then cells contain isotope-labelled amino acids in their proteins. Cells are collected and lysed for labeled proteomes preparing. The labeled proteomes are either pretreated with free compound of interest or untreated, then applied to affinity purification and can be identified quantitatively by MS (**Figure 8C**).[140] The labeled proteomes can also be used for affinity purification with the biotinylated active compounds (heavy-labelled proteomes) and the biotinylated inactive compound (light heavy-labelled proteomes), after that two pulldown samples were combined, separated by SDS-PAGE, digested by trypsin followed by identification using nano-HPLC-MS/MS.[78] This method is a powerful tool for target identification but there is still limited use for labeling cells in case harvested cells cannot be maintained long time for completely labeling.[141]

As SILAC method which is critical for distinguishing specific and nonspecific binders, isobaric tags for relative and absolute quantitation (iTRAQ) is the most commonly used method at this time too.[142] iTRAQ method is based on the principle of isobaric mass tag and chemical labeling of tryptic peptides with isobaric tag peptides.[142] iTRAQ reagent consists of three elements including a reporter group, a mass balance group and a group reacting with peptides.[141] For example, this method was successfully used to identify new targets of kinase inhibitors[143] (**Figure 8B**).

Various approaches have been developed to complement affinity chromatography by increasing artificially the concentration of target proteins, such as the three-hybrid systems, mRNA display, phage display, or protein microarray (see detail in section 1.2.1.1).[121]

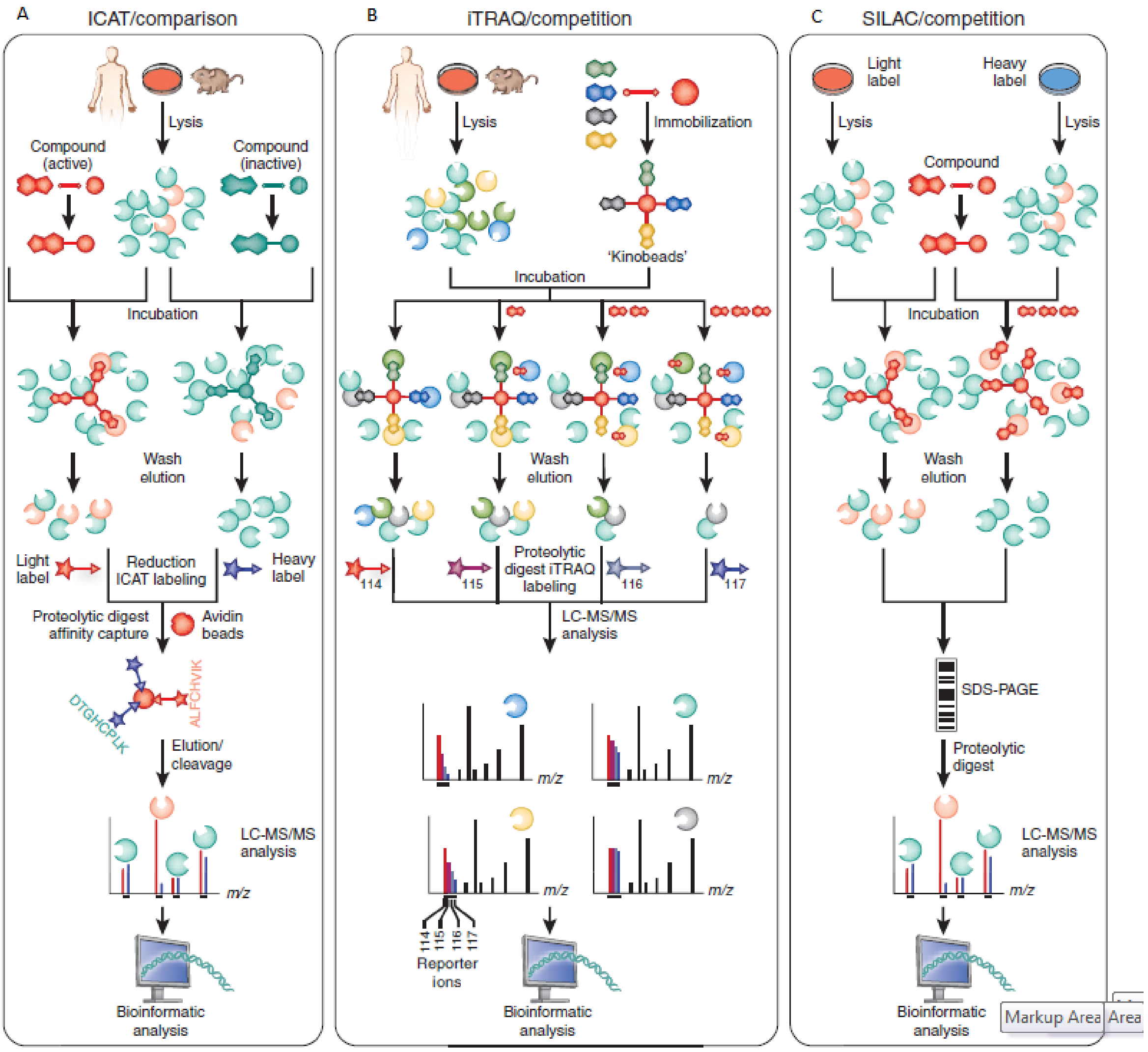
A
ICAT/comparison
Lysis
Compound (active)
Compound (inactive)
Incubation
Wash elution
Light label
Reduction ICAT labeling
Heavy label
Proteolytic digest affinity capture
Avidin beads
DTGHCPLK
ALFCHVIK
Elution/ cleavage
LC-MS/MS analysis
m/z
Bioinformatic analysis
B
iTRAQ/competition
Lysis
Immobilization
'Kinobeads'
Incubation
Wash elution
114
115
Proteolytic digest iTRAQ labeling
116
117
LC-MS/MS analysis
m/z
m/z
m/z
m/z
114 115 116 117
Reporter ions
Bioinformatic analysis
C
SILAC/competition
Light label
Heavy label
Lysis
Lysis
Compound
Incubation
Wash elution
SDS-PAGE
Proteolytic digest
LC-MS/MS analysis
m/z
Bioinformatic analysis
Markup Area
Area

Figure 8: Affinity chromatography using stable isotope labeling and quantitative mass spectrometry.[144] **A**. Competition approach employing ICAT: two similar cell populations are treated either with the active (red) or the inactive (gray) molecule respectively. After affinity purification with either active compounds or inactive compounds and elution of target proteins, both set of proteins are differently modified on their cysteine residues using the ICAT labeling technology and digested. Labeled-peptides are isolated form the mixture by incubation with avidin beads, and then cleaved to remove biotin part. The distinction between their ICAT tags permits their quantification by mass spectrometry. **B**. Competition approach employing ITRAQ: Cell populations are cultured and used for preparing proteomes (lysis) which is incubated with mixed-kinase inhibitors matrix ('kinobeads'). Immobilized kinobeads are incubated with the lysate in presence of free compound as competitor to enrich the binding proteins. Proteins are isolated from the mixture, separated by SDS-PAGE, digested by trypsin and followed by four-channel iTRAQ labeling of obtained peptides, followed by analysis using LC-MS/MS. **C**. Competition approach employing SILAC: Two cell populations are cultured heavy or light stably isotope-labelled amino acids and used for preparing labelled proteomes. Immobilized active compound is incubated with the labeled lysates in presence or absence of free compound as competitor to enrich the

binding proteins. Labeled-proteins are isolated from the mixture, separated by SDS-PAGE, digested by trypsin and followed by analysis using LC-MS/MS.

1.2.1.3 Expression-cloning-based methods

Expression-cloning methods including phage display, ribosome and mRNA display, yeast three-hybrid systems for target identification and drug-western method developed to increase the concentration of target proteins which might be useful for targets with low-expression in cells. Phage display, ribosome and mRNA display, yeast three-hybrid systems are described in detail in below.

1.2.1.3.1 cDNA phage display

Phage display has been an important tool for both basic research and drug discovery from 1985.[145] In this methodology, peptides or proteins are displayed on the surface of phages and are used to select specific interacting peptides and proteins with high affinity.[146-149] Phage display was originally developed for the filamentous phage M13 for the generation of antibody libraries to select the specific target of an antigen.[145] Later it was used to identify protein interaction partners,[145] and it is also useful to identify drug-binding proteins (**Figure 9).** Several experiments hat employed phage M13 displaying peptides or protein libraries to identify the target of small molecule were successful.[150-155] Further, a phage display system based on the bacteriophage T7 has been developed.[156] This approach is easy to use and can display peptides up to 50 amino acids in high copy number (415 per phage), and proteins up to 1200 amino acids in low copy number approximately 1 per phage of 10%-100% phages in population).[156] For example, Jung *et al.* have successfully used T7 phage displayed cDNA library to identify the protein UQCRB (Ubiquinol-cytochrome c reductase binding protein) as a target of terpestacin. Furthermore, this target was validated using surface plasmon resonance (SPR) to monitor the binding of UQCRB to terpestacin.[157]

In order to display potential target proteins on the surface of the phage, a library of DNA sequences is cloned into the phage genome as a fusion to the gene coding coat protein of the phage. This phage library is infected and amplified in bacterial cells until host cell lysing and collected the amplified-phage library and then exposed to the immobilized small molecule, resulting in the capture of phages that have the appropriate affinity for the drug molecule. Non-binding phages are washed off, and the binding phages are eluted and transfected into bacterial host cells for amplification. This amplified phage population is greatly enriched in phages which display proteins that bind to the small molecule. After iterative rounds of affinity enrichment, a monoclonal phage population can be selected, and then DNA isolation and sequencing are used to identify the binding protein based on sequence-similarity searches.

A significant advantage of phage display over other display methods such as mRNA display or drug western is that the iterative amplification steps allow the identification of low-abundant targets and of low-affinity targets. Evaluating the results after early selection rounds might be useful for the identification of additional binding proteins, given that the specific target will be increased during the rounds of selection.[158] Then, once the affinity selection process is completed, clones that express high-affinity proteins will largely dominate in population. Low abundance clones which are reduced following several affinity selection rounds will disappear in population. This affinity selection explains why several targets with lower affinity might be lost during the selection cycles.[116]

There are some limitations for this method due to several reasons. Phage display cDNA libraries do not code for the entire protein and the binding region of a small molecule might not be displayed or not properly folded. Moreover, cloned cDNAs might contain untranslated mRNA regions or might not be in-frame resulting in an early termination of translation or in the generation of non-natural proteins. Additionally, phage display will not be an appropriated method, when a complex composed of two or more proteins is needed for the binding to the small molecule.[159] Another issue associated with this approach is the lack of posttranslational modifications of proteins (PMT) Phage display will not be an appropriated method for target ID in case PMT is needed for the binding of the small molecule to its target protein.[116]

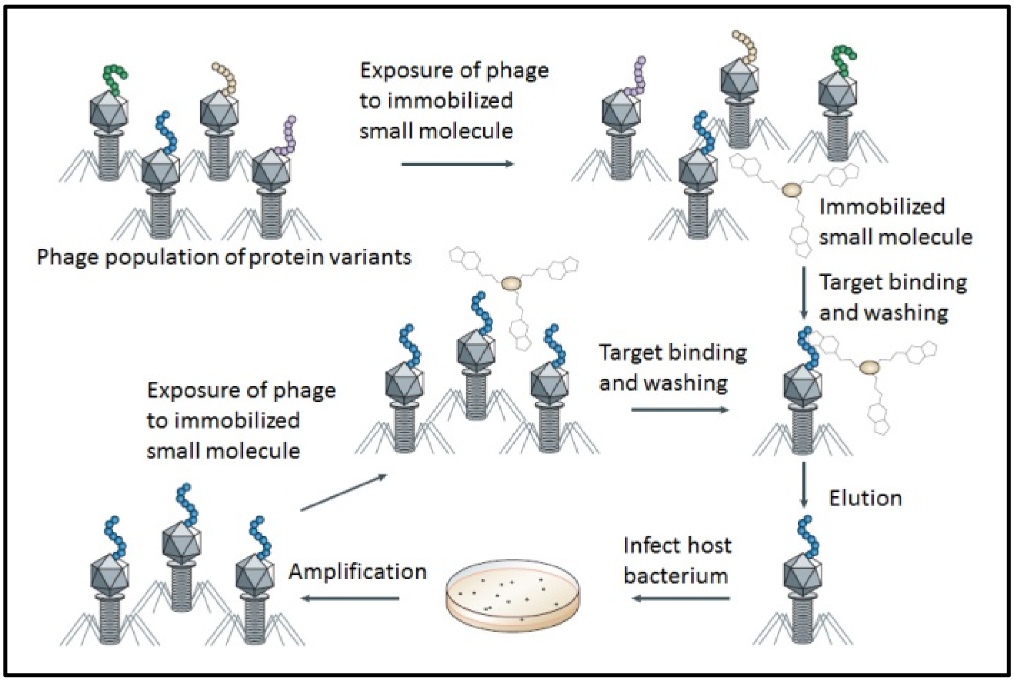
Exposure of phage
to immobilized
small molecule
Phage population of protein variants
Immobilized
small molecule
Target binding
and washing
Exposure of phage
to immobilized
small molecule
Target binding
and washing
Elution
Infect host
bacterium
Amplification

Figure 9: Phage display for target identification. A phage population displaying potential target proteins on their surface is exposed to an immobilized small molecule. After each cycle of affinity selection, the eluted phage population is amplified and subjected to further rounds of affinity enrichment. At the end of the procedure, the monoclonal phage population can be analyzed using sequencing of to identify the target proteins.[116]

1.2.1.3.2 Ribosome and mRNA display

Ribosome and mRNA display are known as *in vitro* technique to study protein-protein interactions.[160] The principle of ribosome display is transcribed DNA into mRNA which can be translated into peptides or proteins *in vitro*. Ribosome display is a method which allows *in vitro* translation and selection for proteins and peptides from large libraries. The DNA library coding for library of binding proteins is fused to a spacer sequence lacking a stop codon which allows the stabilizing the complex consisting of the ribosome, the mRNA and the nascent polypeptide during *in vitro* translation.

The advantage of the method is that diversity of the library does not depend on the transformation efficiency of bacterial cells and just depends on the number of ribosomes and different mRNA molecules present in the test tube which can be controlled and random mutations can be introduced easily after each selection round. Therefore, diversity of the library brings the evolution of binding proteins over several generations and this selection of peptide or proteins from libraries is the coupling of genotype (RNA, DNA) and phenotype (protein). Such complexes can be stabilized and directly used for selection of target proteins binding to immobilized compounds for target identification. mRNA that is incorporated in bound mRNA-ribosome-protein complexes is purified, then reverse transcribed and used for selection experiments. The DNA strand is recovered from the complementary mRNA and amplified by PCR.[161]

mRNA method was initially developed to increase the number of peptides displayed in the phage display method for *in vitro* protein selection.[162] This method is similar to ribosome display, but it is modified by ligation of puromycin to mRNA (**Figure 10**). For example, mRNA display has been used to identify the target of tacrolimus (also FK-506 or fujimycin), an immunosuppressive drug.[159] McPherson *et al.* could achieve a successful selection of full-length FKBP12, a ubiquitous receptor of FK506, and they could identify proteins which were further confirmed as target proteins by an *in vitro* protein binding assay.[159]

mRNA display offers several advantages over ribosome display. The covalent mRNA–protein complexes are generated by ligation of a DNA linker with a small adaptor molecule (puromycin) to reduce non-specific binders in the selection cycle.[162] In addition, very large libraries of up to 10^{13} different proteins can be generated in a single tube. The sequence complexity is 10^{4}-fold superior to that of phage display and 10^{6}-fold superior to that of yeast display or yeast two- or three-hybrid systems.[162] This approach can be used to create mRNA-display libraries bearing an unnatural amino acids residue. Furthermore, mRNA appears to improve the solubility of the attached protein, enabling functional selection of sequences that can aggregate or are only partially soluble when naturally expressed.[163] One of the issue and therefore limitation of mRNA-display is that full-length translation rarely happens. Therefore, normally polypeptides with relatively short chain lengths (10–110 amino acids) have been used. Synthesis products resulting from an incomplete translation are very likely not to be folded properly, and consequently, to bind nonspecifically.[163]

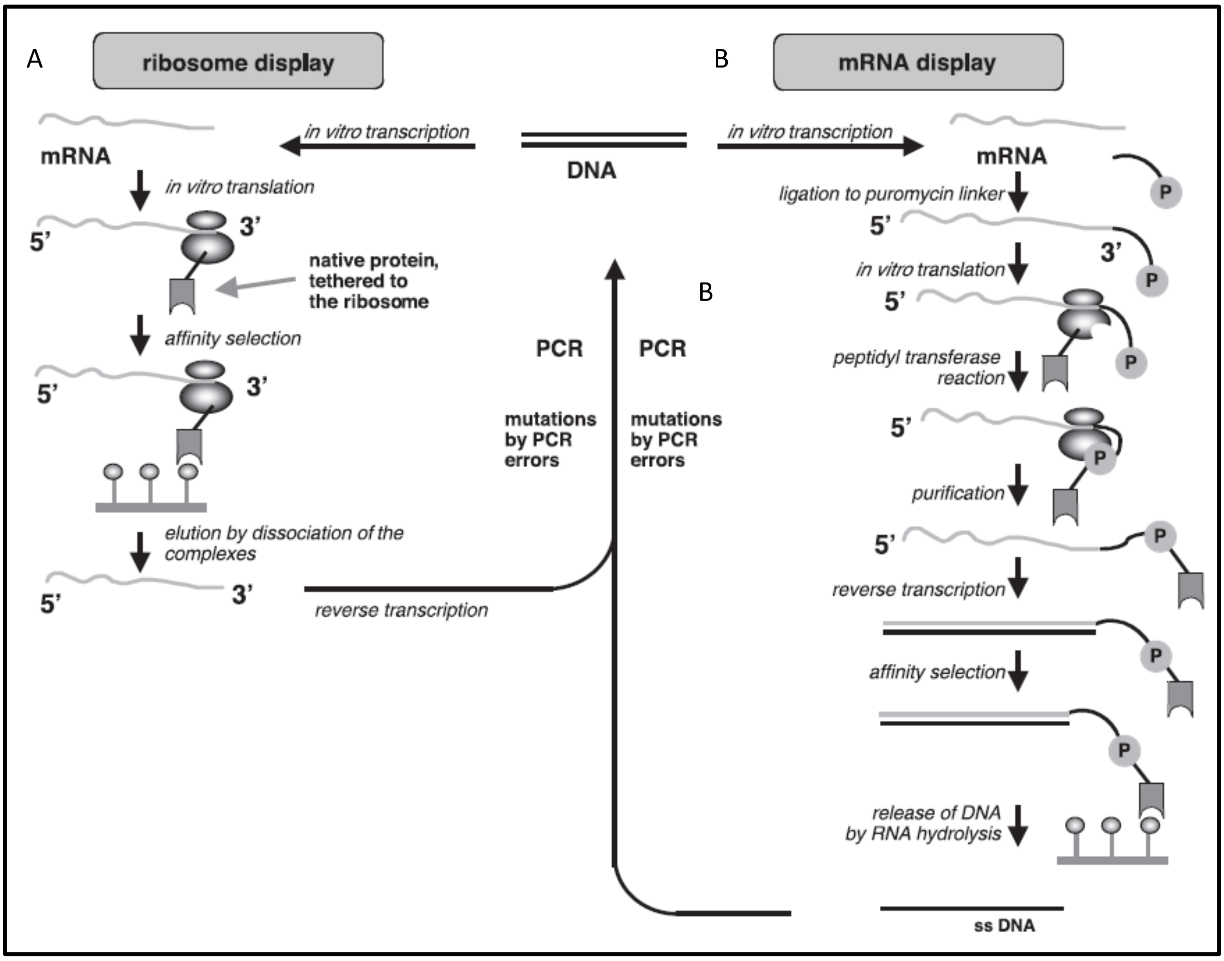
A
ribosome display
B
mRNA display
in vitro transcription
in vitro transcription
DNA
mRNA
mRNA
in vitro translation
ligation to puromycin linker
P
5'
3'
5'
3'
native protein, tethered to the ribosome
in vitro translation
B
5'
affinity selection
PCR
PCR
peptidyl transferase reaction
5'
3'
mutations by PCR errors
mutations by PCR errors
5'
purification
elution by dissociation of the complexes
5'
5'
3'
reverse transcription
reverse transcription
affinity selection
release of DNA by RNA hydrolysis
ss DNA

Figure 10: Ribosome and mRNA display for target identification. A. Ribosome display. DNA is transcribed *in vitro into mRNA*. Given that mRNA lacks a stop codon to maintain the peptide or protein in complex of translation, so mRNA–ribosome–protein complexes are formed during *in vitro* translation. Such complexes can be stabilized and directly used for selection of target proteins binding to immobilized compounds. mRNA that is incorporated in bound mRNA-ribosome-protein complexes is purified. And reverse transcribed and used for selection experiments. The DNA strand is recovered from the complementary mRNA and amplified by PCR. **B**. mRNA display. Covalent mRNA–protein complexes are generated by ligation of a DNA linker that is coupled to a small adaptor molecule, puromycin, to the *in vitro*-transcribed mRNA, which lacks a stop codon. The mRNA is translated *in vitro*, and the ribosome stalls at the RNA–DNA junction. Puromycin then binds to the ribosomal A-site, and the nascent polypeptide is thereby transferred to puromycin (puromycin as an aminoacyl-tRNA). The resulting covalently linked mRNA–protein complex is isolated, reverse transcribed and used for selection experiments. The DNA strand is recovered from target-bound complexes by hydrolyzing the complementary mRNA at high pH and is then amplified by PCR.[162]

1.2.1.3.3 A yeast three–hybrid system

Yeast three-hybrid system (Y3H) which has been developed by Liu *et al.*[164,165] is a newly developed method for target identification, which has be modified from the yeast two-hybrid technology.[166] In this system, one hybrid protein contains a DNA-binding domain fused to a ligand-binding domain (for example, dihydrofolate reductase DHFR) and the other contains a transcriptional activation domain fused to a protein encoded by a cDNA library that includes potential target proteins. The third hybrid is a small molecule that is covalently linked to a ligand (for example, methotrexate which will bind to DHFR) in order to connect the first hybrid with the second. A successful interaction of the three hybrid components will generate a trimeric complex. Formation of such a complex will result in the activation of a reporter gene leading to the generation of a signal which can be monitored. Cells expressing the reporter gene are selected, and then their DNA extracted and sequenced allowing the identification of the target proteins by sequence-similarity searches (**Figure 11**). The yeast three-hybrid system has been successfully used to identify the targets of the kinase inhibitor purvalanol B and identified cyclin dependent kinase such as CDK2 and casein kinase 1 (CK1 or CSNK1) as its targets.[167] All targets were subsequently confirmed using enzymatic kinase assay, affinity purification and immunoblotting experiments.[167]

The advantage of the yeast three-hybrid system over other expression-cloning approaches is that the interaction between a small molecule and a target protein occurs in intact cells rather than *in vitro*. In addition, yeast can be manipulated easily using modern robotics and automation technology. Like all technique, there are also some problems usually associated with this technique such as variability in activation domain (AD)-fusion protein expression, the folding of the target proteins, low affinity of the AD-fusion protein for the small molecule and low abundance of presented cDNA in library.[116,168]

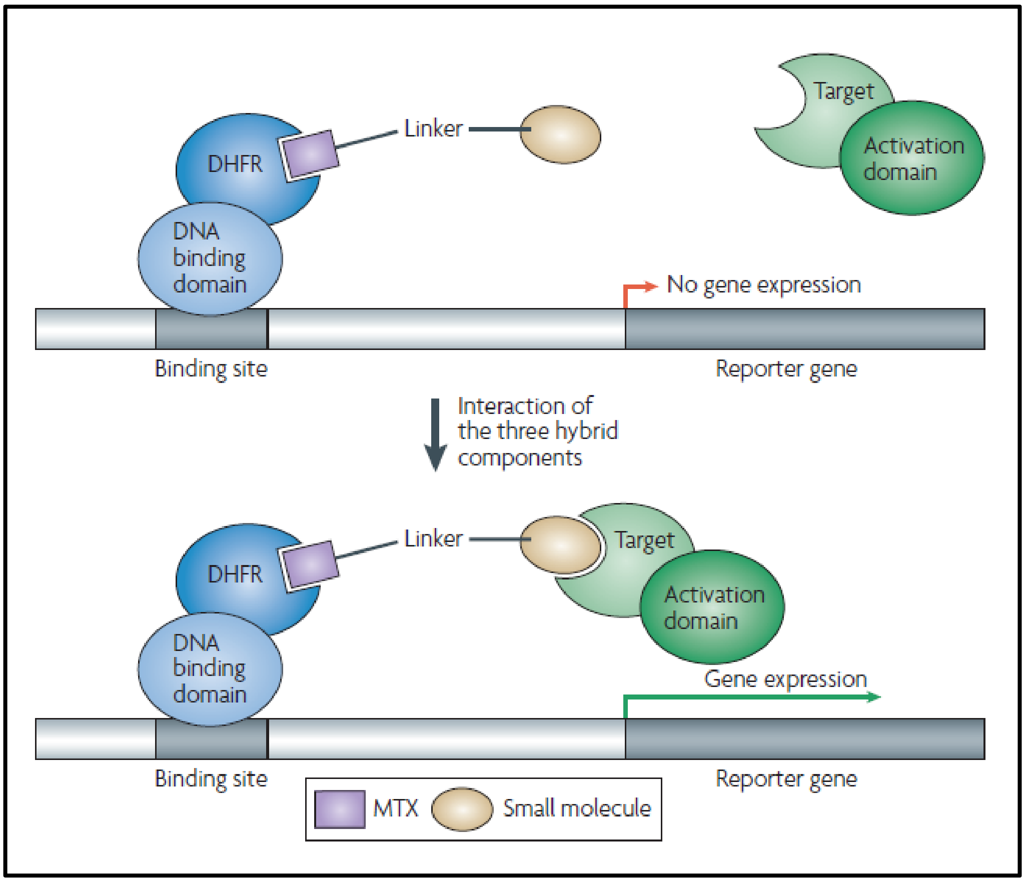
Target
Activation domain
DHFR
Linker
DNA binding domain
No gene expression
Binding site
Reporter gene
Interaction of the three hybrid components
DHFR
Linker
Target
Activation domain
DNA binding domain
Gene expression
Binding site
Reporter gene
MTX
Small molecule

Figure 11: Yeast three-hybrid systems for target identification. This system comprises one hybrid that consists of a DNA-binding domain fused to a ligand binding domain (e.g. DHFR: dihydrofolate reductase), one hybrid that consists of a ligand molecule (MTX: methotrexate) linked to a small molecule, and one hybrid that consists of a transcriptional activation domain fused to a protein from a cDNA library. The binding of the small molecule to its target protein results in the interaction of the three hybrid components, which leads to the formation of a trimeric complex. This complex then activates the expression of a reporter gene, providing a method for detection of the interaction.[116]

1.2.2 Target validation

Target validation plays an important role in chemical biology. Target proteins must be validated by further analysis to remove potential false-positive proteins.[116] The development of protein databases has proven very useful tool distinct between positive and false targets. This can be done by literature search for the protein function.[169,170] Various methodologies have been developed to quantify the binding of a small molecule to its target such as the surface plasmon resonance (SPR) in solution,[26,157] or SRS on surface.[107] The binding affinity can also be determined by fluorescence polarization[18] or by enzyme-linked immunosorbent assay (ELISA)[78] or by microscale themophoresis.[171,172] Conformational changes resulting from the binding of the small molecule to the target protein can be monitored by circular dichroism CD spectroscopy or fluorescence-based thermal shift assays. Thermal stabilization of the protein upon ligand binding is determined and used to binding affinity.[173] Confirmation of a protein as a target can also be achieved employing competition with the unmodified compound during affinity purification or by means of after the pulldown and detection of the protein in immunoblotting.[26] Fluorescence lifetime imaging microscopy (FLIM) is useful to investigate the specific binding of target protein and small molecule in cells.[25,174] In addition, knockdown of the target gene may copy the phenotype that is caused by the small molecule. After gene knockdown less compound may be required to produce a certain phenotype. In analogy to this, overexpression of the target gene may render cells resistant towards the compound. Alternatively, overexpression of the target gene may require higher amount of compound to induce a given phenotype.[116]

1. 3 The cytoskeleton, cell cycle and M-phase

1.3.1 Cytoskeleton

The network of filamentous proteins in cells which remain insoluble when the membrane is disrupted by detergents is generally called the cytoskeleton. The cytoskeleton is composed of microfilaments, intermediate filaments and microtubules.[175]

1.3.1.1 Microfilaments (actin filaments)

One main component of the eukaryotic cytoskeleton is filamentous actin (F-actin). Actin is the most abundant protein in many eukaryotic cells. In 1942, Straub isolated monomeric actin, as a globular actin also called G-actin which is an ATP binding protein.[176,177] G-actin is unpolymerized form of actin and F-actin is the polymerized form of actin.[178] Microfilaments are linear polymers of G-actin with a diameter of 7-8 nm. The globular monomer polymerizes into filamentous actin (F-actin or filament). The polyelectrolyte nature of F-actin is likely to be relevant for its interaction with membrane phospholipids. The filament has polarity (plus (+) and minus (-) end) and the polymerization of actin occurs at high rates at the (+) end of the F-actin polymer. This polymerization requires the presence of actin monomer at high concentration and ATP. The polymerization of actin *in vivo* causes the hydrolysis of one actin-bound ATP for each subunit added to the filament.

Actin filaments are major cytoskeletal structures to form cell morphology, so characteristic shapes of cells are supported by the actin cytoskeleton. During mitosis, Actin cytoskeleton is reorganized to form rounded cells and then is re-established after mitosis, so that allows cells to recover their shape. The network of actin filaments is not only important in cell shape but also in cell cycle progression, mitosis and regulatory interactions such as cytoskeleton signaling, cell–cell/cell–matrix adhesions.[179] Actin filaments provide the basic infrastructure for maintaining cell morphology and functions such as adhesion, motility, exocytosis, endocytosis, and cell division. Alterations of actin polymerization, or actin remodeling, plays a pivotal role in regulating the morphologic and phenotypic events of a malignant cell.[180]

1.3.1.2 Intermediate filaments

Intermediate filaments (IFs) are thicker than microfilaments and thinner than microtubules. They are approximately 10 nm in diameter and reach from the plasma membrane to the nucleus. Intermediate filaments are formed from polymers of fibrous proteins and their subunit proteins are members of the large and evolutionarily unrelated K-M-E-F (keratin, myosin, elastin, and fibrinogen) group of protein.[181] Whereas actin and tubulin are acidic proteins, different intermediate filament proteins can be either acidic or basic. Several eukaryotic cells do not contain intermediate filaments at all (for example, IFs were found in neurons and epithelial, glial, and connective tissue cells (fibroblasts) but not in muscle cells in case of the Mollusca Helix.[181] Polymerization of IF does not require nucleotide hydrolysis or any other obvious irreversible reaction. The kinetics of their assembly and disassembly appears to be quite different and much slower than those of actin filaments or microtubules. IF-associated proteins that control IF polymerization have been less thoroughly studied compared to mitogen-activated protein MAPs or actin binding proteins.[182,183] IFs are one component of the eukaryotic cytoskeleton. Ifs are contributed in the network of cytoskeleton by their interactions with microtubule, microfilament, and cytoplasmic face of the plasma membrane.[181]

1.3.1.3 Microtubules

Like actin, tubulins are abundant cytoskeletal proteins. Microtubules are much stiffer than actin filaments. They are important for cell shape, cell division and cell motility. Microtubules

(MT) are composed of α/β-tubulin heterodimers which are similar proteins of approximately 55 kDa each. A microtubule consists of 13 protofilaments which form hollow cylinders of approximately 25 nm diameter and they can be more than 100 µm long (**Figure 12A**). Protofilaments are polymers of linearly arranged α/β heterodimers. The walls of the microtubule are composed of linear protofilaments arranged in parallel. The polarity of the tubule is created by the α/β axis with the β-tubulin at the (+) end and α-tubulin at the (-) of the microtubule. Tubulin is a GTP-binding protein and GTP is required for tubulin polymerization. GTP binds to both α- and β-tubulin, but affinity α - and β-tubulin for GTP is different. When GTP is depleted and subunits at the end of a microtubule are GDP-bound, the microtubule will rapidly disassemble.[184]

Microtubules are nucleated and organized by microtubule organizing centers (MTOCs), such as the centrosome. Microtubule nucleation is a process of several tubulin molecules interact to form microtubules (for example of microtubule nucleation in purified tubulin is shown in **Figure 12B**. *In vitro*, microtubule nucleation is enhanced by addition of γ-tubulin or complex of γ-tubulin. In living cell, microtubule nucleation occurs on centrosome and is mediated by complex of γ-tubulin.[185]

Dynamics of MT depends on the assembly and the disassembly at the (+) end of a microtubule and determines the switch between growing and shrinking phases in this region (**Figure 12C).** During MT polymerization, both α- and β tubulin of the tubulin dimer are bound to one molecule of GTP. α-tubulin bound GTP and plays a structural function. However, GTP bound to β-tubulin can be hydrolyzed to GDP shortly after assembly with the microtubule. GDP-bound tubulin is a factor for MT depolymerization. Tubulin can be added onto the (+) end of MT only in the GTP-bound state which protect MT from disassembly.[186-188] Microtubule stability, structure and polymerization are also affected by microtubule associated proteins (MAPs) and post-translational modifications of microtubules. For instance, MAP can increase the rate of MT polymerization *in vitro*.[184,189,190]

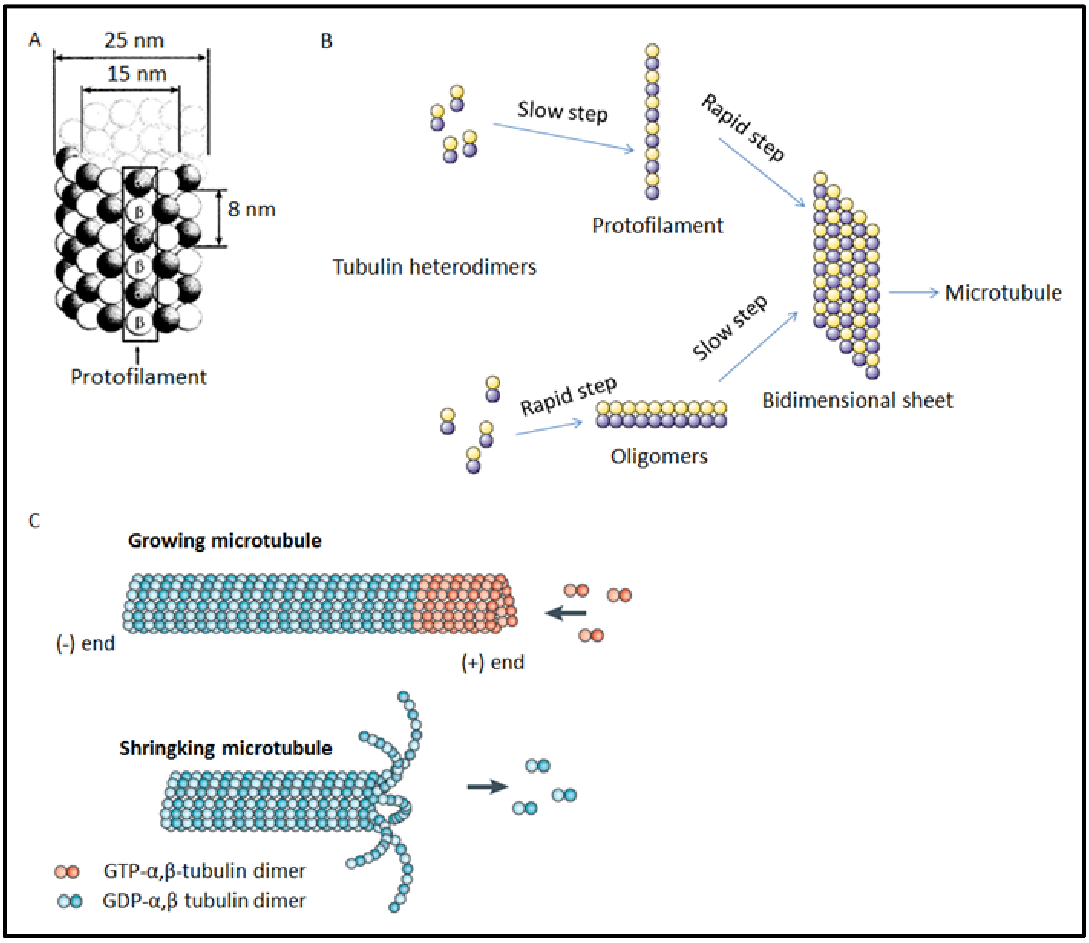
A
25 nm
15 nm
8 nm
β
Protofilament
B
Slow step
Rapid step
Protofilament
Tubulin heterodimers
Microtubule
Slow step
Rapid step
Bidimensional sheet
Oligomers
C
Growing microtubule
(-) end
(+) end
Shringking microtubule
GTP-α,β-tubulin dimer
GDP-α,β tubulin dimer

Figure 12: Microtubules structure and dynamics. A. Structure of microtubules.[191] **B**. Microtubule nucleation in purified solution (adapted from Job *et al.*).[185] Tubulin heterodimers aggregate to form either protofilament (which reaction is slow) or oligomeric tubulin. Tubulin sheet and micrptubule can be formed rapidly from protofilament or slowly from oligomeric tubulin.[185] **C**. Microtubule dynamics in state growing and shrinking microtubule (adapted from Howard *et al.*).[192] GPT-tubulin at the (+) end of microtubules (GTP cap) stabilizes growth phage of microtubules. So microtubules are stable by polymerization (adding) of GTP-tubulin (as growing microtubule). Microtubules are unstable if GDP at the (+) end of microtubules (GDP cap). Microtubules with GDP cap are rapidly depolymerized (as shrinking microtubule).[192]

Microtubules are intracellular filaments as one of three major cytoskeletal components in eukaryotic cells, which are important for cell division, cell transport, cell motility, chromosome movement, maintenance of cell shape and form.[193,194] Microtubules play a role in mitotic spindle function, mitosis and replication of cells since microtubule dynamics is inhibited, chromosome congression and segregation cannot occur.[191,195]

In interphase of endothelial cells, the microtubules are dynamic polarized structures, and during cell migration, plus ends of the microtubule polymers are fast-growing and interact with several proteins which modify the MT stabilize.[195,196,] In contrast, ends of the microtubule are normally stabilized through contact with the perinuclear microtubule organizing center (MTOC) which is known as the centrosome in interphase cells (**Figure 13A**) in vertebrates and spindle pole body (SPB) in fungi, [196] or spindle poles in mitotic cells (**Figure 13B**).[197]

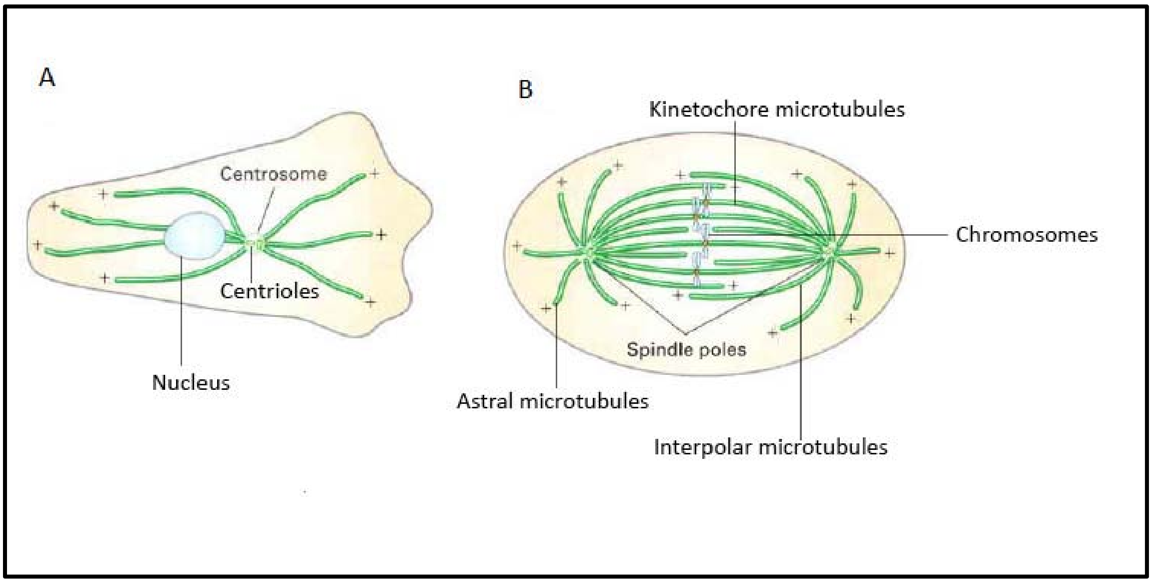

Figure 13: Microtubules are assembled from microtubule organizing centers (MTOCs) (adapted from Przewloka *et al.*).[198] **A**. An interphase cells, the MTOC is called a centrosome. **B**. A mitotic cell, two MTOCs are called spindle poles and microtubule (MT) network (microtubule spindle) as kinetochore MT, astral MT and interpolar MT.[199]

1.3.2 Cell cycle

Cell division consists of two mainly processes which are DNA replication and segregation of replicated DNA into two daughter cells.[200] The cell cycle of eukaryotic cells morphologically can be divided into mitosis (known as dividing phase) and interphase (known as growing phase).[201] The mitosis contains prophase, prometaphase, metaphase, anaphase and telophase (see detail in section 1.3.3). The interphase includes G1, S and G2 phase.[200] In S phase, cell is synthesizing DNA.[201] G1 and G2 phases are considered as gaps which occur between DNA synthesis (S phase) and mitosis (M phase) of cell cycle.[201] The first gap, the G1 phase, is a main stage which permits the cell progression enter either a new cell division or a resting state (Go).[202] The G1 phase also plays the role in preparation for DNA replication[200] and control DNA integrity before the onset of DNA replication.[202] Another gap, the G2 phase is preceded by S phase and followed by M phases. In G2 gap, cell prepares for mitosis by checking the completion of DNA replication and the genomic integrity before cell enter mitosis. Thus, G1 gap and G2 gap which are considered as are two cell-cycle checkpoints regulate the cell-cycle transitions (G1–S and G2–M) and DNA replication correctly before allow the cell entering the cycle of cell division.[202] When cells are in Go phase, cells are accounted for the non-growing and non-proliferating cells.[200] After cell division, two daughter cells with the same genetic material as the parent cell are produced. It represents the DNA segregation (mitosis) and the following separation of the cytoplasmic content (or cytokinesis) which terminates into the generation of two daughter cells.[201,203]

The cell cycle is regulated by several checkpoints and cyclin-dependent kinases (CDKs) and their regulatory proteins including cyclins, CDK inhibitors (*e.g.* p16, p15 and p18 which are belong to INK4 family or p21, p27 which are belong to CIP/KIP family, p53), CDK activating kinase (e.g.CDK7/cyclin H) and Cdc25 phosphatase.[204] Cyclin-dependent kinases (CDK) are the motor of cell cycle and regulate the transition from one phase of the cell cycle to the next. CDKs need an appropriate cyclin protein for activation. When activated, CDKs induce downstream processes by protein phosphorylating.[205]

Different cyclins are required at different phases of the cell progression. In G1 phase, cyclin D binds to kinase CDK4 and CDK6 to form cyclin D-associated kinase CDK4 and CDk6 complexes, as well as cyclin E binds CDK2 to form cyclin E–CDK2 complexes and these complexes can phosphorylate pRb (retinoplasma protein) leading to releasing E2F which transcripts the necessary genes needed for G1 to S transition in cell cycle progression.[201,204] Cyclin A binds to CDK2 to form complex which is required during S phase.[206] Cyclin A complexes with CDK1 promote entry into the late G2 and early M phase. Mitosis is further regulated by cyclin B in complex with CDK1 (**Figure 14**).[207,208]

During cell cycle progression (**Figure 14**), cells are in quiescent phase (Go) and they can enter the cell cycle by controlling of restriction point which is dependent on the external stimuli (e.g. nutrients or mitogen activation).[204] Another checkpoint which is replication checkpoint regulates the cell progression through S phase and ability of cells entering M phase.[204] This checkpoint is related to DNA-damage and DNA replication including the activation of ATM (Ataxia telangiectasia mutated), ATR (Ataxia-telangiectasia-mutated and Rad3-related), DNA-

PK (DNA-dependent protein kinase) kinases with following by activation of Chk1 an Chk2 and results in either DNA repair or cell cycle arrest or apoptosis (the results is dependent on the extent of DNA damage).[204]

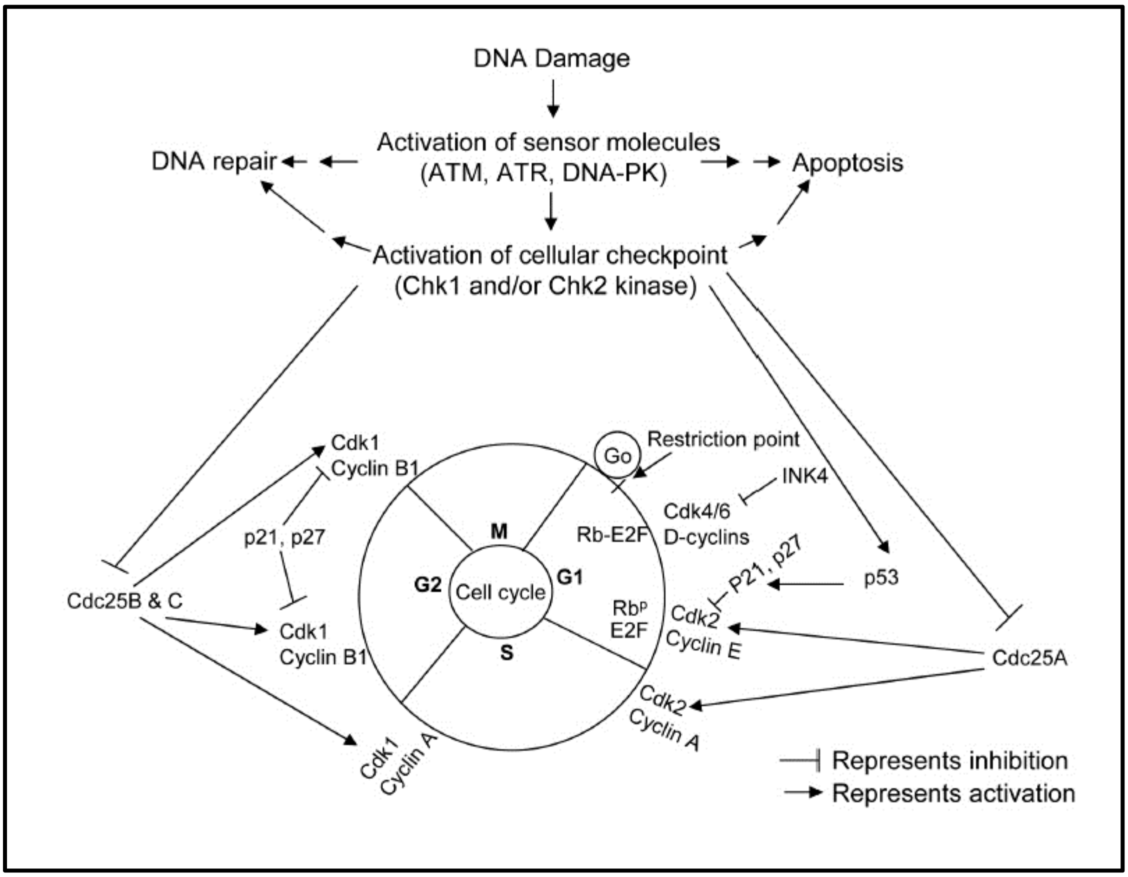
DNA Damage
Activation of sensor molecules
(ATM, ATR, DNA-PK)
DNA repair
Apoptosis
Activation of cellular checkpoint
(Chk1 and/or Chk2 kinase)
Cdk1
Cyclin B1
p21, p27
Cdc25B & C
Cdk1
Cyclin B1
Cdk1
Cyclin A
M
G2
Cell cycle
G1
S
Go
Restriction point
INK4
Rb-E2F
Cdk4/6
D-cyclins
P21, p27
p53
Rbp
E2F
Cdk2
Cyclin E
Cdc25A
Cdk2
Cyclin A
Represents inhibition
Represents activation

Figure 14: Cell cycle regulation involving cyclins-CDKs-CDK inhibitors, Cdc25 phosphatase, cellular checkpoint and DNA damage sensors.[204] The cell cycle consists of four phases. The G1 phase is needed for cell growth. During the S-phase, DNA is synthesized. G2-phase is a further phase of cell growth and cell prepares for mitosis. M-phase consists of mitosis and cytokinesis. The cell cycle is regulated by several checkpoints and cyclin-dependent kinases (CDKs) and their regulatory proteins including cyclins, CDK inhibitors including INK4 family or CIP/KIP family (e.g. p21, p27) and p53, or CDK activators Cdc25 phosphatase.

1.3.3 M-phase (mitosis and cytokinesis)

In vertebrate cells, mitosis is normally subdivided into five stages. After DNA replication in interphase, the sister chromatids are held together by cohesins.[209] In the first stage, prophase, replicated DNA of interphase condenses into well-created chromosomes.[210] The duplicated centrosomes migrate to opposite ends of the cell which form the spindle poles and at the same time the bundle of microtubules (mitotic spindle) which are required for cell division begin to form[191] and extends from the centrosome (nucleating dynamic microtubules). Inside the nucleus, the nucleolus also disappears from view for next state staring of prometaphase (**Figure 15A**).[210] In prometaphase, the spindle microtubule attach to chromosome (sister chromatids) at the kinetochores of center chromosome which is complexes of proteinaceous structures (**Figure 15B**). The interaction of mitotic spindle and paired sister chromatids is bipolar and stable that help to segregate the attached sister chromatids to opposite poles. The bipolar attachment is formed by microtubule bundles emanating from opposite poles of spindle.[210] Prometaphase ends for starting metaphase when all chromosomes bind to spindle and migrate to an equatorial plane, the metaphase plate. During metaphase, all the chromosomes maintain on the spindle until they undergo bipolar attachment. After all chromosomes are on bipolar attachment, cohesion of sister chromatids is lost[210] since the complexes of sister chromatids and cohesins are disrupted via the proteolytic cleavage of cohesion subunit (Scc1)[209] to separate sister chromatids that triggers by a caspase-related activity of separase at the onset of anaphase. Separase is inhibited by securin, which associates with separase in most of cell cycle**.**[209] In anaphase, sister chromatids are then attached the spindle and move to the poles (anaphase A) and the spindle poles themselves also migrate further to the cell cortex (anaphase B). Finally stage of mitosis, telophase, the separated chromosomes are at the poles and spindle disassemble. Nuclear envelopes reform around the decondensing chromosomes and ending of mitosis.[210] Further, process of M-phase for cell division, cytokinesis, cytoplasm which is remained surrounding the nuclei begins divides for nuclear partition and giving two new daughter cells.[191]

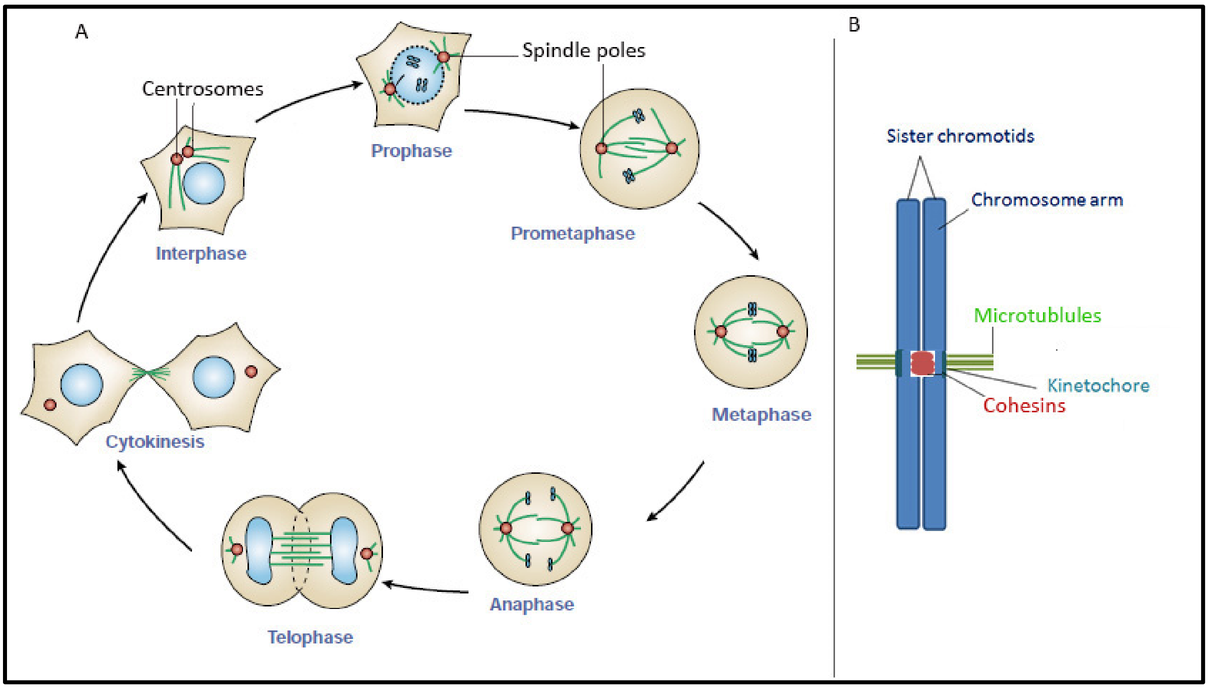

Figure 15: Stages of mitosis. **A.** Process of five stages in mitosis: prophase, prometaphase, metaphase, anaphase and telophase (adapted from Nigg *et al.).* DNA is shown in blue, microtubules in green and spindle poles in orange.[210] During prophase, replicated DNA condenses into well-created chromosomes and migrates to opposite ends of the cell which form the spindle poles. At the same time, the nucleolus also disappears from view for next state staring of prometaphase. In prometaphase, the spindle microtubules attach to chromosomes at the kinetochores. During metaphase, all the chromosomes maintain on the spindle until they undergo bipolar attachment. In anaphase, sister chromatids are then attached the spindle and move to the poles. The spindle poles themselves also migrate further to the cell cortex. In telophase, the separated chromosomes are at the poles and spindle disassembles. Nuclear envelopes reform around the decondensing chromosomes and ending of mitosis. Finally of M-phase, cytokinesis, cytoplasm divides for nuclear partition and giving two new daughter cells. **B**. Schematic of a bi-oriented chromosome and localization of kinetochore (adapted from Musacchio *et al.*). The sister chromatids are held together by cohesins and kinetochore is located at the site of microtubule and chromosome interaction.[209]

1.4 Cancer and cancer inhibitors

1.4.1 Cancer

Cancer occurs as a result of a disturbed balance between cell growth and cell death. There are several factors causing cancer. Carcinogenesis is considered as a multistep process by genetic alterations which influence the cell growth and development[211] and result in an unrestrained cell proliferation.[200] Oncogenes are from cellular or from viral (infected into the cell by a virus) genes and their expression and activation can cause the development of cancer. Proto-oncogenes are normal cellular genes (e.g. *C-MYC*, *RAS*, *BCL2* or *MDM2* gene) and they can be conversed to oncogenes. Tumor suppressors (known as anti-oncogenes, e.g. *p53, pRb, E-cadherin*) are cellular genes.[212] When tumor suppressors are inactivated loading to the probability of tumor formation and restoration of their functioning may suppress the growth of tumor cells.[212] Thus, changes in expression of proto-oncogenes, oncogenes and tumor suppressor genes can cause carcinogenesis.[212] Dysfunction of their protein (products of their genes) results in abnormal regulation of signaling pathways which affect the cell cycle, apoptosis, genetic stability, cell differentiation, and morphogenetic reactions.[212]

In normal cells, proto-oncogenes express at different levels along the pathway to stimulate cell proliferation, but mutated proto-oncogenes or oncogene can induce the tumor growth.[200] In cancer, mutations usually occur in proto-oncogene and tumor suppressor genes. For example, mutation of tumor suppressor genes *p53* and *pRb* cause dysfunction of proteins leading to inhibition of cell cycle progression.[200] Additional, mutations or overexpression of genes encoding proteins which regulate cell signaling pathway such as cyclin, CDK, CDK-activating enzymes, CKI, CDK substrates, Cdc25 phosphatase and checkpoint proteins have been found in cancer cells.[200] For examples, mutation of CDK4 was observed in cancel cells (human melanoma),[213] or abnormal expression of cyclin D1 have been identified in human breast cancer,[214] or mutation of pRb (the main substrates for cyclin D-CDK4 and cyclin D-CDK6 complexes)[212] has been observed in human retinoblasma and lung cancer cells,[200] or overexpression of Cdc25 phosphatase (Cdc25A and B) have been observed in numerous human tumors.[204]

Oncogenes and tumor suppressors genes that regulate the cell cycle or cell proliferation are also related to apoptosis. Thus, inhibition of apoptosis may cause increasing cell number which manifest in cancer.[215] For example, p53 protein is a tumor suppressor protein (also a checkpoint protein which binds specifically to DNA sequence and is able to stimulate either cell cycle arrest or apoptosis at cell cycle checkpoint) encoded by the *p53* (*TP53)* gene.[200] This protein is an important transcription factor and has a role in apoptosis, development, differentiation, DNA replication, chromosomal segregation, genomic stability, and inhibition of angiogenesis.[216] p53 activates DNA-repair proteins upon DNA damage leading to arrest cells at the G1/S phase in order to provide time for DNA-repair proteins repairing the damaged DNA and allows the cell cycle to continue. Alteration or DNA damage in *p53* gene (mutated p53) causes cancer[216] and *p53* gene mutations are common in human cancers.[217]

Cancer cells consist of migration and invasion mechanisms which permit them to change position within the tissues.[218] The process of invasion and metastasis of tumor cells starts with local invasion, then intravasation by migration of primary tumor cells which enter lymphatic vessels or the bloodstream and transit of cancer cells through the lymphatic and hematogenous systems, followed by getting out of cancer cells from the lymphatic vessels into the parenchyma of distant tissues (extravasation). Further, small nodules of cancer cells (micrometastases) are formed and finally developed into macroscopic tumors as ′′colonization′′ for end of metastasis process of tumor cells.[219] The migration of cancer cells from the primary tumor cells can be either individual cells or collective migration (e.g. movement of cell sheets or cell clusters).[218] The metastasis of cancer is the most dangerous manifestation of tumor progression and the reason for deaths of oncological patients.[212]

1.4.2 Cancer inhibitors

1.4.2.1 Small molecules targeting microtubules

As described above (1.3.1.3), microtubules are filamentous cytoskeletal proteins and involved in the replication of cells. If microtubule dynamics is inhibited, chromosome congression and segregation cannot occur, so microtubules are considered as targets of several anti-cancer strategies.[220] As a consequence, cells cannot divide and hence the tumor cannot grow.[191] Because of the important roles of microtubules in cell motility, cell polarity and cell division, microtubules are a relevant target for in drug developmental programs of anticancer therapy for decades until now to treat cancer.[221-224]

Many small-molecule inhibitors of tubulin-and microtubule function were discovered[191] and many of them are antimitotic agents which bind microtubule dynamics and inhibit cell proliferation.[225] There are typically classified into two main groups containing the microtubule-destabilizing agents and the microtubule-stabilizing agents.[225] Currently, two mode of binding site of microtubule-destabilizing agents on tubulin which are well-known are the vinca site or the colchicine site. Vinca-site binders consist of the vinca alkaloids, the cryptophycins and the dolastatins.[225] Colchicine-site binders consist of colchicine and its analogues. Other microtubule-destabilizing agents bind to tubulin at a distinct site of either vinca site or colchicine site such as noscapine, hemiasterlin, estramustine, and, herbicides.[225] Most of the microtubule-stabilizing agents (e.g taxanes, paclitaxel and docetaxel) bind to taxoid-binding site on β-tubulin which is located on the inside surface of the microtubule, or to an overlapping taxoid-binding. The known binding sites are shown in **Figure 16A**.[225]

Due to microtubule dynamics, compounds that bind to tubulin heterodimers and inhibit tubulin polymerization also have effect on microtubules disassembling[186,226] (e.g. colchicine, vinblastine, vincristine, nocodazole). Colchicine is well-known a plant alkaloid that inhibits polymerization of tubulin and disrupts microtubules.[191] Furthermore, colchicine inhibits migration of a wide range of cell types.[191,227-229] Vinca alkaloids like vinblastine and vincristine are indole alkaloids found in periwinkle extracts.[191] Vinblastine and vincristine bind to one site on β-tubulin which is called vinca site (at a site distinct from the colchicine-binding site) and induce the destabilization of polymerized tubulin (**Figure 16A**).[191] The vinca alkaloids have been shown to inhibit cell migration which can be applied for cancer treatment.[230-232] Nocodazole is the most active synthetic benzimidazole derivative that destabilizes microtubules with a level of potency similar to that of the vinca alkaloids. Nocodazole is a competitive inhibitor of colchicine for binding to tubulin to colchicine (nocodazole is a colchicine site binder).[191] Nocodazole, like the other microtubule-disrupting drugs, inhibits animal cell motility.[233-235] On the other hand, small molecules that stabilize microtubules promote new microtubule assembly and lead to formation of unusual microtubule structures in cultured cells (e.g. taxol, epothilone B, eleutherobin).[236] Taxol (paclitaxel), a natural product from the Pacific yew Taxus brevifolia, stabilizes microtubules[237,238] and induces assembly of new microtubules,[239,240] leading to a reorganization of the microtubule network and formation of bundles of microtubules in cells.[236] Taxol is an antimitotic agent which is now clinically used to treat ovarian and breast cancer.[191] Some popular small molecules targeting microtubules are showed in **Figure 16B**.[229,238,241,242]

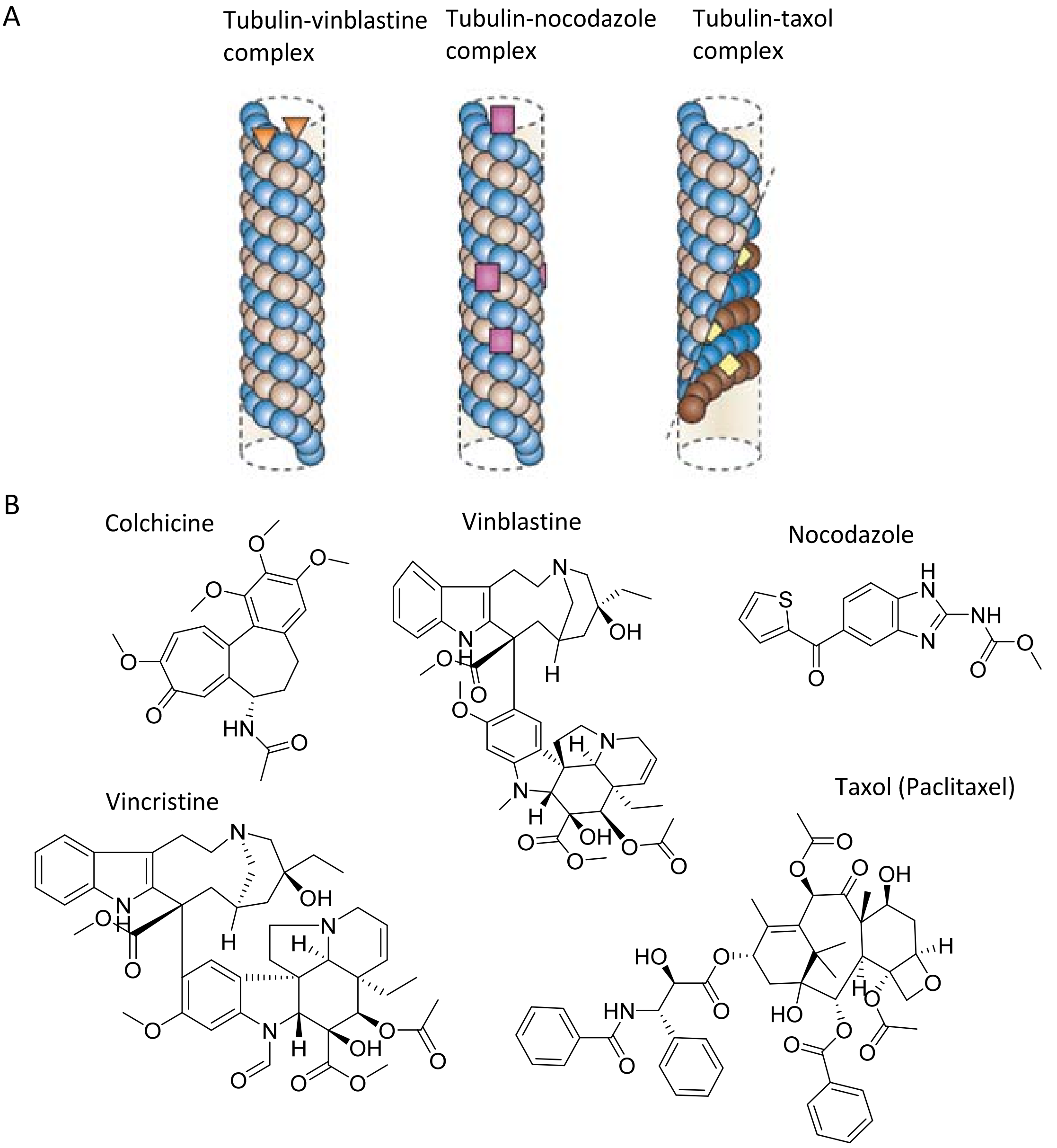
A
Tubulin-vinblastine complex
Tubulin-nocodazole complex
Tubulin-taxol complex
B
Colchicine
Vinblastine
Nocodazole
Vincristine
Taxol (Paclitaxel)

Figure 16: Microtubule agents. **A**. Binding sites of microtubule agents. For examples of vinca-site binders, vinblastine bind to microtubule ends (orange triangles) and colchicine binds to soluble dimers (purple squares). For an example of taxoid-site binder, taxol binds along the interior surface of the microtubule (yellow diamonds).[225] **B**. Structures of some popular microtubule agents.

1.4.2.2 Inhibitors of mitosis and cell cycle signaling

Tubulin and microtubule are known as targets of many antimitotic reagents and other protein targets can be targeted by small molecules which inhibit mitosis. For example, centrocountins which caused cell cycle arrest at the mitotic stage by targeting the centrosome-associated proteins nucleophosmin and Crm1.[25] Many proteins which are related to cell cycle signaling and regulate cell cycle have been considered as an ideal strategy for cancer therapy such as cyclin-dependent kinases (CDKs), cyclin-dependent kinases inhibitors (CKI), Cdc25 phosphatase, RAS and checkpoint proteins (e.g. p53) are potential targets.[208,243] For CDKs strategies, the catalytic activity of CDK can be inhibited directly or indirectly by overexpressing CDK inhibitors or decreasing the level of cyclin. Currently, the direct inhibition of kinase activity of CDK is most employed for development of cell cycle inhibitors.[208,244] For example, butyrolactone, a selective inhibitor of CDK1 and CDK2[245] inhibits phosphorylation of pRb and of histone H1 and then causes the cell cycle arrest at G1/S and G2/M.[246] Another example for CDK inhibitor, SU9516, analog of indolinoes (a novel 3-substituted indolinone) obtained from HTS with CDK2, inhibits the activity of CDK1, CDK2 and CDK4 and leads to apoptosis induction with cell cycle arrest G2/M in colon carcinoma cells (RKO and SW480 cells).[247] There are several CDK-selected- inhibitors are in clinical trial such as AT7519 (Aster) which caused Go-G1 phase and G2-M phase cycle arrest and resulted in cell apoptosis or flavopiridol (Sanofi-Aventis) which caused G1-S and G2-M phase cycle arrest and resulted in cell apoptosis.[244] Various Cdc25 phosphatase inhibitors have been reported in phase I clinical trials such as ARQ-501 for tumor treatment.[204]

RAS protein has been known as a regulator of the cell cycle,[248] so development of agents which inhibit RAS or RAS signaling pathways[26] are considered as promising. For example, palmostatin B inhibits depalmitoylation of RAS in cells by inhibiting the acyl-protein thioesterases (APT1) which affects RAS localization and signaling.[249,250,251] Many small molecules targeting RAS downstream effectors were developed including various MEK inhibitors such as PD 98059[252] and MEK/ERK inhibitor U0126 (abbreviations: MEK, mitogen-activated protein kinase kinase; ERK: extracellular signal-regulated kinase).[253] In RAS/mitogen-activated protein (MAP) kinase signaling, MEK/ERK is a signaling downstream of RAS since RAS in GTP-bound state will interact with RAF protein kinase which stimulates the MAP kinase kinase MEK, then MEK activates the MAP kinase ERK.[254] RAS Activation of ERK pathway causes increasing proliferative rate of tumor cells.[255] Another sample for development of drug discovery oncogenic RAS, small molecule deltarasin which targets PDEδ and inhibits the KRAS-PDEδ interaction impairs oncogenic KRAS signaling and suppresses *in vitro* and *in vivo* proliferation of KRAS-dependent human pancreatic ductal adenocarcinoma cells.[174]

p53 protein is tumor suppressor and tumor suppressor function can be impaired because of its mutation or mediators of p53 such as MDM2 (murine double minute 2)[256] or a homolog of MDM2, MDMX (known as MDM4 or HDM4 in human).[257] *MDM2* gene is a proto-oncogenic gene. MDM2 and p53 have an autoregulatory feedback to control each other.[258] p53 control the transcription of *MDM2* gene because *MDM2* gene consists of p53-promoter and in turn, MDM2 protein binds to p53 at transactivation domain to inactivate function of P53 or promotes the degradation by exporting p53 out of nucleus or by ubiquitination as an E3 ubiquitin ligase function leading to proteasome–mediated degradation. MDMX inhibits the function of p53 by binding to the transactivation domain of p53 but does not promote the degradation of P53.[256,258] The negative regulation of MDM2 on the transcriptional activation function of p53 is essential in normal cells, but this regulation is abnormal when MDM2 is overexpressed[258] which may lead to development of cancers (e.g. in human sarcomas, p53 mutations were not found and only found overexpressed *MDM2* gene).[256] Thus, the inhibitor of p53/MDM2 interaction is interesting target for anticancer drug discovery. The inhibitors block the p53/MDM2 interaction, then results in p53 accumulation and activation the p53 pathway.[258] Several small molecules which were developed for inhibiting of the MDM2-p53 interaction such as MI-219, Nutlin (most potent nutlin-3a), TDP665759 are in preclinical stage of human cancer as MDM2 inhibitors.[259] For another example, small molecule RO-5963 inhibits the binding of p53 to MDM2 and MDMX by inducing the MDMX/MDMX or MDMX/MDM2 dimerization in MCF7 cells. RO-5963 activates p53 pathway in cancer cells (HCT166 cells) expressing the wild-type p53.[257]

1.5 CAS (CSE1L) and cancer

1.5.1 CAS (CSE1L) gene and protein

CSE (chromosome segregation) genes which include CSE1 and CSE2 are yeast genes required for chromosome segregation during mitosis. Xiao *et al*. identified both genes in 1993.[260] CSE1 is an essential gene and has functions in cell proliferation and division. Defects in CSE1 lead to abnormal chromosome segregation in yeast. The human homologue to the yeast CSE1 gene, CSE1L (chromosome segregation 1-like, or cellular apoptosis susceptibility gene, CAS) is located on the chromosome 20q13.[261,262,263] Several candidate oncogenes (e.g. ZNF217, a transcription factor; AIB1, a steroid receptor coactivator; BTAK, a serine/threonine kinase; or the Src oncogene) are found on this chromosomal region.[262,264,265] The CAS gene is amplified in several cell lines such as breast, colon, and bladder cancer cells. The CAS gene consists of 25 exons. There are various CAS cDNAs because of alternative mRNAs splicing.[266]

CAS protein is a nuclear transport (exportin 2) which recycling importin alpha from nucleus back to cytoplasm. In normal cells, the CAS protein is essential for cell proliferation and early embryonic growth.[267] This protein is highly expressed during in cell proliferation.[261,268] CAS is considered to have a "switch" function that determines whether a cell will proliferate or will undergo apoptosis.[269] It also plays an important role in the mitotic spindle checkpoint, which controls genomic stability during cell division.[270]

There are 4 isoforms of the CSE1L protein.[271] Nuclear transport function may be controlled by different isoforms of CAS.[266] The N-terminus of CAS is homologous to the RAN-binding domain of importin beta[263] and it binds to RAN. It also acts as a nuclear transport factor for importin alpha by recycling it from the nucleus to the cytosol and is crucial for a variety of proteins that have function in mitosis and apoptosis. This may explain the function of CAS in apoptosis and proliferation as a cancer-related gene or pro-oncogene.[266,272]

1.5.2 Studies related to CAS (CSE1L)

Pathological studies showed that CAS is highly expressed in most cancers and correlates with the high cancer grade and stage.[261,262,268,273-276] CAS was also reported to be a secretory protein and to regulate the invasiveness and metastasis of cancer cells.[277-281] Furthermore, CAS binds to tubulin, enhances microtubule assembly and the migration of MCF-7 cancer cells.[282]

Ogryzko *et al.* reported that CAS is important for mitosis. Reduction of the CAS protein level by antisense cDNA perturbed the progression of HeLa cells because of accumulation of cells in G2 phase or mitosis (G2/M arrest) and preventing cyclin B degradation (increased levels of cyclin B).[283] Knock-down of CAS by siRNA treatment increased cell apoptosis and cell adhesion and led to decrease in cell viability in HCT116 and SW480 cells.[262]

CAS knock-down reduced UV-C-induced apoptosis in MCF-7 cells. However, it was not clearly demonstrated whether CAS is as a pro-apoptosic or pro-arrest factor.[284] CAS expression induced polarity of HT-29 cells. CAS binds to E-cadherin and stimulates the formation of E-cadherin/β-catenin complex which is important for normal epithelial cell-cell adherence and tissue architecture.[285,286] Deregulation in association or function of this complex results in loss of intercellular adhesion and is related to cell transformation and tumor progression.[285] An anticancer drug screening was established by Liao *et al.* in 2008 for high-sensitivity and high-throughput anticancer drug screening based on the coexpression of CAS.[287] Liao *et al.* transfected HT-29 human colorectal cancer cells with CAS- and GFP-expressing vectors (pcDNA-CAS and pcDNA-GFP) or the control and GFP-expressing vectors (pcDNA3.1 and pcDNA-GFP).[287,288] They found that CAS over-expression enhanced the cytotoxicity of some anti-cancer compounds like 5-fluorouracil, doxorubicin, cisplatin, and tamoxifen. In transfected HT-29 cancer cells that were treated with chemotherapeutic drugs, CAS over-expression enhanced the accumulation of p53 and drug-induced apoptosis. However, another study demonstrated that CAS inhibits taxol-induced apoptosis.[288] In 1996, Brinkmann *et al.* found out that CAS also plays an important role in mediating apoptosis in MCF-7 cells induced by immunotoxins like pseudomonas exotoxin, diphtheria toxin, and tumor necrosis factor α, β (TNF α, β), but not by staurosporine, cycloheximide or etoposide. They suggested that CAS might play a role in selected pathways of apoptosis.[269]

2 Objective

In chemical proteomics, a small molecule is often immobilized on a solid support for the isolation and identification of binding proteins from an entire proteome. This affinity chromatography approach is the technique currently used widely for protein target identification. However, this technology also has some limitations. An alternative methodology employs the link between the protein and its corresponding gene called “genotype–phenotype link”. There are several possibilities for creating a genotype–phenotype link, such as mRNA display and ribosome display. Currently, the phage display is the potential method for target identification of small molecules. The real advantage of phage display originates from the phage amplification by infection into *E. coli* and its subsequent subjection to affinity selection with the immobilized small molecule. Non-binding phages are washed off, and the binding phages are eluted and transfected into bacterial host cells for amplification and the amplified phage population is used for next affinity selection and affinity selection are repeated with several rounds. One significant advantage of phage display over other expression-cloning-based methods is that the iterative amplification steps allow the identification of low-abundant targets and of low-affinity targets. For this reason, the first objective of this thesis was to establish a cDNA phage display protocol for affinity isolation of target proteins binding to small molecules of interest as an alternative to the affinity-based approach, which utilizes cell lysates and subsequent mass spectrometry analysis. After establishing the protocol, the aim was to confirm already known target proteins for biotinylated small molecules and to apply it in the target deconvolution for new biologically active compounds.

A separate study focused on the biological evaluation of hit compounds from phenotypic high content screening that monitors changes in cytoskeleton and DNA. Screening of tetrahydropyran library that was synthesized in the department identified some derivatives as mitosis modulators. The most active compound tubulexin A inhibits tubulin polymerization by targeting the vinca alkaloid binding site of tubulin. By means of the affinity purification approach, tubulin and chromosome segregation 1-like protein CSE1L (CAS, exportin-2) were identified as proteins that bind to biotinylated tubulexin. Furthermore, a collection of natural products was subjected to the phenotypic screen to monitor changes in the cytoskeleton and DNA and identified podoverine A as a potent mitotic inhibitor.

Molecules interfering with microtubule dynamics are among the most successful therapeutics for the treatment of cancer. Despite the availability of many tubulin targeting agents, cells can become resistant towards the drugs. Hence, there is high demand for the identification of new anti-tubulin agents that are able to overcome anti-tubulin drug resistance. Within this work, the aim was to further validate the effects of tubulexin A and podoverin A and characterize their mode of action.

Despite the high relevance of CAS as a target in cancer, there is no small molecule selectively targeting CAS published yet. Therefore, additional focus of this work was to discover further compounds that bind to CAS which might interfere with CAS function and thus might inhibit growth of cancer cells. A reverse chemical genomics-approach was chosen in collaboration with the group of Prof. Osada (RIKEN-Wako-Japan). This strategy is based on a chemical array screening to identify compounds that bind to CAS. The resulting hit compounds needed to be validated in respect to binding properties and phenotypic changes in HeLa cells.

3 Materials

3.1 Instruments and laboratory devices

Name		Company
HPLC machine	AKTA (FPLC)	Amersham Biosciences
Hi-Trap Ni-NTA column	Hi-Trap HP TM (Ni Sepharose 1 and 5mL) column prepacked with precharged Ni^{2+} and sepharose	GE Healthcare, Sweden
PCR machine	Thermo cycle machine	Thermo scientific, Germany
Autoclave	Varioklav®400	Thermo scientific, USA
Safety cabinets	Hera Safe type HS12	Kendro laboratory, Germany
	NUAIRE, class II	Integra Biosciences, Germany
CO_2-incubator	NUAIRE IR Autoflow and NUAIRE DHD Autoflow	Integra Biosciences, Germany
	Odyssey Infrared Imaging System	LI-COR Biosciences, Germany
Electrophoresis system	DNA and protein electrophoresis	BioRad, USA
pH meter	Mettler Toledo FiveEasy	Mettler Toledo, State
Semi-dry protein transfer device	Trans-Blot ® SD	BioRad, USA
Power supply device	Power PAC 1000	BioRad, USA
Sonicator for cell lysis	Sonoplus HD2070	Bandelin, Germany
Vacuum concentrator	5301	Eppendorf, Germany
Vortex device	Vortex Genie 2	Carl Roth, Germany
Centrifuge device	Centrifuge 5415R	Eppendorf, Germany
Balance	BP301S	Sartorius, Germany
Cell culture flask s	BD Falcon ™ 175 cm2	BD Biosciences, USA

	BD Falcon ™ 75 cm2	BD Biosciences, USA
Falcon tubes	50 ml falcon tube	Sarstedt, Germany
	15 ml falcon tube	Sarstedt, Germany
Centrifuge tubes	Safe lock tube (0.5-2 mL)	Eppendorf, Germany
CD-Spectrometer J-815	*Spectrometer*	Jasco® GmbH, Germany
Microscopes	Zeiss Axiovert	Visitron, Germany
	Zeiss observer Z1	Zeiss, Germany
	Thermomixer comfort	Eppendorf, Germany
Plate readers	Infinite M200	Tecan, Austria
	Safire II XFluor4	
96-well plates, black with black bottom measurement	Corning Costar® plate	Corning Incorporated, USA
96-well clear plates	Corning cellBind Surface	Corning Incorporated, USA
96-well black imaging plates FC with clear fluorocarbon film bottom	96-well black imaging plates	PAA Laboratories GmbH, Germany
24-well black imaging plates FC with clear fluorocarbon film bottom	24-well black imaging plates	PAA Laboratories GmbH, Germany
Pierce High Binding Capacity Streptavidin coated plates (HBC), 96-well, clear	Streptavidin Coated Plate	Thermo Scientific, USA
Dialysis membrance tubing		Thermo Scientific, USA
PVDF-transfer membrane	Immobilon®-FL	Millipore, USA
X-ray Films	CL-Xposure ™ film	Thermo scientific, USA
T7 phage capture 96-well plate	T7 Phage Capture Plate	Novagen, Germany
Pierce High Binding Capacity Streptavidin coated plates (HBC), 8-well strips, clear	Streptavidin Coated High Capacity Plates	Thermo Scientific, USA
Cell counting chamber	Neubauer Cell counting chamber	Carl Roth, Germany
Cell scrapers	BD Falcon TM Cell scrapers	BD Biosciences, USA

3.2 Chemicals and reagents

Chemicals and reagents	**Company**
Developing solution for Western Blot	TETENAL-Eukobrom, Germany
Fixing solution for Western Blot	TETENAL-Eukobrom, Germany
Ethanol absolute	Sigma Aldrich, Germany
Formaldehyde 37%	Fischer Sicentific, Germany
Concentrated 37% HCl	J.T. Baker, Netherlands
Methanol	J.T. Baker, Netherlands
Bradford Reagent - Bio-Rad-protein assay	Bio-Rad laboratories, Germany
Acrylamid 4K- solution 30%	AppliChem , Germany
Complete Mini EDTA-free protease inhibitor cocktail	Roche Diagnostics, Germany
Dimethylsulfoxyde (DMSO) research grade	Serva, Germany
1,4-Dithio-D,L-threitol (DTT)	Gerbu Biotechnik, Germany
HEPES sodium salt	Serva, Germany
Ethylenglycol-bis(2-Aminoethylether)-N,N,N’,N’-tetraacetic acid (EGTA)	Sigma Aldrich, Germany
Glycerol 99%	Sigma Aldrich, Germany
Glycin 99%	Carl Roth, Germany
TRIS-HCl	Carl Roth, Germany
Bromophenol blue – sodium salt	Serva, Germany
Coomassie Brilliant Blue G-250	Serva, Germany
NaCl	Sigma Aldrich, Germany
KCl	J.T. Baker, Holland
Na_2HPO_4	Merck, Germany
KH_2PO_4	J.T. Baker, Netherlands
N,N,N’, N’-tetramethylethylendiamine (TEMED)	Sigma Aldrich, Germany
NP-40 Alternative	CalBiochem, Germany
Tween 20	Serva, Germany
Streptavidin magnetic beads	New england Biolabs, Germany

Super Signal ® West Pico Chemiluminescence substrate	Thermo Scientific, Germany
Super Signal ® West femto Chemiluminescence substrate	Thermo Scientific, Germany
Amonium persulfate	Serva, Germany
Sodium dodecylsulfate	Gerbu Biotechnik, Germany
Tryptan blue solution	Fluka, Germany
Odyssey blocking buffer	LI-COR, Germany
Penicillin (10,000U/mL) and Streptomycin (10 mg/mL)	Sigma Aldrich, Germany
DMEM high glucose (4.5g/l) mit L-glutamine	PAA, Austria
RPMI 1640 medium	Invitrogen, Japan
Fetal calf serum	Nichirei Biosciences, Japan
Sodium pyruvate solution (100 mM)	Sigma Aldrich, Germany
Trypsin-EDTA 0,05%	PAA, Austria
Fetal bovine serum (FBS)	Invitrogen, Germany
Agarose	Invitrogen, Germany
GelRed Nucleotide Acid stain	Biotium, Germany
Tubulin general buffer	Tebu-bio GmbH, Germany (origin Cytoskeleton, USA)
Tubulin glycerol buffer	Tebu-bio GmbH, Germany
TR-FRET buffer	Invitrogen, Germany
Phalloidin-TRITC	Sigma-Aldrich, Germany
4',6-diamidino-2-phenylindole (DAPI)	Sigma-Aldrich, Germany
BODIPY®-FL-Vinblastine	Invitrogen, , Germany
Triton X-100	Serva, Germany
Vinblastine	Sigma-Aldrich, Germany
TMB substrate solution	Cell Signaling, State
Cell proliferation WST-1	Roche, Germany
Bovine serum Albumin, (BSA)	Sigma, Germany
ExoSap-IT	USB, Germnay

Glutathione, reduced, free acid	Merck Millipore, Germany
Non fat dried milk powder (skim milk)	Applichem GmbH, Germany

All other chemical reagents were purchased from the following companies: Sigma-Aldrich, Fluka, Merck, Roche, Roth and Serva in Germany.

3.3 Buffers and solutions

Buffers	**Components**
5X SDS-PAGE loading buffer	0.05% bromophenol blue 0.25 M DTT 50% (v/v) glycerol 10% SDS 0.25 M Tris-HCl, pH 6.8
6X DNA loading buffer	60 mM EDTA 0.03% bromophenol blue 60% (v/v) glycerol 10 mM Tris-HCl, pH 7.6
50X TAE buffer for agarose gels	2 M Tris-Acetate 0.05 M EDTA, pH 8.3
1X TBE buffer	89 mM Tris-base 89 mM boric acid 2 mM EDTA, pH 8.0
SDS-PAGE gel staining buffer)	0.1% coomassie brilliant blue 50% (v/v) methanol 10% (v/v) glacial acetic acid
SDS-PAGE gel destaining buffer	30% (v/v) methanol 10% (v/v) acetic acid
10X SDS-PAGE running buffer	2.5 M glycine 0.25 M TRIS-HCl

	1% SDS
10X PBS	1.37 M NaCl 0.27 M KCl 0.1 M Na_2HPO_4 0.02 M KH_2PO_4 pH 7.4
10X TBS	1.5 M NaCl 0.02 M KCl 0.25 M TRIS-HCl, pH 7.4
PBS-T	0.1% (v/v) Tween 20 in 1X PBS
TBS-T	0.1% Tween 20 in 1X TBS
Transfer buffer for Western Blot	25 mM TRIS-HCl 200 mM glycine 20% (v/v) MeOH
Membrane stripping buffer	6M guanidine hydrochloride
4X PERM buffer	400 mM PIPES/KOH pH = 6.8 40 mM EGTA 4 mM $MgCl_2$ 0.4% (v/v) Triton X-100
Fixation and permeabilization buffer for cell staining	3.7% (v/v)formaldehyde 1X PERM buffer
Blocking buffer for Western Blot	5% skim milk in PBS-T, or Odyssey blocking buffer
Blocking buffer for cell staining	2% BSA in PBS-T
Lysis buffer for HeLa cells	50 mM PIPES, pH 7.4 50 mM NaCl 5mM MgCl2 5mM EGTA

	0.1% (v/v) NP40 0.1% (v/v) Triton X-100 0.1% (v/v) Tween 20 10 mM 2-Mercaptoethanol 1 protease inhibitor cocktail
Washing buffer for affinity purification	50 mM PIPES, pH 7.4 50 mM NaCl 75 mM MgCl2 5 mM EGTA 0.1% (v/v) NP40 0.1% (v/v) Triton X-100 0.1% (v/v) Tween 20
Binding buffer for immunoprecipitation	50 µM Hepes, pH 7.5 200 mM NaCl 10 mM Mg-Ac (magnesium acetate) 50 mM K-Ac (potassium acetate)
Lysis buffer for bacterial cells expression CAS	50 mM TRIS-HCl, pH 8.0 400 mM NaCl 5% (v/v) glycerol 0.1% (v/v) Triton X-100 1 mM DTT 5 mM imidazol 0.025 mM PMSF 3,3 µg DNase for 1 g cells 1 protease inhibitor cocktail
Washing buffer for CAS purification for size exclusion, affinity chromatograph step	500 mM NaCl 10% (v/v) glycerol 1 mM DTT 50 mM TRIS-HCl, pH 8.0

Elution buffer for CAS purification for affinity chromatograph step	500 mM NaCl 500 mM imidazole 10% (v/v) glycerol 1 mM DTT 50 mM TRIS-HCl, pH 8.0
PreScission protease cleavage buffer	400 mM NaCl 5% (v/v) glycerol 1 mM DTT 1 mM EDTA 0.01% (v/v) Triton X-100 40 mM TRIS-HCl, pH 8.0
Size exclusionchromatography buffer for CAS purification	400 mM NaCl 1 mM DTT 5% (v/v) glycerol 40 mM TRIS-HCl, pH 8.0
Lysis buffer for bacterial cells expression of RAN	20 mM Kpi (potassium phosphate), pH 6.5 5 mM $MgCl_2$ 2 mM DTE 1 mM PMSF 3,3 µg DNase for 1 g cells 1 protease inhibitor cocktail tablet
Loading buffer for RAN purification n	20 mM Kpi, pH 6.5 5 mM $MgCl_2$ 2 mM DTE
Elution buffer for RAN purification	20 mM KPi, pH 6.5 1M KCl 5 mM $MgCl_2$ 2 mM DTE

DNA binding buffer	2 mM NaAcetate 9.3 mM NaCl 0.1 mM EDTA
Phenylmethylsulfanoxide (PMSF)	100 mM in 2-propanol
1000X kanamycin	50 mg/mL in H_2O
1000X ampicillin	100 mg/mL in 70% EtOH
1000X chloramphenicol	25 mg/mL in 100% EtOH
Isopropyl β-D-1-thiogalactopyranoside (IPTG)	1 M in H_2O
Dithiothreitol (DTT)	1 M in H_2O
Ammonium persulfate (APS)	10% in H_2O
DEAE-dextran	10 mg/mL in water
Chloroquine diphosphate	8 mM in PBS

3.4 DNA and protein ladders

Product Name	**Company**
PageRuler TM prestained protein ladder plus GeneRuler™ 1 kb DNA Ladder GeneRuler™ 100 bp DNA Ladder plus	Fermentas, Germany

3.5 Plasmids

Plasmid backbones /supplier	**Constructs**
pOPIN Dortmund Protein Facility	pOPINHis
	pOPINHis-CAS
	pOPINHis(n).EGFP
	pOPINHis(n).EGFP-CAS FL
	pOPINHis(n).EGFP-CAS 391N
	pOPINHis(n).EGFP-CAS 570N

	pOPINHis(n).EGFP-CAS 570C
pcDNA3.1 Invitrogen^{TM}	pcDNA3.1-FLAG
	pcDNA3.1-FLAG-CAS FL
	pcDNA3.1-FLAG-CAS 391N
	pcDNA3.1-FLAG-CAS 570N
	pcDNA3.1-FLAG-CAS 570C
pCMV-SPORT6 Open Biosystems	pCMV-SPORT6-CAS
pET-3d Novagen The construction of pET-3d-RAN (from Klebe *et al*)[289]	pET-3d-RAN

3.6 Oligonucleotides for cloning and sequencing

Name	**Sequences (5´-3´)**
pOPIN(n) EGFP-CAS-F	GAAGTTCTGTTTCAGGGTCCCATGGAACTCAGCGATGCAAATCTGC
pOPIN(n) EGFP-CAS-R	TAAACTGGTCTAGAAAGCTTTAAAGCAGTGTCACACTGGCTGC
pOPIN(n) EGFP-CAS391N-R	TAAACTGGTCTAGAAAGCTTTATCGTACCAGATCACAAGCAGCC
pOPIN(n) EGFP-CAS570N-R	TAAACTGGTCTAGAAAGCTTTATTCATTTTCTGAAGAGCCAGGAAGTGTG
pOPIN(n) EGFP-CAS570C-F	GAAGTTCTGTTTCAGGGTCCCATGTATATTATGAAAGCTATCATGAGAAGTTTTTCTCTCC
pcDNA3.1flag-CAS-F	CAGTCTAGAGCCACCATGGAACTCAGCGATGCAAATCTGC
pcDNA3.1flag-CAS-R	GGAGGATCCAAGCAGTGTCACACTGGCTGCCTGAAGGTAC
pcDNA3.1flag-CAS391N-R	GGAGGATCCTCGTACCAGATCACAAGCAGCCCTGCG
pcDNA3.1flag-CAS579N-R	GGAGGATCCACTTCTCATGATAGCTTTCATAATATATTCATTTTC
pcDNA3.1flag-CAS579C-F	CAGTCTAGAGCCACCATGAGTTTTTCTCTCCTACAAGAAG
T7 Select Down	AACCCCTCAAGACCCGTTTA
T7 Select up	GGAGCTGTCGTATTCCAGTC
Ec-Hd3 linker 1	GCTTGAATTCAAGC

Ec-Hd3 linker 2	GCTTGGAATTCCAAGC
Ec-Hd3 linker 3	GCTTGGGAATTCCCAAGC

3.7 Enzymes and kits

Products	**Company**
Pfu and Taq DNA Polymerase; shrimp Alkaline Phosphatase (SAP); T4-Ligase; restriction enzymes; klenow-Fragment; RNase A; DNase I; Oligo (dT)	Fermentas, Germany
PCR purification Kit DNA Gel-extraction Kit	Qiagen GmbH, Germany
Pre-made T7Select® Human Breast cDNA Library Pre-made T7Select® Human liver cDNA Library	Merck KGaA, Germany (origin from Novagen)
Apo-ONE® Homogenous Caspase-3/7 Assay Kit	Promega, Germany

3.8 Antibodies

3.8.1 Primary antibodies

Antigen	**Organism**	**Type and stock**	**Company**	**Dilution**
Importin alpha	Rabbit	Polyclonal (#ab70160) 1 mg/mL	Abcam	WB 1:10,000 IF: 1:500
RANBP1	Rabbit	Polyclonal (#ab97659) 1 mg/mL	Abcam	IF: 1:200
CAS	Mouse	Monoclonal (#sc-101226) 100 µg/mL	Santa Cruz Biotechnology, Inc	WB: 1:1000 IF: 1:100
CAS	Rabbit	Polyclonal (#sc-28233) 200 µg/mL	Santa Cruz Biotechnology, Inc	IF: 1:100
CAS	Goat	Polyclonal (sc-1708)	Santa Cruz Biotechnology, Inc	WB: 1:1000 IP: 1:30

		200 µg/mL		
α-tubulin	Mouse	Monoclonal (#T9026) 1 mg/mL	Sigma-Aldrich	IF: 1:500
α-tubulin	Rabbit	Polyclonal (#ab18251) 0.5 mg/mL	Abcam	IF: 1:500
RAN	Mouse	Monoclonal (#610341) 250 µg/mL	BD Biosciences	WB: 1:1000 IF: 1:200
Flag-tag	Rabbit	Polyclonal (#2368) 100 µg/mL	Cell Signaling Technology®	WB: 1:1000
His-tag	Mouse	Monoclonal (#GE.2747100)	*GE* Healthcare	WB: 1:1000 IF: 1:100
pHistone H3	Rabbit	Polyclonal (#ab5176) 500 µg/mL	Abcam®	IF: 1:500

WP: Western Blot; IF: immunofluorescence

3.8.2 Secondary antibodies

Antigen	**Host**	**Description**	**Company**	**Dilution**
Rabbit IgG (H+L)	Goat	Polyclonal, Horseradish peroxidase (HRP) conjugate	Thermo Scientific	WB: 1:15000
Mouse IgG (H+L)	Goat	Polyclonal, HRP conjugate (#31430)	Thermo Scientific	WB: 1:15000
Goat IgG (H+L)	Donkey	Polyclonal, HRP conjugate (#sc2033)	Thermo Scientific	WB: 1:15000
Rabbit IgG (H+L)	Goat	Alexa Fluor® 488 conjugate (#A11076)	Invitrogen	IF: 1:500
Mouse IgG (H+L)	Goat	Alexa Fluor® 488 (#4408)	Cell Signaling Technology®	IF: 1:500
Mouse IgG (H+L)	donkey	IRDye800CW conjugate	LI-COR® Biosciences	WB: 1:10000

Rabbit IgG (H+L)	Donkey	IRDye700CW conjugate	LI-COR® Biosciences	WB: 1:10000
Goat IgG (H+L)	Donkey	IRDye800CW conjugate	LI-COR® Biosciences	WB: 1:10000
Mouse IgG (H+L)	Goat	Cy5 conjugate	Invitrogen™	Microarray: 1:100

3.9 Organisms and culture media

3.9.1 Bacterial strains

***E. coli* strains**	**Genotype**	**Company**
DH10B	F-, *mcrA*, Δ(*mrr*, *hsdRMS*, *mcrBC*), φ80d (*lacZΔM15*, Δ*lacX74*), *deoR*, *recA1*, *araD139*, Δ(*ara*, *leu*)7697, *galK*, λ-, *rpsL*, *endA1*, *nupG*	Stratagene
BL21-codon Plus(DE3)-RIL	*F- ompT hsdS(*r_B^- m_B^-) *dcm*$^+$ Tet^r *gal* λ(DE3) *end*A Hte [argU ileY*leuW* Cam^r]	Stratagene
BLT5615	*F- ompT hsdS$_B$*(r_B^- m_B^-) *gal dcm* pAR5403 (amp^R)	Novagen
Rosetta-gami™ B5615	F$^-$ *ompT hsdS*$_B$(r_B^- m_B^-) *gal dcm lacY1 ahpC gor522*::Tn*10* (Tc^R) *trxB*::kan pRARE2 (Cm^R) pAR5615 (Ap^R)	Novagen

3.9.2 Mammalian cell lines

Name	**Description**
HeLa	Human cervical carcinoma cells
KB-V1	Derivative of HeLa cells, a multidrug-resistant cells due to mutations[290]
HeLa Fucci (fluorescent ubiquitination-based cell cycle indicator)	Derivative of HeLa cells stably expressing Kuzabira orange-Cdt1 and Azami green-Geminin as sensors for cell cycle progression in live cells.[291]
HEK293T	Human Embryonic Kidney 293 cells stably expressing the SV40 large T antigen
COS-7	African green monkey kidney cells

3.9.3 Cell Culture media

Organisms	**Media**	**Components**
Bacterial strains (*E. coli*)	LB (Luria Bertani)	1% bacto-tryptone 0.5% yeast extract 1% NaCl
	SB (Super Broth)	3.2% peptone 2% yeast extract 0.5% NaCl
	SOB (Super Optimal Broth)	2% peptone 0.5% yeast extract 10 mM NaCl 2.5 mM KCl 10 mM $MgCl_2$
	SOC (Super Optimal broth with Catabolic repressor)	SOB + 20 mM glucose
HeLa HeLa Fucci COS-7	DMEM, 4.5 g/l Glucose, L-Glutamine	10% (v/v) FBS 1000 U/mL penicillin 1 mg/mL streptomycin 1% (v/v) non essential amino acids
KB-V1	DMEM, 4.5 g/l Glucose, L-Glutamine supplemented with 200 ng/mL vinblastine	10% (v/v) FBS 1000 U/mL penicillin 1 mg/mL streptomycin 1% (v/v) non essential amino acid 10 mM sodium pyruvate
HEK239T	RPMI 1640	10% (v/v) FBS 1000 U/mL penicillin 1 mg/mL streptomycin 1% (v/v) non essential amino acids

3.10. Proteins

Proteins	Supplier
Porcine tubulin	Tebu-bio GmbH, Germany
Importin alpha	From Ms. Carolin Koerner (MPI-Dortmund) (Thank to Ms. Carolin Koerner regarding this protein)

4 Methods

4.1 General methods in molecular biology

4.1.1 Polymerase chain reaction (PCR) and colony PCR

Polymerase chain reaction (PCR) is a technique used to amplify given DNA sequence. The reaction mixture consists of desoxynucleotides (DNA) template, primers (oligonucleotides) which are duplicates of nucleotide sequences of the piece of DNA of interest, Mg^{2+} ions, DNA polymerase and is performed in a thermal cycler. There are three basic steps in the PCR amplification process. During the denaturation step the DNA template is heated to 90-96°C to disrupt the hydrogen bonds between complementary bases thus yielding single-stranded DNA). In the following annealing step the oligonucleotides (primers) hybridize with the single-stranded DNA template to form primer-DNA template hybrid. The enzyme DNA polymerase binds to this hybrid and catalyzes the synthesis of the complementary DNA strand during the extension (or elongation) step.

Colony PCR is employed when *E. coli* colonies are used as a DNA template to rapidly detect the correct recombinant clones after cloning and transformation of plasmids into *E.coli*.

The PCR reaction (**Table 1**) was prepared in a PCR tube and incubated in a thermal cycler (Thermo scientific, Germany) using the PCR cycling protocols described in **Table 2**.

Table 1: PCR reaction composition.

Reagent	**Final concentration**
10X DNA polymerase buffer	1X
dNTPs mix, 2 mM each	0.2 mM of each
Primers	0.1 µM
DNA template	10-100 ng (or *E. coli* colony)
DNA polymerase	0.025 U/µL
Water	add to 50 µL
Total volume	**50 µL**

Table 2: PCR cycling protocol.

Step	**Temperature**	**Time**
Initial DNA denaturation	95 °C	3 min
PCR cycles (30 cycles)		40 s
Denaturation	95 °C	30 s
Annealing	55-60 °C	1-5 min (dependent on the enzyme and the size of the PCR product)
Extension	72 °C	
Final extension	72 °C	15 min
Final hold	4 °C	short-time storage

4.1.2 DNA digestion

DNA vectors or PCR products were digested using DNA restriction nucleases according to the manufacturer's manual (Fermentas, Germany). Briefly, PCR products were subjected to agarose gel electrophoresis (see section 4.1.7) to analyse the size of the detected DNA. Afterwards the DNA was purified using the PCR Purification Kit (Qiagen), followed by determination of the DNA concentration. 3 µg DNA were digested using 7 units of the restriction enzyme for for 2 hours (h) at 37 °C. Finally, the enzyme was inactivated at 65-80 °C for 10-15 minutes (min).

4.1.3 DNA dephosphorylation

Digested DNA typically contains a 5' phosphate group, which is required for ligation. In order to prevent self-ligation of a restricted plasmid during DNA ligation 5' phosphates were removed by dephosphorylation. This step improves the efficiency of DNA insertion into a vector. There are several phosphatases can be used for dephosphorylation such as Shrimp Alkaline Phosphatase (SAP), Calf Intestinal Alkaline Phosphatase (CIP) and Antarctic Phosphatase. In this work, linearized vectors were incubated in the supplied reaction buffer with 2 units SAP (Thermo Scientific) per µg DNA vector for 30 min at 37 °C followed by heat inactivation at 65 °C for 15 min.

4.1.4 DNA ligation

DNA ligation step was performed according to the cloning guide of NEB (New England Biolabs). In this work the ligation was performed in a volume of 20 µL using 2.5 units of T4 DNA ligase (NEB), 100 ng vector and 100-150 ng DNA insert. Amounts of DNA inserts are dependent on the size of DNA insert by formula of (3 x (kb of insert/ kb of vector) x ng of vector) in the supplied reaction buffer for 2 h at 22 ^{o}C, followed by heating for enzyme inactivation at 65 ^{o}C for 15 min.

4.1.5 DNA purification

PCR products that were generated for cloning were purified using Qiagen PCR purification kit. PCR products that were prepared for sequencing were purified using ExoSap-IT (USB) prior to sending them to StarSEQ (Germany). Plasmid purification was performed by means of the plasmid mini/midi purification kit (Qiagen). All purification steps were carried out according to the manufacturer's protocol.

4.1.6 Transformation of *E. coli* with plasmid DNA

DNA transformation is the process of introduction of foreign DNA into cells. For this work, DNA transformation is performed by heat shock transformation to chemically competent bacteria. Competent *E. coli* cells were prepared by the method of Inoue *et al.*[292] and the frozen competent cells were stored at -80 ^{o}C. Before transformation, competent cells were thawed on ice. At the same time, LB agar plates that were supplemented with the appropriate antibiotic and tubes with 1 mL SOC media were pre-warmed at 37 ^{o}C. Vector DNA (10-100 ng) or insert DNA were gently mixed into 50 µL of competent cells. The mixture was incubated on ice for 20-30 min. Heat shock was then performed by placing the tube to 42 ^{o}C water bath for 45-60 seconds (sec) followed by immediate cooling on ice for 2-5 min. 1000 µL of pre-warm SOC media (without antibiotic) were added to the cells. Cells were incubated at 37 ^{o}C in a shaker for 45 min. Different amounts of transformed cells were plated onto pre-warm LB agar plate to obtain the single colony. Plates were incubated at 37 ^{o}C overnight.

4.1.7 DNA electrophoresis

This method is employed for checking the size of DNA or separating DNA fragments based on their size. DNA migrates from the negative to the positive electrode because of the negative charge of DNA.

Agarose gels were prepared in 1X TAE buffer. An appropriate amount of agarose powder was added to 100 mL 1X TAE buffer and was heated in a microwave oven to dissolve it. The agarose solution is cooled down to 50-60 ^{o}C in a water bath at room temperature before GelRed Nucleotide Acid stain solution (Biotium) was added in a 1:10000 dilution. The gel casting tray was prepared and the comb was placed. The agarose solution was poured into the casting tray. Once the gel solidified, the casting tray was placed into the electrophoresis chamber and the comb was removed. The electrophoresis chamber was filled with running buffer (1X TAE). DNA samples were mixed with DNA loading buffer and were carefully loaded into the wells of the gel to avoid air bubbles. DNA ladder was loaded in one well which enables to estimation the size of the analyzed DNA. The bromophenol blue dye in the DNA loading buffer permits to monitor the DNA migration during electrophoresis. The electrophoresis chamber was connected to a power supply and the voltage was set to 120 volts. After finishing electrophoresis (i.e. after 20-30 min dependent on the size of DNA products and the percentage of the agarose gel), DNA bands were visualized using Gel Logic 200 imaging system device with UV lamp (Kodak Gel Logic 200 imaging system device).

4.1.8 Cultivation and storage of *E. coli*

The growth of *E. coli* cells is characterized by four major phases: lag phase, log phase, stationary phase, and death phase. In the lag phase, the cell density increases slowly. In the log phase, *E. coli* cells grow exponentially and have doubling time of 20-30 min. In the stationary phase (the saturation phase), *E. coli* cells are stressed due to limited nutrients in the growth media and metabolic products that inhibit cell growth and might lead to a loss of cell viability (death phase).

For induction of protein expression or generation of competent cells, *E. coli* cells that are in the log phase were used. Bacterial cell growth can be monitored by measuring the absorption at 600 nm (optical density at 600nm: OD_{600}) several time points until the value of OD_{600} of 0.5 to 0.6 which correspond to the log phase (OD_{600} of 0.4 shows early log phase).

For storage or short maintenance (i.e. one day), *E. coli* cells were grown in LB medium. Cells were plated on LB agar plates and stored at 4 ^{o}C for four to seven days. For long-term storage, *E. coli* cell suspension was containing 10% glycerol can be kept at -80 ^{o}C. Bacterial cells were grown in SB media for protein expression. To obtain a pre-culture (small volume of culture which will be used for next culture of big volume) always a single colony was selected.

4.1.9 Biochemical methods

4.1.9.1 Determination of protein concentration

Protein concentration was determined by the Bradford assay. In principle, the Bradford assay is a protein determination method is based on the binding of coomassie brilliant blue G-250 dye to proteins. Since the dye binds to protein, the protein-dye complex which is blue is generated and can be detected at $OD_{595.}$

For this work, 1-2 µL of a protein sample wad added into 1 mL of Bio-Rad Protein Assays solution (Bio-Rad). After 5 min of incubation at room temperature and absorbance at 595 nm was measured using Biophotometer 6131 device (Eppendorf Biophotometer 6131). Only absorbance value between 0.1 and 1 were considered for the calculation of protein concentration. Protein samples were appropriately diluted if the absorbance value was higher than 1. In order to determine the protein concentration, BSA solutions with defined concentrations (0-5 mg/mL) were used to generate a standard curve. This curve determines the linear relationship between protein quantity and absorbance value which enables to determine the protein concentration of a given sample.

4.1.9.2 Protein gel electrophoresis

Sodium dodecyl sulfate polyacrylamide gel (SDS-PAGE) electrophoresis is based on electrophoresis and SDS-PAGE. In principle, electrophoresis is the process of moving charged molecules through in solution using a power supply. SDS-PAGE can be employed for proteins and nucleotides, most popular for proteins using. For proteins application, SDS-PAGE electrophoresis is a process of separating proteins according to their size on SDS-PAGE with denature proteins (e.g. unfold) because of SDS adding in gel.

The SDS polyacrylamide gel (SDPAGE) gel consists of stacking and resolving gel. The stacking gel is poured on top of the resolving gel after the completed polymerization of the resolving gel and a gel comb is inserted in the stacking gel. The percentage of acrylamide in the gel determines the range of proper separation of proteins and is chosen according to the size of the protein of interest. Two glass plates were assembled in the casting frames on the casting stands. Then the solution for the resolving gel (see **Table 3**) was prepared and was pipetted into the gap between the glass plates. The gel was covered with ethanol or 2-propanol to obtain a flat gel surface. While the resolving gel was polymerizing the stacking gel was prepared. Upon polymerization the ethanol or isopropanol layer was removed and the remaining space between the glass plates was filled with the stacking gel solution (see **Table 3**). Afterwards the comb was inserted rapidly. After complete polymerization, the gel can be used directly or stored at 4 °C.

Table 3: Composition of 12% resolving gel and the stacking solution.

Components	**Volume**	
	Resolving gel (for 10 mL)	**Stacking gel (for 1 mL)**
Water	3.3 mL	0.68 mL
30% acrylamide mix	4.0 mL	0.17 mL
1.5M TRIS-HCl (pH 8.8)	2.5 mL	_
1M TRIS-HCl (pH 6.8)	_	0.13 mL
10% SDS	0.1 mL	0.01 mL
10% APS	0.1 mL	0.01 mL
TEMED	0.01 mL	0.001 mL

4.1.9.3 Staining of proteins

After polyacrylamide electrophoresis, the gel was boiled in coomassie staining for 45-60 sec in a microwave oven (or until the gel was stained blue). The staining solution was discarded and the gel was rinsed briefly with MilliQ water and boiled for two to three minutes in the microwave oven. The gel was then incubated in a de-staining solution containing 40% methanol and 10% acetic acid) which was replaced every 10-20 min until bands are observed. Finally, the gel was rinsed with MilliQ water.

4.1.9.4 Semi-dry protein transfer

Transfer of proteins is process of transferring proteins from a gel to a membrane (e.g. nitrocellulose or polyvinylidene difluoride (PVDF)), where proteins are probed and detected using antibodies specific to the target protein. Transfer of proteins can be done by semi-dry transfer (which is faster and requires less buffer than wet transfer) or wet transfer using the transfer device.

In this work, protein transfer was performed by means of the semi-dry protein transfer (semi-dry electroblotting) technique using the transfer device (Bio-Rad) according the manufacturer's manual. PVDF membrane was used which was first activated by 100 % methanol for 5 min. Then, the membrane, the protein gel and 4 pieces of filter paper were equilibrated in transfer buffer for 5 min. Subsequently a sandwich composed of the gel, the membrane and the filter paper was assembled in the transfer device. Two pieces of pre-wetted filter paper were put onto the platinum anode (+) and were covered by the membrane. The gel was placed on top of the membrane and was covered by two pieces of pre-wetted filter paper. All air bubbles between the layers were removed because they may affect the quality of the protein transfer. The voltage or time needed for the transfer was chosen depending on the size of the membrane. Usually the transfer was performed at 22 V for 45 min.

4.1.9.5 Detection of proteins on membrane supports

Proteins that were using SDS-PAGE were transferred to a PVDF membrane by means of semi-dry protein transfer (section 4.1.9.4). Afterwards, the membrane was blocked in blocking buffer for one hour at RT to block non-specific binding to the membrane. For chemiluminescent detection, 5% nonfat dry milk in PBS-T was used. For fluorescent detection by means of the Odyssey Fc imaging system (LI-COR) membranes were blocked in LI-COR blocking buffer). The membrane was then washed 3 times with PBS-T buffer for 10 min at room temperature (RT). Afterwards, the membrane was incubated with the primary antibody which was diluted in an appropriate blocking buffer for one hour at RT (antibody dilution was showed in section 3.8.1). Upon incubation the membrane was washed three times with PBS-T for 10 min at RT to remove unbound antibodies and was subsequently incubated with the secondary antibody for one hour at RT. Prior detection membranes were washed again with PBS-T (3 times for 10 min at RT). For chemiluminescent detection of bound antibodies that are coupled to horseradish peroxidase (HRP), the Super Signal West Pico or Super Signal West Femto chemiluminescent substrate system (Thermo Scientific) was used to detect the chemiluminescence by exposing to X-ray film in dark room or using the Odyssey Fc imaging system (LI-COR® Biosciences). For fluorescent detection, secondary antibodies were labelled with IRDye 800/700 (LI-COR® Biosciences) and bound antibodies were detected using the Odyssey Fc imaging system (LI-COR® Biosciences).

4.1.9.6 Stripping PVDF-membranes

PVDF-membranes can be used several times when it is necessary to investigate different immunoblotting conditions. Incubation of the membrane into stripping buffer until it becomes transparent one (1-2 min). This step permits to wash away bound antibodies. After washing several times with PBS-T or TBS-T (3 times × 10 min), the original aspect of the membrane is recovered, blocked before to be re-used. This process can usually be performed 2 to 3 times without affecting the results.

4.2 General methods for phage display affinity selection and target validation

4.2.1 Growth of T7 lysates and liquid lysate amplification

This step was done following by T7Select® System Manual (TB178 Rev.B 0203, Novagen). *E. coli* strain BLT5615 and Rosseta-gami^{TM} B5615 were designed for carrying ampicillin–resistant plasmid that supplies extra 10A capsid protein and contains lacUV5 promoter. So both cells require the IPTG induction for capsid protein expressing prior to phage infection.

T7 phage grows rapidly on logarithmically growing cells. So for this work, 50 mL host cells grown at log phage when OD_{600} reached to 0.5 were induced by IPTG at 1 mM for 30 min before phage infection. The induced cells should be used in one day. Cells were infected with phage library at an MOI of 0.001-0.01 (means that one pfu per 100-1000 cells). The host cells can be calculated. For example, a host cells with OD_{600} of 0.75 contains cells per mL by formula: $OD_{600} \times (2 \times 10^8$ cells/mL)/0.5 $OD_{600} = 0.75 \times 2 \times 10^8/0.5 = 3 \times 10^8$ cell/mL. This culture can be infected with 3×10^5 to 3×10^6 pfu per 1 mL of cells.

Infected cells were grown until lysis is observed for 1-3 h at 37 ^oC and made the clarity lysate by centrifuging at 8,000 × g for 10 min. The supernatant was transferred into the sterile tube for either tittering the lysate by plaque assay (section 4.2.2) or storing at 4 ^oC (several months without a loss of titer for short-term of experiment) or storing at -70 ^oC in 10% sterile glycerol (for longer-term storage).

4.2.2 Plaque assay

In principle, this assay was also done following by T7Select® System Manual (TB178 Rev.B 0203, Novagen). For this work, 50 mL host cells grown until OD_{600} reached to 1 which can be used directly for assay or stored at 4 ^oC no longer than 48 h. At the same time, a melting top agar (0.7% in LB media) was prepared and hold at 50 ^oC in water bath. At the same time, pre-warm LB agar plate supplemented with 1 mM IPTG and antibiotic at 37 ^oC. Phage dilution was prepare in LB media supplemented with 1 mM IPTG, made dilution from 10^2 to 10^8 by adding 10 µL of phage in 990 µL LB media. Further, a series 12-mL tube was prepared by adding 3 mL of melting agar and 250 µL of host cells for each tube, followed by adding 100 µL of phage dilution. All mixture of top agar from step 3 was added to pre-warm LB agar plate and waited until the top agar hardens then reverted and incubated for 3-4 h at 37 ^oC or overnight at RT.

The plaques were counted and calculated the phage titer. The phage titer described in plaque forming units (pfu) per unit volume is the number of plaques on the plate times the dilution times 10 (plaques are counted on plate for 0.1 mL of dilution plated). For an example, 50 plaques are on plate from a $1/10^7$ dilution, the titer of sample is $50 \times 10^7 \times 10 = 5 \times 10^9$ pfu/mL.

The total number of phage in sample is determined by multiplying the titer with the total volume. For sample, a packaging reaction is used 1 µg of vector DNA and final volume of reaction is 0.3 mL, then the total number of pfu in the packaging reaction is 5×10^9 pfu/mL × 0.3 mL = 1.5×10^9 pfu/mL. For packaging, the efficiency is 1.5×10^9 pfu/ µg since 1 µg DNA is used.

4.2.3 Biopanning

In principle, the biopanning was also done following by T7Select® System Manual (TB178 Rev.B 0203, Novagen). For this work, 50 mL host cells were prepared as above (section 4.2.1) for selected phage eluted from selection cycle. Based on the phage titer, the number of phage used for screening can be desired. Normally, 100 µL of 10^8-10^9 pfu/mL was used for biopanning. 1 nmol of biotinylated compound was immobilized on a streptavidin-coated well at RT for 1 h, washed by TBS-T buffer (5 times × 5 min) and incubated with 100 µL phage library for 1h at RT. Further, the well was washed by TBS-T buffer (5 times × 5 min) before phages were eluted either with 1% SDS or specific compound. Eluted phages were used for titer or amplification which was a lysate-preparation step for next selection cycle. This cycle was repeated 6 rounds.

4.2.4 PCR-based analysis and *Hinf*I fingerprinting

After six rounds of binding and selection, phage particles were used as templates for the amplification of the encoded genes by means of PCR employing the primers T7SelectUP and T7Selectdown. 48-96 plaques (phage clones) were analyzed per a sample. PCR products were checked using agarose gel electrophoresis before being digested. The PCR products were then analyzed by means of *Hinf*I fingerprinting using the *Hinf*I restriction enzyme (recognizes G^ANTC sites) to digest PCR products. PCR products were digested by *Hinf*I (0.2 U/µL) in 1X supplemented buffer R (Thermo Scientific) at 37 ^{o}C for 2 h. After finishing digestion, reaction was added with DNA loading dye, heated 65 ^{o}C for 15 min and checked using agarose gel electrophoresis. After *Hinf*I fingerprinting, phage clones were chosen to amplify again of the encoded genes by means of PCR employing the primers T7SelectUP and T7Selectdown. PCR products were purified and followed by DNA sequencing using primers T7SelectUP or/and T7Selectdown.

4.3 Making phage display cDNA library and target validation

4.3.1 RNA extraction

RNA Extraction was following by the Qiagen´s manual using the RNeasy mini kit. HeLa cells were cultured and collected (section 4.8.1). Cells pellet of 2 × 10^6 HeLa cells were used for

RNA extraction. After finishing extraction, RNA was checked using agarose gel electrophoresis in 1X TBE buffer and measured RNA concentration. After checking, RNA can be used directly for cDNA synthesis or can be stored in DEPC-treated water at -20 °C.

4.3.2 Linker preparation

Based on the original linker of Novagen (OrientExpress TM cDNA manual, protocol TB247 Rev. B1109JN), other two linkers were designed (see detail of linker sequence in section 3.6). There are 3 primers; one linker was formed from each primer by hybridization reaction containing 1.9 nmol of primer in 1X SSC (150 mM NaCl, 15 mM Na3Citrate). Process of reaction: 85 °C for 15 min, then 65 °C for 15 min, following by RT for 30 min. Linkers can be stored at -20 °C or used directly for next reaction.

4.3.3 Generation of T7 phage display HeLa cDNA library

This work was done by using the Kit and based on the instruction manual (OrientExpress TM cDNA manual, protocol TB247 Rev. B1109JN) of Novagen. In principle, cDNA synthesis is primed with oligo (dT) or *Hind*III Random primers and methylation dNTP (5-me dCTP) which will be incorporated in both strands to protect certain internal restriction sites from being cut during digestion. The cDNA then is treated with T4 DNA polymerase to flush the ends and ligated with *Eco*RI/*Hind*III linkers. Following linker ligation, the cDNA is then digested with *Eco*RI and *Hind*III. Further, the cDNA is passed through a small gel filtration column to discard the small cDNA products (<300 bp) and excess linkers. Finally, the digested-cDNAs are inserted into *Eco*RI/*Hind*III-digested vector arms. This ligated vector is packaged with T7 packaging extracts *in vitro* to form phage clones.

There are mainly 7 steps (1/ first and second cDNA stand synthesis; 2/ modification of end cDNA; 3/ Ligation to directional *EcoR*I/*Hind*III linkers; 4/ *Eco*RI and *Hind*III digestion; 5/ site fractionation; 6/ ligation of prepared-cDNA to vector vector arms; 7/ packaging in T7 packaging extracts) which will be descripted in detail below:

4.3.3.1 First and second cDNA strand synthesis

- **First strand synthesis**

HeLa-RNA prepared (section 4.3.1) was used as template for first cDNA strand synthesis in 40 µL reaction containing 4 µg RNA, 2 µg primers (either oligo (dT) or *Hind*III Random primer) and followed by heating at 70 ^{o}C for 10 min to reduce the RNA secondary structure which may allow more efficient priming and cDNA synthesis. Further, reaction was chilled quickly on ice for adding other components (17 µL of water, 20 µL of 5X first strand synthesis buffer (250 mM Tris-HCl pH 8.3, 375 mM KCl, 15 mM MgCl2), 10 µL of 100 mM DTT and 5 µL of methylation dNTP mix), and gently mixed and equilibrated for 1 min at 37 ^{o}C. Finally, reaction was added 800 units of enzyme MMLV reverse transcriptase (8 µL), gently mixed and incubated at 37 ^{o}C for 60 min. This step was done for the first cDNA strand synthesis.

- **The second cDNA strand synthesis**

100 µL of fisrt strand reaction above was used for the second strand in of 500 µL of reaction. 100 µL of first strand synthesis was chilled on ice and added the other components including 270. 8 µL of water, 100 µL of 5X second strand synthesis buffer (250 mM Tris-HCl pH 7.5, 425 mM KCl, 22 mM MgCl2), 12 µL of 100 mM DTT, 4 µL of methylation dNTP mix, 10 µL of DNA polymerase I (10 units/µL), 3.2 µL of RNase H (1 unit/µL)) to 500 µL in final volume. Reaction was gently mixed, incubated at 15 ^{o}C for 90 min and followed by adding 500 µL PCA (phenol:chloroform:isoamyl alcohol) (25:24:1), vortexing 30 sec and centrifuging at 12,000 rpm for 3 min. The aqueous phase was collected, transferred to a fresh tube and added 2 µL of glycogen, 500 µL of ammonium acetate and 600 µL isopropanol, then inverted several times to mix well. Further, reaction was incubated 5 min at RT and centrifuged at 12,000 rpm for 10 min. Sample was carefully discarded the supernatant and rinsed the pellet with 0.5 mL of 70% ethanol and then 100% ethanol, followed by centrifuging 12,000 rpm for 5 min for each rinse. The pellet was dried thoroughly and resuspended in 40 µL TE buffer. This solution can be used with end modification (in next below, section 4.3.3.2) or stored at -20 ^{o}C.

4.3.3.2 End modification of cDNA

cDNA is flushed with T4 DNA polymerase for creating blunt ends. 40 µL of the prepared DNA-solution above (section 4.3.3.1) was added the other reaction components (2 µL of water 6 µL of 10X reaction buffer, 3 µL of 100 mM DTT, 6 µL of 1 mM dNTPs, 3 µL of T4 DNA polymerase (1 unit/µL)) to 60 µL of total volume, gently mixed and incubated at 11 ^{o}C for 20 min. Further, reaction was added 40 µL TE, 100 µL of PCA, and followed by vortexing, centrifuging at 12,000 rpm for 4 min and collecting the aqueous phase to a fresh tube. The aqueous phase was added 100 of chroroform:isoamyl alcohol (24:1), vortexed and centrifuged as above. The aqueous phase was collected to a fresh tube, and added 2 µL of glycogen, 100 µL of ammonium acetate and 500 µL of 100% ethanol, then mixed well. Reaction was hold at -20 ^{o}C for 1.5 h, then centrifuged 12,000 rpm for 15 min and discarded the supernatant. The pellet was collected and rinsed with 500 µL of 70% ethanol, and then 100% ethanol by centrifuging 12,000 rpm for 5 min for each rinse. The pellet was dried thoroughly and resuspended in 22 µL TE buffer and used 2 µL for DNA measurement and 20 µL for linker ligation (next section below, section 4.3.3.3) or stored at -20 ^{o}C.

4.3.3.3 Ligation to directional *Eco*RI/*Hind*III linkers

Directional *Eco*RI/*Hind*III linkers prepared above (section 4.3.3.2) were phosphorylated by a brief incubation with T4 polynucleotide kinase and immediately used for ligation. To do this reaction, 10 µL of blunt-ended cDNA prepared above (section 4.3.3.2) was added other reaction components including 2 µL of 10X ligation buffer (200 mM Tris-HCl pH 7.6, 100 mM MgCl2, 240 µg/mL BSA), 2 µL of 1 mM ATP, 2 µL of 100 mM DTT, 2 µL of directional *Eco*RI/*Hind*III linkers, 0.5 µL of T4 polynucleotide kinase (5 units/µL) and incubated for 5 min at 37 ^{o}C. The tube of reaction was placed on ice, added 2 µL of T4 DNA ligase (4 units/µL), and incubated at 16 ^{o}C overnight (8-12 h).

4.3.3.4 *Eco*RI and *Hind*III digestion

After the ligation above (section 4.3.3.3), the ligase in reaction was inactive by heating at 70 ^{o}C for 15 min and hold sample at RT to reduce the temperate slowly. Further, reaction was added other reaction components (56.5 µL of water, 10 µL of 10X *Hind*III buffer, 10 µL of *Hind*III (10 units/µL)) to 100 µL of total volume and incubated at 37 ^{o}C for 2 h. Furthermore, reaction was added 10 µL of *Eco*RI (10 units/µL) and 10 µL of 10X *Eco*RI adjustment buffer and incubated at 37 ^{o}C for 4 h. Finally, reaction was added 120 µL of PCA to denature enzymes, gently mixed and collected the aqueous phase to a fresh tube for doing size fractionation (next section below, section 4.3.3.5).

4.3.3.5 Size fractionation

This step helps to discard the small cDNA products (<300 bp) and excess linkers that produces cDNA ready for ligation with vector arms. For this work, first the gel filtration resin column was prepared by using 2 mL resin suspended in storage buffer onto Mini column, equilibrated the column with column buffer (5 × 1 mL). The column buffer was drained to the drop of column bed, carefully transferred the cDNA solution prepared above (section 4.3.3.4) onto the column. After the cDNA has settled into the resin, sample was gently added 200 µL 1X column buffer without disturbing the gel bed surface, then added 250 µL 1X column buffer and collected the eluted sample. The eluted sample was added 1 µL of 10 mg/mL glycogen and 150 µL of isopropanol, vortexed and mixed for 5 min. Further, sample was centrifuged at 10,000 rpm for 10 min then discarded the supernatant and collected the pellet. Furthermore, the pellet was rinsed in 500 µL of 70% ethanol and then 100% ethanol as above. Finally, the pellet was dried at RT and resuspended in 20 µL of TE. This ample can be used for ligation to vector arms stored at -20 ^{o}C (next section below, section 4.3.3.6).

4.3.3.6 Ligation of prepared-cDNA to vector arms

This reaction was done in 5 µL after adding reaction components (1.5 µL of insert DNA (approximately 0.02 pmol), 1 µL of T7 select vector arms (0.02 pmol), 0.5 µL of 10X ligase buffer, 0.5 µL of 100 mM DTT and 1 µL of T4 DNA ligase) and incubating at 16 ^{o}C for overnight (8-12 h). This sample be used for packaging (section 4.3.3.7) or stored at 4 ^{o}C until use.

4.3.3.7 cDNA packaging in T7 packaging extracts

The prepared-ligation above (section 4.3.3.6) was directly added to T7 packaging extracts *in vitro* in 30 µL of final volume (5 µL of prepared-ligation above and 25 µL of extract). Reaction was incubated at 22 ^{o}C for 2 h, followed by adding 270 µL LB media to stop the reaction. Finally, plaque assay was performed (section 4.2.2) to calculate the number of recombinant phages generated. At the same time, phages are also amplified for phage storage (section 4.2.1).

4.3.3.8 Phage enzyme-linked immunosorbent assay for validation

B5615 *E. coli* cells were infected either UQCRB–displayed phages or T7 phages as control. Cells were grown in LB media until lysing. The lysed *E. coli* containing amplified library was then clarified by centrifuging to be used in assay. An anti-T7 tail fiber antibody-coated plate was blocked by blocking buffer for 1 h at RT (2% BSA in PBS-T buffer), then washed by PBS-T buffer (3 times × 5 min) and followed by incubating with either lysed *E. coli* containing UQCRB–displayed phages or lysed *E. coli* containing T7 phages for 1 h at RT. After washing out unspecific binding (3 times × 5 min) by PBS-T buffer, the plate was then incubated with the biotinylated molecule provided in different concentrations for 1 h at RT. The plate was then washed thoroughly prior to incubation with streptavidin coupled to HRP which was diluted in blocking buffer for 1 h at RT. After washing by PBS-T buffer (3 times × 10 min, at RT), TMB substrate (Cell signaling) was added. The reaction was stopped with 1 N HCl and absorbance was measured at 450 nm.

4.4 Expression and protein purification of CAS

4.4.1 Expression of CAS in *E. coli*

E. coli strain BL21-codonPlus(DE3)-RIL was transformed DNA (pOPINHis-CAS or pOPINHis.EGFP-CAS) and placed on a LB agar plate supplemented with 100 µg/mL Amp and 25 µg/mL Cam at 37 ^{o}C overnight. Single colony from the agar plate was picked and pre-culture in 100 mL SB media supplemented with 100 µg/mL ampicillin (Amp) and 25 µg/mL chloramphenicol (Cam) at 37 ^{o}C overnight until transferred into bigger culture media. Pre-cultured bacteria were grown in 10 L of SB (in six big flasks) medium supplemented with 100 µg/mL Amp and 25 µg/mL Cam at 28-30 ^{o}C on incubator with shaking at 160 rpm until the value of absorbance at 600 nm (OD_{600}) reached approximately 0.6 and cold them to 18-20 ^{o}C for induction of protein expression. Expression was induced with 0.4 mM IPTG at OD_{600} of 0.6 at 18-20 ^{o}C on incubator with shaking 160 rpm for 18-20 h. During this time, protein expression should be checked. Small amount of cells (100-200 µL cells) were collected, centrifuged and added SDS loading buffer to final 1X, further heating at 95 ^{o}C for 5 min and run on SDS-PAGE gel. This gel was stained by coomassie blue to visualize the protein overexpression before sample harvesting of 10 L.

4.4.2 *E. coli*-lysate preparation and protein purification

After 18-20 h IPTG (isopropyl β-D-1-thiogalactopyranoside) induction, cells were harvested by centrifuging at 6000 rpm, 4 ^{o}C for 15 min (Beckman), discarded the media carefully and followed by washing with cold PBS. After washing step and collect the cell pellet by centrifuging, cells were either frozen in liquid nitrogen and immediately stored at -80 ^{o}C for further protein purification or used for purification directly.

Harvested cells were suspended in lysis buffer (section 3.3) and lysis was performed by sonication. The cell lysate was clean by centrifuging at 30,000 rpm at 4 ^{o}C for 30 min using ultracentrifuge (Beckman). After centrifugation the supernatant was loaded with flow rate of 2 mL/min on a 5 mL Hi-Trap Ni-NTA column which has been equilibrated with washing buffer (section 3.3). After washing step with washing buffer at flow rate of 2 mL/min until the value of absorbance showed the baseline, proteins were eluted with gradient of elution buffer (section 3.3) at a flow rate 1 mL/min and collected 1.5 mL per fraction in 2 mL-eppendoft tube. The collected fractions were combined and digested with PreScission protease (3C protease) to removed His-EGFP (approximately 0.5 unit of PreScission protease per 100 µg proteins) in PreScission buffer (section 3.3) at 4 ^{o}C overnight in dialysis membrane tubing at 4 ^{o}C, followed by 2 times of buffer exchanging (section 3.3) to discard EDTA for 4 h and re-loading sample on a 5 mL Hi-Trap Ni-NTA column to remove His.EGFP and uncut His.EGFP-CAS with flow rate at 2 mL/min to collect fractions. Further fractions of proteins were combined and purified by size exclusion chromatography using Sephadex G-200 column for CAS FL (full-length CAS) or Sephadex G-75 column for CAS fragments with a flow rate at 1 mL/min and 1.5 mL per fraction. Proteins were concentrated and removed salt by centriguging using Amicon tube; finally proteins were checked and stored at -80 ^{o}C.

4.5 RAN preparation

4.5.1 Expression and protein purification of RAN

The pET-3d-Ran was transformed in *E. coli* BL21-codonPlus(DE3)-RIL. Bacteria were grown in LB medium supplemented with 100 µg/mL ampicillin at 37 ^{o}C overnight. Expression was induced with 0.1 mM IPTG at OD_{600} of 0.6. The cells were grown at 25 ^{o}C overnight. Harvested cells were suspended in lysis buffer (section 3.3) and lysis was performed by sonication. After centrifugation, the supernatant was loaded on the Fractogel column with loading buffer (section 3.3) and eluted to collect protein in elution buffer (section 3.3). Further proteins were precipitated in 3.9 M ammonium sulfate and centrifuged to collect protein pellet. This protein pellet was resuspended in loading buffer and removed salt by centrifuging using Amicon tube; finally proteins were checked and stored at -80 ^{o}C. This work was done by Ms. Christine Nowak.

4.5.2 Nucleotide exchange of RAN

Nucleotide exchange reaction was done with 0.42 µmol RAN (10 mg) and 1.67 µmol nonhydrolyzable GTP analogue guanosine 5'-O-(beta, gamma-imidotriphosphate) (GPPNHP) in reaction (which contains 100 mM ammonium sulfate, 0.1 mM ZnCl2, alkaline phosphatase (5-10 U/mg protein), 20 nM KPi, pH 7.0) at 4 ^{o}C overnight on the rotating wheel. Further protein purification was done in loading buffer (section 3.3) using HiTrap desalting column, protein fractions then were concentrated and measured protein concentration using Bradford assay. Nucleotide exchange was checked with HPLC. This work was done by Ms. Christine Nowak.

4.6 Biochemical methods

4.6.1 Enzyme-linked immunosorbent assay for binding study

1 nmol of biotinylated tubulexin A was immobilized on a streptavidin coated 96-well plate (High Binding Capacity Streptavidin Coated Plate, Thermo Scientific) at RT for 1 h. The plate was washed with PBS prior to blocking with blocking buffer (2 % BSA in PBS-T buffer) for 30 min followed by washing in washing buffer (PBS containing 0.1% BSA and 0.05% Tween 20, 3 times × 10 min, at RT). The plate was incubated for 2 h at RT with different concentrations of CAS protein in blocking buffer. After washing, a goat anti-CAS antibody (Santa Cruz) which was diluted at 1:1000 in in blocking buffer is added to the wells and incubated for 2 h at RT. The plate was washed again prior to incubation with donkey anti-goat IgG coupled to HRP (Santa Cruz) which was diluted at 1:10,000 in blocking buffer. After washing 3 times with washing buffer (3 times × 10 min, at RT), TMB (Cell signaling) was added. The reaction was stopped with 1 N HCl and absorbance was measured at 450 nm.

4.6.2 Tubulin polymerization *in vitro* assay

4.6.2.1 *In vitro tubulin* polymerization assay by measuring absorption

The test compounds including controls were incubated to 10 µM porcine-tubulin (Cytoskeleton) in reaction (80 mM Na-PIPES pH 6.9, 1 mM MgCl2, 1 mM EGTA and 0.88 mM Na-glutamate) at RT for 30 min, then the samples were cooled at 4 °C for 15 min and pipet samples in a microtiter plate (Corning 96 Flat Bottom Transparent Polystyrol Half area, Corning Incorporated). Polymerization was induced by the addition of 0.5 mM GTP and was monitored by means of absorption at 340 nm (measured by turbidity) at 37 °C in the Inifinite® M200 plate reader (Tecan, Grödig, Austria) for 90 cycles (around 60 minutes). Blank values were subtracted from all sample values.

4.6.2.2 *In vitro* tubulin polymerization assay by measuring DAPI fluorescence[293,294]

The test compounds including controls were dissolved in general tubulin containing 5% DMSO. An aliquot (5 µL) of each compound solution was transferred to a 96-well plate at RT. The tubulin solution was prepared by dissolving a purified tubulin in the tubulin reaction (2.0 mg/mL tubulin, 1 mM GTP, 10 µg/mL DAPI, 61% (v/v) general tubulin buffer and 16.1% (v/v) tubulin glycerol buffer). An aliquot (50 µL) of this tubulin solution was added to the solutions containing the compounds or control (0.5% DMSO) in a microtiter plate (Costa 96-well black non-binding surface plate, Corning Incorporated) at 4 °C. The polymerization was recorded by reading the increase in fluorescence at excitation/emission 340 nm/ 460 nm in the Inifinite® M200 plate reader (Tecan, Grödig, Austria) at 37 °C for 90 cycles (around 60 minutes).

4.6.3 DNA binding studies based on fluorescence dyes

DNA sonication and purification was performed according to the Williams´s protocol.[295] R89 was titrated in a solution of 20 µM sonicated calf thymus DNA and 2 µM either DAPI or EtBr in DNA binding buffer (section 3.3) in a microtiter plate (96-well plate with non-binding surface black polystyrene, Corning incorporated). Two dyes were employed in this assay. EtBr binds to DNA by intercalation, whereas DAPI binds to the minor grooves of DNA. Both dyes bind to DNA and increase the fluorescent signal. When a compound binds to DNA at the same binding site using the same binding mode it will compete with the other dyes and will cause the reduction of the fluorescent signal. Fluorescence intensity was measured (for DAPI at excitation/emission 358 nm/461 nm or EtBr at excitation/emission 540 nm/594 nm). The fluorescence value of the sample was normalized to the value of the DMSO as a control.

4.6.4 Affinity purification for target protein validation

Streptavidin magnetic beads (S1420S, New England Biolabs) were resuspended the by shaking the bottle, then transferred 500 µL (2 mg) beads of resuspended beads into a new tube, placed the tube in the magnetic rack for 1-2 min, until the beads separated from the solution, removed the supernatant with a pipette, washed the beads two times with PBS buffer. Further, 500 µL of 10 µM biotinylated compound which was diluted in PBS buffer was added to the beads and incubated 1 h at RT. Finally, the tube was placed in the magnetic rack for 1-2 min to remove the supernatant with a pipette, and washed the beads two times with PBS buffer. The beads were then incubated for 1 h with 500 µg cellular extract or 2 µg purified CAS at 4 ^{o}C. The beads were then washed with lysis buffer (4 times × 10 min) and one time with PBS buffer at 4 ^{o}C before the proteins were eluted by various concentration of tubulexin A or heating at 95 ^{o}C for 5 min in 2X SDS loading buffer. Proteins were resolved on 12 % SDS-PAGE and transferred to a PVDF membrane by means of semidry electroblotting (section 4.1.9.4), followed by immunoblotting detection (section 4.1.9.5).

4.6.5 Colchicine competition assay for binding site study

The tubulin-colchicine complex was formed by incubating 5 µM tubulin with 50 µM colchicine in reaction mixture (1 mM GTP, 5% (v/v) general tubulin buffer, 16.9% (v/v) tubulin glycerol buffer and 76.6 % (v/v) TR-FRET buffer) for 30 min at RT. The podoverine A or nocodazole was then incubated with the preformed tubulin-colchicine complex for 30 minutes at RT. Fluorescence intensity was measured in a microtiter plate (Costa 96-well black non-binding surface plate, Corning Incorporated) using Safire2 plate reader (Tecan) at excitation/ emission 365 nm/ 435 nm. Blank values were subtracted from all sample values. Values were normalized to the DMSO control.

4.6.6 BODIPY FL-vinblastine competition assay for binding site study

The tubulin-vinblastine complex was formed by incubating 2.5 µM tubulin with 2 µM BODIPY-FL-vinblastine (Sigma, Deisenhofen, Germany) in reaction mixture (in 1mM GTP, 5% (v/v) general tubulin buffer, 16.9% (v/v) tubulin glycerol buffer and 76.6 % v/v TR-FRET buffer) for 30 minutes at RT. The podoverine A or vincristine was then added and the samples were incubated for 30 minutes at room temperature. Fluorescence intensity was measured in (Costa 96-well black non-binding surface plate, Corning Incorporated) using Safire2 plate reader (Tecan) at excitation/ emission 470 nm/ 514 nm. Blank values were subtracted from all sample values. Values were normalized to the DMSO control.

4.6.7 Pulldown procedure based on immunoprecipitation (IP)

4.6.7.1 Preparing of G protein beads

100 µl protein G sepharose beads (GE Healthcare Life Sciences) which was stored in 20% ethanol was washed twice by PBS buffer by centrifuging and blocked non-specific binding by 2% BSA in PBS buffer 1 h at RT, then washed them twice with PBS buffer. This protein G sepharose beads were ready to be used for pulldown assay.

4.6.7.2 Preparing complex of proteins and compound

Complex preparation was incubated with 5 µM importin alpha and 10 µM RANGPPNHP and 5 µM CAS in binding buffer (section 3.3)[272] for 30 min on ice, then added goat anti-CAS antibody (Santa Cruz Biotechnology) in 200 µL reaction to obtain final amount 7.5 µg/mL (1.5 µg) and incubated 1 h at RT. Finally, this solution was added either 500 µM tubulexin A or DMSO as a control. This complex of proteins, antibody and compound pre-incubated was ready to use.

4.6.7.3 Pulldown assay

Based on previous preparing steps, prepared-protein G Sepharose beads (section 4.6.7.1) were incubated with complex (complex of proteins, antibody and compound pre-incubated (section 4.6.7.2) at 4 ^{o}C overnight. After incubation, the beads and complex were washed 5 times with binding buffer (section 3.3) before the proteins were collected by adding 100 µl

2.5X SDS buffer and heating at 95 °C for 5 min. Proteins were resolved on 12 % SDS-PAGE and transferred to a PVDF membrane by means of semidry electroblotting (section 4.1.9.4), followed by immunoblotting detection (section 4.1.9.5).

4.6.8 Microscale thermophoresis (MST)

This method is based on the direct movement of molecules in optically microscopic temperature gradients generated by an IR-Laser (infrared laser). The movement is determined by the entropy of the hydration shell around molecules or by a change in size. Stability and conformation of molecules alters this hydration shell. The readout method of the interaction analysis is based on fluorescence, e.g. fusion proteins expressed with GFP/YFP/RFP and also biomolecules labeled with fluorescent dyes.

The experiment setup includes an infrared (IR)-laser coupled into the path of the fluorescence excitation/emission using an IR dichroic mirror (**Figure 17A**). The IR-laser is focused into the samples through the same optics of fluorescence detection that allows for a localized temperature increase on the order of a few hundred micrometers. The MST signal can be obtained by an MST instrument which is based on timescales and IR-laser heat source (**Figure 17B**). These MST events are defined as “Initial fluorescence” (the fluorescence of sample without laser heating), “MST temperature jump or MST T-Jump” (fluorescence change induced by sample heating before the themophoresis molecule transport sets in), “themophoresis” (fluorescence change induced by themorphoretic motion, “inverse T-Jump” (induced by sample cooling after turning of IR-Laser) and “Backdiffusion” (fluorescence recovery triggered by pure mass diffusion of molecules.[296]

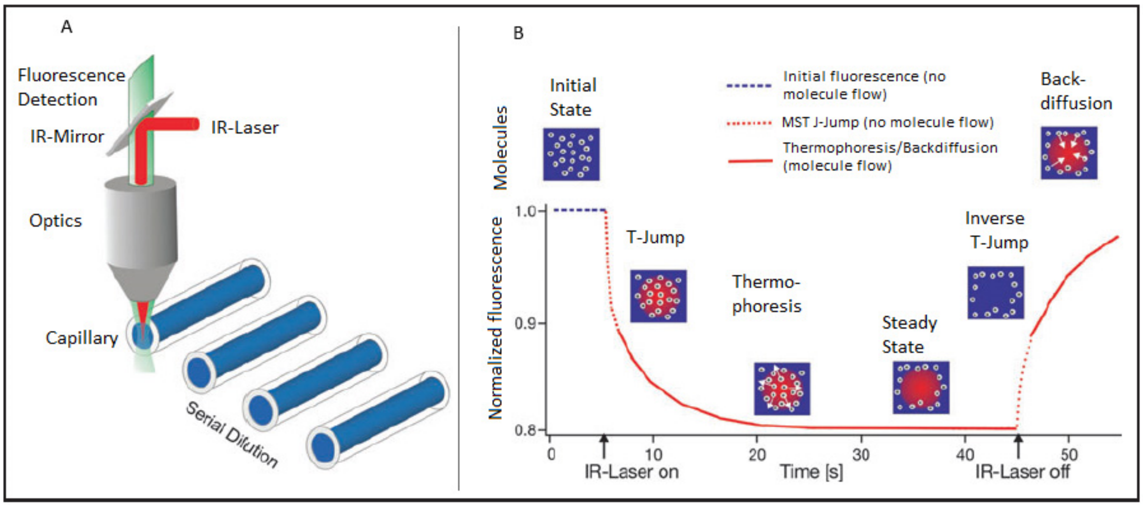
A
Fluorescence Detection
IR-Mirror
IR-Laser
Optics
Capillary
Serial Dilution
B
Initial State
Initial fluorescence (no molecule flow)
MST J-Jump (no molecule flow)
Thermophoresis/Backdiffusion (molecule flow)
Back-diffusion
Molecules
Normalized fluorescence
1.0
0.9
0.8
T-Jump
Thermo-phoresis
Steady State
Inverse T-Jump
0
10
20
30
40
50
IR-Laser on
Time [s]
IR-Laser off

Figure 17: MST instrument with experimental setup and process of MST.[296] **A**. MST instrument with experimental setup. An IR-Laser is applied to locally heat the sample in capillaries and the fluorescence within the capillary is excited and measured through the same optical element. T-Jump (temperature jump) and thermophoresis are directly measured via fluorescence change at different time scales. **B**. Process of MST. Initially, before IR-laser turned on, the molecules are homogeneously distributed and a constant ''initial fluorescence'' is measured. When the infrared (IR)-Laser is turned on, a fast temperature jump (T-Jump) is occurred, followed by thermophoretic molecule motion. The fluorescence decrease is measured for about 30 second (s). When the IR-Laser is turned off, an inverse T-Jump is observed, followed by the ''backdiffusion'' of molecules.[296]

The dissociation constant was determined using the MST device (Microscale_Thermophoresis V030, Monolith NT.115 Blue Green). The measurement was run in PBS buffer containing 100 nM His.EGFP-CAS. Compound titration series up to 16 dilutions was prepared in a protein solution (start from 100 µM of compound). After incubating at RT for 30 min and centrifuging (13,000 rpm at 4 ^{o}C for 5 min) to remove the aggregated protein. The reaction then was aspirated into a glass capillary. Further the capillary was placed on a tray. The tray contained up to 16 capillaries placed in the instrument. Within 10 minutes, it automatically measured the thermophoresis signal of each sample, and the instrument automatically recognized the presence of properly filled capillaries on the tray. The data can be used for calculate the dissociation constant with the Monolith NT.115 software. In this work, the binding affinity was assessed by means of MST, whereby the change of the fluorescence intensity or the change of concentration ratio of small molecule after IR-Laser heating (hot) and before IR-Laser heating (cold) value (Hot/Cold) or the temperature jump was used for K_d determination.

4.6.9 Circular dichroism for studying protein thermal stability shift

Protein melting points of CAS in the presence and absence of small molecules were detected with circular dichroism spectroscopy (Jasco J-815, 0,1cm path length cell). Melting curves were recorded in PBS buffer containing 20 µM CAS and either 50 µM of compound or 0.5% DMSO as control. CAS unfolding was detected at 233 nm (heating rate 1 ^{o}C per minute, starting from 25 ^{o}C to 90 ^{o}C).

4.7 Cell biological methods

4.7.1 Mammalian cell culture

Cells were cultured in suitable media supplemented with antibiotics, amino acid, sodium pyruvate and FBS for 3-4 days to obtain sufficient numbers of 70-80% confluent cells for experiment. When cells were confluent (70-80%), then subcultured or passaged to new flask using trypsinization. After discarding the old growing media, cells were washed with PBS and incubated with trypsin for 2-5 min at 37 ^{o}C, 5% CO_2. Trypsin digests the proteins which enable the cells to adhere to the vessel, makes cells detach from the surface of flask and become cell suspension. After trypsinization, cells were added with fresh media containing 10% FBS which inhibits trypsin and counted (section 4.7.4). Finally step, cells were diluted in fresh media and incubated at 37 ^{o}C, 5% CO2 for next culture.

4.7.2 Thawing the cells

The previously stored in liquid nitrogen, cell aliquot was immediately thawed with gentle shaking at 37 ^{o}C in a water bath for 2-3 min and quickly transferred into a 75 cm2 cell culture flask containing 10 ml of pre-warmed media. After incubation of the cells at 37 ^{o}C for 24 h, the old media is subsequently replaced by fresh media in order to remove the DMSO originally contained into the cell aliquot. Cells were cultured in suitable media to be confluent (70-80%), then subcultured or passaged to new flask (section 4.7.1).

4.7.3 Freezing cells

Cells were grown to a confluence of 80% in 75 cm2 cell culture flask and used for cells trypsinization (section 4.7.1). After trypsinization, centrifugation and discarding the old media, cell pellet was resuspended in cold PBS buffer and counted (section 4.7.4), followed by centrifuging again (1500 rpm for 5 min) and discarded PBS. The cell pellet was resuspended in DMEM media containing 10% DMSO and 10% FBS in absence of antibiotic with corresponding volume to 2 × 10^6 cells/mL. Furthermore, 0.5 mL of this cell stock was gently transferred to each cold cryovial. These cryovials were subsequently stored in an isopropanol filled-freezing container. This occurred within 24 h at -80 ^{o}C to reduce slowly temperature (1 ^{o}C/min) before being placed in liquid nitrogen for long-term storage.

4.7.4 Cell counts

The cell number can be counted using a Neubauer cell-counting chamber. The cell suspension were diluted with trypan blue to distinguish living cells and dead cells, with dead cells stained in blue. The cell suspension was pipetted into the counting chamber and was counted under microscope. The cells were counted in 4 large squares (0.1 µL per a large square which contains 16 small squares). The values obtained were averaged and the cell number determined by multiplying a factor of 10^4 to have the calculated number of cells (cells/mL) in sample.

4.7.5 DNA transfection to mammalian cells

4.7.5.1 DNA transfection to COS-7 cells

COS-7 cells were cultured in DMEM medium supplemented with 10% FBS and antibiotic (section 3.5) in humidified atmosphere containing 37 ^{o}C and 5% CO2. The day before transfection, 8 x 105 cells were seeded per 60-mm dish (50-80% confluent after 18-24 h) to be used for DNA transfection. The cells were discarded the old media and changed to fresh medium and transfected DNA (4µg DNA per dish) to them using DEAE-Dextran transfection based on the protocol of Schenborn and Goiffon.[297] Cells are cultured for next 48 h for lysate preparation.

4.7.5.2 DNA transfection to HEK293T cells

HEK293T cells were cultured in RPMI 1640 medium supplemented with 10% FCS and antibiotic in humidified atmosphere containing 37 ^{o}C and 5% CO2. 4-8 x 10^5 cells were seeded in 60-mm dish for 24 h. The cells were discarded the old media and changed to fresh medium and transfected DNA (1µg DNA per dish) using Effectene transfection reagent according to Qiagen's manual. Cells are cultured for next 48 h for lysate preparation.

4.7.6 Preparation cells lysate of mammalian cells

4.7.6.1 Preparation cells lysate of HeLa cells for affinity purification

HeLa cells were cultured in DMEM medium supplemented with 10% FBS and antibiotic (section 3.9.3) in incubator at 37 ^{o}C and 5% CO2. HeLa-cell pellet of 4 × 10^7 cells was resuspended in 1 mL lysis buffer (section 3.3), incubated then on ice for 20-30 min and vortexed every 5 min to lyse cells, finally centrifuged at 12,000 rpm for 15 min at 4 ^{o}C. The cell supernatant was transferred to another new tube. Furthermore protein amount of lysate was measured using Bradford protein assay (Bio-Rad) (section 4.1.9.1). Cell lysate was stored on ice until to be used for affinity purification.

4.7.6.2 Preparation cells lysate of HEK293T cells for chemical array

After 48 h of DNA transfection (section 4.7.5.2), HEK293T cells were discarded the old media and washed by PBS buffer to remove remaining medium and collect the cells in PBS buffer by pipetting, followed by centrifuging 5000 × g for 5 min at 4 ^{o}C. Cell pellet were then resuspended in PBS buffer and sonicated to lyse cells, finally centrifuged at 15,000 × g for 15 min at 4 ^{o}C. The cell supernatant was transferred to another new tube. Further protein expression was detected. For EGFP fluorescent-fused proteins (His.EGFP or His.EGFP-CAS), proteins were detected by means of the fluorescence signal of EGFP using SDS-PAGE gel scanning by Typhoon TM 9400. For protein lacking fluorescent tag (His-CAS), protein was detected by means of immunoblotting using specific antibody (anti-His tag antibody). Furthermore protein amount of lysate was measured using Bradford protein assay (Bio-Rad) (section 4.1.9.1). Cell lysate was stored on ice until to be used for screening.

4.7.7 Determination of cell proliferation using WST-1 reagent

4000 HeLa or KB-V1 cells were seeded in 96-well plate with clear bottom and after one day treated with the compounds for 48-72 h in quadruplicates. Then WST-1 reagent (Roche, Germany) was added to the media to a final concentration of 10%. After 25-45 min of incubation the absorbance was determined at 450 nm with the Infinite® M200 plate reader (Tecan, Grödig, Austria) and blank values were subtracted from all readings. Values were normalized to the DMSO control (n=4). The half maximal inhibitory concentration (50% growth inhibitory effect) (IC_{50}) was estimated by a sigmoidal fitting curve (OriginLabs Origin v. 6.0, Northhampton, USA).

4.7.8 Time-lapsed images using Metamopth

4.7.8.1 Time-lapsed images using Metamopth for HeLa cells

16,000 HeLa cells were seeded per well in a 24-well plate (PAA Laboratories GmbH) and incubated overnight. R89 was added to the wells at various concentrations in fresh media. 0.3% DMSO was used as a control. The effects of the compound were recorded using a time-lapse mode for 24 h with time intervals of 15 min. Cells were exposed for 60ms at 5% CO_2 at 37 °C. Image acquisition was performed with a Zeiss Axiovert microscope and the MetaMorph software using a brightfield mode and with a 20X objective.

4.7.8.2 Time-lapsed images using Metamopth for HeLa Fucci cells

16,000 HeLa cells were seeded per well in a 24-well plate (PAA Laboratories GmbH) and incubated overnight. R89 was added to the wells at various concentrations in fresh media. 0.3% DMSO was used as a control. The effects of the compound were recorded using a time-lapse mode for 24 h with time intervals of 40 min. Cells were exposed for 20ms at 5% CO_2 at 37 °C. Image acquisition was performed with a Zeiss Axiovert microscope and the MetaMorph software using a fluorescence mode (Azami and mKO) and with a 20X objective.

4.7.9 Caspase-3/7 activation analysis

Apoptosis induction was determined by measuring the activity of caspase-3 and caspase-7. 5000 HeLa cells were seeded per well in black 384-well plate, and after one day were treated in quadruplicates with the compounds for 20-24 h. Caspase-3/7 activation was determined by means of the Apo-ONE® Homogenous Caspase-3/7 Assay (Promega, Germany) after incubation with the substrate in the dark at room temperature for 3 h. Fluorescence intensity was measured at excitation/emission 485 nm/535 nm in the Beckman DTX880 plate reader and blanks were subtracted from all readings. Values were normalized to the DMSO control.

4.8 Immunofluorescence

4.8.1 General protocol for cell staining

Cells were washed with PBS buffer and fixed and permeabilized with 3.7% (v/v) formaldehyde in 1X PREM buffer for 20 min at RT. After blocking the unspecific binding with a blocking buffer (either with 1% BSA and 10% goat serum in PBS-T buffer for importin alpha, RANBP1 and pHistone H3 staining, or 2% BSA in PBS-T buffer for tubulin staining), the primary (rabbit anti-RANBP1 which was diluted at 1:200; mouse or rabbit anti-tubulin, rabbit anti-importin alpha and rabbit anti-pHistone H3 antibody which were diluted at 1:500 in blocking buffer) antibody was added and incubated for 1 h at RT. Samples were rinsed 3 times in PBS-T buffer prior to incubation at RT for 1 h with secondary goat anti-rabbit (or mouse) IgG antibody coupled to Alexa Fluor 488 (which was diluted at 1:500 in blocking buffer) to detect importin alpha (or RANBP1, pHistone H3, tubulin), and DAPI to detect DNA.

4.8.2 Mitotic cells staining and cytoskeleton staining on coverslip

20,000 HeLa cells were seeded per well in a 24-well plate containing coverslips overnight. R89 was added in the fresh media at 15 µM either 15 h for mitotic cells checking or 19 h for cytoskeleton checking. Cell staining was performed by general staining-protocol above (section 4.8.1) and TRIC-phalloidin was used to detect actin. After rinsing in PBS-T buffer, coverslips of stained cells were mounted with Aqua Polymount overnight and images were taken using a Zeiss Observer microscope with a magnificent objective lens of 63X.

4.8.3 Phenotypic screening in HeLa cells

4000 HeLa cells were seeded at per well in a microtiter plate (96-well plate with black bottom, Corning Incorporated) overnight, and then the compound was added to fresh media at 30 µM for 24 h. Cell staining was performed by general staining-protocol above (section 4.8.1) and TRIC-phalloidin was used to detect actin. After rinsing in PBS-T buffer cells were stored in PBS buffer at 4 °C until images were acquired using Zeiss Axiovert Screening microscope and MetaMorph software. Images were taken automatically with a 20X objective.

4.8.4 Importin alpha screening in HeLa cells

4000 HeLa cells were seeded per well in a microtiter plate (96-well plate with black bottom, Corning Incorporated) overnight. The compound was added in the fresh media at 30 µM for 4 h. Cell staining was performed by general staining-protocol above (section 4.8.1). After rinsing in PBS-T buffer cells were stored in PBS buffer at 4 °C until images were acquired using Zeiss Axiovert Screening microscope and MetaMorph software. Images were taken automatically with a 20X objective.

4.8.5 Importin alpha and RANBP1 staining on coverslip

20,000 HeLa cells were seeded per well in a 24-well plate containing coverslips overnight. R89 was added in the fresh media with various concentrations for 2 h. Cell staining was performed by general staining-protocol above (section 4.8.1). After rinsing in PBS-T buffer, coverslips of stained cells were mounted with Aqua Polymount overnight and images were taken using a Zeiss Observer microscope with a magnificent objective lens of 63X.

4.8.6 Mitotic maker pHistone H3 analysis

4000 HeLa cells were seeded per well in a 96-well plate overnight. R89 was added with various concentrations in fresh media or 0.3% DMSO as a control and 1 µM nocodazole for the positive control for 15 h and then removed from the media. Cell staining was performed by general staining-protocol above (section 4.8.1). After rinsing in PBS-T buffer cells were stored in PBS buffer at 4 °C until images were acquired using a MetaMorph microscope. Images were taken automatically with a 20X objective. Images were analyzed using the MetaMorph software for image analyses of cell cycle included the nuclei size, DNA staining intensity after subtracting the local background signal, and fluorescence intensity value of the pHistone H3 staining after subtracting the local background signal. The obtained data on the number of mitotic and total cell were exported to an excel file.

4.8.7 Doulink II fluorescence

This work done based on the manual of OLINK Bioscience (the Duolink In Situ Fluorescence, OLINK Bioscience). In principle, Adherent cells are prepared (with or without compound treatment), then fixed and pre-treated with blocking buffer for primary antibodies incubation. Further the secondary antibodies conjugated with oligonucleotides (PLA prober MINUS and PLA prober PLUS) are added in reaction and incubated. Furthermore, the ligation solution consisting of two oligonucleotides and ligase is added to reaction to permit oligonucleotides hybridize to two probes PLA and join to a closed circle if they are in close proximity. Finally, the amplification solution consisting the nucleotides and fluorescently labelled oligonucleotides and polymerase are added to reaction. The reaction is that the oligonucleotide arm of one PLA probe acts as a primer for a rolling-circle amplification (RCA) reaction and the ligated circle acts as a template for generating repeated sequences. The fluorescently labelled oligonucleotides will hybridize to the RCA to form the fluorescent spot which can be visible and analyzed by fluorescence microscope. In this work, experiments were done by process below:

4.8.7.1 Cell preparation

4,000 HeLa cells were seeded per well in a 96-well plate (PAA Laboratories GmbH) overnight. The compound was added in the fresh media at 30 µM for 4 h, then discarded and washed by PBS buffer. Further cells were fixed and permeabilized with 3.7% (v/v) formaldehyde in 1X PREM buffer for 20 min at RT.

4.8.7.2 Blocking and primary antibodies incubation

After blocking the unspecific binding site with a blocking buffer (2% BSA and 5% goat serum in PBS-T buffer), cells were incubated with primary antibodies for 1 h at RT in a humidity chamber. There were two primary antibodies which diluted at the same time in blocking buffer. There were three stocks of primary antibodies: rabbit anti-tubulin (diluted 1:500) and mouse anti-CAS (1:100), rabbit anti-importin alpha (diluted 1:500) and mouse anti-CAS (1:100), mouse anti-RAN (1:200) and rabbit anti-CAS (1:100). After this incubation step, cells were washed by PBS-T (3 times × 5 min at RT), then cells were stored in PBS buffer for next step.

4.8.7.3 PLA probes

PLA were prepared by mixing the PLA probe minus and the PLA probe plus by ratio 1:1 in blocking buffer and incubated for 20 min at RT. Further, 20 µL of this probe solution was added to each well of prepared-cells above after discarding PBS buffer (which was used for storing cells in step above), following by incubation for 1 h at 37 ^{o}C in a pre-heated humidity chamber. After antibodies incubation, cells were washed by PBS-T (3 times × 5 min at RT), and stored in PBS buffer for next step.

4.8.7.4 Ligation

Cells were discarded PBS buffer and added 20 µL of ligase which was diluted at a 1:40 dilution in ligation buffer per well and incubated for 30 min at 37 ^{o}C in a pre-heated humidity chamber. After this incubation step, cells were washed by PBS-T (3 times × 5 min at RT), and stored in PBS buffer for next step.

4.8.7.5 Amplification

Cells were discarded PBS buffer and added 20 µL of polymerase which was diluted at a 1: 80 dilution in 1X amplification buffer per well and incubated for 100 min at 37 ^{o}C in a pre-heated humidity chamber. After this incubation step, amplification reaction was discarded and cells were washed by PBS-T containing DAPI diluted at 1:2000 for the first washing time (10 min), then other 2 times (2 times × 10 min at RT) with 1X wash B and one time with 0.1X wash B for 10 min. Finally, cells were stored in PBS buffer for imaging and analyzing in a fluorescence microscope. During storing the cells in PBS buffer, plate was stored at 4 ^{o}C in the dark.

4.8.7.6 Extra step for tubulin staining to mark cells

This step does not mention in the kit, this staining step is optimal step to mark the cell area. After PLA assay, the second staining for tubulin was done by a general protocol for cell staining above (section 4.8.1) and cells were used for another fluorescence imaging.

4.9 Microarrays on glass slides

4.9.1 Screening of microarray slides

Array slides were incubated with 1% skim milk in TBS-T buffer at RT for 1 h to block non-specific binding, followed by washing step (3 times × 5 min with TBS-T buffer on shake, 1min for spin dry). Further, array slides were incubated with either 50 µL purified protein sample (1 µM or 3 µM) at 30 ^{o}C for 1 h or 50 µL cell lysate (150 µg) at 4 ^{o}C for 1 h, then followed by another washing step (3 times × 5 min with TBS-T buffer, 1 min for spin dry). Furthermore, array slides were incubated 50 µL mouse anti-His tag antibody which was diluted at 1:100 in TBS-T buffer (GE Healthcare) at 30 ^{o}C for 1 h. This incubation was followed by another washing step (3 times × 5 min with TBS-T buffer on shake, 1min for spin dry) and incubation with 50 µL secondary antibody coupled to Cy5 (goat anti-mouse IgG, Invitrogen) at 30 ^{o}C for 1 h. After the final washing step (3 times × 5 min with TBS-T buffer, 1 min for spin dry) slides were scanned at 635 nm on a GenePix 4200AL microarray scanner (Amersham Biosciences, Foster city, CA).

Two copies were used for every slide; one was used for target protein (His-CAS or His.EGFP-CAS in 1% skim milk in TBS-T buffer) and another one for control (either His-EGFP in 1% skim milk in TBS-T buffer or only 1% skim milk in TBS-T buffer).

4.9.2 Data analysis for scanned arrays

The results of two array slides (one for target protein and one for control) were painted green and red respectively using Photoshop 5.5 software. The colour images were merged. The positive signals were detected as red signals and the false positive signals caused by binding of ligands to antibody or by auto-fluorescent signals of the ligand itself were detected as green or yellow signals.

The fluorescent signal was quantified using GenePix 6.1 software with local background subtraction. Fluorescent signal of each compound in array was corrected by the local background subtraction and the fluorescence intensity of the corresponding control slide (Equation 1). A relative ranking was used to select hit compound obtained (Equation 2).

Equation 1: $\Delta I = I(\text{sample}) - I(\text{reference})$

Equation 2: $\Delta I = \overline{\Delta I} + n \cdot SD$

Relative ranking: $n \geq 1: +; n \geq 2: ++; n \geq 3: +++$

I: Fluorescence Intensity of compound spot

SD: standard deviation

$\overline{\Delta I}$: mean fluorescence intensity of all compound spots

5 Results

5.1 Establishing a phage display protocol for target identification

The goal of this study was to establish a cDNA phage display protocol for affinity isolation of target proteins binding to small molecules of interest as an alternative to the affinity-based approach. After establishing the protocol, the already known target proteins of biotinylated small molecules had to be confirmed and possible additional new candidate targets were to be identified. To establish the method, a commercial cDNA phage display library (T7 phage displayed cDNA library of Human Breast Tumor cDNA library from Novagen) was used. The size of the library was $1.1*10^7$ primary phage clones.

Three different approaches that are based on biopanning were used for establishing the protocol (**Figure 18**). The principle of this method was described in section 1.2.1.3.1. In the first approach was performed without pre-incubation of the cDNA library with any control such as streptavidin-biotin or inactive analog before biopanning selection (**Figure 19A**) and 1% SDS were used for phage elution (first approach). Alternatively, the cDNA library was pre-incubated with streptavidin-polyethylene glycol (PEG)-biotin (in case affinity probe contained a PEG linker) to reduce nonspecific binding and bound phages were eluted with 1% SDS (second approach). In the third approach the cDNA library was pre-incubated with either streptavidin-PEG-biotin or inactive compound prior to the biopanning cycle and unmodified active compound was used for specific elution. The general steps of the second and the third approach are shown in **Figure 19B**.

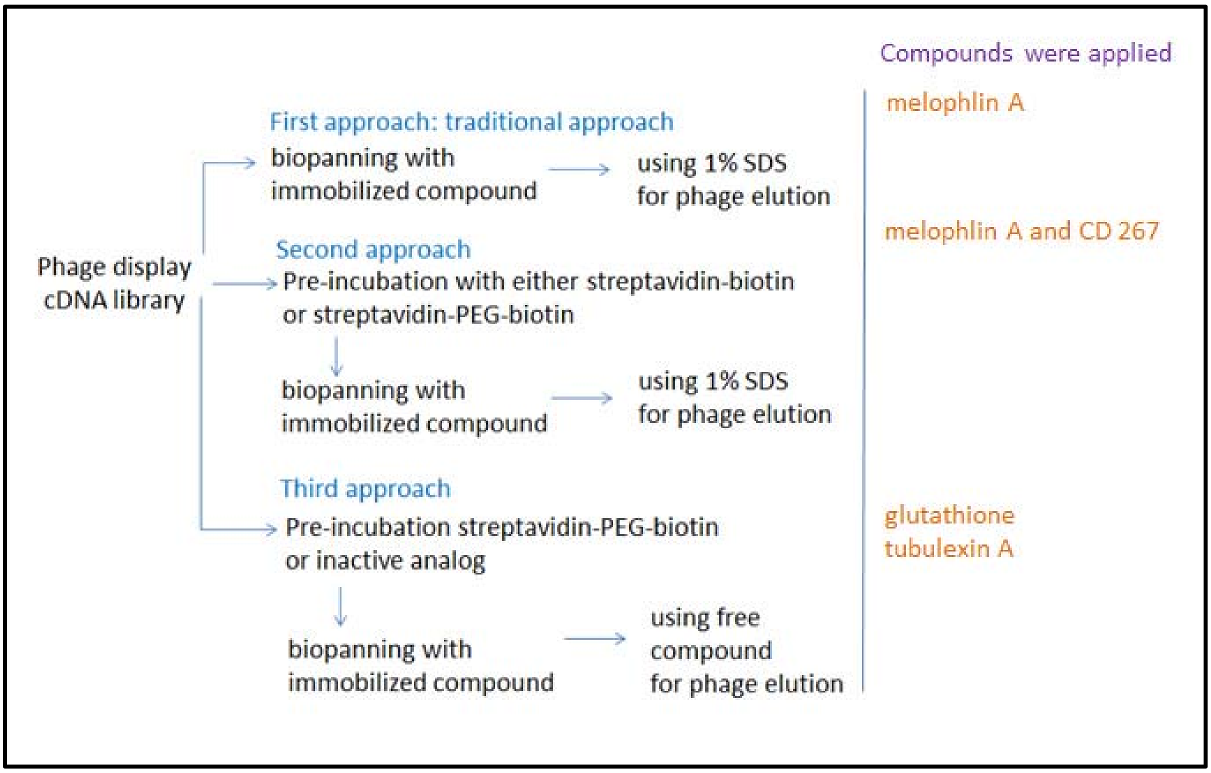
Compounds were applied
Phage display cDNA library
First approach: traditional approach
biopanning with immobilized compound
using 1% SDS for phage elution
melophlin A
Second approach
Pre-incubation with either streptavidin-biotin or streptavidin-PEG-biotin
biopanning with immobilized compound
using 1% SDS for phage elution
melophlin A and CD 267
Third approach
Pre-incubation streptavidin-PEG-biotin or inactive analog
biopanning with immobilized compound
using free compound for phage elution
glutathione
tubulexin A

Figure 18: Approaches that were employed for establishing a protocol for phage display.

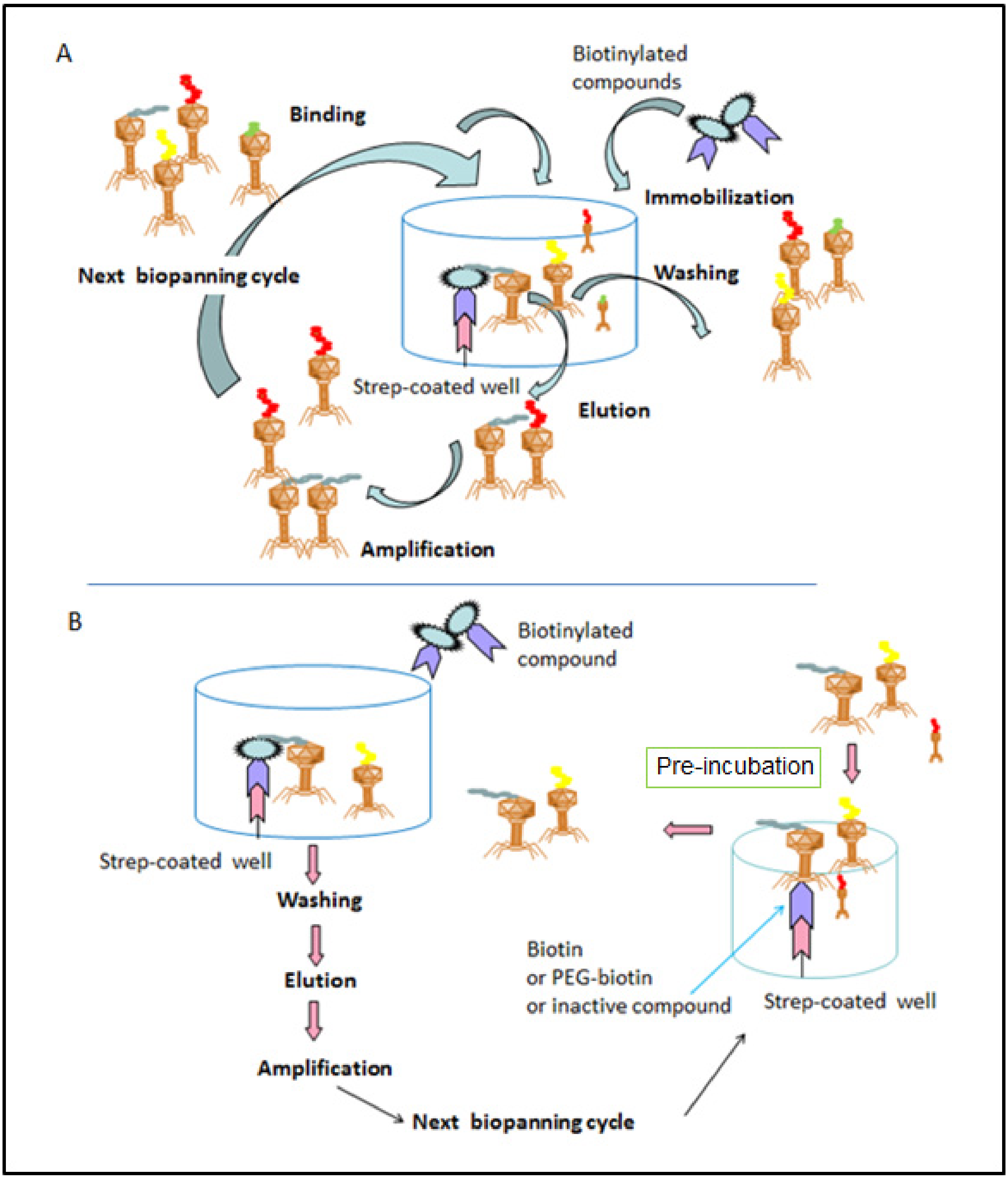
A
Biotinylated compounds
Binding
Immobilization
Next biopanning cycle
Washing
Strep-coated well
Elution
Amplification
B
Biotinylated compound
Pre-incubation
Strep-coated well
Washing
Elution
Amplification
Biotin
or PEG-biotin
or inactive compound
Strep-coated well
Next biopanning cycle

Figure 19: Biopanning cycle. **A**. Biopanning cycle without pre-incubation. **B**. Biopanning cycle with pre-incubation of the phage library with streptavidin-biotin, streptavidin-PEG-Biotin or inactive compound.

As a start, an active biotinylated melophlin A derivative and an inactive biotinylated analog of melophlin A (referred to as TK311) were subjected to phage display. Melophlin A reverses the phenotype of H-ras transformed NIH3T3 cells and of H-ras transformed MDCK-F3 cells.[298] This compound also promotes neurite outgrowth in PC12 cells.[298] Melophlin A causes reduction of MAP kinase phosphorylation in HeLa cells.[299] Using an affinity-based approach, human dynamin I-like protein, dynamin I, and dynamin II were identified as targets of melophlin A.[299] In this study melophlin A (**Figure 20A**) and biotinylated melophlin A as an active analog (structure containing X=$C_{15}H_{31}$, **Figure 20B**) and inactive analog (structure containing X=C_4H_9, **Figure 20B**).

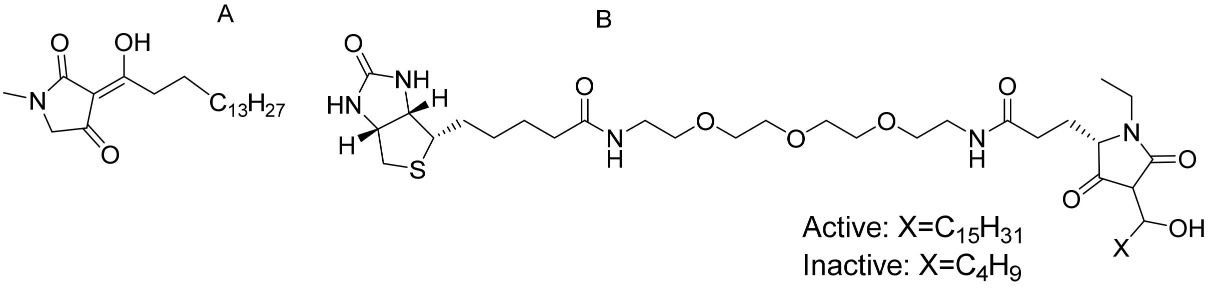

Figure 20: Chemical structures of probes based on melophlin A (A), biotinylated analog of active and inactive melophlin A (B).

For biopanning, the primary library was first amplified by infecting *E. coli* BLT5615 at a mid-log-phase (i.e. OD_{600} = 0.5-0.6) using a multiplicity of infection (MOI) of 0.001-0.01. *E. coli* lysates, which contained the phages, were clarified by centrifuging prior to further usage (see section 4.2.1). 10 µM of biotinylated compounds in PBS buffer were immobilized on streptavidin-coated 96 well plates (see section 4.2.3). For each binding-selection cycle, phage particles were incubated with the immobilized compounds and wells were washed with PBS-T buffer to remove non-specific binders. The bound phage particles were eluted with 1% SDS and immediately used for determination of phage titer. *E. coli* BLT5615 cells were infected with eluted phages and phages were amplified for the next round of selection. After six rounds of binding and selection, phage particles were used as templates for the amplification of the encoded genes by means of PCR employing the primers T7SelectUP and T7Selectdown. The PCR products were then analyzed by means of *Hinf*I fingerprinting using the *HinfI* restriction enzyme to digest PCR products. This step allowed identification identical phage clones prior to sequencing. Selected phage particles were employed as DNA of templates for a PCR with subsequent DNA sequencing using primers T7SelectUP or/and T7Selectdown (see section 4.2.4).

5.1.1 Identification of proteins that bind to melophlin A

The diversity of the phage clones in phage populations was analyzed using PCR of single phage plaques. Biopanning was employing immobilized biotinylated melophlin A (MeA) and TK311 as control. After round to round 6 binding-selection cycles, bound phage particles of phage population were eluted with 1% SDS and were used as DNA templates for PCR. PCR products were resolved by means of agarose gel electrophoresis. *Hinf*I fingerprint was employed for analysis of the phages obtained from round 6.

Single phage plaques from round 2 to round 5 were employed and 19 phage clones for each immobilized compound were investigated per round. The PCR analysis revealed that DNA fragments of different length are amplified and more phage clones bound to MeA than to TK311. Moreover, the diversity of the phage clones in the population was reduced by increasing the number of biopanning cycles (**Figure 21**). After round 5, the length of the PCR products for immobilized MeA was different, while the size of PCR products, which was approximately 250 bp, for immobilized TK311 was almost similar to the background control (without immobilized compound) (**Figure 22**). The result showed clearly different diversity of the phage clones which bind to the compounds.

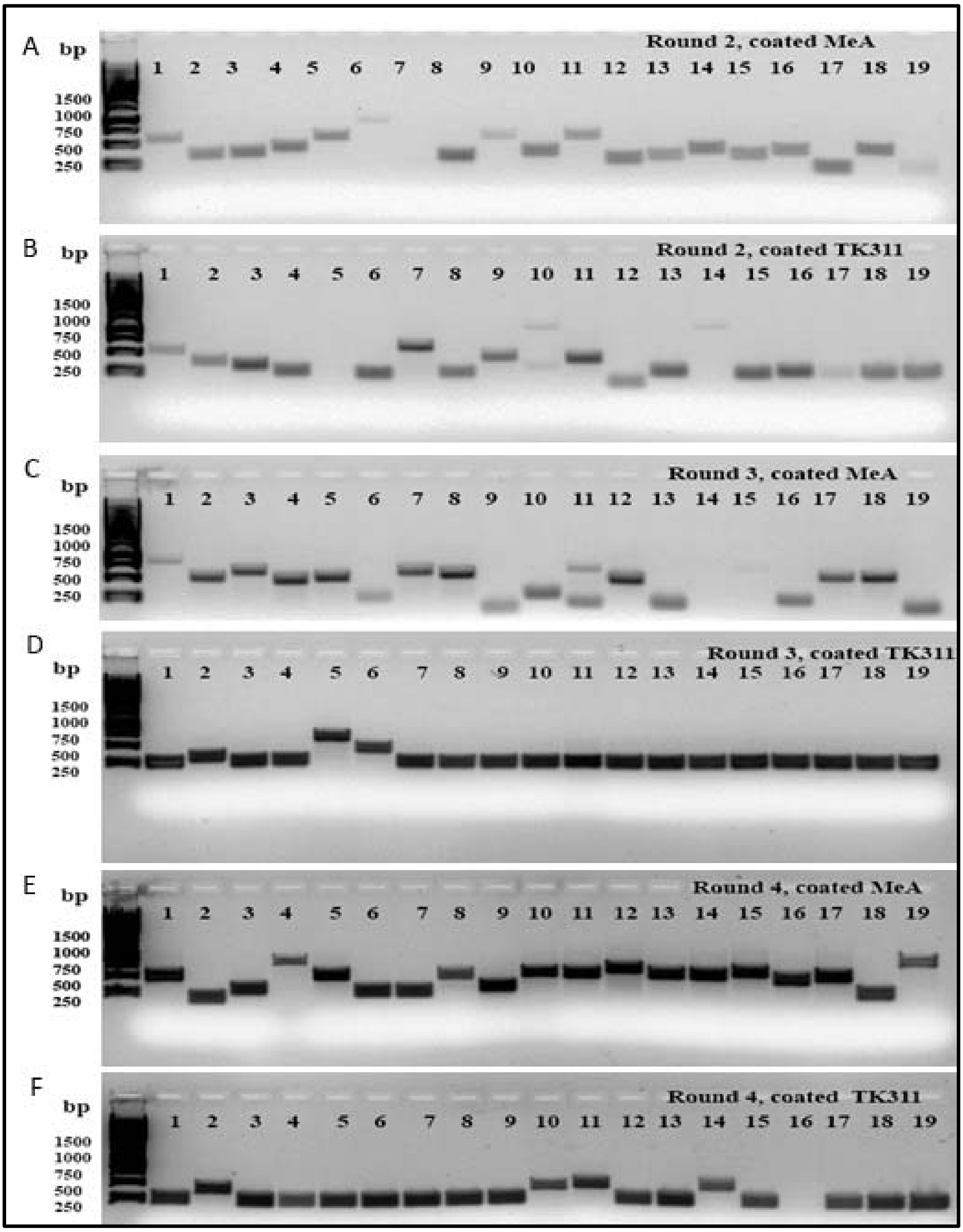
A
B
C
D
E
F
bp
1500
1000
750
500
250
Round 2, coated MeA
Round 2, coated TK311
Round 3, coated MeA
Round 3, coated TK311
Round 4, coated MeA
Round 4, coated TK311
1 2 3 4 5 6 7 8 9 10 11 12 13 14 15 16 17 18 19

Figure 21: PCR products after biopanning obtained from round 2 to round 4 using immobilized biotinylated melophlin A (MeA) or TK311. After several binding-selection cycles, bound phage particles were eluted with 1% SDS and used as DNA templates for PCR. PCR products were resolved on an agarose gel using a red dye as staining and images were recorded under UV light. **A**, **C** and **E**: PCR products using phage clones obtained from biopanning from round 2 to round 4 using immobilized biotinylated melophlin A (MeA). **B**, **D** and **F:** PCR products using phage clones obtained from biopanning from round 2 to round 4 using immobilized biotinylated inactive analog TK311.

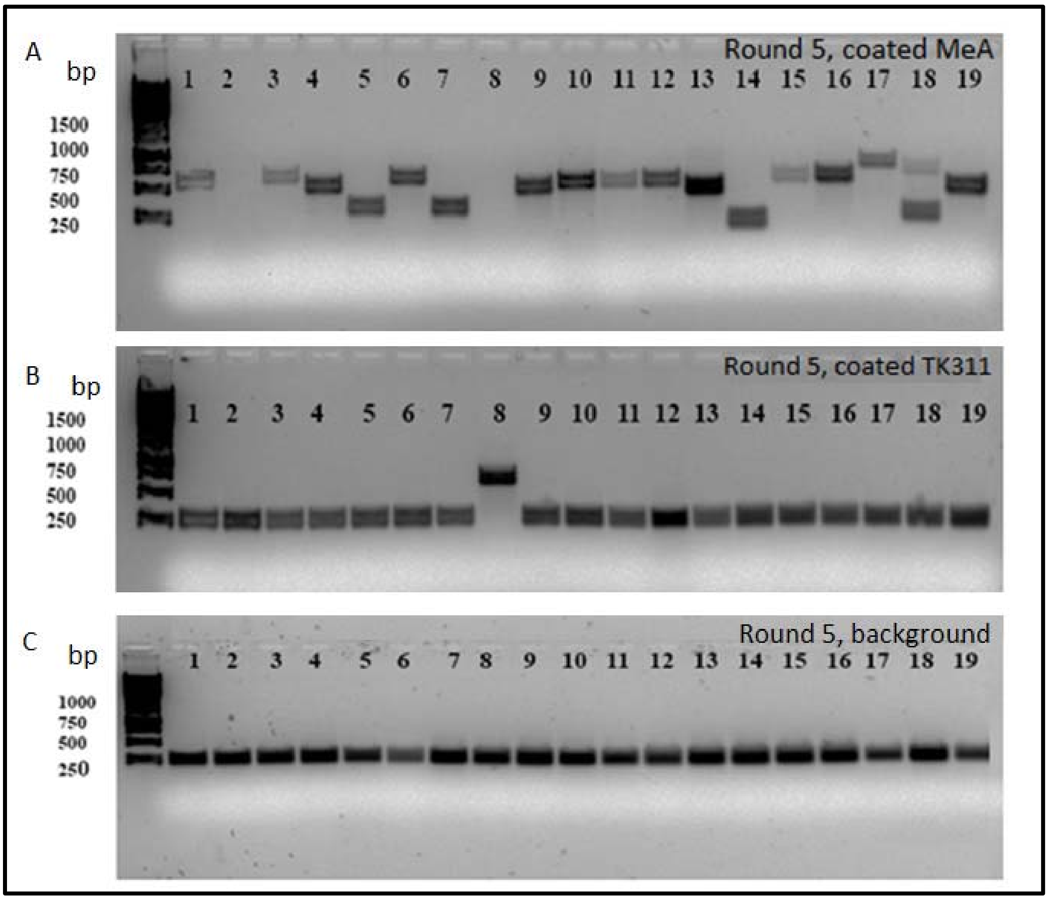
A
bp
1500
1000
750
500
250
Round 5, coated MeA
1 2 3 4 5 6 7 8 9 10 11 12 13 14 15 16 17 18 19
B
bp
1500
1000
750
500
250
Round 5, coated TK311
1 2 3 4 5 6 7 8 9 10 11 12 13 14 15 16 17 18 19
C
bp
1000
750
500
250
Round 5, background
1 2 3 4 5 6 7 8 9 10 11 12 13 14 15 16 17 18 19

Figure 22: PCR products of biopanning obtained in round 5 using biotinylated melophlin A (MeA) or TK311. After several binding selection cycle, bound phage particles were eluted with 1% SDS and used as DNA templates for PCR. PCR products were resolved on an agarose gel using a red dye as staining and images were recorded under UV light. **A.** PCR products of biopanning obtained in round 5 using immobilized active biotinylated melophlin A. **B**. PCR products of biopanning obtained in round 5 using immobilized biotinylated inactive analog TK311. **C**. PCR products of biopanning obtained in round 5 without compound immobilization (as background binders, using streptavidin coated-well only).

For further analysis, the diversity of phage clones in the population obtained after round 6 was analyzed not only using PCR of single phage clones but also by *HinfI* fingerprinting. *HinfI*-digested PCR products do not only permit to study the diversity of phage populations, but also allow to determine identical clones and to select clones for DNA sequencing. For example, for phage clones 1 and 3 the same size of PCR products of approximately 500-750 bp was obtained (**Figure 23A**). After *HinfI* digestion, the DNA fragments of clone 1 and 3 have the restriction pattern and thus the phages are grouped in one group (1st group). Phage clones 6, 7 and 8 give rise to PCR products of similar size as clone 1 and 3. However, *HinfI* digestion of the DNA fragments display similar pattern for clones 6, 7 and 8, which differs from the pattern of clone 1 and 3. Thus, clones 6, 7 and 8 are classified as a second group (2^{nd} group) (**Figure 23B**). After restriction analyses many clones were assigned to the same group. For this reason, only few samples of each group were chosen for DNA sequencing to the reduce costs for sequencing.

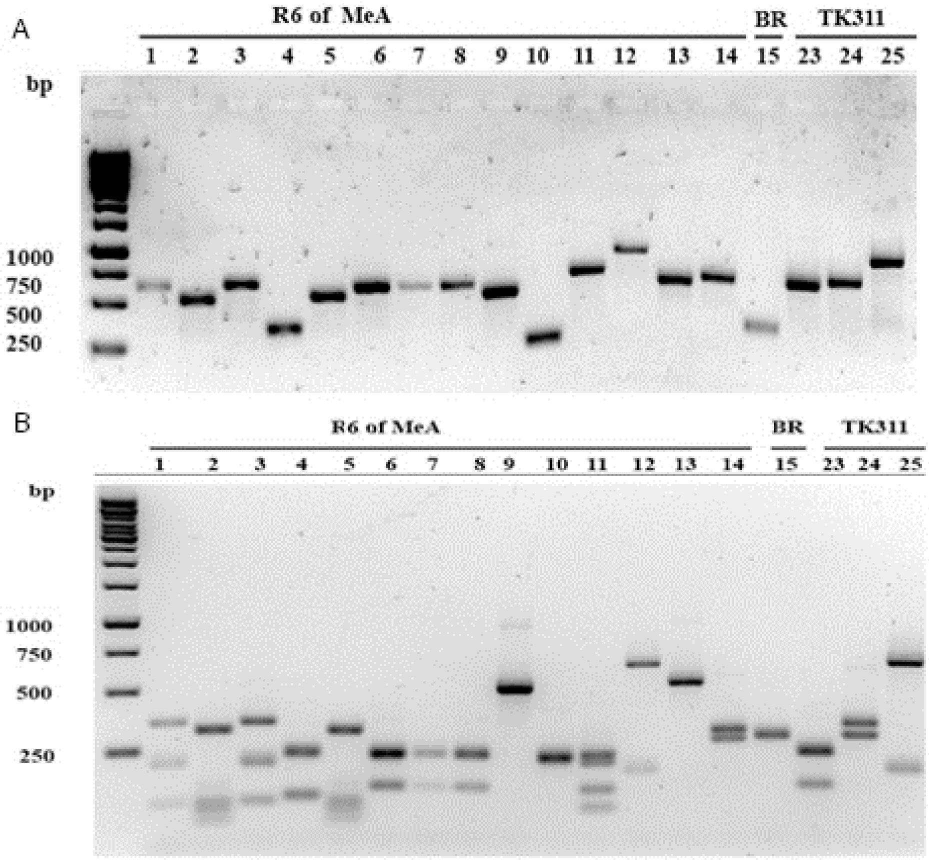

Figure 23: Biopanning using MeA and T7 phage displayed human breast tumor cDNA. **A**. PCR products obtained using phage clones as DNA templates were detected by means of agarose gel electrophoresis. 1-14: PCR products of phage clones after biopanning with MeA; 15: PCR products of phage clone for the background (BR); 23-25: PCR products of phage clones for biopanning with TK311. **B**. *HinfI* fingerprinting. PCR products were digested by *HinfI*. DNA products were detected by means of agarose gel electrophoresis. 1-14: Digested PCR products of phage clones after biopanning with MeA; 15: Digested PCR products of phage clones for the background; 23-25: Digested PCR products of phage clones for TK311.

DNA sequence analysis of the selected clones allows identification of the binding proteins based on sequence homology search employing the GenBank database of NCBI (The National Center for Biotechnology Information) and the BLAST tool. As potential hit proteins human proteins are considered.

The affinity-based proteomics approach led to the identification of importins, catenin-delta 1, dynamin II and dynamin-I-like as proteins that bind to MeA in HeLa cell lysate. However, the phage display-based identification of target proteins did not lead to the same result (**Table 4**).

Table 4: Identified proteins that binding to MeA using phage display. After biopanning employing MeA and TK311 phages were eluted with 1% SDS. Proteins are considered as targets when identified with MeA but not with TK311.

Protein name (abbreviation)	**Protein name**	**Function of hit proteins (data from NCBI or UniProtKB)**	**Identified in three independent experiments**
PTGR2	prostaglandin reductase 2	13-prostaglandin reductase activity	1
COL5A1	collagen, type V, alpha 1	extracellular matrix structural constituent	1
COL3A1	collagen, type III, alpha 1	extracellular matrix structural constituent	2
COL1A1	collagen, type I, alpha 1	extracellular matrix structural constituent	1
HTRA2	HtrA serine peptidase 2,	peptidase activity, protein binding	1
RAN	member RAS oncogene family	GTPase and transcription coactivator activity	1
SMYD4	Homo sapiens SET and MYND domain containing 4	methyltransferase activity	1
MUC20	MUC20 protein	cell surface associated	1
CTDSP2	CTD small phosphatase 2	phosphoprotein phosphatase activity	1
COX II	cytochrome c oxidase subunit II	cytochrome-c oxidase activity	1
CAPN2	calpain 2	calcium-dependent cysteine-type endopeptidase activity	1
KTN1	kinectin 1 (kinesin receptor)	kinesin binding in process microtubule-based movement	1
HMGB2	high-mobility group box 2	protein and DNA binding	1
KLC1	kinesin light chain 1	microtubule motor activity	1
NAB1	NGFI-A binding protein 1 (EGR1 binding protein 1)	transcription corepressor activity transcription factor activity	1
STAT-3	signal transducer and activator of transcription 3	transcription factor binding	1

Protein name (abbreviation)	Protein name	Function of hit proteins (data from NCBI or UniProtKB)	Identified in three independent experiments
AHNAK	AHNAK nucleoprotein	protein binding in process of nervous system development	1
MRPS6	mitochondrial ribosomal protein S6	RNA binding and structural constituent of ribosome	1
SPPL3	signal peptide peptidase 3	aspartic endopeptidase	1
AP1G2	adaptor-related protein complex 1, gamma 2 subunit	protein binding protein transporter activity	1
VCP	valosin-containing protein	ATPase activity	1
CAML2	calmodulin 2	delta-phosphorylase kinase	1
PLDN	palladin	cytoskeletal associated protein	1
EEF1A1	eukaryotic translation elongation factor 1 alpha 1	GTPase and translation elongation factor activity	1
SEPT4	septin 4	filament-forming cytoskeletal GTPase	1
PRDX1	peroxiredoxin 1	peroxidase, thioredoxin peroxidase activity	1
ZNF581	zinc finger protein 581	metal ion and DNA binding	1

The experimental procedure was improved by first pre-incubating the amplified phage library with streptavidin-biotin before starting the biopanning cycle to reduce the background binding. All further steps of biopanning and analysis were performed as previously described (section 5.1). However, the identified proteins results differed again from those enriched by means of affinity-based proteomics (**Table 5**).

Table 5: Identified proteins that binding to MeA using phage display employing pre-incubation with streptavidin-biotin. After biopanning employing pre-incubation with streptavidin-biotin, and followed by biopanning for MeA and control TK311. Phages were eluted with 1% SDS. Proteins are considered as targets when identified with MeA but not with TK311.

Protein name (abbreviation)	**Protein name**	**Function of hit proteins (data from NCBI or UniProtKB)**	**Identified in three independent experiments**
COL3A1	collagen, type III, alpha 1	extracellular matrix structural constituent	2
TUBGCP6	tubulin, gamma complex associated protein 6	microtubule binding	1
TYROBP	TYRO protein tyrosine kinase binding protein	receptor signaling protein activity	1
CTNNA1	catenin alpha 1 (also called alpha-E-catenin)	a linking protein between cadherin and actin	1
FUBP1	far upstream element (FUSE) binding protein 3	RNA and DNA binding	1
CHID1	chitinase domain containing 1	chitinase activity	1
ING1	inhibitor of growth family, member 1	zinc ion, protein and methylated histone residue binding	1
HLA-DRA	major histocompatibility complex, class II, DR alpha	MHC class II receptor activity	1
PPP1R12C	protein phosphatase 1, regulatory (inhibitor) subunit 12C	protein binding	2
WDR73	WD repeat domain 73	function in signal transduction and transcription regulation	1
TMUB2	transmembrane and ubiquitin-like domain containing 2	component of membrane	1
TOPBP1	topoisomerase (DNA) I	enzyme in DNA replication	2
TOPBP2	topoisomerase (DNA) II	enzyme in DNA replication	1
GTF2F1	general transcription factor IIF, polypeptide 1	transcription coactivator activity	2
CAPRIN1	cell cycle associated protein 1	RNA binding	1
RPL35A	ribosomal protein L35a	structural constituent of ribosome tRNA binding	2
UBC	Ubiquitin C	protein and protease binding	1
AEBP1	The adipocyte enhancer binding protein 1 (AE binding protein 1)	carboxypeptidase activity	2

Protein name (abbreviation)	**Protein name**	**Function of hit proteins (data from NCBI or UniProtKB)**	**Identified in three independent experiments**
CoxII	cytochrome c oxidase subunit II	cytochrome-c oxidase activity	2
OSBPL2	oxysterol binding protein-like 2	cholesterol binding	1
ZBTB7B	zinc finger and BTB domain containing 7B	transcription factor activity	1
CatSper2	cation channel, sperm associated 2	voltage-gated calcium channel	1
SCAND2	SCAN domain containing 2 pseudogene	transcription factor activity	1
UBE2B	ubiquitin-conjugating enzyme E2B	ubiquitin-protein ligase activity	1
HRS	hepatocyte growth factor-regulated tyrosine kinase substrate	regulating the trafficking of growth factor-receptor complexes through early endosome, up-regulating MAPK	1
TMEM123	transmembrane protein 123	cell surface receptor	1
ZC3H4	zinc finger CCCH-type containing 4	zinc ion, metal ion, and nucleic acid binding	1

So far, pre-incubation of the amplified phage library with a streptavidin-PEG-biotin construct prior to the biopanning cycle reduced the background more efficiently. Comparison of the biopanning results for immobilized MeA using lysate of an enriched phage without pre-incubation and with pre-incubation (either with streptavidin-biotin or with streptavidin-PEG-biotin) showed clearly a background reduction when performing the pre-incubation step (i.e. disappearance of the PCR products with a size of approximately 500 bp). Furthermore, the gene that corresponds to the 500 bp PCR products was found to be the alpha polypeptide of propionyl Coenzyme A carboxylase (**Figure 24A**). The experiment was repeated on with immobilized MeA and the inactive analog TK311 using a lysate pre-incubated with streptavidin-PEG-biotin (**Figure 24B**). The potential binders of MeA that were identified are shown in **Table 6** (this data was not reproduced, only done once).

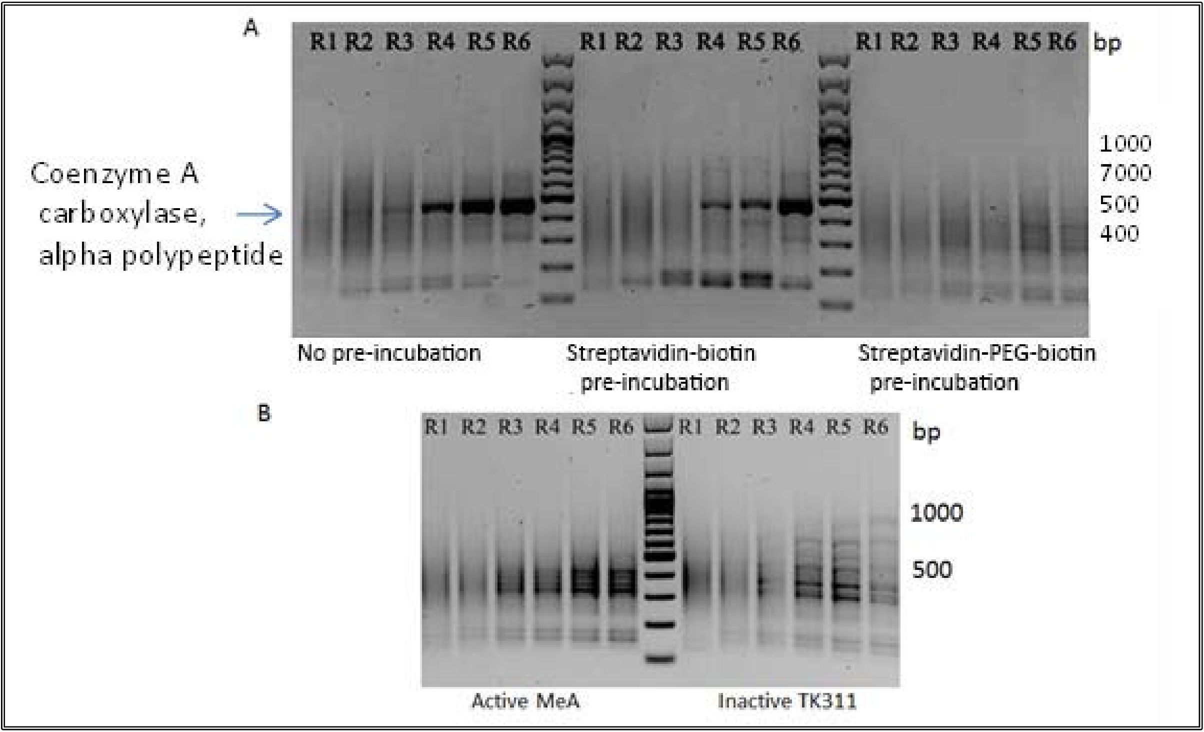
A
R1 R2 R3 R4 R5 R6
R1 R2 R3 R4 R5 R6
R1 R2 R3 R4 R5 R6
bp
1000
7000
500
400
Coenzyme A carboxylase, alpha polypeptide
No pre-incubation
Streptavidin-biotin pre-incubation
Streptavidin-PEG-biotin pre-incubation
B
R1 R2 R3 R4 R5 R6
R1 R2 R3 R4 R5 R6
bp
1000
500
Active MeA
Inactive TK311

Figure 24: PCR products using after phage display employing lysate of enriched phage library with and without preincubation. **A**. PCR products of enriched phage clones after biopanning using immobilized MeA. The lysates of the enriched phage from the first (R1) to the sixth (R6) round of selection with and without preincubation were used as DNA templates for PCR. PCR products were detected by means of agarose gel electrophoresis. **B**. PCR products of enriched phage clones using immobilized MeA and TK311. The lysates of the enriched phage clones from the first (R1) to the sixth (R6) round of selection upon pre-incubation with streptavidin-PEG-biotin were used as DNA templates. PCR products were and detected by means of agarose gel electrophoresis.

Table 6: Identified proteins that binding to MeA using phage display employing pre-incubation with streptavidin-PEG-biotin. After biopanning employing pre-incubation with streptavidin-PEG-biotin, and followed by biopanning for MeA and control TK311. Phages were eluted with 1% SDS. Proteins are considered as targets when identified with MeA but not with TK311 (data was not reproduced, done only once).

Protein name (abbreviation)	Protein name	Function of hit proteins (data from NCBI or UniProtKB)
G2E3	G2/M-phase specific E3 ubiquitin ligase	ubiquitin-protein ligase activity
RPL 8	ribosomal protein L8	structural constituent of ribosome
ZNF592	zinc finger protein 592	DNA and metal ion binding
SLC38A2	Solute carrier family 38, member 2	transmembrane transporter activity

Protein name (abbreviation)	Protein name	Function of hit proteins (data from NCBI or UniProtKB)
NDUFB10	NADH dehydrogenase (ubiquinone) 1 beta subcomplex, 10, 22kDa	NADH dehydrogenase (ubiquinone) activity
MMP9	matrix metallopeptidase 9	gelatinase, type IV collagenase
CoxII	cytochrome c oxidase subunit II	cytochrome-c oxidase activity
UBE2D3	ubiquitin-conjugating enzyme E2D 3	ATP and protein binding
GUK1	guanylate kinase 1	guanylate kinase activity
CBX1	chromobox homolog 1	chromatin, enzyme, protein binding
RPS27	ribosomal protein S27	structural constituent of ribosome
COMT	catechol-O-methyltransferase	catechol O-methyltransferase activity
PTGFRN	prostaglandin F2 receptor negative regulator	inhibits the binding of prostaglandin F2-alpha to its specific FP receptor
SNRNP70	small nuclear ribonucleoprotein 70kDa	nucleotide binding
OSBPL5	oxysterol binding protein-like 2	cholesterol binding
TMEM43	transmembrane protein 43	maintains nuclear envelope structure
EMP2	epithelial membrane protein 2	integrin binding
COL1A1	collagen, type III, alpha 1	extracellular matrix structural constituent
METTL10	methyltransferase like 10	methyltransferase activity
TOMM20	translocase of outer mitochondrial membrane 20	allows movement of proteins through intermembrane of the mitochondrion
RBM12	RNA binding motif protein 12	nucleotide binding
RPLP1	ribosomal protein, large, P1	structural constituent of ribosome
GRB7	growth factor receptor-bound protein 7	RNA and protein kinase binding
CCL5	chemokine (C-C motif) ligand 5	protein kinase activity
HNRNPA2B1	heterogeneous nuclear ribonucleoprotein A2/B1	Nucleotide binding
MDH2	malate dehydrogenase 2, NAD	L-malate dehydrogenase activity
ATP5J	ATP synthase, H+ transporting, mitochondrial F0 complex, subunit F6	transporter activity
DNAJB4	Homo sapiens DnaJ (Hsp40) homolog, ubfamily B, member 4	unfolded protein binding
TMSB4X	thymosin beta 4, X-linked	actin and protein binding

Protein name (abbreviation)	Protein name	Function of hit proteins (data from NCBI or UniProtKB)
SMARCC2	SWI/SNF related, matrix associated, actin dependent regulator of chromatin, subfamily a, member 2	RNA, P53 and chromatin binding DNA-dependent ATPase activity transcription coactivator activity
RBBP6	retinoblastoma binding protein 6	ubiquitin-protein ligase activity
FZD6	frizzled homolog 6	Wnt-activated receptor activity
HIVEP1	human immunodeficiency virus type I enhancer binding protein 1	metal ion, DNA and protein binding
TBX21	T-box 21	transcription factor activity
KDM2A	lysine (K)-specific demethylase 2A	RNA and protein kinase binding
CTSS	cathepsin S	lysosomal cysteine protease
PLXNB2	plexin B2	cell surface receptor
TOP1	topoisomerase (DNA) I	enzyme in DNA replication
OSBPL1A	oxysterol binding protein-like 1A	cholesterol and protein binding
MAPRE1	microtubule-associated protein, RP/EB family, member 1	regulates the dynamics of the microtubule cytoskeleton

As a summary, 27 binders were identified using the first phage display approach (no pre-incubation). 27 proteins were identified when employing phage display including pre-incubation with streptavidin-biotin. 40 binders were found after pre-incubation with streptavidin-PEG-biotin which was not reproduced and not concluded (only done for one time). However, binders found in all three approaches are collagen type III, alpha 1 and cytochrome c oxidase subunit II. Topoisomerase (DNA) I was identified in both experiments with pre-incubation. In addition, proteins identified by phage display to bind to melophlin A differ from the known targets previously identified by affinity purification.

From the results presented, we could determine the optimal conditions allowing us to employ this method for target identification. However, all identified proteins remained to be validated by appropriated methods. To confirm the potential target proteins specific elution with free compounds was employed (see next section 5.1.2).

5.1.2 Identification of proteins that bind to CD 267

One further compound that was included in the second approach was a biotinylated analog of CD267 (affinity probe of Wntepane 1)[60] (**Figure 25A**). As an inactive analog a PEG-biotin linker was employed (**Figure 25B**). CD 267 is a small molecule activator of the Wnt-pathway.[60] CD 267 targets Vangl1. Vangl1 proteins are multipass (more than one transmembrane segment) hydrophobic integral membrane protein and play a role as receptor in the noncanonical Wnt-signaling pathway. Vang1 was validated as a target of compound CD267 by means of Western blot of Vangl1 after doing competitive affinity purification.[60]

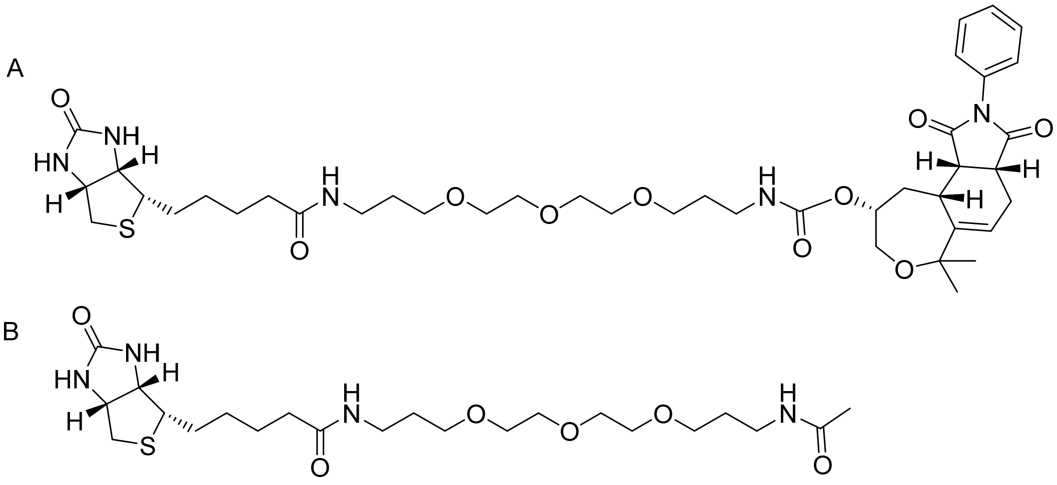

Figure 25: Chemical structures of probes: CD 267 (A) and PEG-Biotin linker (B)

For CD 267 all experiments were performed with the pre-incubation step. Two experiments were done after pre-incubating the amplified phage library with streptavidin-biotin and one done after preincubating the amplified phage library with streptavidin-PEG-biotin. All steps of the biopanning cycle and analysis were performed as described above (section 5.1). The identified potential binders of CD 267 were compared and confirmed with the hits identified from affinity purification methods in **Table 7** and **Table 8**.

Table 7: Identified proteins as potential binders to CD 267 after preincubation with streptavidin-biotin. After biopanning employing pre-incubation with streptavidin-biotin, and followed by biopanning for CD 267 and control. Phages were eluted with 1% SDS. Proteins are considered as targets when identified with CD 267 but not with PEG-biotin linker (data was not reproduced, done only twice).

Protein name (abbreviation)	Protein name	Function of hit proteins (data from NCBI or UniProtKB)	Identified in two independent experiments
SSR2	signal sequence receptor beta	membrane receptor	1
HINT	histidine triad nucleotide binding protein 1	nucleotide and protein kinase C binding hydrolase activity	2
FBR-MuSV	Finkel-Biskis-Reilly murine sarcoma virus	RNA binding structural constituent of ribosome	1
SNX21	sorting nexin family member 21	phosphatidylinositol binding	1
Nucks1	nuclear casein kinase and cyclin-dependent kinase substrate 1	nuclear localization signals, DNA-binding domain	1
LAMB2	laminin, beta 2 (laminin S)	integrin binding, structural molecule activity	1
DNHD1	dynein heavy chain domain 1	microtubule motor activity	1
ACTG1	actin, gamma 1	ATP and protein binding, structural constituent of cytoskeleton	1
GTF2F1	general transcription factor IIF, polypeptide 1	transcription coactivator activity	1
NOLC1	nucleolar and coiled-body phosphoprotein 1	ATP and GTP binding, maintenance of the fundamental component in the nucleolus	1
COL1A1	collagen, type I, alpha 1	extracellular matrix structural constituent	1
ATP5J	ATP synthase, H+ transporting, mitochondrial F0 complex, subunit F6	transporter activity	1
MFNG	MFNG O-fucosylpeptide 3-beta-N-acetylglucosaminyltransferase	O-fucosylpeptide 3-beta-N-acetylglucosaminyltransferase activity	1
HMGN1	high mobility group nucleosomal binding domain 4	nucleosomal DNA binding	1
SMAD2	SMAD family member 2	receptor signaling protein activity	1
DNAJC21	DnaJ (Hsp40) homolog, subfamily C, member 21	nucleic acid, zinc ion, and protein binding	1

Table 8: Identified proteins as potential binders to CD 267 after preincubation with streptavidin-PEG-biotin. After biopanning employing pre-incubation with streptavidin-PEG-biotin, and followed by biopanning for CD 267 and control. Phages were eluted with 1% SDS. Proteins are considered as targets when identified with CD 267 but not with PEG-biotin linker (data was not reproduced, done only one time).

Protein name (abbreviation)	Protein name	Function of hit proteins (data from NCBI or UniProtKB)
ITGB8	integrin, beta 8	receptor activity
MAP3K7IP3	mitogen-activated protein kinase 7 interacting protein 3	MAP kinase activity protein serine/threonine kinase activity
NPAS3	neuronal PAS domain protein 3	signal transducer activity
SNX11	sorting nexins	protein transporter activity
APOL2	apolipoprotein L,2	receptor, lipid and lipoprotein binding
EEPD1	exonuclease/phosphatase family domain containing 1	DNA binding
RGS1	regulator of G-protein signaling 1	GTPase activator activity
CD24	CD24 molecule	protein tyrosine kinase activator activity
HINT	histidine triad nucleotide binding protein 1	nucleotide and protein kinase C binding hydrolase activity
RBBP6	retinoblastoma binding protein 6	ubiquitin-protein ligase activity
HIST1H2AC	histone cluster 1, H2a	core component of nucleosome
VPS39	vacuolar protein sorting 39	small GTPase regulator activity

Binders of CD 267 that were identified in this approach are histidine triad nucleotide binding protein 1 (HINT). Only one protein, SMAD family member 2, was identified using both, phage display and affinity purification, but SMAD has not been validated further more as target of CD 267 compound. From the results presented in the first and second approach, we could determine the optimal conditions allowing us to employ phage display methods for target identification. However, all identified proteins remained to be validated by appropriated methods. To confirm the potential target proteins specific elution with free compounds was employed as the third approach (see next section 5.1.3).

5.1.3 Phage display employing specific elution

Two commercial cDNA phage display libraries (human breast and liver library (Novagen) were employed for phage display followed by phage elution using unmodified compounds (specific elution). Each library consisted of $1.1*10^7$ primary phage clones. Rosetta gami *E. coli* strain was used which is derived from B5615 *E. coli*. This strain permits heterologous protein expression with enhance disulfide bond formation because of mutations in both the thioredoxin reductase (*trxB*) and glutathione reductase (*gor*) genes which allow the cytoplasmic disulfide bond formation.[300] Biotinylated glutathione (Biotin-GSH) was used as control compound for valuation protocol and biotinylated tubulexin A was subjected to phage display to validate the target identification protocol.

5.1.3.1 Identification of glutathione binding proteins

Glutathione (GSH) is an antioxidant that protects cells from reactive oxygen species such as free radicals and peroxides. It is synthesized from the amino acids L-cysteine, L-glutamic acid and glycine. This molecule exists in reduced (GSH) and oxidized (GSSG) states; with a large majority found in its reduced form (more than 90% exists in a reduced form and less than 10% exists in the disulfide form). GSH can be regenerated from GSSG by the enzyme glutathione reductase. GSH is known as a substrate in both conjugation reactions and reduction reactions, catalyzed by glutathione S-transferase enzymes. GSH participates in leukotriene synthesis and is a cofactor for the enzyme glutathione peroxidase. Structures of GSH, biotinylated GSH, GSSG and biotin are shown in **Figure 26**.

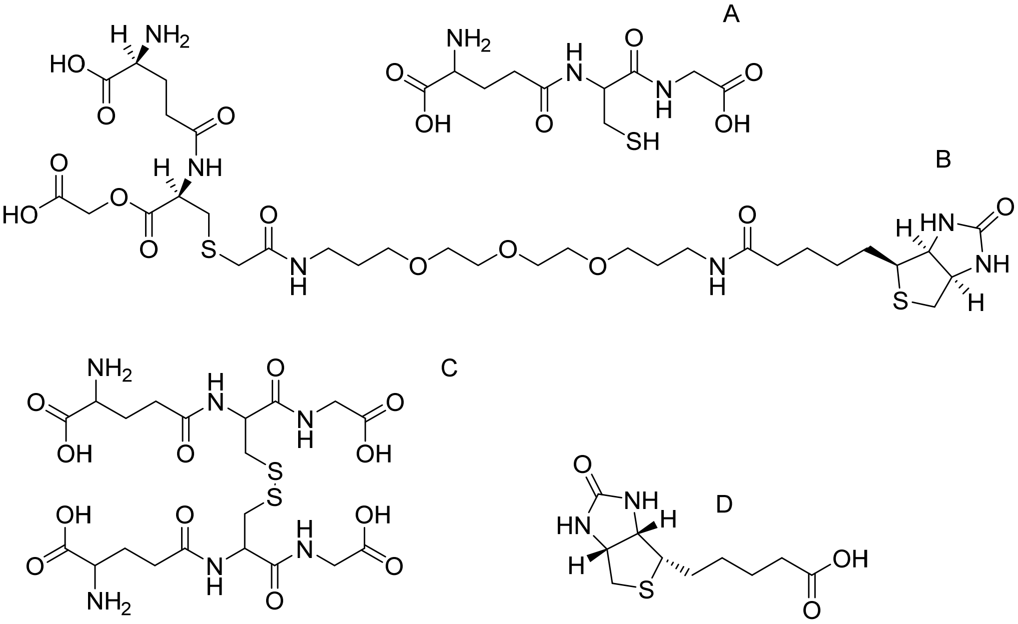

Figure 26: Chemical structures of GSH (A), biotinylated GSH (B), GSSG (C) and biotin (D)

Phage display human breast tumor and liver cDNA libraries were used for biopanning. Libraries were pre-incubated with streptavidin-PEG-biotin before biopanning and 100 µM of GSH was used for specific elution. Glutathione peroxidase was found as a GSH binder only when the breast tumor cDNA library was employed. The identified sequence corresponds to sequence of amino acid 134 to amino acid 184 of human glutathione peroxidase 1 isoform 1 (sequence identificati*on*: ref|NP_000572.2| on NCBI for referent). However, another well-known target of GSH, glutathione S transferase (GST), could not be identified in these experiments.

5.1.3.2 Identification of proteins that bind to tubulexin A

Using SILAC and affinity-based proteomics and, α/β-tubulin and CAS were identified as target proteins of tubulexin A. To compare the proteins that bind to tubulexin A in the proteomics and phage display approach, biotinylated derivative was subjected to phage display. For this, T7 phage display human breast and liver tumor cDNA libraries and two *E. coli* strain (BLT5615 and Rosetta-gami^{TM} B5615) were employed. The amplified phage libraries were pre-incubated with an inactive biotinylated control. 100 µM of unmodified tubulexin A was used for specific elution. The structures of the tubulexin A and derivatives are shown in **Figure 27**.

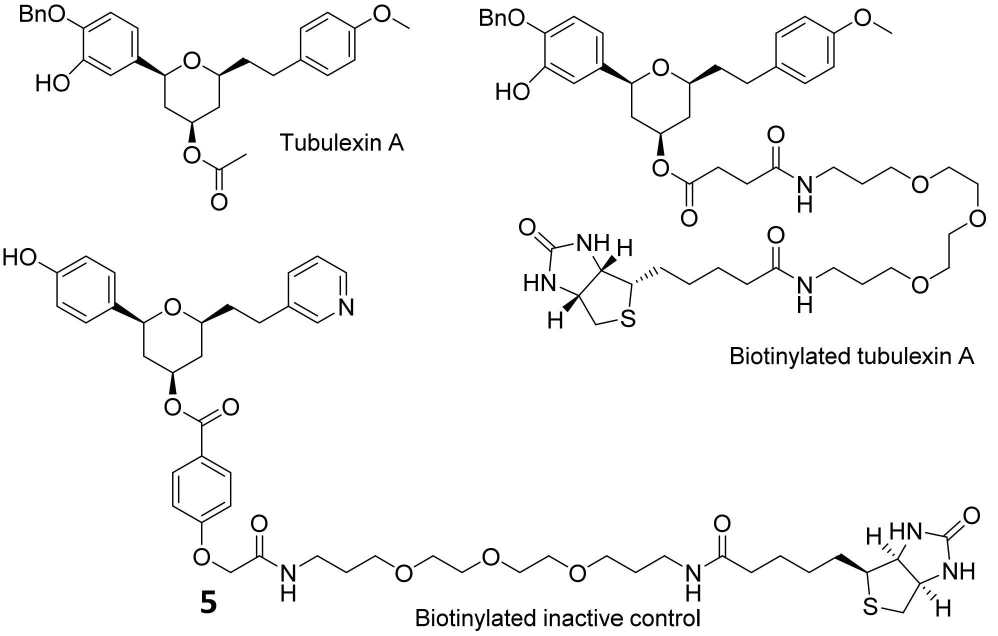

Figure 27: Chemical structures of tubulexin A and derivatives.

Biopanning and phage clone analysis were performed as described (section 4.1) and 94 phage clones for each phage population were analyzed. Identified proteins are shown in **Table 9**. Surprisingly, none of the identified binders matched with the targets that were enriched using the proteomics-based approach. The results may reflect several problems. First, the pre-incubation step might have removed all of the target proteins if the targets also bind to inactive analog event inactive analog has no effect on cells but it still bind to the same protein targets of MeA *in vitro.* Second, target proteins were not presented in sample because of lacking in fame of phage 10B capsid protein. Third, target proteins could not be isolated if the posttranslational modification (PTM) is necessary for the interaction between target and molecule (see more details about the limitation of this method in section 1.2.1.3.1).

Table 9: Identified proteins that bind to biotinylated tubulexin A employing pre-incubation with inactive analog. After biopanning employing pre-incubation with streptavidin-inactive analog-biotin, and followed by biopanning for tubulexin A. Phages were eluted with unmodified tubulexin A (without PEG-Biotin). Identified proteins shown in this table were marked as plus (+) and as minus (-) for unpresented one.

Protein name (abbreviation)	**Protein name**	**T7 phage display human breast tumor cDNA library**		**T7 phage display human liver tumor cDNA library**		**Function of hit proteins (data from NCBI or UniProtKB)**
		rosseta gami B5615	B5615	rosseta gami B5615	B5615	
FABP6	fatty acid binding protein 6	+	+	-	-	transporter activity
USP24	ubiquitin specific peptidase 24	+	+	-	-	deubiquitinating enzymes
EIF3M	eukaryotic translation initiation factor 3, subunit M	+	+	-	-	translation initiation
TOP1	topoisomerase (DNA) I	-	+	-	-	DNA topoisomerase activity
CTNNA1	catenin (cadherin-associated protein), alpha 1	-	+	-	-	structural molecule activity
MAP1B	microtubule-associated protein	-	-	+	-	structural molecule activity
EWSR1	Ewing sarcoma breakpoint region 1	-	-	+	-	Nucleotide and protein, zinc ion binding

5.1.4 Generation of a T7 phage display HeLa cDNA library

5.1.4.1 Strategy to make a T7 phage display HeLa cDNA library

In the affinity-based proteomics approach HeLa cell lysates were employed for enrichment of targets of melophlin A and tubulexin A. However phage display HeLa cDNA library is commercially not available. To better compare proteins identified by phage display and affinity chromatography, first a phage display cDNA HeLa library needed to be designed which based on primers which were employed for reverse transcriptase reaction (mRNA to cDNA such as oligo dT or random oligonucleotides (see step 1 in **Figure 29**) and the linkers employing for enzyme digestion before inserting cDNA into phage vectors (see step 4 in **Figure 29**)

There are two types of primers that hybridize with mRNA and are suitable for cDNA library synthesis: random or oligo dT primers (**Figure 28**). The choice of the primers depends on personal preference or specific use of the developed library. Random primers permit to control the average insert size, and smaller inserts may be desirable for example when screening for functional protein domains. Random primers are often employed in the generation of commercial phage display cDNA library (e.g. from Novagen). Oligo dT primers are regarded as the standard primers for library construction for screening of gene products.[301] Therefore, it is usually worthwhile using both priming strategies in parallel. Therefore, in this study both random priming and oligo dT primers were employed to construct the library.

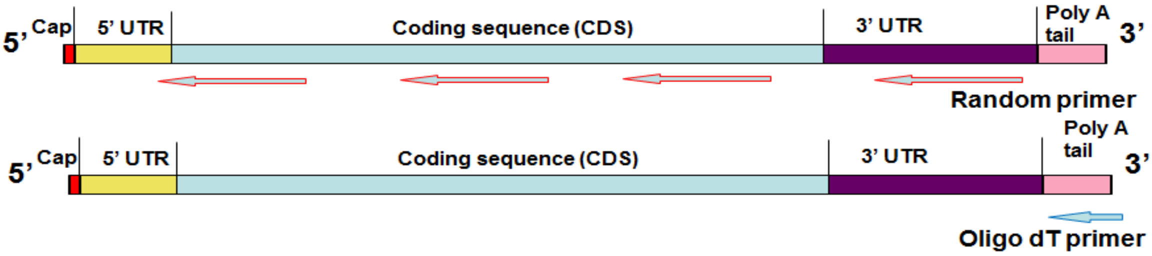

Figure 28: mRNA structure. mRNA consist of coding sequence (CDS), untranslated region at 5´ cap (5´ UTR) or 3´ (3´ UTR) and poly adenine (poly A) tail which can be hybridized with oligo dT primers.

In addition, T7Select10-3 vector and three linkers for recombinant fusion to 10B capsid protein were used. These linkers enable the expression of the cloned sequences in all three reading frames in case of oligo dT primers (**Figure 29**). The vector has cloning capacity of 0–3.6 Kbp and allows the display of an average of 10 copies of recombinant fusions. Proteins are displayed following amino acid (aa) 348 of the 10B capsid protein.

HeLa cell cDNA was synthesized using OrientExpress™ Oligo dT cDNA synthesis kit (Novagen). The cDNA was then prepared for cloning into T7Select10-3b vector using the *Eco*RI/*Hind*III end modification kit, DNA ligation kit, and mini column fractionation kit. All steps were performed according to the manufacturer’s protocol (see section 4.3).

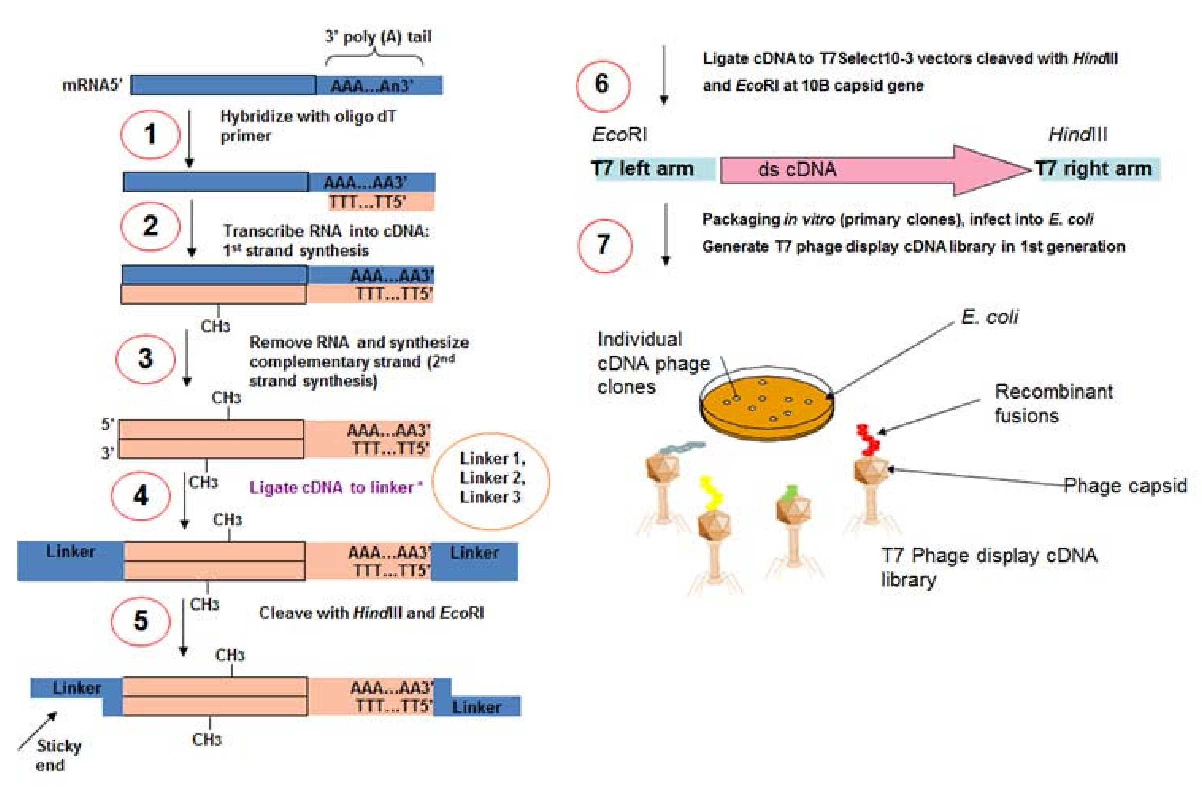
3' poly (A) tail
mRNA5'
AAA...An3'
1
Hybridize with oligo dT primer
AAA...AA3'
TTT...TT5'
2
Transcribe RNA into cDNA: 1st strand synthesis
AAA...AA3'
TTT...TT5'
CH3
3
Remove RNA and synthesize complementary strand (2nd strand synthesis)
CH3
5'
3'
AAA...AA3'
TTT...TT5'
Linker 1, Linker 2, Linker 3
CH3
4
Ligate cDNA to linker*
CH3
Linker
AAA...AA3'
TTT...TT5'
Linker
CH3
5
Cleave with *Hind*III and EcoRI
CH3
Linker
AAA...AA3'
TTT...TT5'
Linker
Sticky end
CH3
6
Ligate cDNA to T7Select10-3 vectors cleaved with *Hind*III and *Eco*RI at 10B capsid gene
*Eco*RI
*Hind*III
T7 left arm
ds cDNA
T7 right arm
7
Packaging *in vitro* (primary clones), infect into *E. coli*
Generate T7 phage display cDNA library in 1st generation
E. coli
Individual cDNA phage clones
Recombinant fusions
Phage capsid
T7 Phage display cDNA library

Figure 29: Synthesis of T7 phage display HeLa cDNAs library using oligo dT primers and three linkers. After extraction, HeLa cells mRNA was hybridized with oligo dT primers allowing reverse transcription of RNA into cDNA. RNA was removed and the second stand of DNA was synthesized. Different linkers were ligated to the double stranded DNA (dsDNA), followed by *Eco*RI/*Hind*III digest prior to ligation into T7Select10-3 vector. Finally, *in vitro* phage packaging was performed to generate primary phage clones. *E. coli* were infected with primary phage clones to produce the first generation T7 phage display HeLa cDNA library.

Upon packaging, *E. coli* were infected with primary phage clones for phage amplification to produce the first generation of T7 phage display HeLa cDNA library and for determination of the phage titer. The results showed that the size of the libraries that were generated using oligo dT primers is higher than when random primers were used (**Table 10**).

Table 10: Comparison of T7 phage display HeLa cDNA library and commercially available libraries.

Library	**T7 phage display HeLa cDNA library (in-house)**				**Commercial libraries**
Primer	Random	Oligo dT			Random
Linker	1	1	2	3	1
Number of primary clones	3.6×10^6	1.9×10^7	1.3×10^8	1.7×10^8	1.1×10^7

5.1.4.2 Target identification of tubulexin A using a T7 phage display HeLa cDNA library

T7 phage display HeLa oligo dT cDNA libraries with different linkers were combined after the first generation for biopanning experiments to identify the targets of biotinylated tubulexin A. First generation of T7 phage display HeLa cDNA library, that has been synthesized using random primers with one linker, was employed in biopanning too. Biopanning was performed in B5615 *E. coli* for six rounds of selection. The amplified phage library was pre-incubated with biotinylated inactive control analog and 100 µM of unmodified tubulexin A were used for specific elution (see structure in **Figure 27**). 90-94 phage clones were analyzed for each library. All steps for biopanning or analysis were done like previously described (section 5.1).

For the T7 phage display HeLa random cDNA library, phage plaque PCR obtained many PCR products of similar DNA size and small size (approximately 300-500 bp) and PCR products of analyzed samples were not cut by *Hinf*I. In addition, many unknown peptides corresponding to two different sequences: SPAGISRELVDKLAAALE and SLLVQRGTALWTLGKNLVERVKNLTPKLAAALE, respectively (**Figure 30**).

For the T7 phage display HeLa oligo dT cDNA library, phage plaque PCR and *Hinf*I fingerprinting revealed many PCR products of similar DNA size (e.g. clones 51, 53, 56, 84, 86, 89, 90 in **Figure 31**). DNA sequencing demonstrated that these products correspond to ubiquinol-cytochrome c reductase binding protein (UQCRB). This protein is a subunit of mitochondrial complex III which suppress hypoxia-induced tumor angiogenesis in tumor cells with unknown mechanism which is related to UQCRB. UQCRB enhances vascular endothelial growth factor receptor type 2 (VEGFR2) signaling by increasing the levels of mitochondrial reactive oxygen species (ROS) in endothelial cells.[302] In addition, many additional unknown peptides such as RFIPLLSHWPAVRNLLTNILYPVPK were identified.

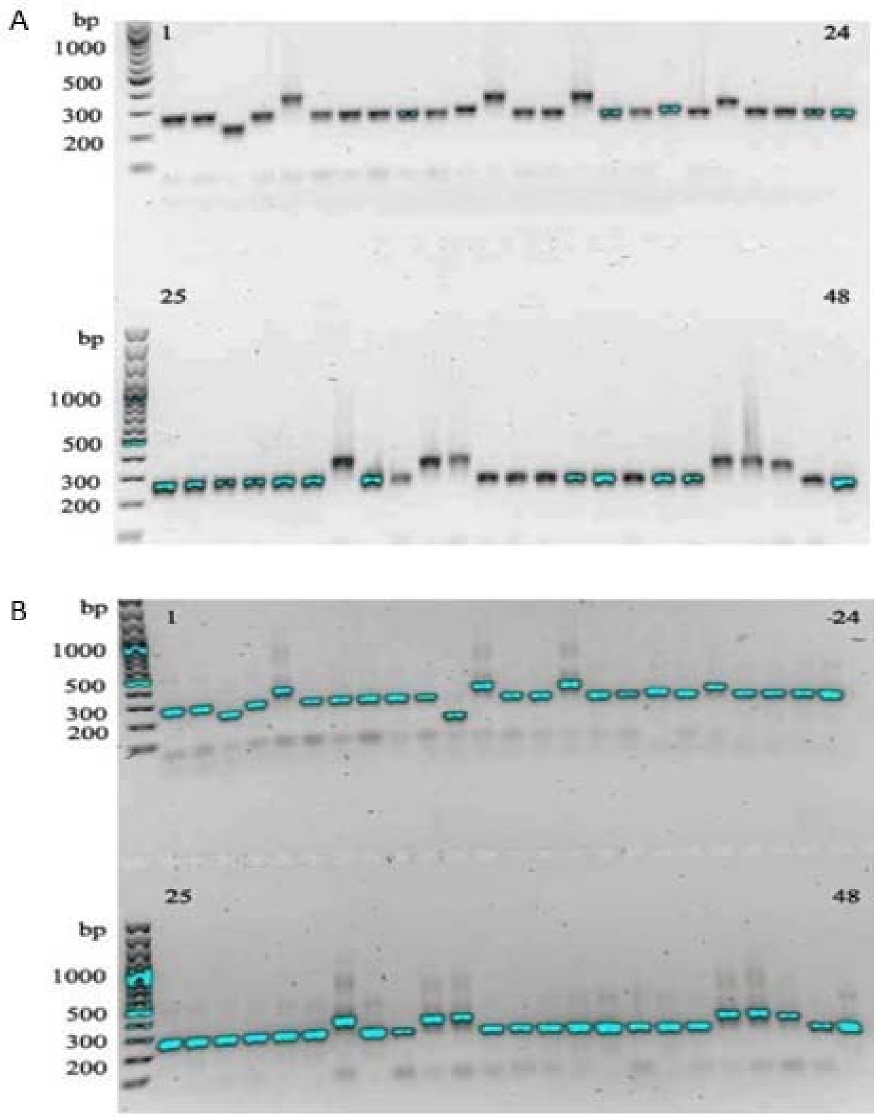
A
bp
1000
500
300
200
1
24
25
48
bp
1000
500
300
200
B
bp
1000
500
300
200
1
24
25
48
bp
1000
500
300
200

Figure 30: Biopanning using tubulexin A using T7 phage display HeLa random cDNA library. **A**. PCR products. Phage clones as DNA template for PCR. PCR products were detected by means of agarose gel electrophoresis. 1-48: phage clones of biopanning of tubulexin A. **B**. *Hinf*I fingerprinting. PCR products which were the same above (A) were digested by *Hinf*I. Restriction products were detected by means of agarose gel electrophoresis.

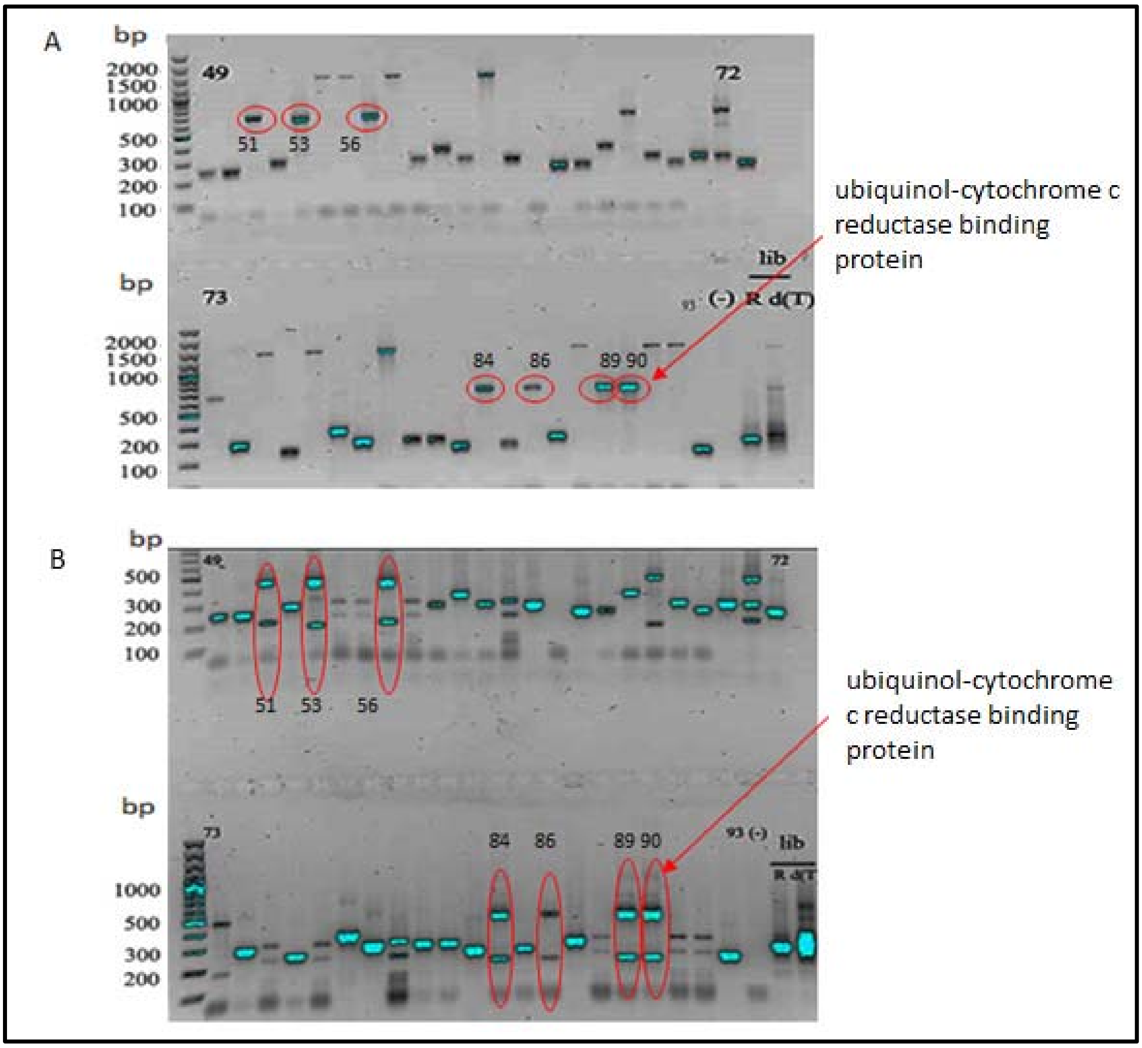
A
bp
2000
1500
1000
500
300
200
100
49
72
51
53
56
ubiquinol-cytochrome c reductase binding protein
73
(-)
lib
R
d(T)
84
86
89
90
B
1000
ubiquinol-cytochrome c reductase binding protein
93 (-)

Figure 31: Biopanning using tubulexin A using T7 phage display HeLa oligo dT cDNA library. **A**. PCR products. Phage clones as DNA template for PCR. PCR products were detected by means of agarose gel electrophoresis. 49-93: phage clones of biopanning of tubulexin A; 94: negative control; 95-96: phage clones of primary library (lib) generating by random primers (R) and generating by oligo dT primers (dT). **B**. *Hinf*I fingerprinting. PCR products which were the same above (**A**) were digested by *Hinf*I. Restriction products were detected by means of agarose gel electrophoresis.

These were unexpected results; even though phage display HeLa cDNA library was used. Identified binders were not matched with the any known targets that were enriched using the proteomics-based approach. The results lead to the same conclusion as above (in section 5.1.3.2).

5.1.4.3 Validation of UCRBP as a target protein of tubulexin A

Target identification of terpestacin identified the protein UQCRB (Ubiquinol-cytochrome c reductase binding protein) as a target.[157] Phage display employing a biotinylated derivative (BT2) was chosen as approach for target deconvolution. For biopanning different T7 phage display encoding human cDNA libraries (liver tumor, normal liver, Alzheimer's brain, normal brain, and normal stomach tissues (Novagen)) were used. UQCRB was validated as a target using surface plasmon resonance (SPR) analysis.[157] The structures of terpestacin and of biotinylated terpestacin (BT2) are showed in **Figure 32**.

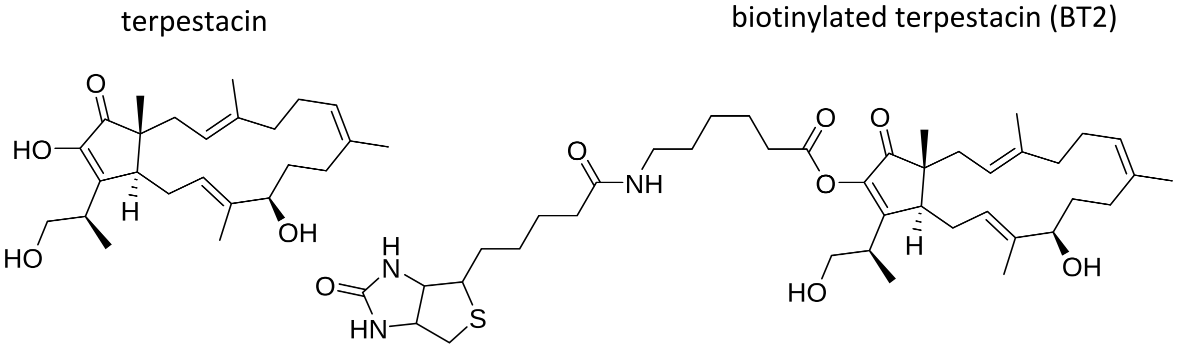

Figure 32: Chemical structure of terpestacin and biotinylated terpestacin (BT2)

The amino acid sequence corresponding to the phage clone that was enriched by biotinylated tubulexin A matches with the protein sequence, which has been reported to bind to TB2 apart from N- and C-terminal extensions when tubulexin A is used (**Figure 33)**.

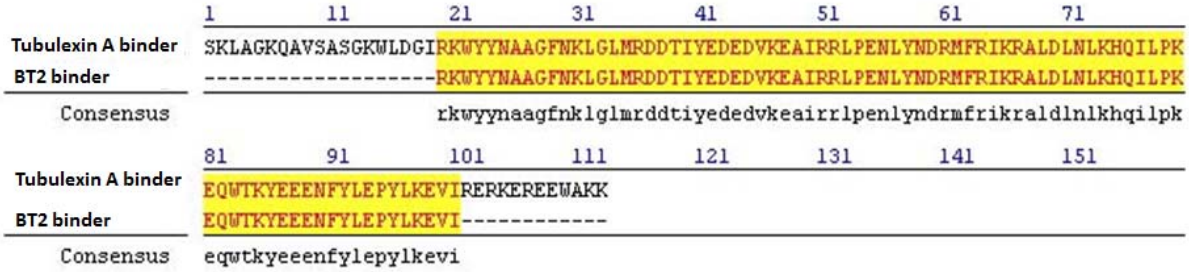
```
                   1         11        21        31        41        51        61        71
Tubulexin A binder SKLAGKQAVSASGKWLDGIRKWYYNAAGFNKLGLMRDDTIYEDEDVKEAIRRLPENLYNDRMFRIKRALDLNLKHQILPK
BT2 binder         -------------------RKWYYNAAGFNKLGLMRDDTIYEDEDVKEAIRRLPENLYNDRMFRIKRALDLNLKHQILPK
Consensus                             rkwyynaagfnklglmrddtiyededvkeairrlpenlyndrmfrikraldlnlkhqilpk
                   81        91        101       111       121       131       141       151
Tubulexin A binder EQWTKYEEENFYLEPYLKEVIRERKEREEWAKK
BT2 binder         EQWTKYEEENFYLEPYLKEVI------------
Consensus          eqwtkyeeenfylepylkevi
```

Figure 33: Alignment of the amino acid sequences identified after biopanning using of biotinylated tubulexin A or terpestacin derivative BT2.

The affinity of the interaction between phage-displayed UQCRB peptide and tubulexin A was evaluated by means of the enzyme-linked immunosorbent assay (ELISA). An anti-T7 tail fiber antibody-coated plate was incubated either with UQCRB–displayed phages or T7 phages as a control. After removing unspecific binders, the plate was incubated with different concentrations of either biotinylated tubulexin A or biotinylated inactive analog. The plate was then washed thoroughly prior to incubation with streptavidin coupled to horseradish peroxidase (HRP). TMB was used as a HRP substrate to detect HRP (section 4.3.3.8). Result showed that UQCRB–displayed phages bind to both biotinylated active and inactive of tubulexin A. Binding affinity of UQCRB–displayed phages to biotinylated inactive analog was not significantly higher than active analog (**Figure 34**). Thus, UQCRB is not a target of tubulexin A, but only a non-specific binder.

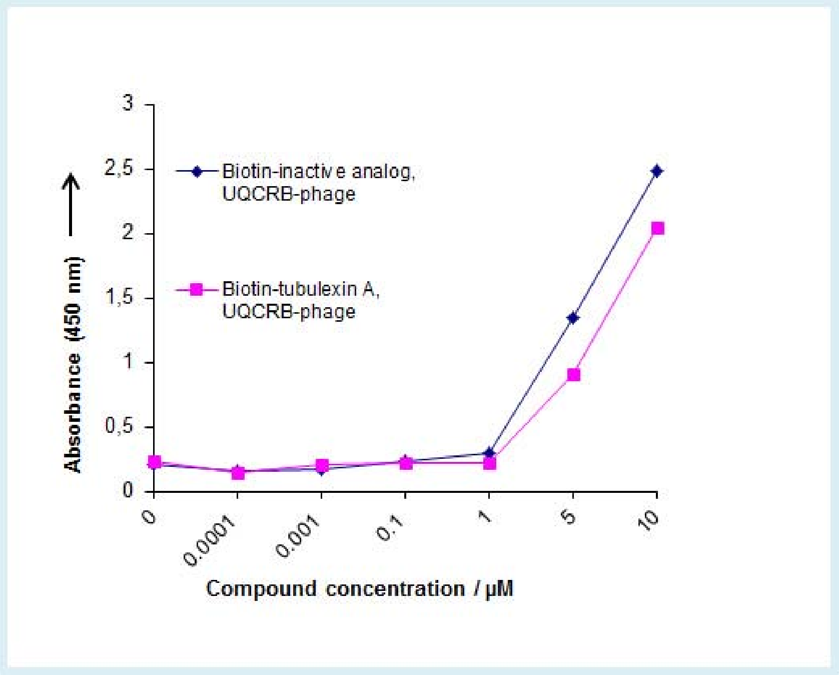

Figure 34: Binding of UQCRB phage displayed peptide to biotinylated tubulexin A. After incubation of anti-T7 tail fiber antibody-coated plate with either UQCRB-displayed phages or with T7 phage library as a control, different concentrations of biotinylated compounds were added to the plate. Binding was monitoring is by means of ELISA using a streptavidin coupled to HRP for detection.

In parallel, affinity purification using HeLa cell lysate was performed to address if UQCRB is indeed targeted by tubulexin A. HeLa cell lysate was incubated with either immobilized biotinylated tubulexin A or a negative control (PEG-biotin or inactive biotinylated analog) on streptavidin-coated beads. After washing, bound proteins were collected by boiling in SDS sample buffer at 95 ^{o}C for 5 min. UQCRB was then detected by means of immunoblotting using anti-UQCRB antibody. The results showed that UQCRB can bind to either biotinylated active tubulexin or control (PEG-biotin or biotinylated inactive analog TK311) (**Figure 35**). This result is in accordance with the data obtained by ELISA and demonstrates that UQCRB binds non-specifically to biotinylated tubulexin A.

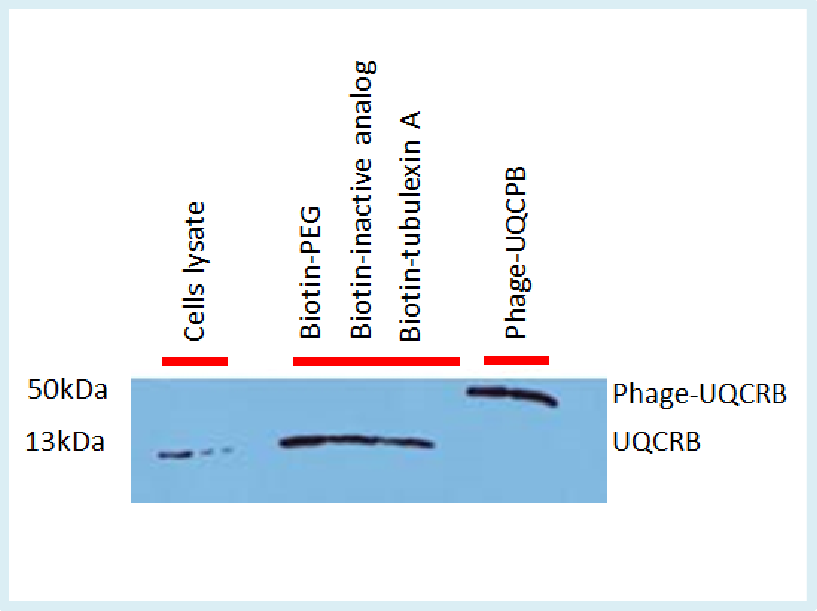

Figure 35: Evaluation of UQCRB enrichment by biotinylated tubulexin A using affinity purification. HeLa cell lysate was incubated with biotinylated tubulexin A or control compound, which were immobilized on streptavidin beads. After affinity purification, bound proteins were collected by heating and detected by immunoblotting using anti-UQCRB antibody.

Evaluation of the mode of action of tubulexin A

5.2 Influence of tubulexin A on vinblastine-resistant KB-V1 cells

Compounds that interfere with microtubule dynamics are among the most successful therapeutics for the treatment of cancer. However, these agents suffer from severe adverse effects and development of resistance.[303,304] Thus, novel anti-tubulin agents are in high demand. Using a high content screening, the tetrahydropyran tubulexin A was identified as mitotic inhibitor. Proteins enriched by biotinylated tubulexin A and identified by means of stable isotope labeling by amino acids in cell culture (SILAC)-based affinity chromatography are α-tubulin, β-tubulin, CAS (chromosome segregation 1-like-CSE1L, cellular apoptosis susceptibility, exportin 2), leucine–rich repeat-containing protein 59Guanine nucleotide binding protein like 3 and Dna homolog sub family A member 1.[305] The structure of tubulexin A, the biotinylated active and the inactive analog of tubulexin A are shown in **Figure 27**.

The multidrug-resistant KB-V1 cell line which is derived of HeLa cells was obtained from human KB carcinoma cells KB-3-1 by Shen and his co-workers in 1986.[306,307] They used an alkylating agent[308] such as ethyl methanesulfonate (EMS) to induce mutations which generated mutagenized cells. This step yielded either colonies or cell populations that were able to grow in the presence of increasing concentrations of vinblastine. KB-V1 cells express high level of MDR-1 gene (MDR: multidrug resistance), a P-glycoprotein and also display high resistance towards vinblastine when compared with KB-3-1 cells. KB-V1 and KB-3-1 had the same release rate, but KB-V1 had a lower uptake rate, so the decreased intracellular drug concentration was mediated by this uptake rate.[309] So the KB-V1 cells are used as a drug-resistant cell line, e.g. vinblastine-resistant cells.

Due to the limitations of vinblastine in the clinic, it was interesting to compare the influence of tubulexin A on the proliferation of HeLa cells and KB-V1 cells. Cell lines were treated with increasing concentrations of the compounds for 48 h. Cell proliferation was determined using the WST-1 cell proliferation reagent. This assay confirmed the resistance of the KB-V1 cells to vinblastine. The half-maximal inhibitory concentration was about 254 fold higher for the KB-V1 cells (IC_{50} 442.06 ± 43.62 nM) compared to HeLa cells (IC_{50} values = 1.74 ± 0.86 nM). In contrast, tubulexin A inhibited the proliferation of KB-V1 cells (IC_{50} 3.75 ± 0.1 µM) and HeLa cells (IC_{50} 4.29 ± 0.03 µM) with nearly identical potency (**Figure 36A-C**). This result shows that tubulexin A overcomes resistance to vinblastine in multidrug-resistant KB-V1 cancer cells.

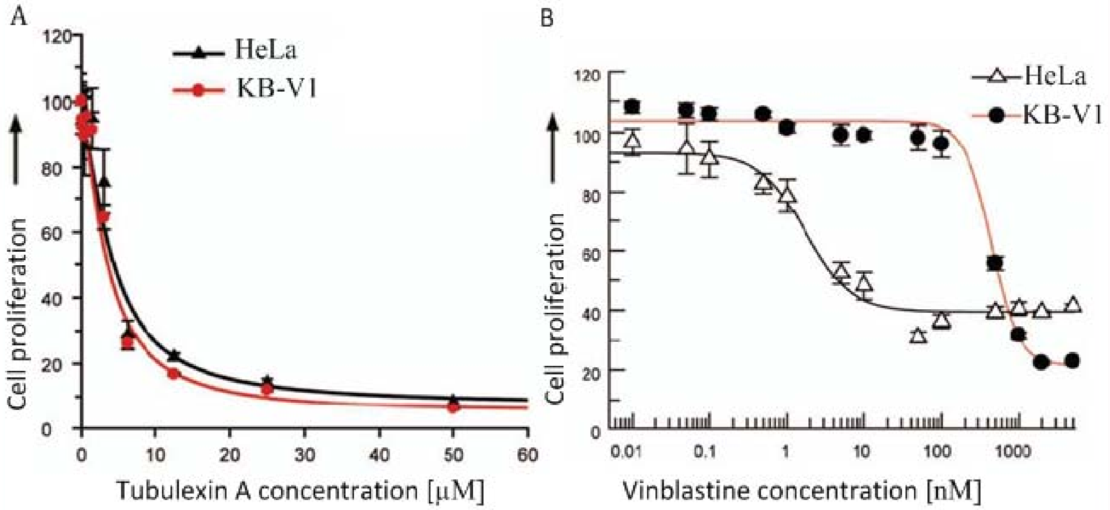

C

Compounds	Cell proliferation IC$_{50}$ HeLa cells	Cell proliferation IC$_{50}$ KB-V1 cells	Resistance factor
Tubulexin A	4.29 ± 0.03 µM	3.75 ± 0.1 µM	0.88
Vinblastine	1.74 ± 0.85 nM	442.06 ± 43.62 nM	254

Figure 36: Tubulexin A overcomes resistance to vinblastine in KB-V1 cells. HeLa and vinblastine-resistant KB-V1 cells were treated with increasing concentrations of tubulexin A (**A**) or vinblastine (**B**) for 48 h. Cell proliferation was determined by using the WST-1 cell proliferation reagent. IC$_{50}$ values for proliferation inhibition were determined using a sigmoidal fitting curve (OriginLabs Origin 6.0). The resistance factor was determined as the ratio of the IC$_{50}$ value in the resistant cell line KB-V1 divided by the IC$_{50}$ value in the sensitive HeLa cells.

5.3 Time-course of the influence of tubulexin A on HeLa cells

Treatment of HeLa cells with tubulexin A for 20 hours induces apoptosis and no necrosis. Fluorescence-activated cell sorting (FACS) analysis showed that this compound induced G2/M cell cycle arrest at a concentration of 5 µM (experiments performed by Dr. Claas Gerding-Reimers). As a next step, the influence of this compound on mitosis was examined in more detail by live-cell imaging of HeLa and HeLa Fucci cell lines. HeLa Fucci cells stably express two fusion proteins Cdt1 (Kusabira-Orange fused Cdt1) and Geminin (Azami-green fused Cdt1). The levels of these proteins change during the cell cycle: high levels of Cdt1 (red) correspond to G1 phase, whereas high levels of Geminin (green) correspond to G2 and M phase. In S phase both proteins are expressed at moderate levels (red and green).

HeLa or HeLa Fucci cells were incubated with 5 µM or 15 µM of tubulexin A or DMSO as a control. Changes in the phenotype were monitored for 24 using live-cell imaging. In HeLa cells tubulexin A caused concentration-dependent accumulation of round shaped cells after 10 h which is indicative of mitotic arrest (**Figure 37**). Many of these cells undergo then apoptosis, since membrane blebbing during apoptosis can be observed.[310] In case of HeLa Fucci cells, treatment with 15 µM tubulexin A led to a clear accumulation of green-stained cells (**Figure 38**), indicating that tubulexin A induced G2/M arrest followed by apoptosis because of DNA fragmentation.[311]

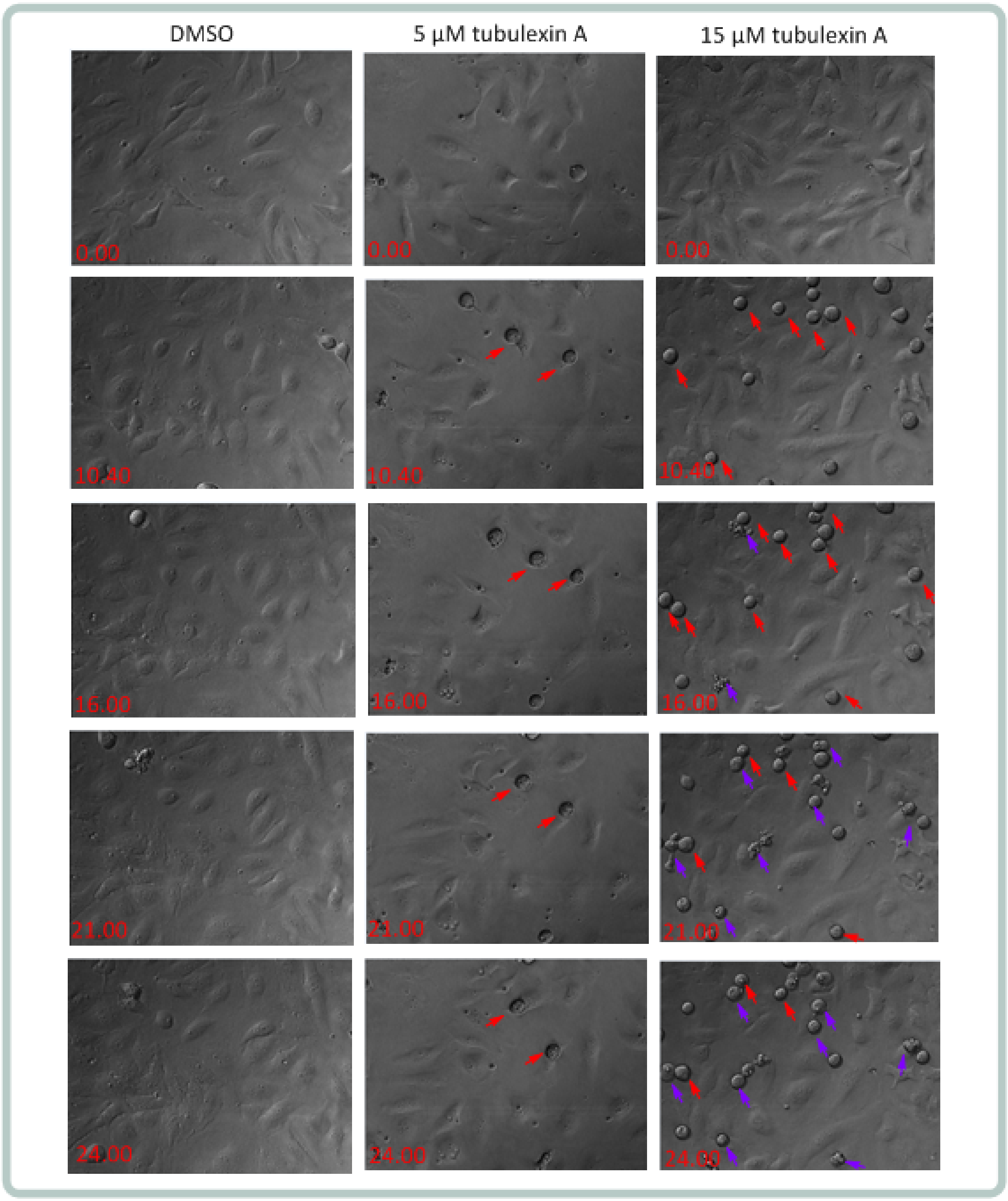
DMSO
5 µM tubulexin A
15 µM tubulexin A
0.00
0.00
0.00
10.40
10.40
10.40
16.00
16.00
16.00
21.00
21.00
21.00
24.00
24.00
24.00

Figure 37: Time-course of the influence of tubulexin A on HeLa cells. HeLa cells were incubated for 24 h with different concentrations of tubulexin A or 0.3% DMSO as a control. Representative images from time-lapse movies at the indicated time-points are shown. Red arrowheads mark cells with rounded shape. Purple arrowheads mark cells undergoing rounded shape. These cells are arrested in mitosis and undergo apoptosis.

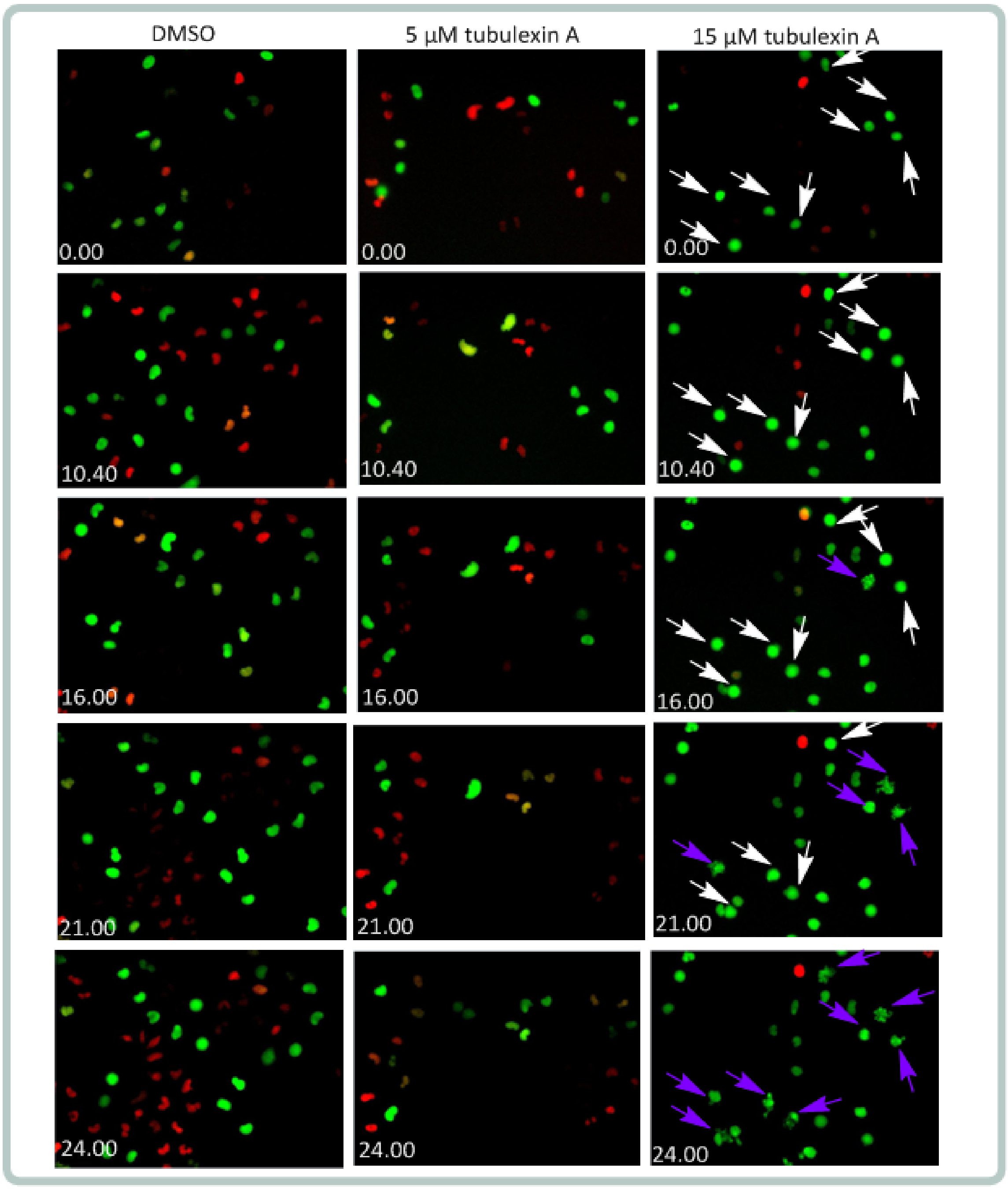
DMSO
5 µM tubulexin A
15 µM tubulexin A
0.00
0.00
0.00
10.40
10.40
10.40
16.00
16.00
16.00
21.00
21.00
21.00
24.00
24.00
24.00

Figure 38: Time-course of the influence of tubulexin A on HeLa Fucci cells. Cells were incubated for 24 h with different concentrations of tubulexin A or 0.3% DMSO as a control. Representative images from time-lapse movies using fluorescence imaging are shown for the indicated time points. White arrowheads mark cells in G2/M phase. Purple arrowheads mark cells arrested in mitosis, which then undergo apoptotic cell Death.

5.4 Confirmation of CAS as target protein of tubulexin A

The protein CAS was identified by Dr. Gerding-Reimers as a potential target of tubulexin A. The binding of tubulexin A to CAS was first analyzed after affinity purification employing HeLa cell lysates and immunoblotting with CAS-specific antibody (Figure 18). After pulldown CAS was enriched only by biotinylated tubulexin A but not with the inactive control. Upon immobilization of either biotinylated tubulexin A or inactive biotinylated compound (**Figure 27**) to streptavidin beads affinity purification using HeLa cell lysate was carried out. Bound proteins were released by heating. Proteins were separated using SDS-PAGE and CAS was detected with a specific antibody. The result showed that CAS is enriched by active biotinylated tubulexin A but not by the inactive biotinylated compound (**Figure 39**).

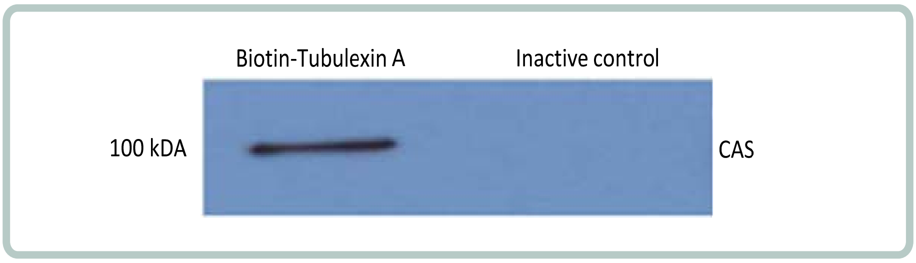

Figure 39: Confirmation of CAS as target protein of tubulexin A by biotinylated tubulexin A using comparison approach of affinity purification. HeLa cell lysate was incubated with immobilized biotinylated tubulexin A and inactive biotinylated analog which were immobilized on streptavidin beads. Upon affinity purification, bound proteins were released by heating and detected by immunoblotting employing goat anti-CAS antibody. The secondary antibody (donkey anti-IgG goat) coupled to horseradish peroxidase (HRP) and was detected detect the chemiluminescence by exposing to X-ray film in dark room.

For further confirmation of the binding of tubulexin A to CAS, purified CAS protein was required. For this, the CAS gene was cloned by the Dortmund Protein Facility (DPF) into pOPINHis(n).EGFP plasmid (section 3.5). Four CAS expressing constructs fused to enhanced green fluorescent protein (EGFP) were generated: full-length CAS (CAS FL, 971 amino acids (aa), with a predicted molecular weight of approximately 107 kDa) fused to EGFP and 6His tag to obtain His.EGFP-CAS FL (1216 aa and a predicted molecular weight of approximately 134 kDa); CAS 391N spans the region from aa1 to aa391 (391 aa with a predicted molecular weight of approximately 45 kDa) fused to His.EGFP to His.EGFP-CAS 391N (636 aa, predicted molecular weight of approximately 74 kDa); CAS 570N from aa1 to aa570 (570 aa, predicted molecular weight of approximately 65 kDa) fused to His.EGFP to His.EGFP-CAS 570N (815 aa, predicted molecular weight of approximately 94 kDa) and CAS 570C with aa570 to aa971 (401 aa, predicted molecular weight of approximately 65 kDa) fused to His.EGFP to His.EGFP-CAS 570N (646 aa, predicted molecular weight of approximately 74 kDa). These CAS constructs were expressed in *E. coli* and purified.

E. coli strain BL21-codonPlus(DE3)-RIL was transformed DNA (pOPINHis-CAS or pOPINHis.EGFP-CAS). Bacteria were grown in SB medium at 37 ^{o}C. Expression was induced with 400 µM IPTG at OD_{600} of 0.6 at 20 ^{o}C. The cells were grown at 20 ^{o}C for 18 h. Harvested cells were suspended in lysis buffer and lysis was performed by sonication. After centrifugation the supernatant was loaded on a Ni-NTA column (Qiagen). After washing step, proteins were eluted at 30 mM imidazole in elution buffer (section 3.3). The collected fractions were digested with PreScission protease to removed His.EGFP (in case His.EGFP-CAS) and were further purified by size exclusion chromatography using Sephadex G200 column (see detail in section 4.4)

Upon purification recombinant proteins fused to His.EGFP were analyzed by means of SDS-PAGE and proteins were stained with Coomassie brilliant blue (**Figure 40A**). His.EGFP-CAS FL, His.EGFP-CAS 391N and His.EGFP-CAS 570N were detected at the predicted size. Proteins were detected by means of immunoblotting (section 4.1.9.4 and 4.1.9.5) using anti-N-terminal of CAS antibody for His.EGFP-CAS FL and all N-terminal fragments of CAS (**Figure 40B**). An antibody against the C-terminus of CAS were employed for detection of His.EGFP-CAS 570C (**Figure 40C**). The results showed that the expected sizes were observed (approximately 134 kDa for His.EGFP-CAS FL, approximately 74 kDa for His.EGFP-CAS 391N and approximately 94 kDa for His.EGFP-CAS 570N). However, the C-terminal construct His.EGFP-CAS 570C could not be detected, although the employed antibody was able to detect His.EGFP-CAS FL (Figure 21C). The purified His.EGFP-CAS 579C was analyzed by means of mass spectrometry. Indeed, the successfully purified proteins (His.EGFP-CAS FL, His.EGFP-CAS 391N, and His.EGFP-CAS 570N) were cleaved by PreScission protease to remove His.EGFP using Ni-NTA column and purified using size exclusion chromatography (section 4.4) (**Figure 40C**).

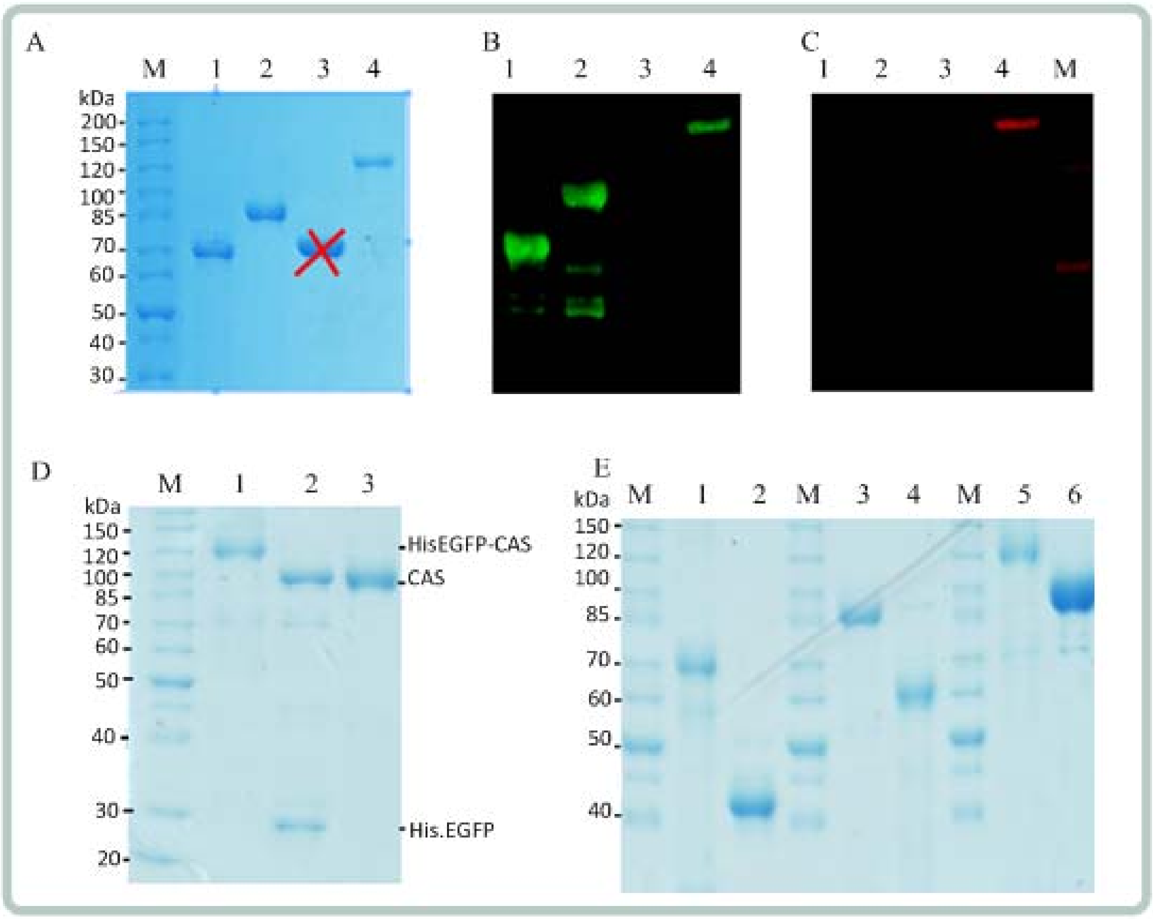

Figure 40: Detection of expressed and purified CAS constructs that were fused to His.EGFP. **A**. Purified proteins were subjected to SDS-PAGE and gels were stained with Coomassie Brilliant blue. **B**. Purified proteins were detected by immunoblotting using an anti-N-CAS antibody and a secondary antibody coupled to IR dye to IRDye800. **C**. Purified proteins were detected by immunoblotting using anti-C-CAS antibody and a secondary antibody coupled to IRDye700 and bound antibodies were detected using the Odyssey Fc imaging system (LI-COR® Biosciences). A, B and C, 1: His.EGFP-CAS 391N; 2: His.EGFP-CAS 570N; 3: His.EGFP-CAS 570C; 4: His.EGFP-CAS FL. IR dye-coupled antibodies were visualized with the Odyssey Fc system. **D**. Purification of CAS FL. Purified protein (uncut or cut with PreScission protease) was subjected to SDS-PAGE and the gel was stained with Coomassie Brilliant blue 1: Uncut His.EGFP-CAS FL; 2: Cleaved His.EGFP-CASFL before loading onto the Ni-NTA column; 3: Cleaved His.EGFP-CAS FL after purification on a Ni-NTA column. **E**. Purification of CAS constructs. Purified proteins (Before and after cleaving His.EGFP) was subjected to SDS-PAGE and the gel was stained with Coomassie Brilliant 1: His.EGFP-CAS 391N; 2: CAS 391N; 3: His.EGFP-CAS 570N; 4: CAS 570N; 5: His.EGFP-CAS FL; 6: CAS FL.

The results of protein purification revealed that it is not possible to express the His.EGFP-CAS 570C fragment in *E. coli* because of toxic or hydrophobic properties of the protein which is difficult to express and purify. For this reason, CAS FL and fragments were cloned in the mammalian expression plasmid pcDNA3.1-FLAG (Plasmid 20011, Addgene) to generate FLAG-tagged proteins. Plasmids were transfected into COS-7 cells using DEAE-Dextran method.[312] 48 hours post DNA transfection, cells lysed and the expression of the proteins were analyzed by means of immunoblotting using antibody against the FLAG tag to detect fusion proteins. Similar to the expression and purification in *E. coli* FLAG-CAS FL, FLAG-CAS 391N and FLAG-CAS 570N, but not FLAG-CAS 570C could be detected (**Figure 41**). Thus, results showed CAS 570C fragment was not expressed even in mammalian cells (COS-7 cells).

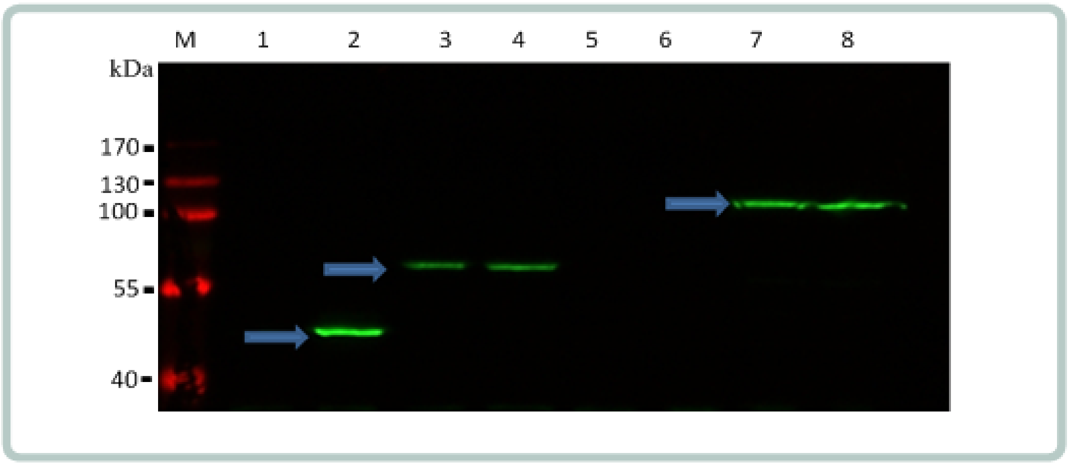

Figure 41: Expression of FLAG-tagged CAS constructs in COS-7 cells. COS-7 cells were transfected using DEAE dextran. 48 h post transfection, cells were lysed and FLAG-tagged CAS proteins were detected by immunoblotting using anti-FLAG tag antibody and secondary antibody coupled to IRDye800cw. Odyssey Fc imaging system was used for image acquisition. 1: cells were transfected pcDNA3.1-FLAG; 2: cells were transfected pcDNA3.1-FLAG-CAS 391N; 3-4: cells were transfected pcDNA3.1-FLAG-CAS 570N; 5-6: cells were transfected pcDNA3.1-FLAG-CAS 570C; 7-8: cells were transfected DNA3.1-FLAG-CAS FL.

5.5 Pulldown of CAS using tubulexin A

To further prove whether CAS can bind to tubulexin A independently of tubulin, a competition approach using purified CAS FL protein was chosen (see the method in section 3.6.4). After immobilization of biotinylated tubulexin A to streptavidin beads and affinity purification using purified CAS proteins, proteins were eluted by increasing concentrations of tubulexin A. In parallel, proteins that remained on the beads were released by heating. Proteins were separated using SDS-PAGE and CAS was detected with specific antibody. CAS could be eluted with 1000 µM of tubulexin A (**Figure 42A**). The amounts of CAS FL that remained bound to the beads were also reduced when 1000 µM of tubulexin A were used for elution (**Figure 42B**). These results indicate that CAS can bind to tubulexin A independently of tubulin free tubulexin A can compete with immobilized tubulexin A for binding to CAS. Thus, CAS is the specific target of tubulexin A.

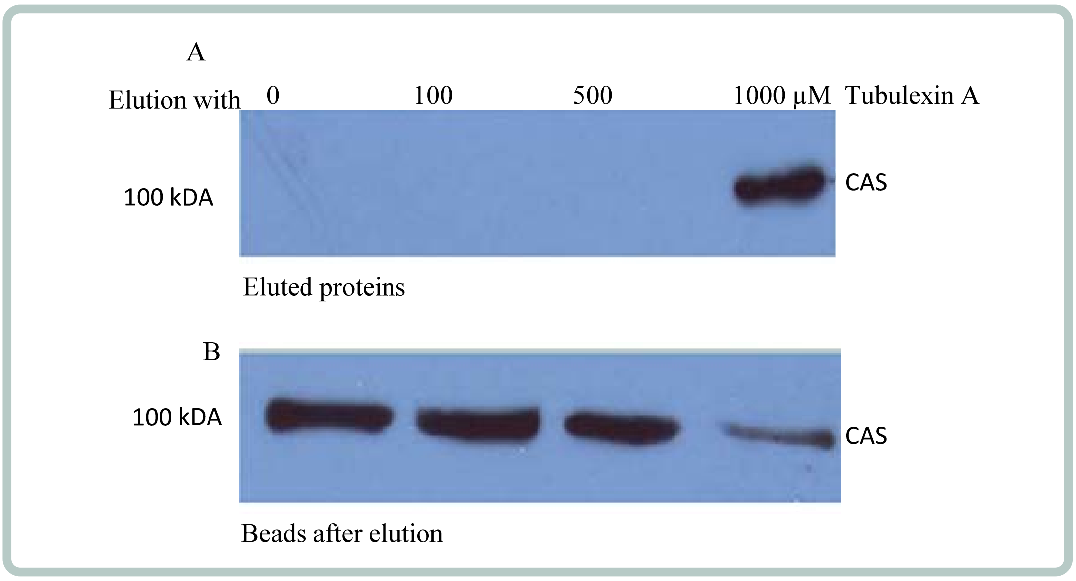

Figure 42: Affinity purification of CAS using biotinylated tubulexin A. **A** and **B:** Competition approach**.** Upon immobilization of biotinylated tubulexin A and affinity purification using purified CAS FL proteins, proteins were eluted by different concentrations of tubulexin A (**A**). Proteins that remained on the beads were collected by heating (**B**). Eluted proteins (**A**) and proteins that were released from the beads (**B**) were subjected to immunoblotting employing goat anti-CAS antibody. The second antibody (donkey anti-IgG goat) coupled to horseradish peroxidase (HRP) and was detected detect the chemiluminescence by exposing to X-ray film in dark room.

5.6 Analysis of the binding affinity of CAS to tubulexin A

The previous results (section 5.5) demonstrate that CAS can bind to tubulexin A independently of tubulin. To determine the binding affinity of this protein to the compound first, an ELISA approach was employed to validate the binding (section 4.6.1). Biotinylated tubulexin A was immobilized on a streptavidin-coated plate and incubated with different concentrations of CAS. Binding was monitored by means of ELISA using an anti-CAS specific antibody and a secondary antibody coupled to HRP. CAS bound to biotinylated tubulexin A with of an apparent K_d value of (0.87 ± 0.05) µM (**Figure 43A).**

Moreover, microscale thermophoresis (MST) (for details see section 4.6.8) was chosen as an alternative method to validate the binding affinity. MST offers the advantage to monitor the binding in solution. MST is based on the movement of molecules along temperature gradients. For this, unmodified tubulexin A was used. 100 nM EGFP-CAS proteins were titrated with different concentrations of free tubulexin A (3 to 10,000 nM). The binding affinity was assessed by means of MST, whereby the change of the fluorescence intensity or the change of concentration ratio of small molecule after IR-Laser heating (hot) and before IR-Laser heating (cold) value (Hot/Cold) or the temperature jump which were used for K_d determination (see detail method in section 4.6.8).

Employing MST method, EGFP-CAS FL bound to tubulexin A with a K_d of (2.3 ± 0.9) µM (**Figure 43B)** which is similar to the value obtained by ELISA (approximately 1 µM). At the same time, the binding of EGFP protein alone to tubulexin A was also studied. 100 nM EGFP was titrated with different concentrations of tubulexin A (3 - 10,000 nM). Thus, the results shown in **Figure 44** that EGFP did not bind to tubulexin A. Weak binding was seen but the K_d could not be determined (**Figure 44)**.

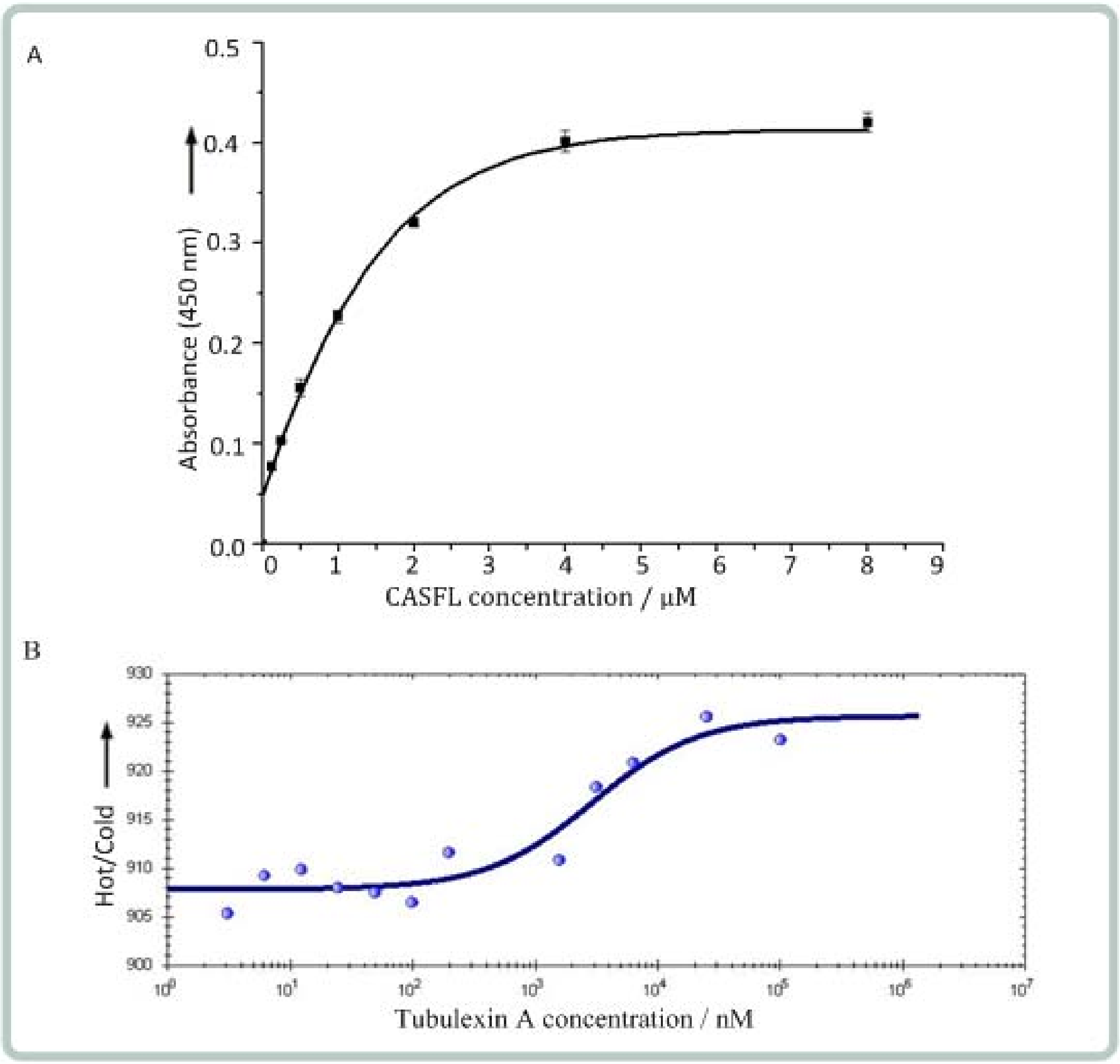

Figure 43: Analysis of the binding of CAS to tubulexin A. **A**. Analysis of the binding of CAS to tubulexin A using ELISA. After incubation of immobilized biotinylated tubulexin A with different concentrations of CAS, binding was monitored by means of ELISA by using an anti-CAS specific antibody and a secondary antibody coupled to HRP. **B**. Analysis of the binding of CAS to tubulexin A using MST. 100 nM EGFP-CAS was incubated with different concentrations of tubulexin A and the binding was monitored by means of MST based on the change of concentration ratio of small molecule after IR-Laser heating (hot) and before IR-Laser heating (cold) value (Hot/Cold).

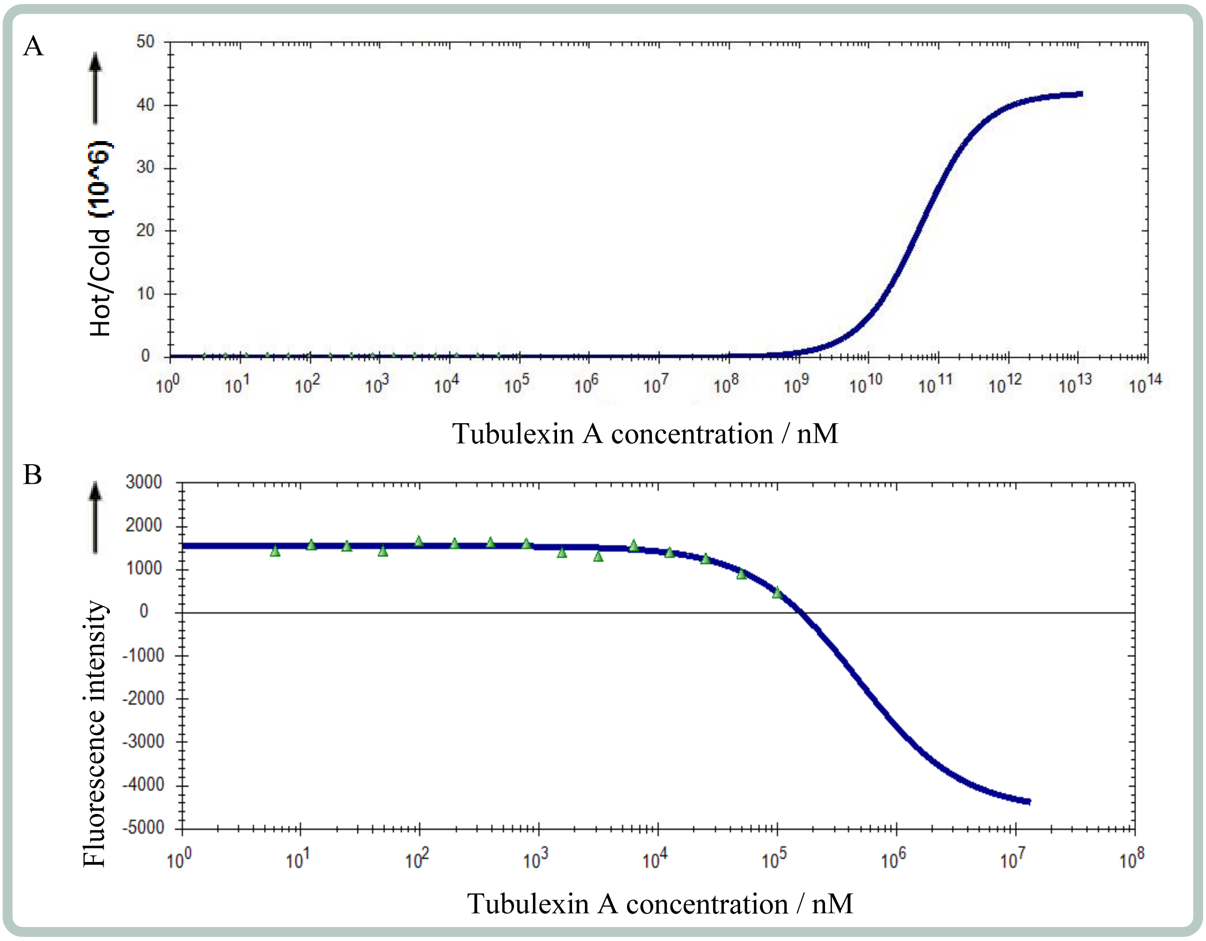

Figure 44: Analysis of the binding of EGFP to tubulexin A. Analysis of the binding of EGFP to tubulexin A using MST. 100 nM EGFP was incubated with different concentrations of free tubulexin A and the binding was monitored by means of MST based on the change of concentration ratio after and before IR-Laser heating (Hot/Cold) value (**A**) or change of fluorescence intensity after IR-Laser heating (**B**).

5.7 Mapping the binding site of tubulexin A in CAS

Based on the finding that purified CAS FL binds to tubulexin A, different CAS constructs were employed to map the binding site for tubulexin A. The binding of CAS 391N and CAS 570N to tubulexin A was determined by means of ELISA and MST.

EGFP-CAS 391N bound to biotinylated tubulexin A with an apparent K_d value of (28.5 ± 16.8) µM when using the ELISA approach (**Figure 45A**). When MST was employed, the binding affinity K_d, which was determined by means of the change of fluorescence intensity was (91.1 ± 51.0) µM (**Figure 45B**).

EGFP-CAS 570N bound to biotinylated tubulexin A with an apparent K_d value of (5.4 ± 1.8) µM in ELISA (**Figure 46A**) and (66.4 ± 18.9) µM using MST (**Figure 46B**). These results demonstrate that CAS 391N and CAS 570N can bind to tubulexin A, but the binding affinity of CAS 391N and CAS 570N to tubulexin A is weaker than the binding affinity of CAS FL to tubulexin A.

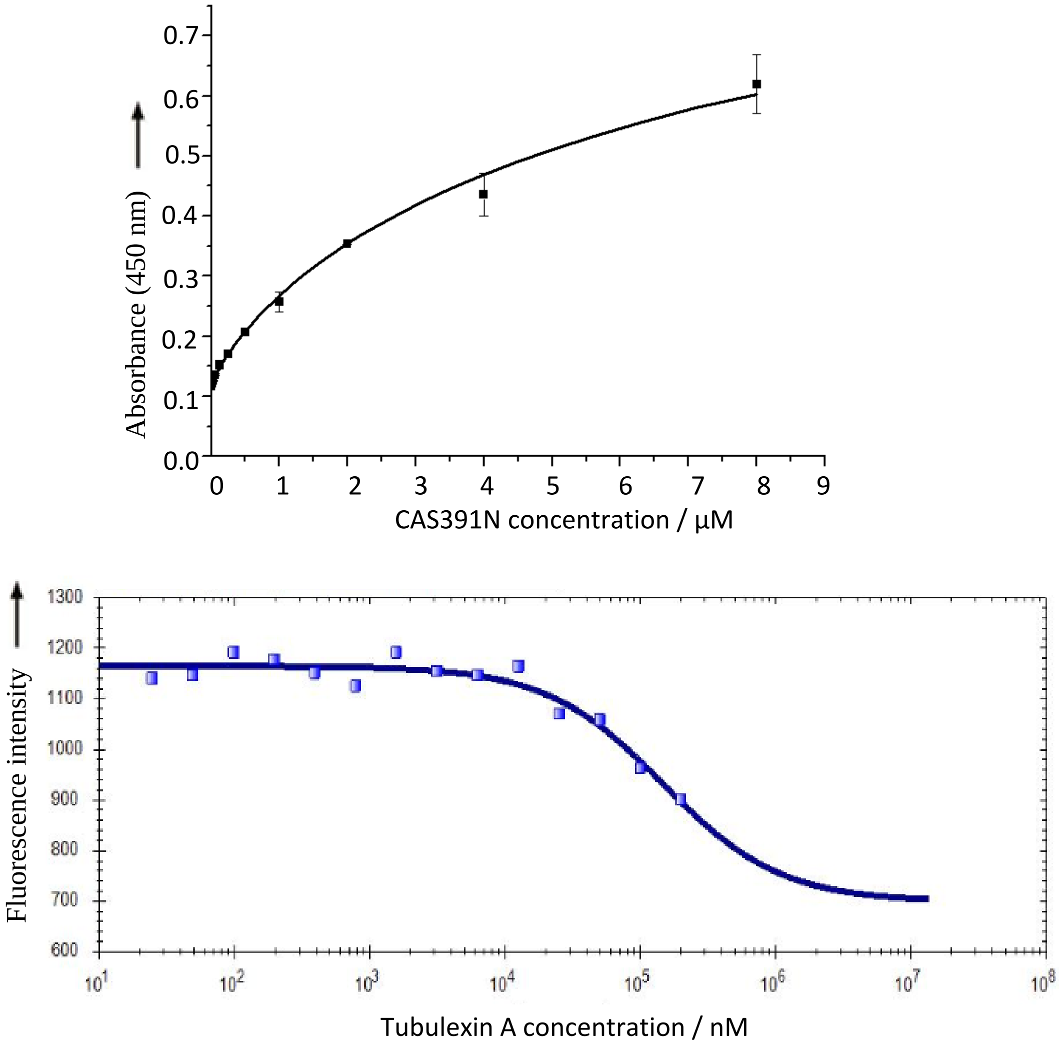

Figure 45: Analysis of the binding of CAS 391N to tubulexin A. **A**. Analysis of the binding of CAS 391N to biotinylated tubulexin A using ELISA. After incubation of immobilized biotinylated tubulexin A with different concentrations of CAS 391N, binding was monitored by means of ELISA by using a specific antibody anti-CAS and a secondary antibody coupled to HRP. **B**. Analysis of the binding of EGFP-CAS 391N to tubulexin A applying MST. Different concentrations of EGFP-CAS 391N were incubated with tubulexin A and binding affinity monitored by means of MST based on fluorescence change after and before IR-Laser heating.

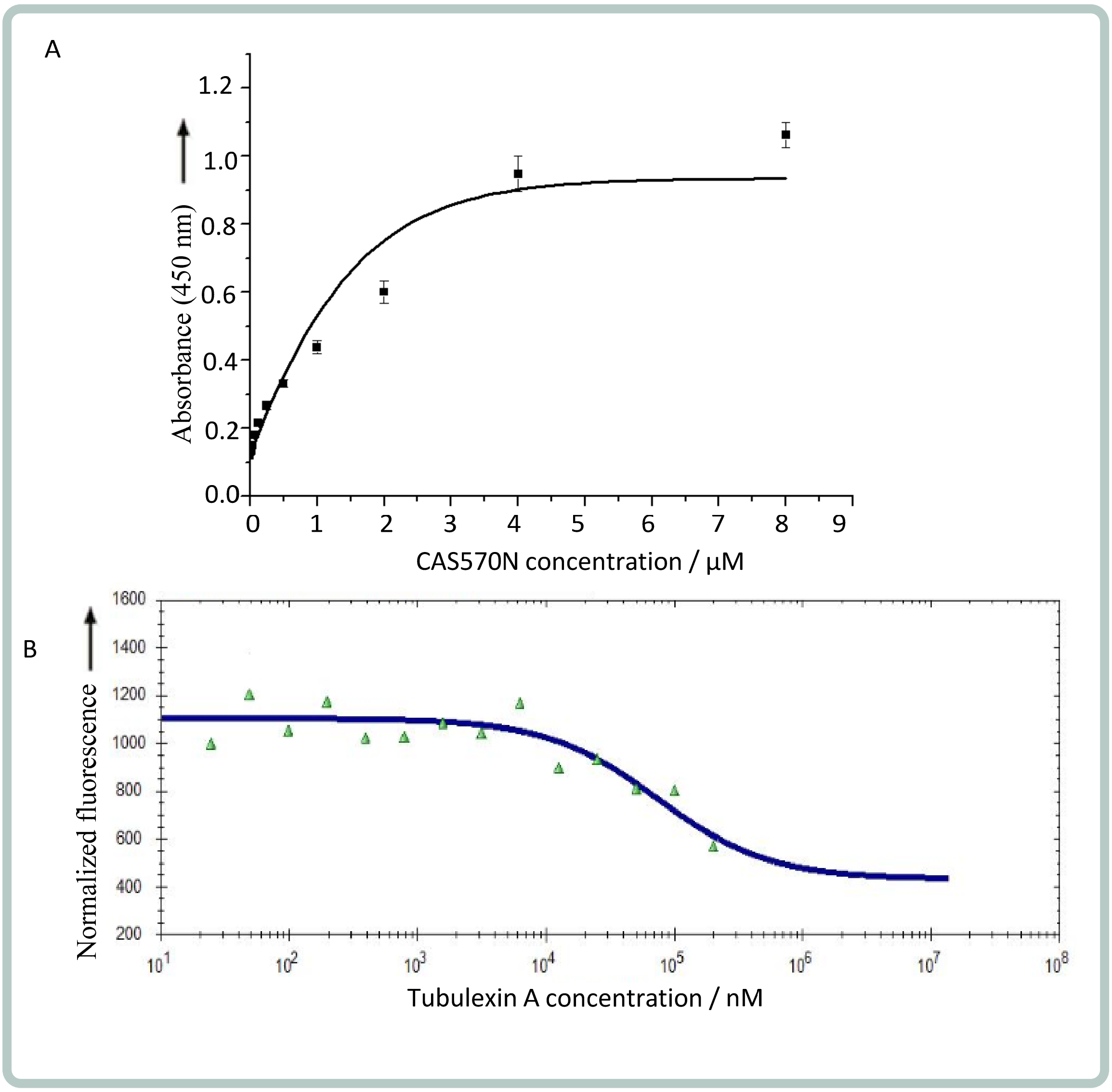

Figure 46: Analysis of the binding affinity of CAS570N to tubulexin A. A. Analysis of the binding affinity of CAS 570N to tubulexin A using ELISA. After incubation of immobilized biotinylated tubulexin A with different CAS 570N concentrations, binding was monitored by means of ELISA by using anti-CAS antibody and a secondary antibody coupled to HRP. **B**. Analysis of the binding affinity of CAS 570N to tubulexin A using MST. Incubation of EGFP-CAS 570N with different concentration of free tubulexin A and the binding affinity monitored by means of MST based on fluorescence change after and before IR-Laser heating.

5.8 Influence of tubulexin A or/and CAS on tubulin polymerization *in vitro*

Previous results by Dr. Gerding-Reimers showed that tubulexin A binds to tubulin and inhibits tubulin polymerization *in vitro* (section 4.6.2.1). Based on this result, the effect of tubulexin A and CAS on tubulin polymerization was studied *in vitro* by means of a turbidity-based assay. In addition, tubulin polymerization assay that is based on the increase in DAPI fluorescence upon binding to assembled with tubulin greater affinity (with a K_d value of 6 ± 2 μM) than to dimeric tubulin (with a K_d value of 43 ± 5 μM)[293,294] has been developed (details in section 4.6.2.2) and was applied to confirm the results of the turbidity assay. In the turbidity assay, tubulin was polymerized to microtubules in a buffer containing the necessary co-factors (GTPs).

Porcine tubulin was pre-incubated with tubulexin A, CAS or tubulexin A and CAS, DMSO and 0.5 μM nocodazole as controls. Afterwards, GTP was added to initiate tubulin polymerization and tubulin turbidity was measured at 340 nm. Results showed that low concentrations of tubulexin A or CAS have only a slight inhibitory influence on tubulin polymerization (the curves for 1 and 5 μM tubulexin look quite similar to the CAS curves). However, when both tubulexin A and CAS were applied together, tubulin polymerization was inhibited. This finding suggests a synergistic mode of inhibition of tubulin polymerization for CAS and tubulexin A (**Figure 47A).** The DAPI fluorescence-based assay was used as an alternative method to confirm this result. For this, tubulin and related co-factors (GTP) are pre-incubated with DAPI and the tubulexin A, CAS and DMSO or nocodazole as controls. When GTP is added, tubulin polymerization starts and DAPI binds to the newly formed microtubules, and consequently an increase in the DAPI fluorescence signal at 460 nm can be measured.[293] Employing this method, it was observed that tubulexin A or CAS alone inhibit tubulin polymerization to a weaker extent compared to the inhibition, which is mediated by tubulexin A and CAS. Thus, CAS and tubulexin A inhibit tubulin polymerization synergistically (**Figure 47B).**

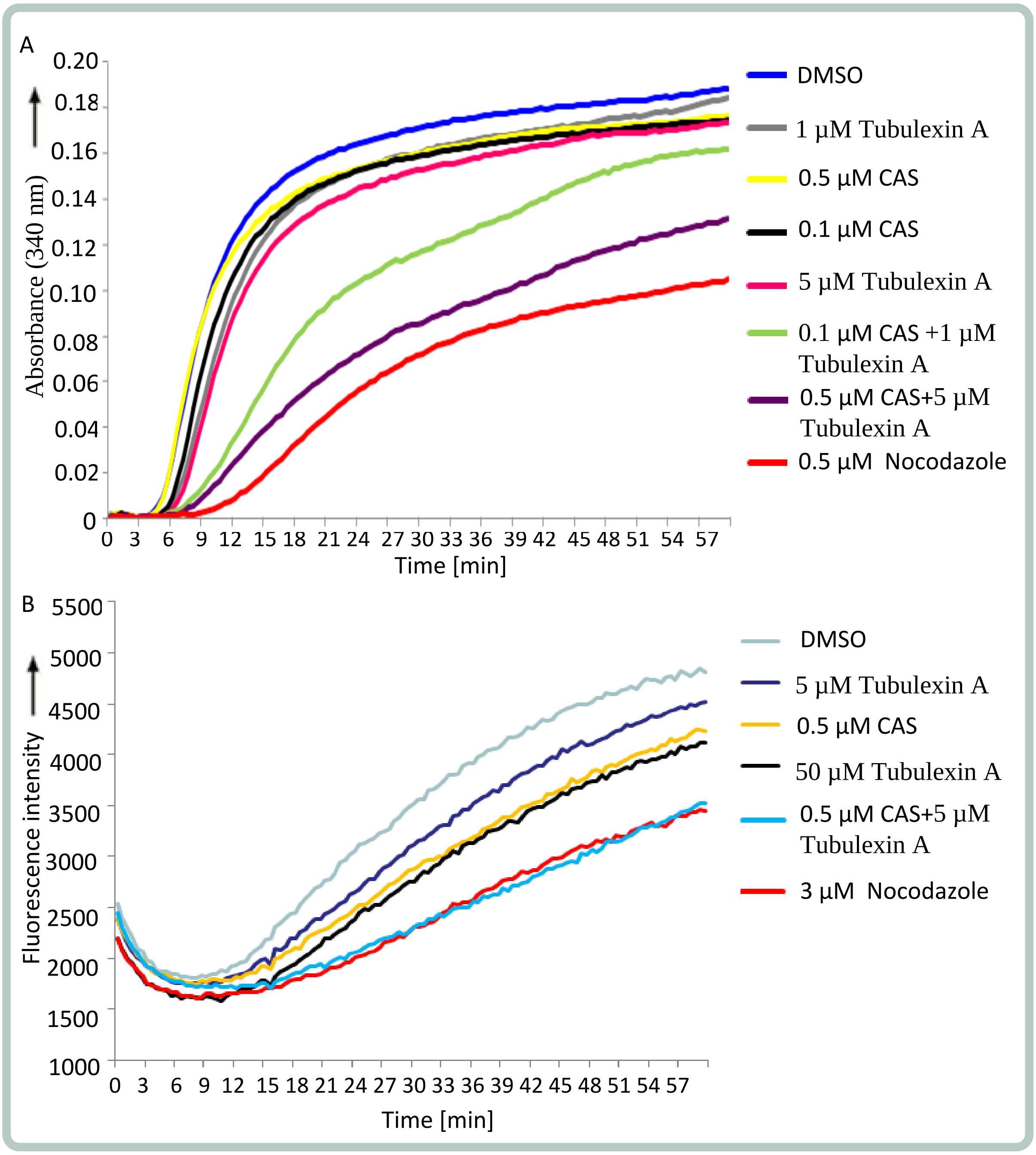

Figure 47: Effect of tubulexin A or/and CAS on tubulin polymerization *in vitro*. A. Turbidity-based assay. *In vitro* polymerization of tubulin was monitored at 340 nm in the presence of tubulexin A and CAS or DMSO and nocodazole as controls. **B.** DAPI fluorescence-based assay. Tubulin polymerization was monitored by fluorescence measurement at 460 nm in the presence of tubulexin A and CAS or DMSO and nocodazole as controls.

5.9 The effect of tubulexin A on nuclear export mediated by CAS

CAS is a nuclear export factor for importin alpha, which recycles importin alpha from the nucleus to the cytosol. To study the influence of tubulexin A on importin alpha localization HeLa cells were treated with various concentrations of the compound for 2 h. The results demonstrated that tubulexin A did not influence the localization of importin alpha in HeLa cells (**Figure 48**).

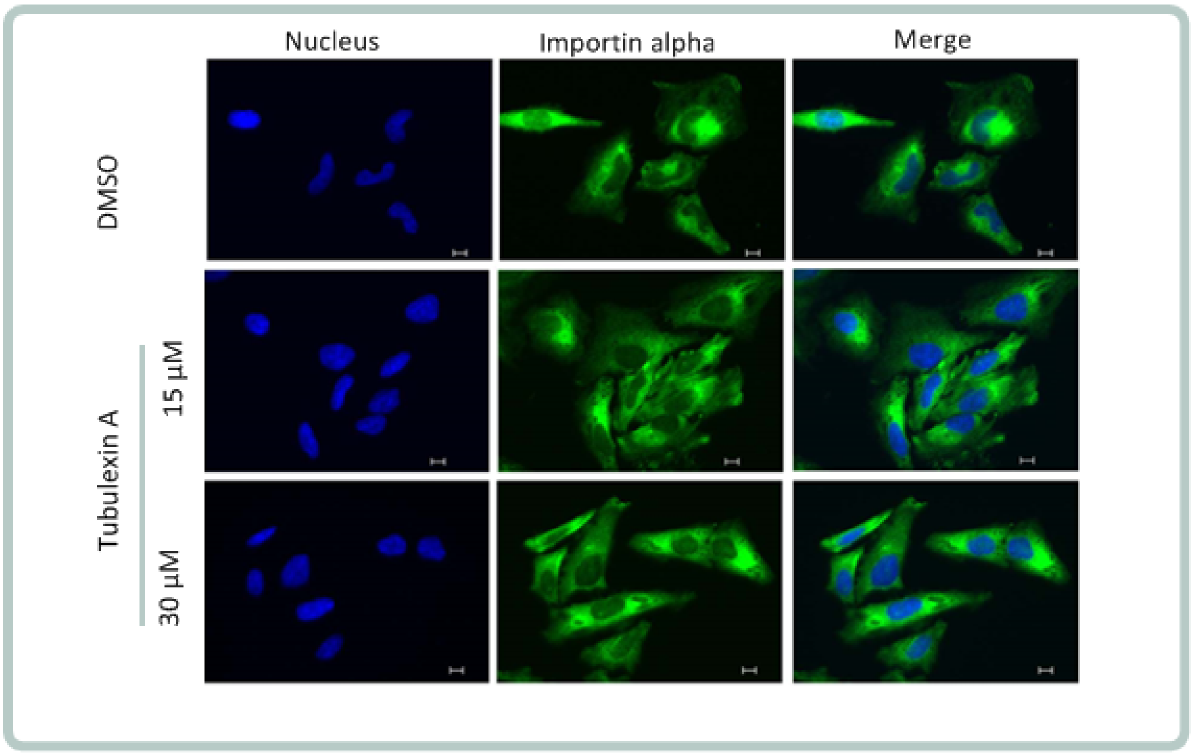

Figure 48: Influence of tubulexin A on importin alpha localization in HeLa cells. Cells were incubated for 2 h either with tubulexin A at concentrations of 15 µM and 30 µM or 0.3% DMSO as a control. Cells were fixed, permeabilized and stained with antibodies specific for importin alpha and DAPI. An antibody coupled to Alexa Fluor 488 was used to detect importin alpha (green) and DAPI was used to stain DNA (blue). Images were taken on a Zeiss Observer microscope. Scale bar: 10 µm.

5.10 Influence of tubulexin A on the interaction of CAS, importin alpha and RAN

5.10.1 Optimization of the pulldown procedure based on immunoprecipitation (IP)

CAS binds strongly to importin alpha in the presence of RANGTP forming an importin alpha/CAS/RanGTP complex.[272] Based on this interaction, the influence of tubulexin A on this complex was analyzed using pulldown. In principle, anti-CAS antibody can be coupled (immobilized) to protein G beads (matrix) either before or after interacting with CAS proteins in complex of CAS, RANGPPNHP and Importin alpha which were pre-incubated with tubulexin A or DMSO as a control. After washing to remove non-binding proteins, bound proteins were collected and detected using Western blot (see detail method in section 4.6.7). RANGPPNHP (GPPNHP: nonhydrolyzable GTP analogue guanosine 5'-O-(beta, gamma-imidotriphosphate)) which is a nonhydrolyzable GTP analogue was employed in this experiment.

In this work, free anti-CAS antibody was incubated with the complex of proteins which may permit the interaction of protein CAS and anti-CAS antibody in solution before immobilization of anti-CAS antibody on the protein G sepharose beads. Further, the complex of proteins and anti-CAS antibody was pre-incubated either with tubulexin A or DMSO as a control before immobilization step, which allows that anti-CAS antibody is coupled to the beads. First, the protein G sepharose beads were prepared and non-specific binding sites were blocked (section 4.6.7.1). Afterwards, the conditions for the specific antibody and the concentration of proteins to form this complex were optimized (detail method in section 4.6.7.2).

As a control, the binding of RANGPPNHP in absent anti-CAS antibody to the prepared protein G sepharose beads was analyzed. For this, beads were with 10 µM RANGPPNHP and the binding of RAN to the protein G sepharose was analyzed by means of immunoblotting using anti-RAN antibody. Results showed that RAN could not bind to G sepharose beads without anti-CAS antibody (**Figure 49A 1-2**). The same observation was made for importin alpha and CAS. When protein G sepharose beads were incubated with 5 µM importin alpha in the absence of anti-CAS antibody, importin alpha could not bind to G sepharose beads (**Figure 49A 3-4**). When 5 µM CAS was incubated with protein G sepharose beads, CAS could not bind to protein G sepharose in the absence of anti-CAS antibody (**Figure 49B 1-2**) and was detected only in presence of anti-CAS antibody (**Figure 49B 3-4**). Still weak bands for RAN and importin alpha were visible in the control experiments (**Figure 49A 3-4**), but they were so weak that the signal could not be due to the pulldown results.

The optimized IP conditions were used with samples containing the complex of 5 µM importin alpha, 10 µM RANGPPNHP and 5 µM CAS (**Figure 49C-D 1-2**), the complex of 5 µM importin alpha and 5 µM CAS (**Figure 49C-D 3-4**) or complex of 10 µM RANGPPNHP and 5 µM CAS (**Figure 49C-D 5-6**). All complexes were incubated with anti-CAS antibody and then added to the protein G sepharose beads (see section 4.6.7.3). Upon pulldown, all proteins were detected by means of immunoblotting using anti-importin alpha, anti-CAS, or anti-RAN antibody. Results showed that CAS can interact with RAN and importin alpha *in vitro* to form the complex of importin alpha/RANGPPNHP/CAS or importin alpha/CAS or RANGPPNHP/CAS (**Figure 49C-D**).

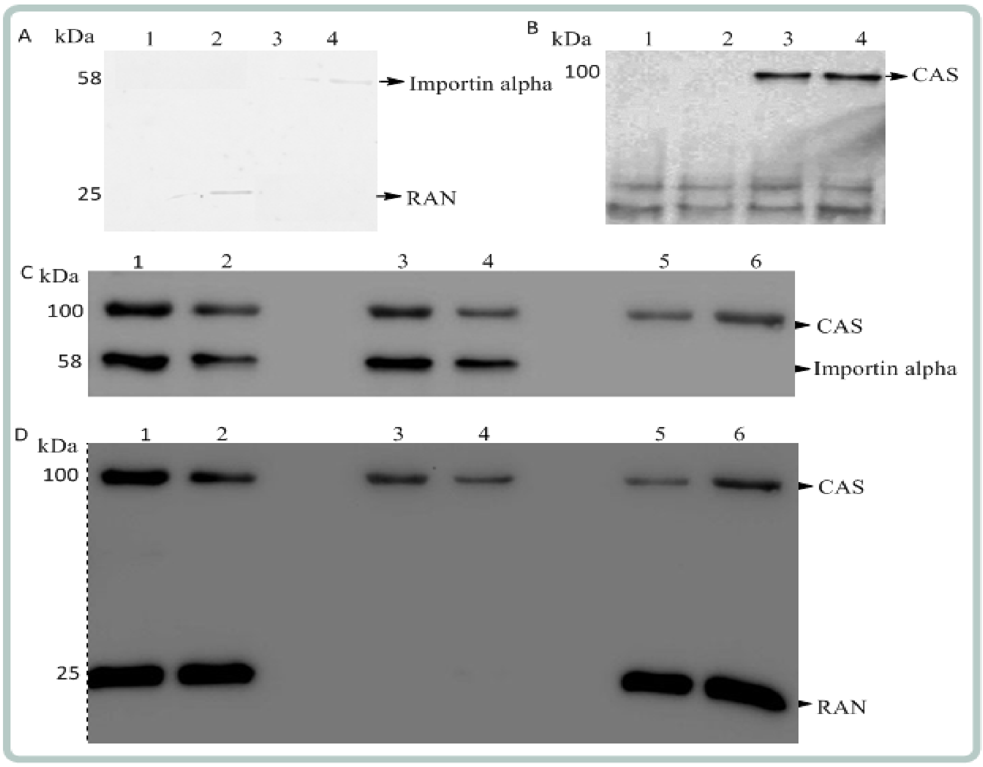

Figure 49: Checking condition for IP assay of CAS/importin alpha/RANGPPNHP complex *in vitro*. A. Testing the binding of RANGPPNHP and importin alpha to the beads. 1-2: The G-protein sepharose was incubated solution containing RAN in the absence of an anti-CAS antibody. Upon pulldown, immunoblotting using anti-RAN antibody was employed to detect RAN. 3-4: The G-protein sepharose was incubated solution containing importin alpha in absence of anti-CAS antibody. Upon IP immunoblotting using anti-importin alpha antibody was performed. **B**. Binding of CAS to protein G beads. 1-2: Protein G sepharose was incubated with CAS in the absence of anti-CAS antibody; 3-4: Protein G sepharose was incubated with CAS in the presence of anti-CAS antibody. Upon IP immunoblotting using anti-CAS antibody was performed. **C-D**: *In vitro* CAS/RANGPPNHP/importin alpha complex formation. Either of the three complexes (importin alpha/RANGPPNHP/CAS, importin alpha/CAS or RANGPPNHP/CAS) was pre-incubated with an anti-CAS

antibody prior to incubation with protein G beads. Upon IP, all proteins were detected by immunoblotting using anti-importin alpha, anti-CAS, and anti-RAN antibody. 1-2: importin alpha/RANGPPNHP/CAS; 3-4: importin alpha/CAS complex formation; 5-6: RANGPPNHP/CAS complex formation.

5.10.2 Influence of tubulexin A on the *in vitro* interaction of CAS, importin alpha and RAN

The optimized IP conditions were applied to study the influence of tubulexin A on the interaction of the three proteins (see section 5.10.1). The proteins were pre-incubated with the anti-CAS antibody. Afterwards, complexes of 5 µM importin alpha/10 µM RANGPPNHP/5 µM CAS (**Figure 50 1-2**), 5 µM importin alpha/ 5 µM CAS (**Figure 50 3-4**) or complex of 10 µM RANGPPNHP/5 µM CAS (**Figure 50 5-6**) were incubated with either 500 µM tubulexin A or DMSO as control prior to addition of protein G sepharose beads (4.6.7.3). Upon IP, proteins were loaded on SDS-PAGE and separated proteins were transferred to PDVF membrane followed by immunoblotting using anti-CAS, anti-importin alpha and anti-RAN antibody. Results showed that tubulexin A did not influence both binding of RAN and importin alpha to CAS or it might be hard to disturb a preformed complex. Further, this experiment should be tried with concomitant incubation of tubulexin A with proteins during complex formation (this idea has not been done).

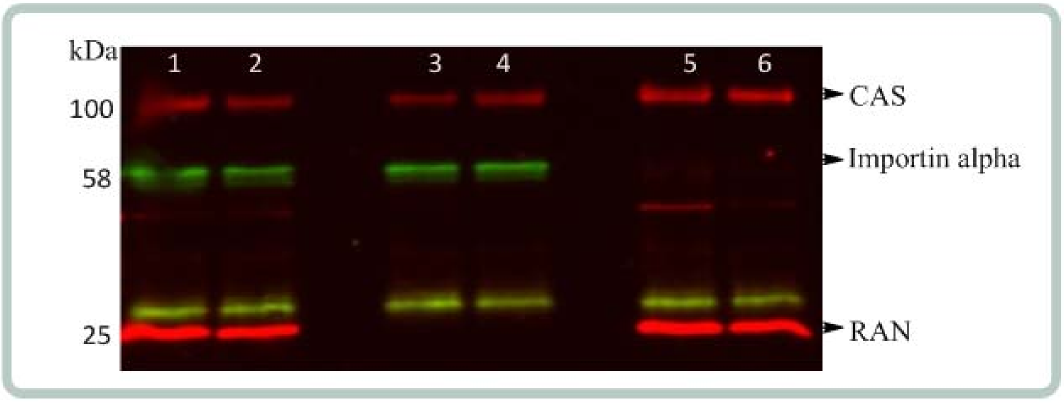

Figure 50: Influence of tubulexin A on the *in vitro* interaction of CAS, importin alpha and RAN. Protein G beads were incubated with solution of protein complexes containing either 500 µM free tubulexin A or DMSO as control. Upon pulldown, proteins were detected by immunoblotting using anti-CAS, anti-importin alpha and anti-RAN antibody. 1,3,5: complexes were incubated with DMSO (control) and 2,4,6: complexes were incubated with tubulexin A. 1-2: the complex of importin alpha/ RANGPPNHP/CAS; 3-4: complex of importin alpha/CAS; 5-6: the complex of RANGPPNHP/CAS

5.10.3 The influence of tubulexin A on the interaction of tubulin, importin alpha and RAN with CAS in HeLa cells

The interaction of CAS with tubulin, importin alpha, and RAN in HeLa cells was studied using Doulink II fluorescence (see detail method in section 4.8.7). In parallel to the in vitro studies of the influence of tubulexin A on the interaction of CAS/importin alpha/RAN, the effect of tubulexin A on the interaction of tubulin, RAN, importin alpha with CAS were investigated in HeLa cells using proximity ligation assay (Duolink in situ PLA, OLINK BIOSCIENCE). HeLa cells were treated with different concentrations of tubulexin A or DMSO as a control. Cells were fixed, pre-treated with blocking buffer for primary antibodies incubation according the manufacturer's manual.[313] Samples were incubated with primary antibodies that bind to the proteins to be detected, followed by incubation with secondary antibodies conjugated with oligonucleotides (PLA probe MINUS and PLA probe PLUS). Upon ligation and amplification (detail method in section 4.8.7), fluorescence was monitored using Zeiss Observer microscope with a magnificent objective lens of 63X. Upon treatment with tubulexin A the interaction of tubulin and CAS was not disturbed (**Figure 51**). Similarly, tubulexin A does not affect the interaction of CAS and importin alpha (**Figure 52**), or of CAS and RAN (**Figure 53**) in HeLa cells.

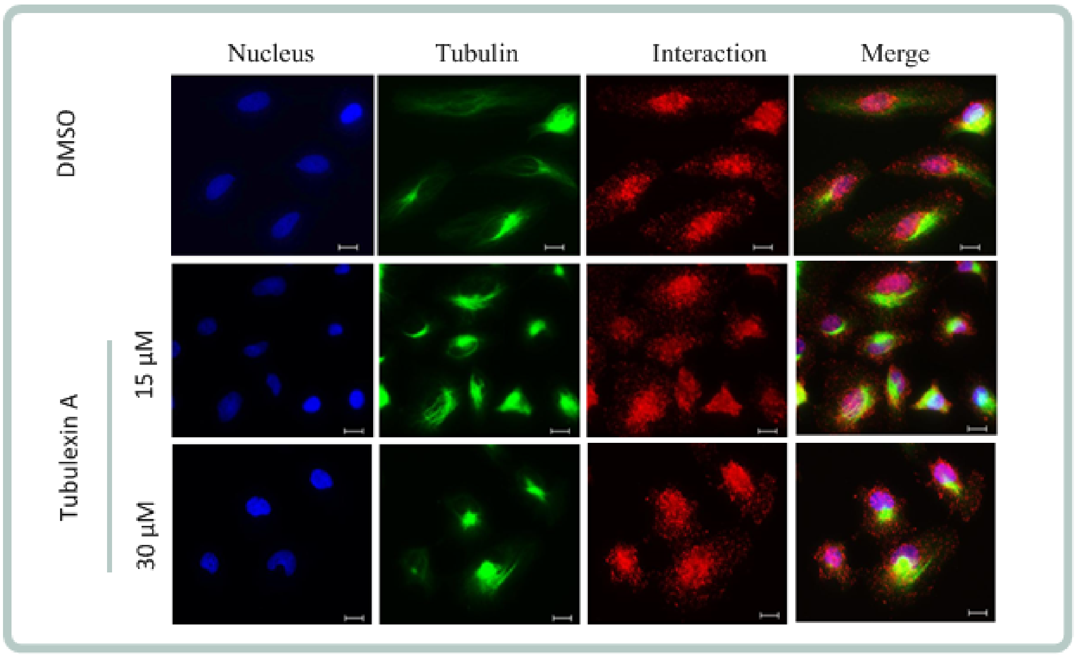

Figure 51: The influence of tubulexin A on the interaction of tubulin and CAS. HeLa cells were treated with different concentrations of tubulexin A or DMSO as a control. Cells were fixed, blocked and incubated with

primary anti-tubulin and anti-CAS antibody, followed by PLA assay. After the PLA assay cells were stained for tubulin antibody coupled with Alexa Fluor® 488 (green) to mark the cells. Stained cells spot were analyzed by fluorescence microscopy. Cells were stained with DNA (blue), tubulin (green), the interaction signal spots (red). Scale bar: 10 µm.

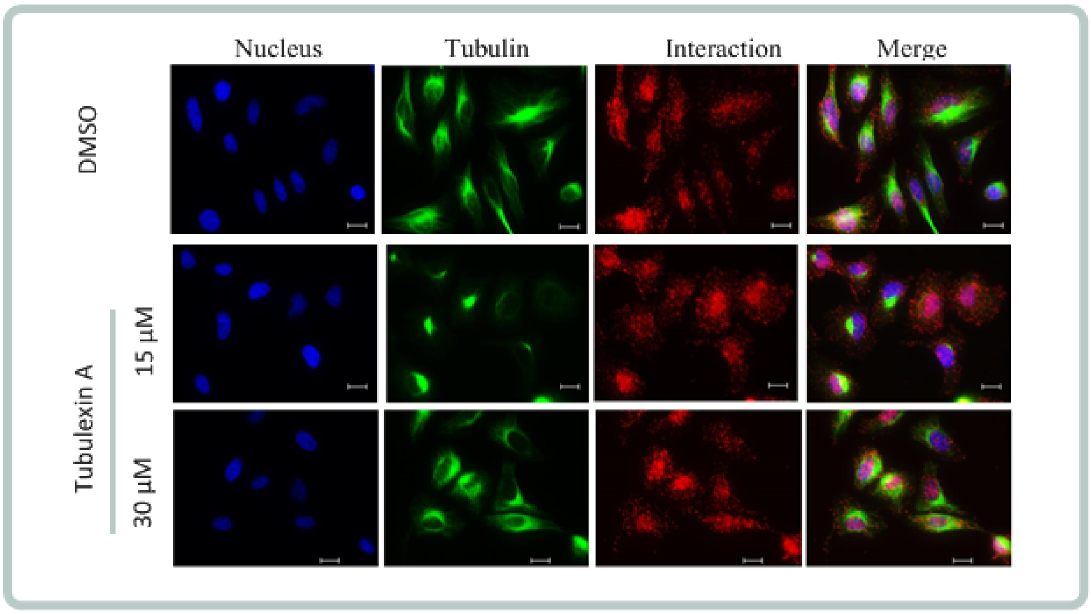

Figure 52: The influence of tubulexin A on the interaction of importin alpha and CAS. HeLa cells were treated with different concentrations of tubulexin A or DMSO as a control. Cells were fixed, blocked and incubated with primary anti- importin alpha and anti-CAS antibody, followed by PLA assay. After the PLA assay cells were stained for tubulin antibody coupled with Alexa Fluor® 488 (green) to mark the cells. Stained cells spot were analyzed by fluorescence microscopy. Cells were stained with DNA (blue), tubulin (green), the interaction signal spots (red). Scale bar: 10 µm.

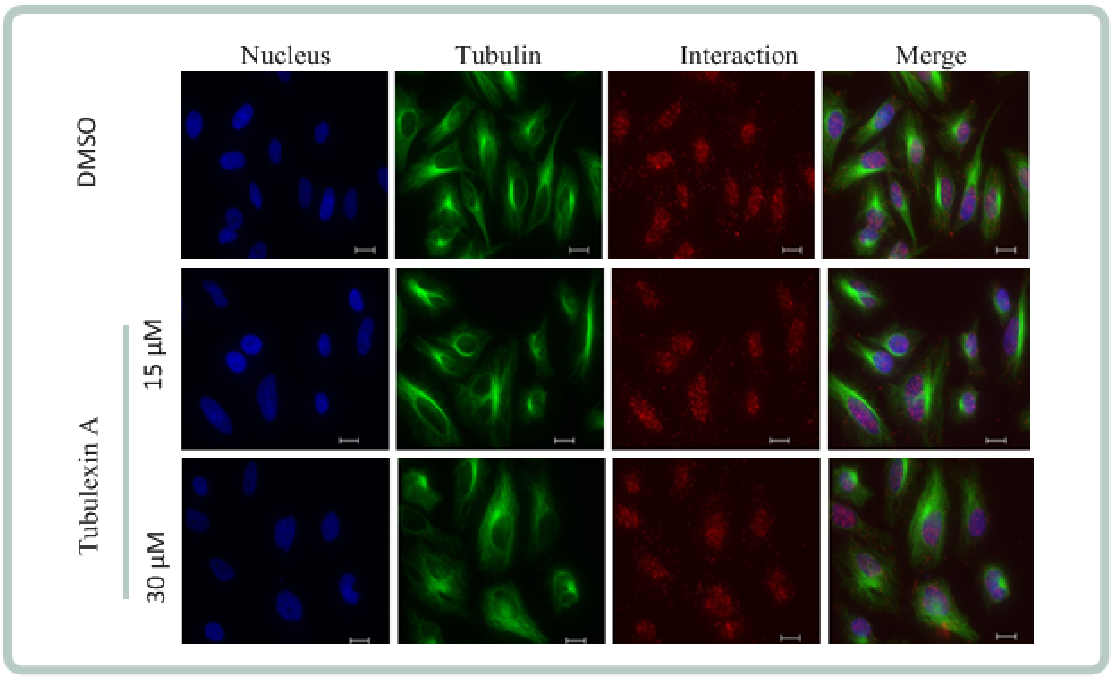

Figure 53: The influence of tubulexin A on the interaction of RAN and CAS. HeLa cells were treated with different concentrations of tubulexin A or DMSO as a control. Cells were fixed, blocked and incubated with primary anti-RAN and anti-CAS antibody, followed by PLA assay. After the PLA assay cells were stained for tubulin antibody coupled with Alexa Fluor® 488 (green) to mark the cells. Stained cells spot were analyzed by fluorescence microscopy. Cells were stained with DNA (blue), tubulin (green), the interaction signal spots (red). Scale bar: 10 µm.

Evaluation of podoverine A as tubulin inhibitor

5.11 Influence of podoverine A on the *in vitro* tubulin polymerization

Previous work done by Dr. Gerding-Reimers showed that the natural product podoverine A was very potent in a phenotypic screen for mitosis modulators, for which a library of natural products was employed. This compound induces G2/M cell cycle arrest and inhibits microtubule regrowth in BSC-1 cells. To validate podoverine A as tubulin inhibitor, *in vitro* tubulin polymerization assay based on turbidity measurement was performed (see detail in section 4.6.2.1). Results demonstrated that podoverine A weakly inhibits tubulin polymerization at 50 µM whereas it does not influence microtubule formation at lower concentrations (**Figure 54)**. Thus, podoverine A inhibits tubulin polymerization which may induce G2/M cell cycle arrest.

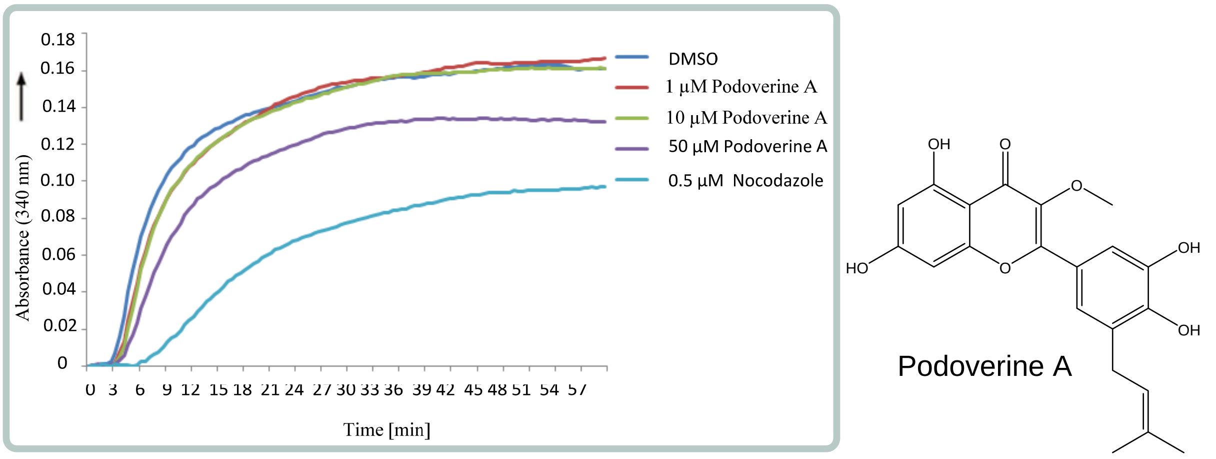

Figure 54: The influence of podoverine A on tubulin polymerization. *In vitro* polymerization of tubulin was monitored at 340 nm in presence of different concentrations of podoverin A or DMSO and nocodazole as controls.

5.12 Evaluation of the binding site of podoverine A in tubulin

There are two well characterized binding sites in tubulin, to which tubulin inhibitors bind, vinca site and colchicine site. To analyze if podoverine A binds to one of these sites competition assays were performed. To study binding to the vinca site (section 4.6.6), tubulin-vinblastine complex was formed by incubating 2.5 µM tubulin with 2.5 µM BODIPY-FL-vinblastine (fluorescent analogue of vinblastine) for 30 min at room temperature. Then, podoverine A or vincristine was added for 30 min. Fluorescence was monitored at excitation/emission 470/514 nm) in black 96 well plates. Results showed that podoverine A displaces BODIPY-FL-vinblastine from tubulin since a concentration-dependent decrease in fluorescence intensity is observed upon addition of different concentrations of podoverine A (**Figure 55A**). Concentration corresponding 50% effect (or half maximal effective concentration, EC_{50}) values for BODIPY-FL-vinblastine displacement was (4.17 ± 1.39) µM for vinblastine and (15.3 ± 1.33) µM for podoverine A.

In parallel, binding of podoverine A to the colchicine site was investigated (section 4.6.5). The tubulin-colchicine complex was formed by incubating 5 µM tubulin with 50 µM colchicine for 30 min at RT. Upon binding to tubulin, the intrinsic fluorescence of colchicine increases. Then, podoverine A or nocodazole (nocodazole is known as a compound binding to colchicine-binding site of tubulin) or DMSO as controls were incubated with the preformed tubulin-colchicine complex for 30 min at RT. Fluorescence readings at excitation/

emission 365 nm/435 nm were performed in black 96 well plates. Results showed that podoverine A cannot displace colchicine from tubulin and thus does bind to the colchicine site (**Figure 55B**). Thus, podoverine A binds to tubulin at vinca-binding site.

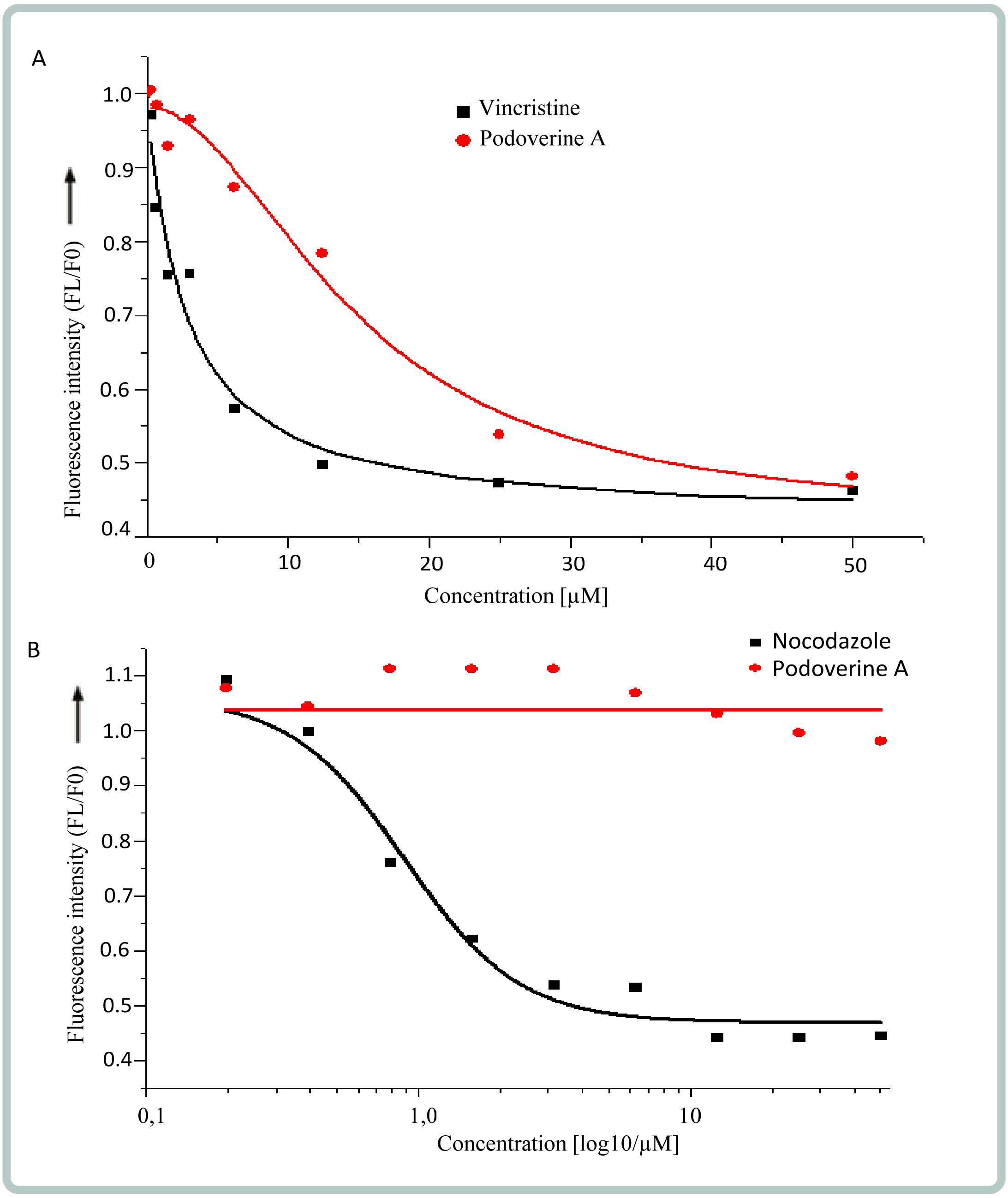

Figure 55: The binding site of podoverine A to tubulin. A. Vinca binding site assay. Tubulin-vinblastine complex was formed and then podoverine A or vincristine and DMSO as controls were added for 30 min at RT. Fluorescence was monitored at excitation/ emission 490/514 nm. **B**. Colchicine binding site assay. Tubulin-colchicine complex was formed and podoverine A or nocodazole and DMSO as controls were incubated with the preformed tubulin-colchicine complex for 30 min at RT. Fluorescence was detected at excitation/ emission 365/435 nm.

Investigation of CAS inhibitors by means of reverse chemical genetics

5.13 Chemical array for screening CAS inhibitors

The goal of this work was to identify small molecules targeting CAS since CAS is overexpressed in cancer and considered as a potential target for cancer treatment. Currently, there is no small molecule targeting CAS yet. Thus, chemical array approach is employed to search small molecules that bind to CAS. This project was carried out within the RIKEN-Max Planck Joint Research Centre for Systems Chemical Biology.

The chemical library "RIKEN Natural Products Depository (RIKEN NPDepo)" including approximately 22,000 compounds was immobilized on glass slides (referred to as RIKEN array). The slides were prepared based on reactivity of the carbene species of compound generated from trifluoromethylaryldiazirine upon UV irradiation. Thousands of small molecules were covalently attached onto glass slides.[103,104,314-316] Chemical array slides were also prepared for approximately 4,000 compounds of the COMAS (Compound Management and Screening Center) library (referred to as MPI array). Both RIKEN and MPI arrays were applied to identify compounds that bind to CAS. As a source of CAS, purified CAS protein and cell lysates of CAS-overexpressing HEK293T cells were used.

After incubating the glass arrays with purified CAS or cell lysate, slides were incubated with first (mouse anti-His tag) and secondary (goat anti-mouse IgG) antibodies coupled to Cy5. The fluorescence of the dried slides was then monitored using GenePix microarray scanner and images were analyzed using Photoshop 5.5. For data analysis the fluorescence intensity of each spot was corrected by the local background and by a blank control (detail of method in section 4.9).

5.13.1 Screening of NPDepo (RIKEN arrays)

5.13.1.1 Targeting purified CAS

Purified His-CAS and His.EGFP(n)-CAS at 1 µM and 3 µM were assayed on one array (NB slide) to determine the optimal conditions of the assay. 3 µM of His-CAS and 1 µM of His.EGFP(n)-CAS were used finally for the screening of all RIKEN arrays. 128 potential hit compounds binding to purified CAS were found.

5.13.1.2 Targeting CAS from DNA transfected-lysate

We used different DNA constructs (pOPINHis(n).EGFP-CAS and pOPINHis(n)-CAS as target vectors) to express CAS in HEK293T cells. HEK239T cells were transfected with DNA and further lysed. Samples were boiled, loaded on SDS gel and transferred to PDVF membrane. His-CAS and His.EGFP-CAS were analyzed by immunoblotting using anti-His tag antibody. Results showed that the vector pOPINHis(n).EGFP-CAS could express His.EGFP-CAS (**Figure 56A**), and the vector pOPINHis(n)-CAS could weakly express His.CAS (**Figure 56B**) in HEK293T cells.

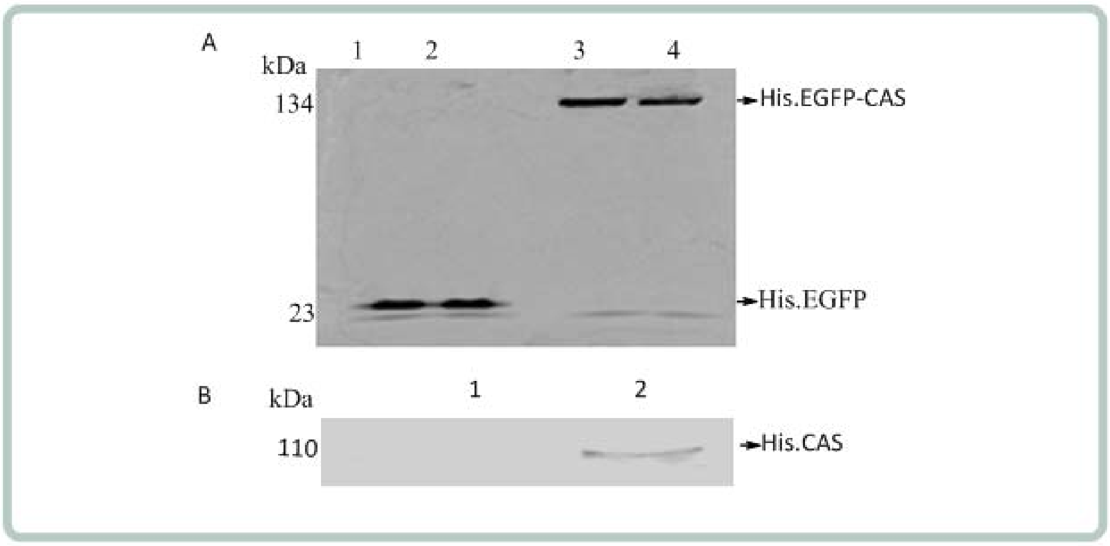

Figure 56: DNA transfected-cell lysate. A. DNA transfection of vector pOPINHis(n).EGFP or pOPINHis(n).EGFP-CAS. HEK293T cells were transfected DNA. Cells then were used for lysate preparing. His.EGFP-CAS or His.EGFP was detected by means of EGFP fluorescence signal using Typhoon scan. 1-2: transfected pOPINHis(n).EGFP; 3-4: transfected pOPINHis(n).EGFP-CAS. **B**. DNA transfection of vector pOPINHis(n) or pOPINHis(n)-CAS. HEK293T cells were transfected DNA, after cells were used for lysate preparing. His.CAS proteins or control lysate were confirmed by immunoblotting using anti-His tag antibody. 1-2: transfected pOPINHis(n); 3-4: transfected pOPINHis(n)-CAS.

Therefore, both pOPINHis(n).EGFP-CAS and pOPINHis(n)-CAS vectors were used for transfection and preparation of cell lysates for further screening CAS inhibitors (detail in section 4.7.6.2). Two control vectors, pOPINHis(n) and pOPINHis(n).EGFP, were used in parallel as controls. Results of the target lysate chemical array and control lysate were compared to identify hits (detail in section 4.9). For an example, 2 chemical arrays were screened for cell lysate containing either His.EGFP-CAS or His.EGFP. R89 is as a potential hit compound because it binds to His.EGFP-CAS (**Figure 57A**) but not to His.EGFP (**Figure 57B**). After screening CAS inhibitors using cell lysates, 19 potential hits binding to CAS proteins were found.

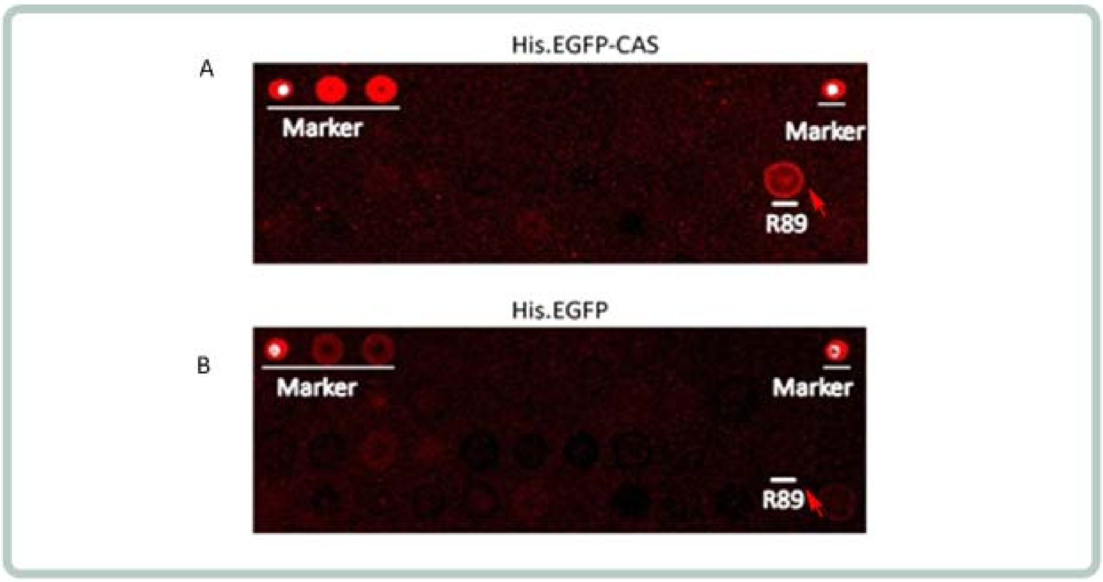

Figure 57: An example of chemical array scanning. Array was incubated with lysate containing either His.EGFP-CAS or His.EGFP. The binding of compounds and proteins were detected by means of the signal of cy5 conjugated antibody anti-His tag. Arrays were scan at 635nm (with optimal PMT (photomultiplier)) using GenePix microarray scanner.

As a summary of RIKEN NPDepo chemical array, 128 hit compounds targeting purified CAS and 19 hit compounds targeting CAS of DNA-transfected cell lysate were obtained (the list of hit structures were showed at appendix, **Table I**).

5.13.2 Screening of MPI compounds

5.13.2.1 Targeting purified CAS

We used 1 µM and 3 µM of both purified His.CAS and His.EGFP-CAS for MPI array screening. 114 potential hit compounds binding to purified CAS were found.

5.13.2.2 Targeting CAS from DNA transfected-lysate

DNA transfection, protein expression and proteins amounts were done and cell lysate was used for MPI array screening (see 5.13.1.2). 2 hit compounds targeting CAS of DNA-transfected lysate were found.

As a summary of MPI arrays, 114 hit compounds targeting purified CAS and 2 hit compounds targeting CAS of DNA-transfected lysate were obtained (the list of hit structures were showed at appendix, **Table II**).

5.14 The influence of array-based potential hits on importin alpha localization

The obtained hits from the chemical array screening at RIKEN (21293 compounds from RIKEN NPDepo and 3931 compounds from the COMAS library) were applied to study the localization of importin alpha. Compounds were screened at a concentration of 30 µM for 4 h, and cells were fixed and permeabilized. Chromosomes were stained with DAPI for visualizing the DNA. Rabbit primary antibody anti-importin alpha and secondary goat anti-rabbit IgG antibody coupled to Alexa Fluor 488 were used to detect importin alpha.

We were looking for small molecules inhibiting nuclear export function of CAS which leads to accumulation of importin alpha in the nucleus. We could not find any hits from this screening. Due to the lack of known modulators of CAS, the applicability of the assay may be doubtful; we could not discuss this result.

5.15 The influence of array-based potential hits on the phenotype of HeLa cells

The potential hits were screened at a concentration of 30 µM for phenotypic changes in HeLa cells after treatment for 24 h. Cells were fixed and permeabilized. Mouse primary anti-α-tubulin antibody and secondary goat antibody anti-mouse IgG antibody coupled to Alexa Fluor 488 were used to detect tubulin. TRITC-phalloidin was used to detect actin. DAPI was used to detect DNA.

263 hit compounds containing 147 RIKEN hits and 116 COMAS hits were tested. 22 hit compounds induced phenotypic changes, among them 13 RIKEN (**Figure 58**) and 9 COMAS hits (**Figure 60**). Phenotypic changes included accumulation of round shaped cells, small and

long shaped cells, and reduction of cells number versus cells that were treated with DMSO (**Figure 59 and 61**).

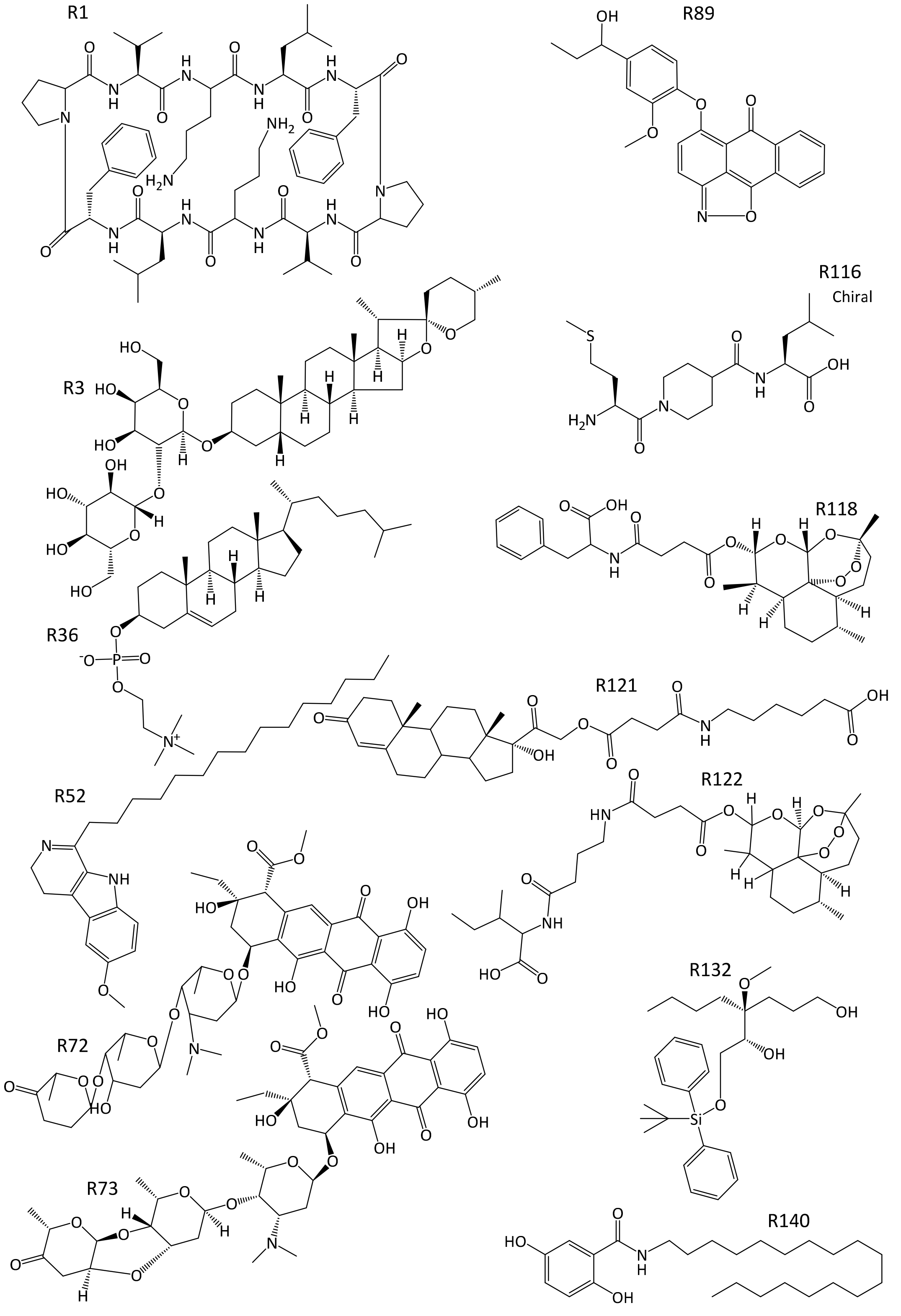
R1
R89
R116
Chiral
R3
R118
R36
R121
R52
R122
R72
R132
R73
R140

Figure 58: Structures of RIKEN hits which affect the phenotype of HeLa cells.

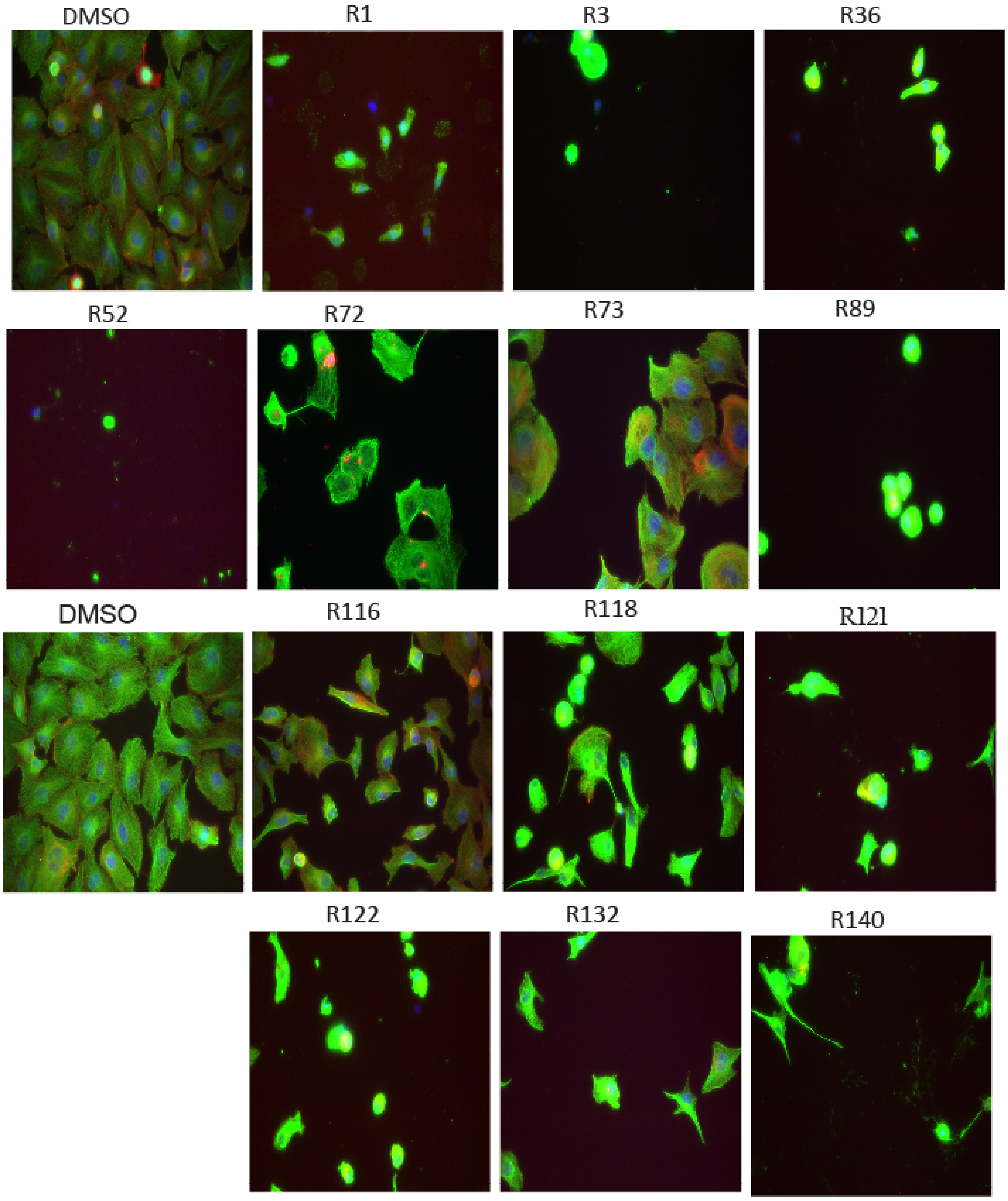
DMSO
R1
R3
R36
R52
R72
R73
R89
DMSO
R116
R118
R121
R122
R132
R140

Figure 59: The influence of RIKEN hit compounds in HeLa cells. Cells were incubated for 24 h either with 30 µM compounds or 0.3% DMSO as a control. Cells were fixed, permeabilized and stained for tubulin (green), actin (red) and DNA (blue). Antibody coupled to Alexa Fluor 488 was used to detect tubulin, TRITC-phalloidin was used to stain actin and DAPI was used to visualize DNA.

M10

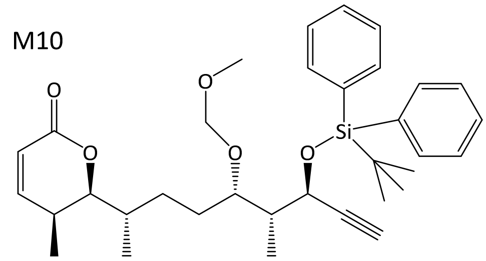

M104

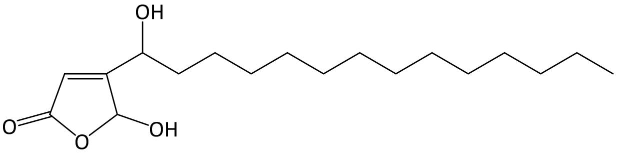

M19

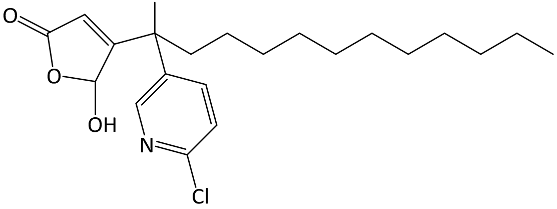

M116

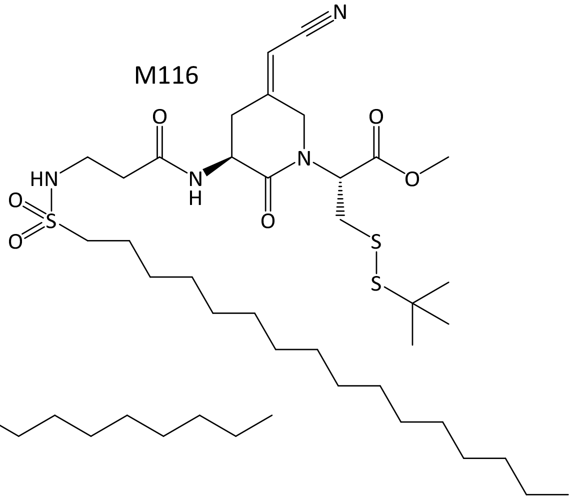
N
O
O
O
HN
N
H
N
O
O
S
O
O
S
S

I⁻ M43

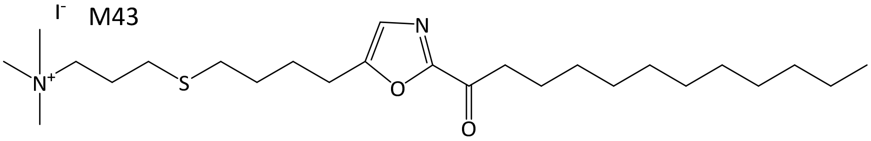

M50

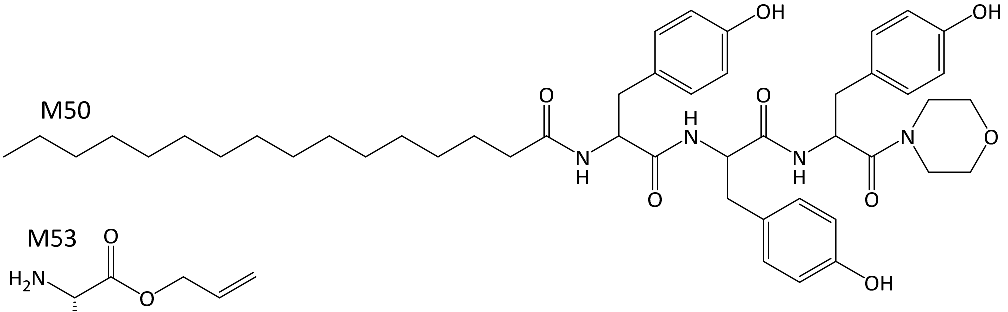
OH
OH
O
H
O
N
N
N
O
N
H
H
O
O
OH

M53

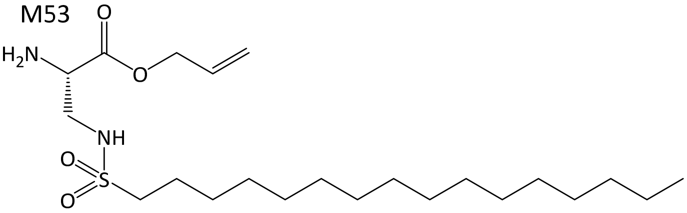
O
H2N
O
NH
O
S
O

M69

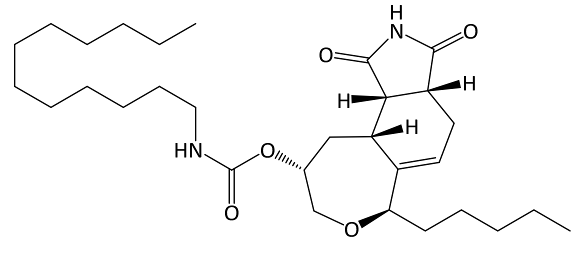
H
N
O
O
H
H
H
HN
O
O
O

M98

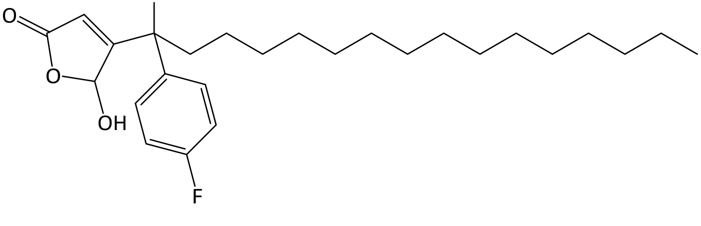

Figure 60: Structures of COMAS hits which affect the phenotype of HeLa cells.

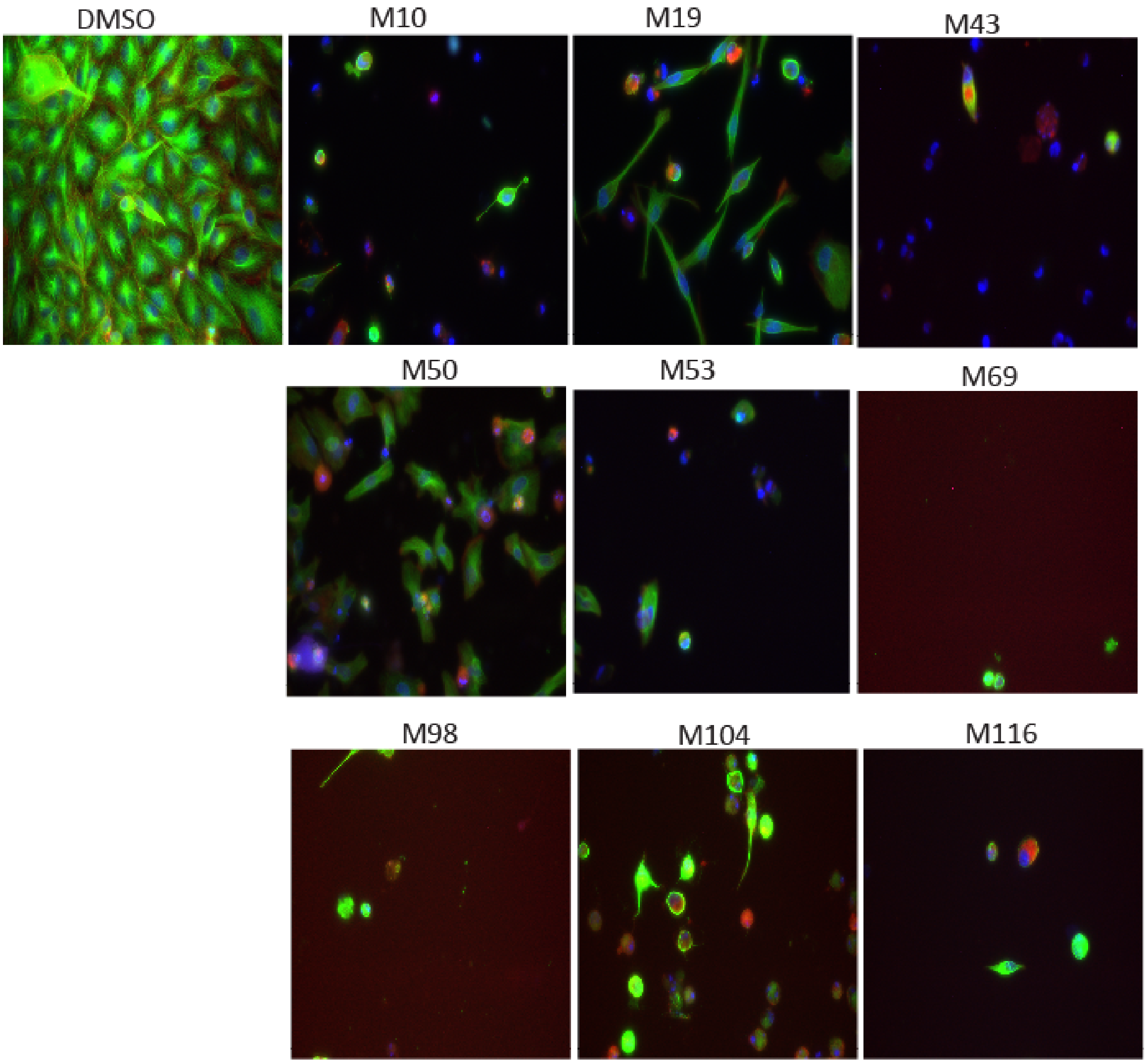

Figure 61: The influence of COMAS hit compounds on HeLa cells. Cells were incubated for 24 h either with 30 µM compounds or 0.3% DMSO as control. Cells were fixed, permeabilized and stained for tubulin (green), actin (red) and DNA (blue). Antibody coupled to Alexa Fluor 488 was used to detect tubulin, TRITC-phalloidin was used to stain actin and DAPI was used to visualize DNA.

5.16 The influence of array-based potential hits on the thermal stability of CAS

For further hit validation the identified compounds were subjected to study protein thermal stability shift using circular dichroism (CD) spectroscopy. When a compound interacts with a given protein, it may change the conformation of the protein or increase its stability which may result in increased melting point of the protein. We analyzed the melting point of 20 µM CAS in presence and absence of 50 µM of the compounds. Similar results were obtained for all compounds. The melting point of 20 µM CAS without the compounds was approximately 54 °C, and the melting curves did not change upon addition of the compounds (see sample in **Figure 62**). Thus, the hit compounds do not affect the thermal stability of CAS. One reason might be the large size of the protein (approximately 100 kDa) which may prevent the change in conformation or inducing the folding of protein upon binding of the small molecules.

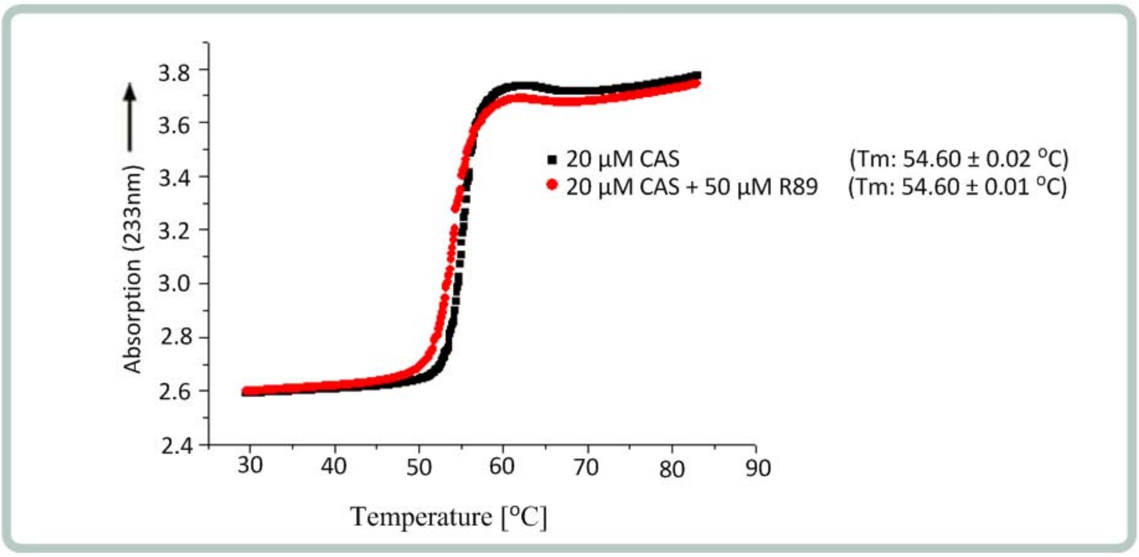

Figure 62: The influence of R89 on the thermal stability of CAS. 20 µM CAS was incubated with either 50 µM compound or 0.5% DMSO for 1 h. The melting point was determined at a wavelength of 233 nm within the temperature range from 25 °C to 90 °C by using circular dichroism spectroscopy (Jasco J-810).

5.17 Determination of binding affinities of array-based potential hits and CAS

To further study the hit compounds targeting CAS, the binding was analyzed by means of themophoresis using MST. We could detect the binding of 3 RIKEN compounds (R72, R73 and R89) to CAS. Results showed that the strongest CAS binder was R89 with a dissociation constant of 3.4 ± 0.4 µM for R89 compared to 32.4 ± 6.9 µM for R72 and 6.8 ± 2.6 µM for R73 (see an example in **Figure 63**).

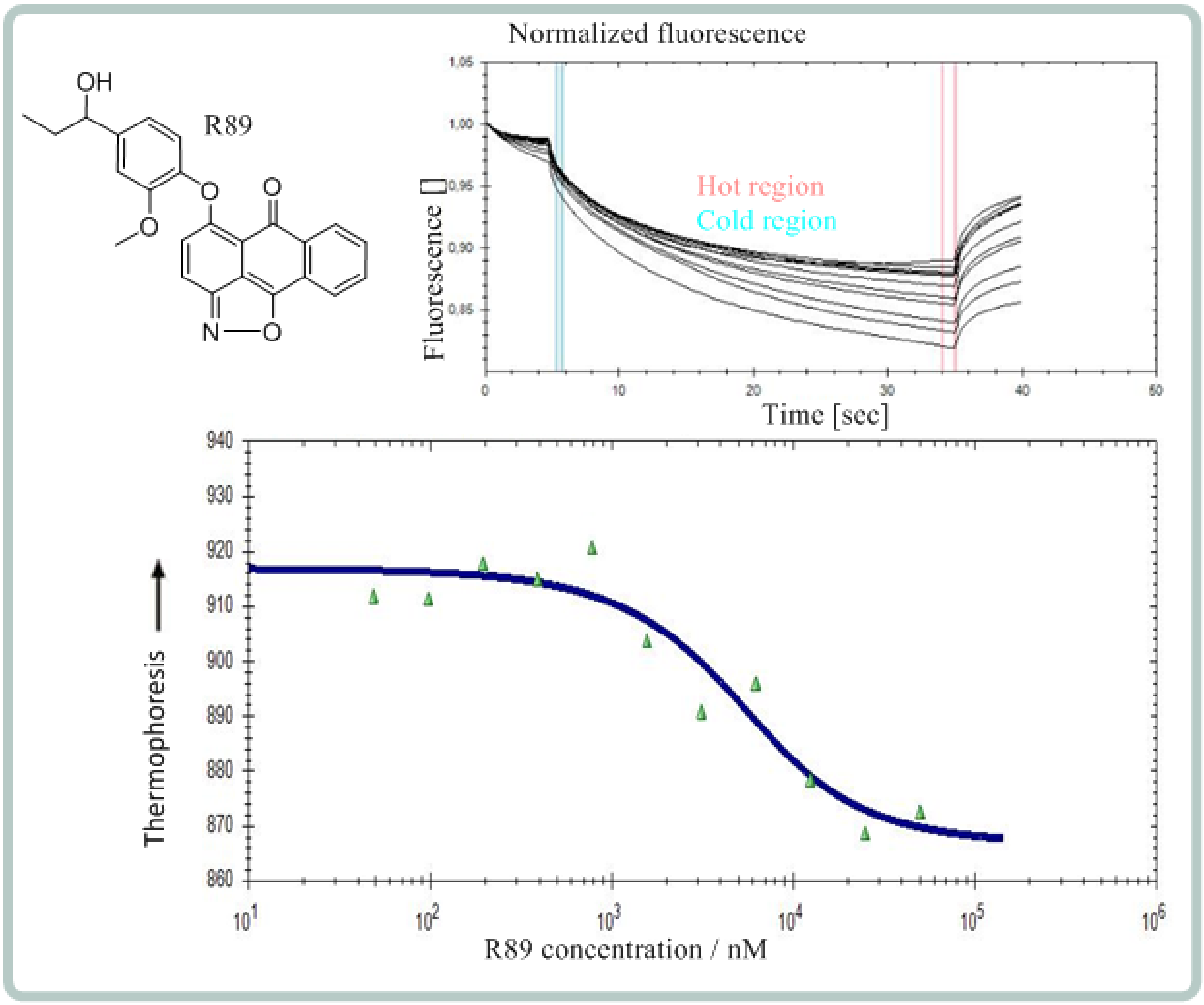

Figure 63: Themophoresis measurement for determination of the binding affinity of R89 to CAS. 100 nM fluorescent proteins (His-EGFP-CAS) were incubated with different concentration of R89 and the binding affinity monitored by means of MST based on themophoresis with temperature jump.

We then performed a search using Scifinder to obtain available information on compounds related to R72, R73 and R89. There are 119 similar substrates to R72-Cinerubin A (57 similarity structures with score from 90 to 94; 44 similarity structures with score from 95 to 98; and 18 similarity structures with score around 99) and 81 similar substrates to R73-Cinerubin B (62 similarity structures with score from 90 to 94; 8 similarity structures with score from 95 to 98 similarity structure; and 11 similarity structures with score around 99). There were many studies on cinerubins. Cinerubin A and B are antibiotics, and were used as antiparasitic agents. They were also used in anticancer studies.[317] Cinerubins form complexes with DNA to inhibit DNA-dependent RNA and DNA synthesis *in vitro*.[318] Thus, we were no longer interested in the validation of cinerubin A and B. The most interesting candidate compound is R89 because there was no published information about this compound and there are only 5 similar substrates with scores from 74-84 in Scifinder. Notably, most of them were patented including studies to identify cysteine protease or cysteine protease-like proteins inhibitors or studies to identify modulators of the survival protein MCL-1. Moreover, a third report aimed to discover inhibitors of mitogen-activated protein kinase (MAPK) phosphatase-1 (MKP-1) dual-specificity phosphatase. Thus, we further focused on R89 for further validation.

5.18 The influence of R89 on cell proliferation, cell cycle and cytoskeleton in HeLa cells

The influence of R89 on the proliferation of HeLa cells was performed by mean of WST-1 proliferation assay after treatment with the compound for 48 h. R89 inhibited the cell proliferation in a dose-dependent manner with a half-maximal inhibitory concentration (IC_{50}) of 8.42 ± 1.24 µM (**Figure 64A**).

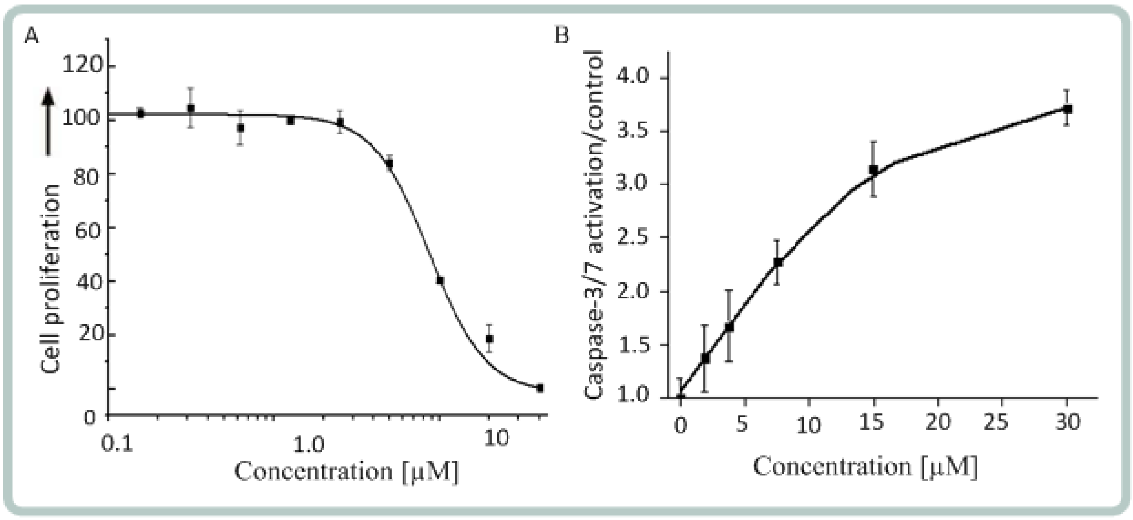

Figure 64: Influence of R89 on proliferation and apoptosis in HeLa cells. **A**. HeLa cells were incubated with R89 for 48 h and cell proliferation was determined using WST-1 assay. **B**. The influence of R89 on apoptosis was determined by means of Caspase-3/7 activation. Cells were incubated with R89 for 24 h and the activity of Caspase-3/7 was measured.

Induction of apoptosis was monitored by means of caspase-3 and caspase-7 activity in HeLa cells after compound treatment for 24 h. As depicted in **Figure 64B** a clear concentration-dependent increase in caspase-3/7 activity was observed for R89.

Our previous results showed that in HeLa cells R89 induces the accumulation of round shaped cells and reduces cell number at 30 µM after 24 h treatment. We studied the influence of various concentrations of R89 on the phenotype of HeLa cells after 15 h of treatment. Similar effects were detected as depicted in **Figure 65A**. A clear dose-response correlation was observed. To determine whether the round shaped cells were apoptotic or mitotic cells, mitotic HeLa cells were detected using the mitotic marker phospho-Histone H3 (pHistone H3). After 15 h of incubation with R89 cells were fixed and permeabilized. Primary rabbit anti-pHistone H3 antibody and secondary goat anti-rabbit IgG antibody coupled to Alexa Fluor 488 were used to detect pHistone H3. DAPI was used to stain DNA. Results showed that pHistone H3 was observed at 7.5 µM R89 treatment, but was not observed at 15 µM and 30 µM R89 treatments even though R89 induced accumulation of round shaped cells at all of these concentrations (**Figure 65B**).

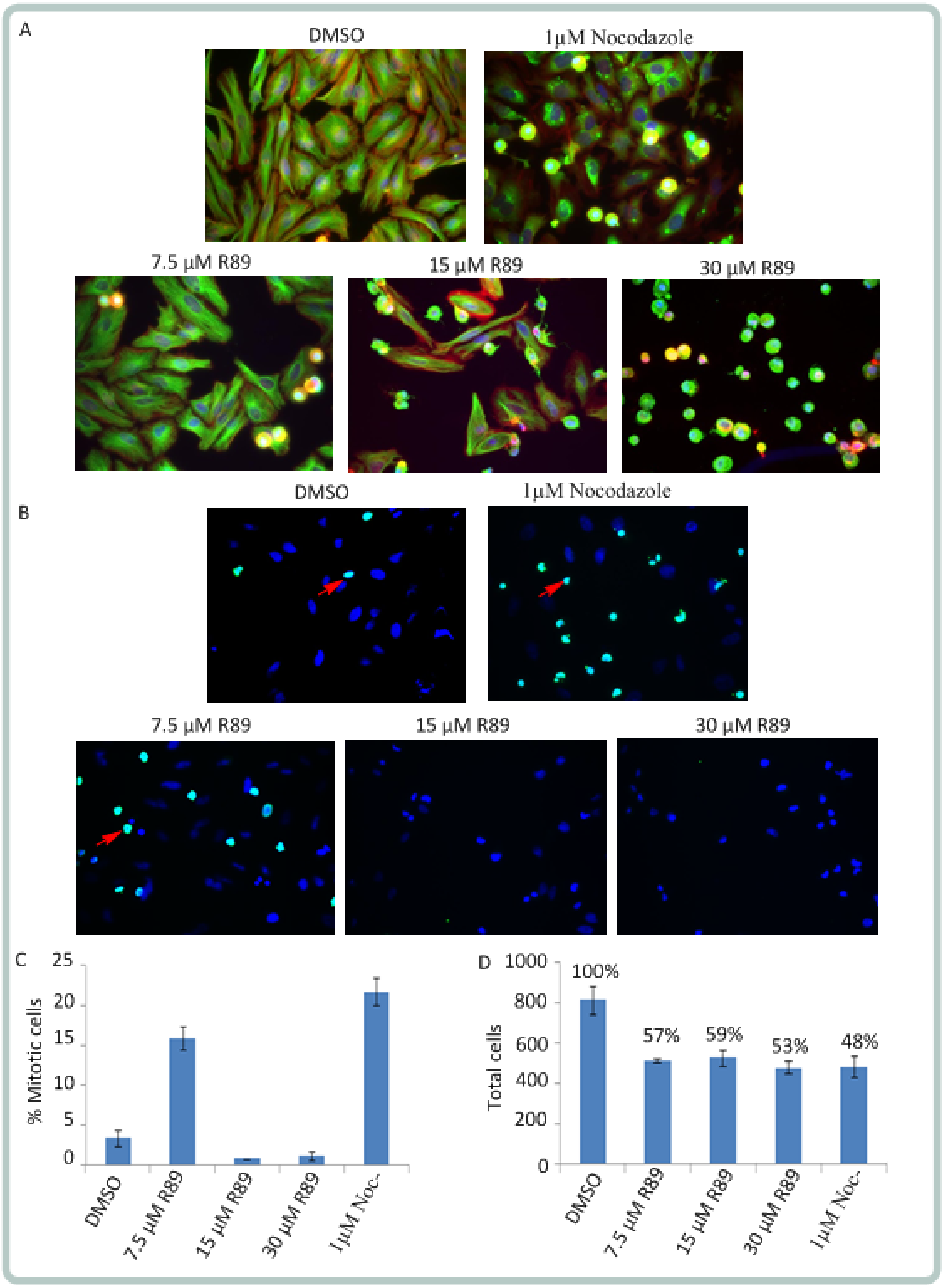
A
DMSO
1µM Nocodazole
7.5 µM R89
15 µM R89
30 µM R89
B
DMSO
1µM Nocodazole
7.5 µM R89
15 µM R89
30 µM R89
C
% Mitotic cells
0
5
10
15
20
25
DMSO
7.5 µM R89
15 µM R89
30 µM R89
1µM Noc.
D
Total cells
0
200
400
600
800
1000
100%
57%
59%
53%
48%
DMSO
7.5 µM R89
15 µM R89
30 µM R89
1µM Noc.

Figure 65: The influence of R89 on phenotype and mitosis of HeLa cells. **A.** Phenotypic changes in HeLa cells. Cells were incubated for 15 h either with different concentrations of R89 or 0.3% DMSO or 1 µM nocodazole as controls. Cells were fixed, permeabilized and stained for tubulin (green), actin (red) and DAPI (blue). Antibody coupled to Alexa Fluor 488 was used to detect tubulin, DAPI was used to stain DNA and TRITC-phalloidin was used to stain actin. **B**. Mitotic cells were detected using the mitotic marker pHistone H3. Cells were fixed, permeabilized and stained for pHistone H3 (green), and DNA (blue). Antibody coupled to Alexa Fluor 488 was used to detect pHistone H3 and DAPI was used to stain DNA. **C**. Percentage of mitotic cells. **D**. Total cells number in sample.

Then we treated HeLa cells for 24 h with different concentrations of R89 and recorded the changes in phenotype using live cell imaging. The time lapse experiments demonstrated again that R89 caused the accumulation of round shaped cells. After treatment with 7.5 µM R89 mitotic cells accumulated, and remained arrested in mitosis for 10 h before undergoing apoptosis. Treatment with 15 µM or 30 µM of R89 caused a very rapid apoptosis (after only 2 h of treatment) (**Figure 66**). Notably, chromosome congression defects and formation of multipolar mitotic spindles were observed (**Figure 67A**). Only a weak influence on cell morphology and tubulin cytoskeleton was detected in interphase cells after treatment for 15 h (**Figure 67B).**

This compound did not disturb the microtubule and the actin cytoskeleton in HeLa cells during 19 h of treatment at 15 µM (**Figure 68**). The target prediction tool SEA[319] (SEA search tool) suggests tubulin as a target of R89. However, R89 only weakly inhibited tubulin polymerization *in vitro* at 50 µM independently on the presence of CAS (**Figure 69).**

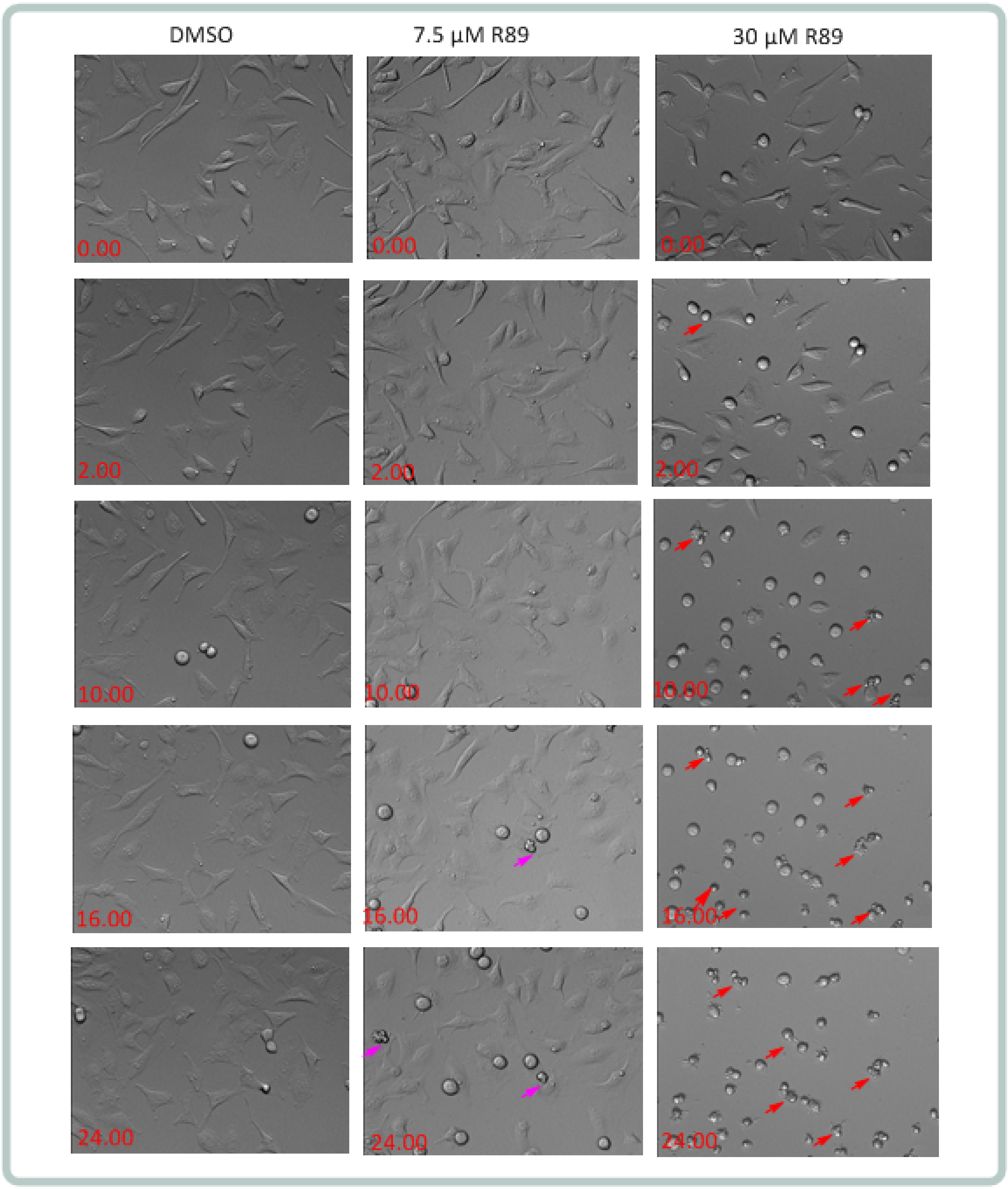
DMSO
7.5 µM R89
30 µM R89
0.00
0.00
0.00
2.00
2.00
2.00
10.00
10.00
10.00
16.00
16.00
16.00
24.00
24.00
24.00

Figure 66: Time-course of influence of R89 on HeLa cells. HeLa cells were incubated either with various concentration of R89 or with 0.3% DMSO as a control for 24 h and representative images from time-lapse movies are shown. Purple arrowheads mark cells undergoing mitosis. These cells become arrested in mitosis and die. Red arrowheads mark cells undergoing apoptosis.

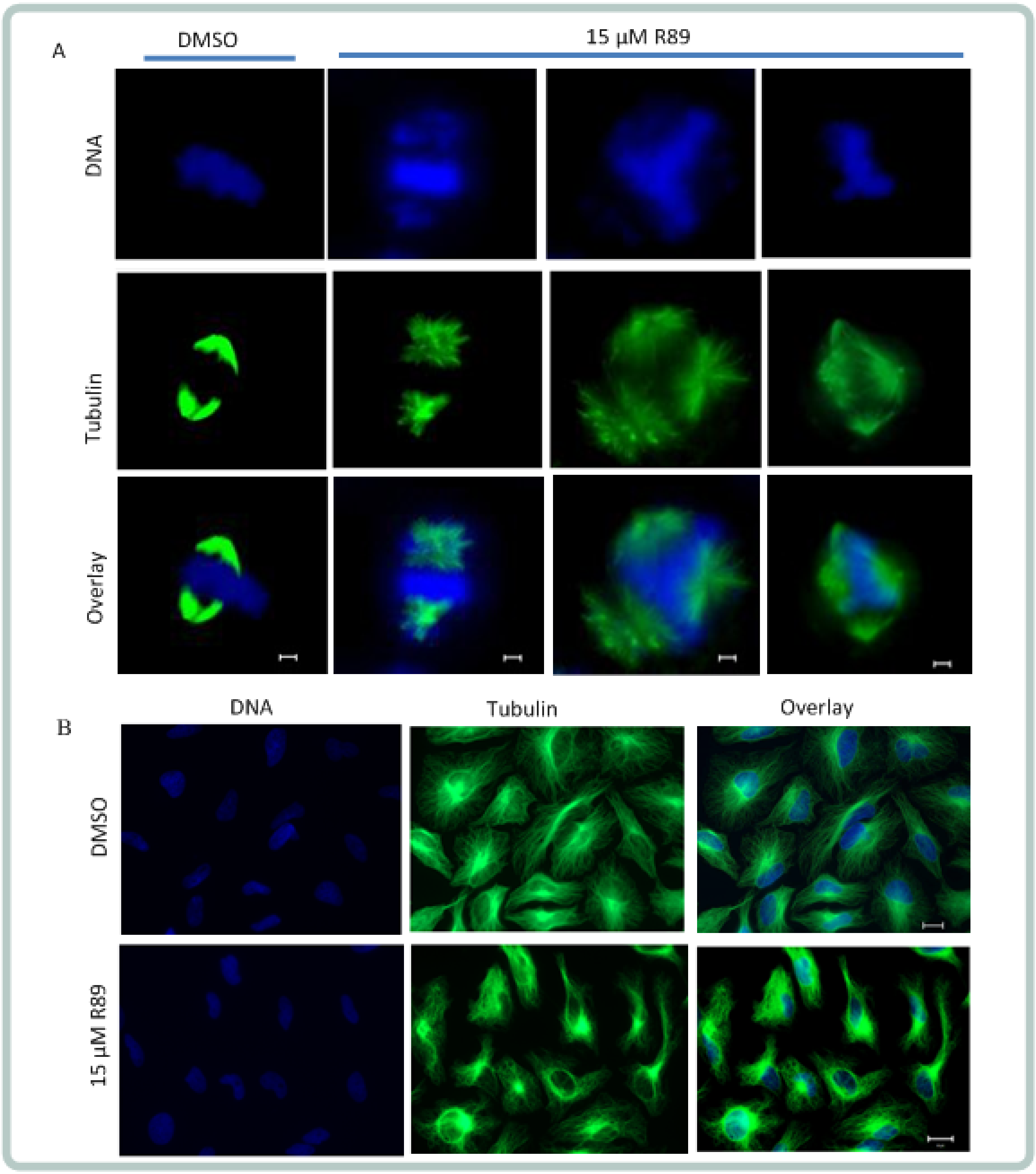
A
DMSO
15 µM R89
DNA
Tubulin
Overlay
B
DNA
Tubulin
Overlay
DMSO
15 µM R89

Figure 67: Influence of R89 on mitosis and interphase of HeLa cells. **A**. Influence of R89 on mitosis of HeLa cells. **B**. Influence of R89 on interphase of HeLa cells. Cells were incubated for 15 h either with 15 µM R89 or 0.3% DMSO as a control. Cells were fixed, permeabilized and stained for tubulin (green), and DAPI (blue). Antibody coupled to Alexa Fluor 488 was used to detect tubulin; DAPI was used to stain DNA. Images were taken with a fluorescent microscope with a magnificent objective lens of 63X; Scale bar: 10 µm.

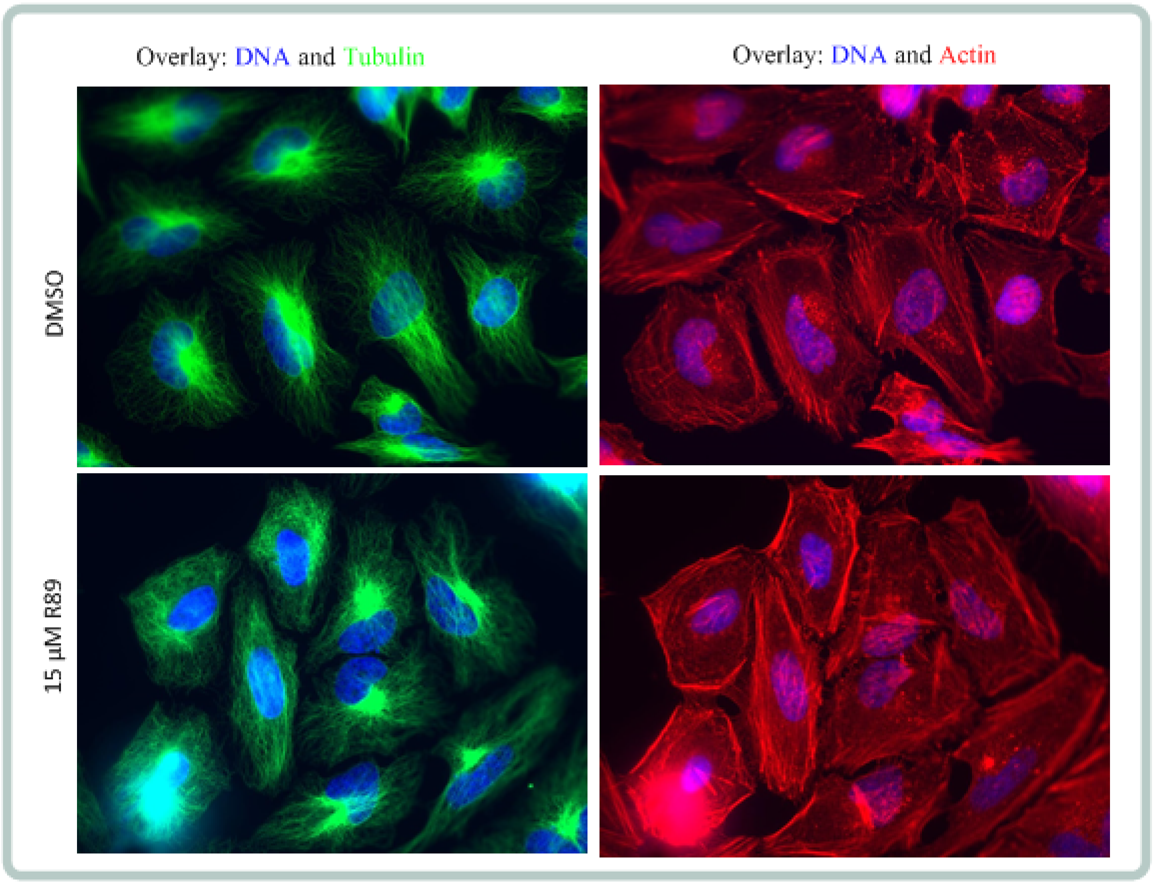
Overlay: DNA and Tubulin
Overlay: DNA and Actin
DMSO
15 µM R89

Figure 68: Effect of R89 on tubulin and actin cytoskeleton of HeLa cells. Cells were incubated for 19 h either with 15 µM R89 or 0.3% DMSO as a control. Cells were fixed, permeabilized and stained for tubulin (green), actin (red) and DAPI (blue). Antibody coupled to Alexa Fluor 488 was used to detect tubulin, DAPI was used to stain DNA and TRITC-phalloidin was used to stain actin. Images were taken with a fluorescent microscope with a magnificent objective lens of 63X.

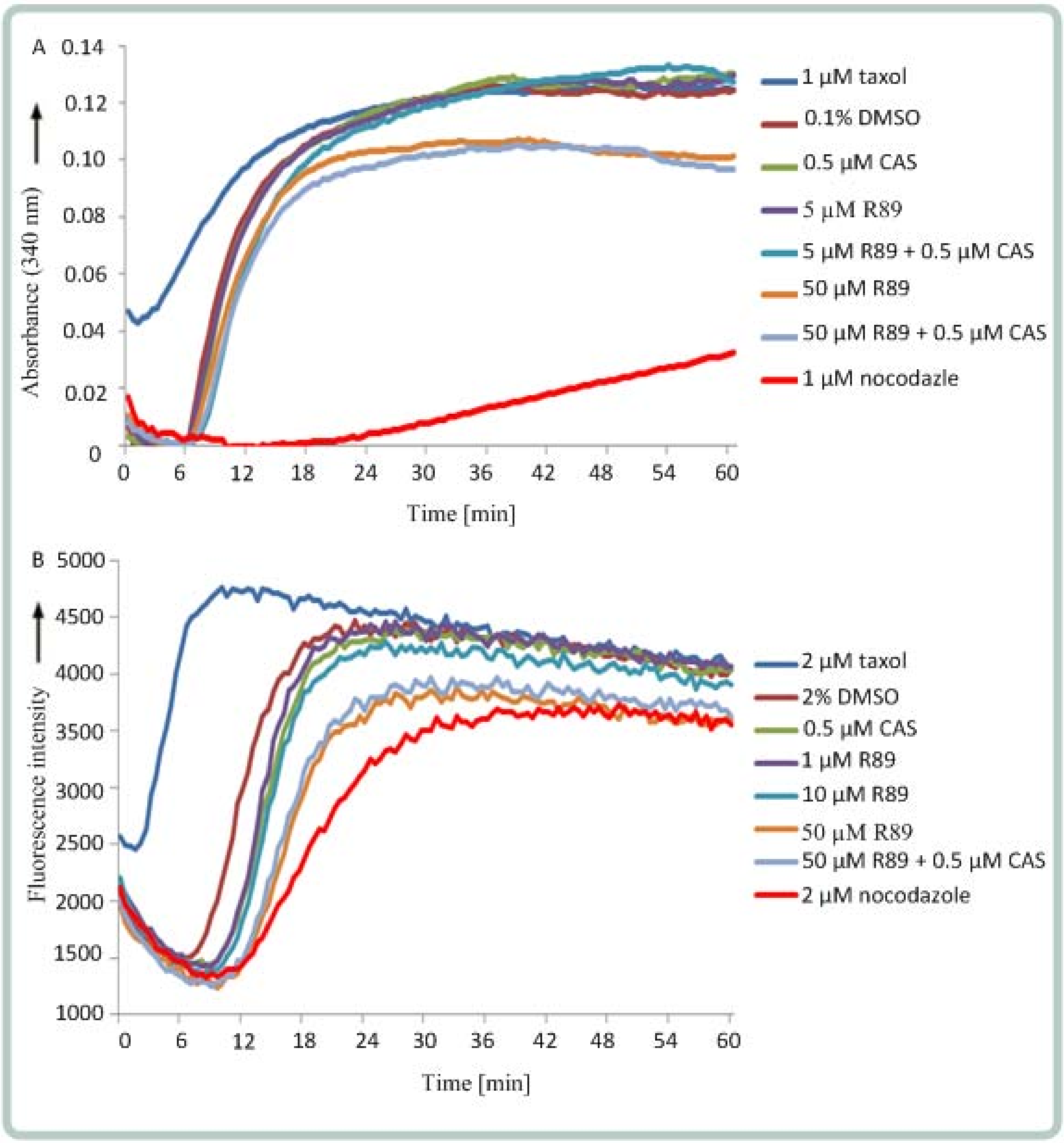

Figure 69: The effect of R89 on tubulin polymerization *in vitro.* **A**. Turbidity-based assay. Tubulin polymerization was monitored by turbidity measurement of polymerized microtubule. Tubulin polymerization was induced by the addition of GTP and was monitored by means of absorption at 340 nm. **B.** DAPI-based assay. Tubulin polymerization was monitored by fluorescence measurement at excitation/emission 340/460 nm. The polymerization was recorded by reading enhanced DAPI fluorescence upon binding to microtubules.

Next we studied whether R89 is a DNA binding small molecule. The interaction of R89 and DNA was determined based on two different DNA binding modes developed by Williams *et al.*[295] The binding of R89 to DNA was investigated by means of ethidium bromide (EtBr)-intercalating dyes[320] and the minor-groove binder DAPI[321] *in vitro*. EtBr binds to double-stranded DNA or single stranded RNA containing local base pairing whereas DAPI interacts with the minor grooves of DNA by strongly binding to A-T rich regions and also to G-C region.[295] Results showed that R89 does not interact with DNA in either DNA binding modes. Berenil was used as a positive control because it interacts with DNA either in EtBr-DNA binding mode or by binding to the minor grooves of DNA. Berenil displaced EtBr and DAPI from DNA by competing with the binding site on DNA, and thus reduced the fluorescent signal (**Figure 70**).

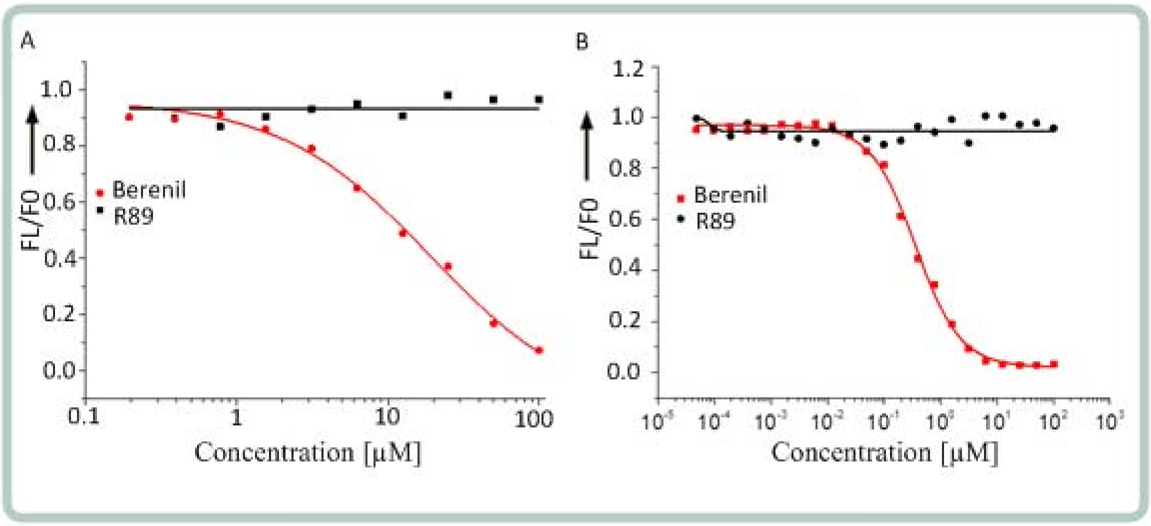

Figure 70: The binding of R89 to DNA. A. Ethidium bromide-DNA binding mode. R89 was titrated in a solution of 20 µM sonicated calf thymus DNA and 2 µM EtBr. Fluorescence intensity was measured at excitation/emission 540 nm/594 nm. **B**. DAPI-DNA binding mode. R89 was titrated in a solution of 20 µM sonicated calf thymus DNA and 2 µM DAPI in acetate buffer. Fluorescence intensity was measured at excitation/emission 358 nm/461 nm. The fluorescence value of the sample was normalized to the value of the DMSO as a control.

5.19 The influence of R89 on nuclear export of importin alpha and RANBP1

As described before, none of the hit compounds affected the localization of importin alpha after 4 h of treatment at 30 µM. For R89, the influence on importin alpha localization was performed with various concentrations for 2 h of treatment (7.5 µM and 15 µM). Again the results demonstrate that R89 does not influence the localization of importin alpha in HeLa cells (**Figure 71**).

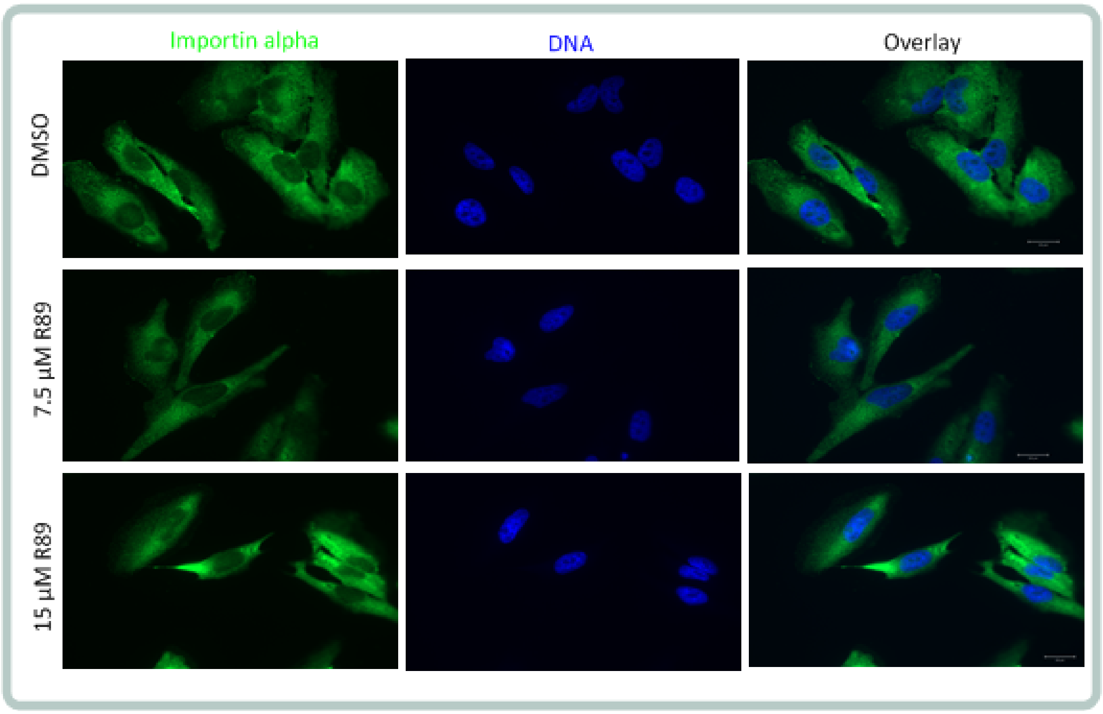

Figure 71: Influence of R89 on importin alpha localization in HeLa cells. Cells were incubated for 2 h either with various concentration of R89 (7.5 µM and 15 µM) or 0.3% DMSO as a control. Cells were fixed, permeabilized and stained for importin alpha (green), and DAPI (blue). Antibody coupled to Alexa Fluor 488 was used to detect importin alpha, DAPI was used to stain DNA. Images were taken with a fluorescent microscope with a magnificent objective lens of 63X.

The RAN-specific binding protein 1 (RANBP1) binds specifically to RANGTP, but not to the RANGDP. RANBP1 is a cargo of CRM1 (exportin 1) and not a cargo for CAS (exportin 2). However, RANBP1 interacts with RANGTP and importin beta to form a complex. CRM1 can dissociate this complex by displacing importin beta.[322] Moreover, RANGTP and cargo molecules can bind to several exportins, including CRM1 and CAS.[272]

RANBP1 must be localized specifically in the cytosol because of its function. RANBP1 mislocalization (e.g. nuclear accumulation) may cause toxicity to the cells.[322] There are some factors which can lead to RANBP1 nuclear accumulation, including competitors of CRM1 (proteins containing NES like REV protein),[323] chemical inhibitors such as leptomycin B (leptomycin B inactivates CRM1 by covalent modification at a cysteine residue in the central region)[324] or indoloquinolizine (indoloquinolizine targets both the centrosome-associated proteins NPM and CRM1).[25]

We studied the influence of R89 on RANBP1 localization. After incubation for 2 h with R89, cells were fixed and permeabilized and stained with anti-RANBP1 antibody. Leptomycin B was used as a positive control since it inhibits the function of CRM1 and traps RANBP1 in the nucleus. Our results showed that R89 induced nuclear accumulation of RANBP1 at 15 µM even though not all cells in the cell population were affected (**Figure 72**).

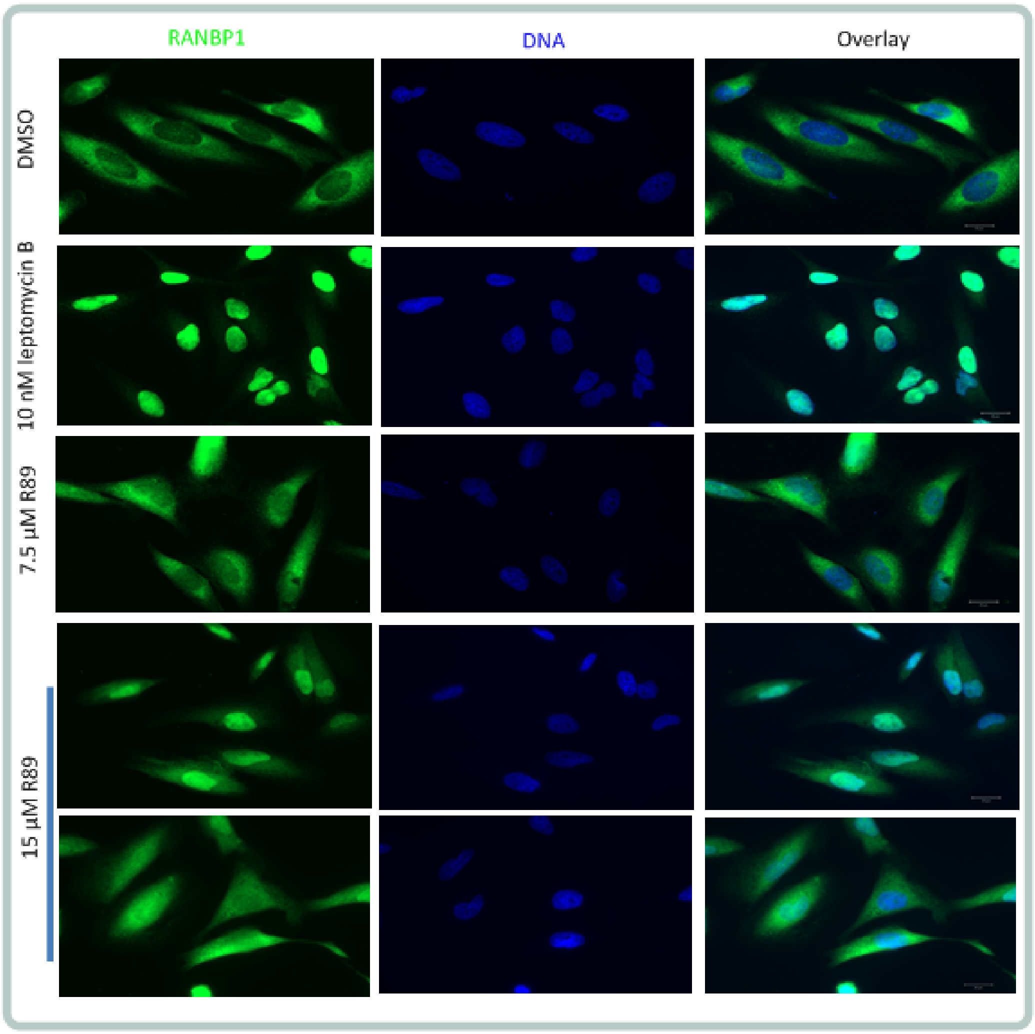

Figure 72: Influence of R89 on RANBP1 localization in HeLa cells. Cells were incubated for 2 hours either with various concentration of R89 (7.5 µM and 15 µM) or 0.3% DMSO as a control. Cells were fixed, permeabilized and stained for RANBP1 (green), and DAPI (blue). Antibody coupled to Alexa Fluor 488 was used to detect RANBP1; DAPI was used to stain DNA. Images were taken with a fluorescent microscope with a magnificent objective lens of 63X.

6 Discussion

6.1 Establishing a phage display for target identification protocol

We could succeed in establishing a protocol with the optimal conditions determined. Pre-incubation of the library with streptavidin-biotin or streptavidin-PEG-biotin or inactive compound before biopanning step is useful to reduce the non-specific background. The alternative phage elution step by using free compound is specific to collect the identified binders. For control glutathione, a binder was found to be glutathione peroxidase which is a known binder to GSH. However, there is unlikely to get the same hits of affinity purification for melophlin A, CD 267 and tubulexin A. In Addition, many unknown peptides were found in all those previously described experiments.

Although it is difficult to use phage display cDNA library for target identification, it still provides an opportunity to study the target of small molecules when lacking instrument to identify proteins (e.g. mass spectrometric techniques). Target identification could get through amplification (PCR) and DNA sequences of the attached gene to identify the binders.

To explain the reason leading to unsuccessful result, there are some limitations described (see detail in 1.2.1.3.1). Additionally, the ability to select target with desired properties is highly dependent on the quality of the initial library. For example, if the initial library is of insufficient size, poor, or inappropriate diversity will not allow successful target identification. Sometimes coding sequences of the optimal clones (e.g. highest affinity) in the displayed library may not be isolated because they are not displayed correctly on the phage surface. Other sequences may be toxic to *E. coli* or interfere with phage display assembly, or be sensitive to bacterial proteases. In many cases, the over-selection has been caused by the dominant clones. For this reason, the selection pressure for binding affinity becomes ineffective given that all clones present nearly the same affinity. Finally, binders with weak affinity, which are displayed at very high levels, are very likely to be selected.[325]

6.2 The binding and influence of podoverine A on tubulin polymerization *in vitro*

Podoverine A is the most active mitosis modulator in natural product library. This compound induces G2/M cell cycle arrest and can bind to vinca site of tubulin and inhibits tubulin polymerization *in vitro* and microtubule regrowth in BSC-1 cells. This compound is a potential target for further study on natural product as mitosis modulator to use for anticancer drugs, also used as natural product scaffold for synthesis library.

Furthermore, the time-course influence of this compound on mitosis would be interesting to know in more detail on life cell imaging of HeLa and of HeLa Fucci cell lines. Another interesting approach would be to check the influence of podoverine A on GTPase activity of α/β tubulin by means of Malachite green test. In addition, the influence of podoverine A on the conformation changes of α/β tubulin by means of determination the intrinsic tryptophan fluorescence changes or the fluorescence changes of fluorescent probes 1,8-ANS and Bis-ANS would be checked.[326] The information of structure–activity relationship (SAR) will be very useful to further study both for synthesis and an affinity probe for target identification which may be considered too.

6.3 Time-course of influence of tubulexin A on HeLa cells

Previous results showed that tubulexin A is a mitotic modulator. Furthermore, the time-lapse experiments demonstrated again that tubulexin A caused the accumulation of round shaped cells in mitosis after 10 hours leading to cells that were driven to apoptosis 16 hours at 15 µM. Experiments with HeLa FUCCI cells demonstrated an accumulation of cells in the G2/M phase. Most cells in the population were in apoptosis after 24 h compound treatment. This result of mitotic arrest can be explained by compound targeting tubulin and CAS. There are already well known compounds targeting tubulin (nocodazole,[327] vinblastine[328]), but no inhibitors are known for CAS, making the compound more interesting. Additionally, previous studies already showed that CAS also plays an important role in mitosis,[269] and that CAS protein reduction perturbed the progression of HeLa cells by G2 arrest.[283] The observed phenotypic effects of tubulexin A demonstrated by the possible of this compound targeting of CAS.

6.4 CAS expression, purification and the binding of CAS to tubulexin A

CAS FL and two N-terminal CAS fragments (391N and 570N) could be expressed in *E. coli* and purified. CAS 570C fragment could not be obtained. This result may be influenced by characteristics of CAS proteins such as shape, net charge, isoelectric point and hydrophobicity leading to the different of solubility and folding of proteins.

To explain the unsuccessful expression and purification of CAS 570C fragment, the “peptide property calculator”[329] was used to calculate the isoelectric point, and represented amino acids. Result showed that CAS FL and N-terminal CAS fragments contained isoelectric point from 4.46 to 5.55 and ratio of hydrophobic amino acids per hydrophilic amino acids from 1.49 to 1.96, but the isoelectric point of terminal CAS 570C is increased to 6.67 and the ratio of hydrophobic amino acids per hydrophilic amino acids is 2.5 (**Figure 73**). It was suggested that the increasing basic and hydrophobic characteristics may cause the failed results of expression and purification for this C-terminal fragment.

Tubulexin A binds to CAS with independent of tubulin. Tubulexin A can bind to N-terminus of CAS but less affinity than to CAS FL; there is no conclusion for influence of tubulexin A on C-terminal fragment of CAS. It may be suggested that protein folding of full CAS is necessary for the binding site of tubulin to CAS proteins.

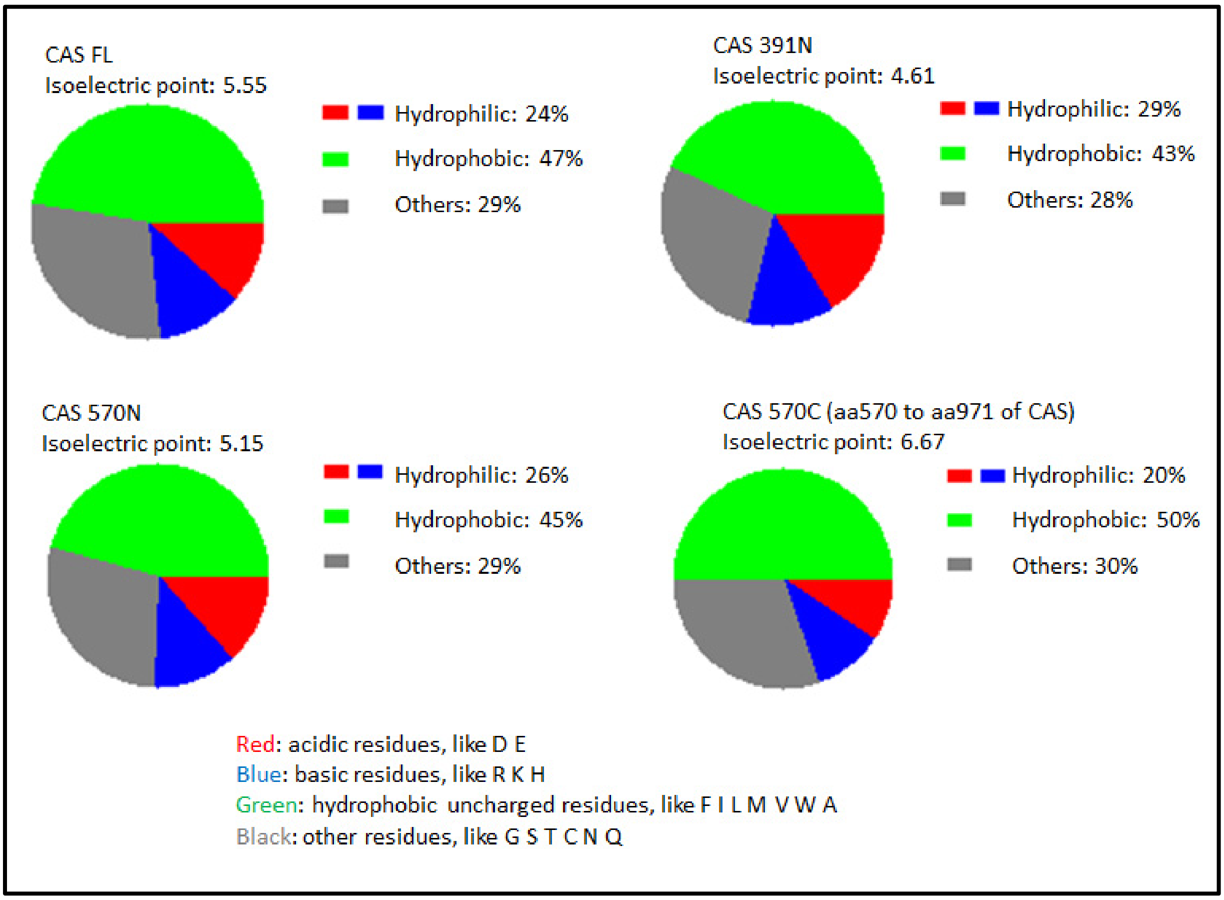

Figure 73: Characteristics of CAS full-length and fragments.

6.5 Influence of tubulexin A or/and CAS on tubulin polymerization *in vitro*

Investigation of the influence of tubulexin A on the assembly of microtubules in the presence of CAS revealed that 1-5 µM tubulexin A or 0.1 µM CAS only moderately decreased the polymerization of tubulin, but tubulin polymerization was inhibited in a synergistic manner in the presence of both tubulexin A and CAS *in vitro*.

Tubulexin A is a new anti-tubulin agent, simultaneously targeting CAS and α/β tubulin at the vinca binding site. The dual mode of action of tubulexin A is different from tubulin-binding small molecules. The synergistic mode of action of tubulexin A and CAS on tubulin polymerization and microtubule growth may be related to modulation of CAS. CAS is overexpressed in several cancers and associates with microtubules. CAS binds to α/β-tubulin heterodimer and stabilizes them leading to increasing of formation of microtubules in cells.[330] CAS binds to tubulin leading to enhancement microtubule assembly and migration of MCF-7 cancer cells.[282] This enhancement may be linked to the prevention of tubulin phosphorylation, which inhibits the disassembly of microtubules, through the binding of CAS to tubulin. The results of microtubule polymerization assay *in vitro* showed that CAS alone does not have a tubulin-stabilizing but rather a weakly destabilizing influence. The binding of tubulexin A to CAS may impair the binding of CAS to tubulin and generates unprotected α/β-tubulin polymer which may stimulate the disassembly of microtubules. In addition, tubulexin A binds to the vinca alkaloid binding site on tubulin thus induces depolymerization into α/β dimers.

6.6 Influence of tubulexin A on vinblastine-resistant KB-V1 cells

Investigation of the influence of tubulexin A on the proliferation of HeLa cells and KB-V1 cells (a multidrug-resistant (mdr) subclone of the HeLa cell line KB-3-1)[290,306,331] by means of a WST-1 proliferation assay confirmed the resistance of the KB-V1 cells to vinblastine (254 fold increase in IC_{50} values for KB-V1 cells compared to HeLa cells. In contrast, tubulexin A inhibited the proliferation of KB-V1 cells (IC_{50} values = 3.75 ± 0.1 µM) and HeLa cells (IC_{50} values = 4.29 ± 0.03 µM) with nearly identical efficiency. The dual mode of action of the tubulexin A and CAS might enable them to overcome the resistance mechanisms of cancer cells based on the binding of the vinca alkaloids.[332]

We have used vinblastine-resistant KB-V1 cells because vinblastine (also available as vinblastine sulphate) is an anticancer drug disrupting microtubule dynamics,[333] and many kinds of cells became resistant. The majority of the resistances acquired by cancer cells are related with MDR gene expression and the presence of P-glycoprotein (P-gp) which pumps out the intracellular drug.[334] KB-V1 cells expressed high level of MDR-1 gene and P-glycoprotein. Based on results of overcome vinblastine-resistance, tubulexin A can become a promising antimitotic drug for cancer treatment with the dual mode of action of the tubulexin A and CAS.

6.7 Influence of tubulexin A on function and protein interaction of CAS

For the CAS target validation, it was demonstrated that tubulexin A binds to CAS but it does not affect the interaction of RAN and importin alpha *in vitro* and in HeLa cells. No solid conclusions about the effects of tubulexin A on the nuclear export machinery can be formulated since there is no available control compound to confirm the method. However, tubulexin A does not have an effect on the interaction of CAS and importin alpha, and it may not influence the nuclear export function of CAS recycling importin alpha from nucleus to the cytoplasm.

6.8 Validation of array-based CAS inhibitors

Hit screening and validation of array-based CAS inhibitor is summarized in the **Figure 74.** The chemical array identified 263 potential compounds binding to CAS. Further validation of the hits showed that any of this identified hits affected the CAS thermal shift, neither any effect was observed on the nuclear export function of CAS. Nevertheless, is not possible to make a solid conclusion because of lacking of the control compound and the difficulty to study thermal shift with big proteins.

Furthermore, the binding of 22 potential hits induced the changes of HeLa phenotype to CAS were checked by using MTS. Among 3 hits with potent K_d, we have considered and studied one substance binding to CAS (R89). R89 is the identified hit using cell lysate of DNA pOPINHis(n).EGFP-CAS) transfected cells.

A chemical array approach was applied using cell lysates from cells transfected with DNA of target proteins. This method has the advantage that the cell lysates contain the proteins with PTM that could be important for the interaction with potential hits. By contrast, this approach can be only applied when the exogenous proteins (target proteins expressed by transfected DNA) are more abundant compared to the endogenous proteins.

Alternatively, purified proteins expressed in *E.* coli could be applied to find all the possible hits that can interact with the target proteins independently of the PTM and also potential hits with weaker binding. Moreover, using purified proteins is possible to control the concentration of protein and perform specific assays to determine the binding mode. Ideally, the best material will be to use purified proteins expressed in mammalian cells, but it is not easy to obtain. Therefore, both approaches (DNA transfected-lysate of mammalian cells and purified proteins expressed in *E. coli*) were applied. An important point to consider is that in the chemical array the compounds are attached and a number of orientations are not possible, therefore some false negatives could occur in the screening.

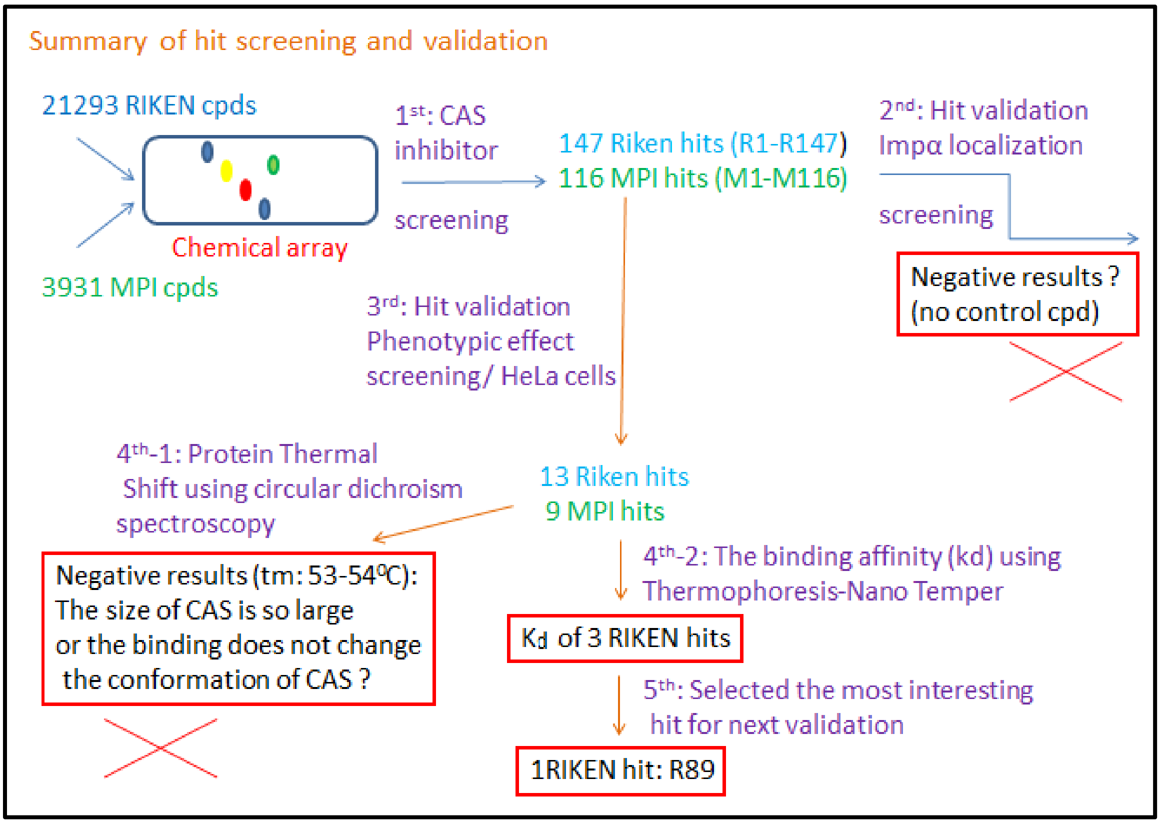
Summary of hit screening and validation
21293 RIKEN cpds
3931 MPI cpds
Chemical array
1st: CAS inhibitor screening
147 Riken hits (R1-R147)
116 MPI hits (M1-M116)
2nd: Hit validation Impα localization screening
Negative results ? (no control cpd)
3rd: Hit validation Phenotypic effect screening / HeLa cells
13 Riken hits
9 MPI hits
4th-1: Protein Thermal Shift using circular dichroism spectroscopy
Negative results (tm: 53-54ºC): The size of CAS is so large or the binding does not change the conformation of CAS ?
4th-2: The binding affinity (kd) using Thermophoresis-Nano Temper
Kd of 3 RIKEN hits
5th: Selected the most interesting hit for next validation
1RIKEN hit: R89

Figure 74: Summary of CAS inhibitors screening and validation.

6.9 Influence of R89 on HeLa cells

R89 inhibited the cell proliferation by affecting mitosis at low concentrations (without significantly influencing tubulin dynamics) or directly inducing apoptosis at higher concentrations. This compound does not interact with DNA and has no clearly inhibitory effect on tubulin polymerization *in vitro*. R89 binds to CAS with a K_d of 3.4 ± 0.4 µM and leads to chromosomal misalignment, multipolar mitotic spindles and induces nuclear accumulation of RANBP1.

Previously studies showed that CAS also plays an important role in the mitotic spindle checkpoint and the function of CAS is important for mitosis,[269] and CAS protein reduction perturbed the progression of HeLa cells and resulted in G2/M arrest.[283] CAS is considered to have a “switch” function that determines whether a cell will proliferate or will undergo apoptosis.[269] These functions of CAS may contribute for results of influencing of R89 with affecting mitosis at low concentrations and affecting apoptosis at high concentration. It is interesting to have the first mitotic chemical inhibitor without targeting tubulin. Most mitotic inhibitors target tubulin such as nocodazole, vinblastine.

We have studied the influence of R89 on the localization of importin alpha and RAN-binding protein 1 (RANBP1). Importin alpha is transported from nucleus to cytoplasm by CAS (see detail in **Figure 75A**) and RANPB1 is a factor for the release of RANGTP and CAS from the complex of CAS/importin alpha/RANGTP in cytoplasm to set CAS free for transporting back into the nucleus through the pore (**Figure 75B**).[335,336]

Results showed that R89 does not influence the importin alpha export function of CAS but induces nuclear accumulation of RANBP1. Results of RANBP1 accumulation might be caused by the interaction of R89 directly with CAS, resulting in the influence indirectly to related protein RANGTP and RANBP1 in nuclear export cycling or by the interaction of R89 both on CAS and NPM.

We suggest to further study the influence of R89 on RANBP1 localization by performing a Western Blot analysis for the RANPB1 using cell fractionation with and without R89 treatment to quantify the amount of this protein. Further biological characterization is needed to understand the mode of action of this small molecule. Moreover, design and synthesis of derivatives of R89 may provide more potent compounds.

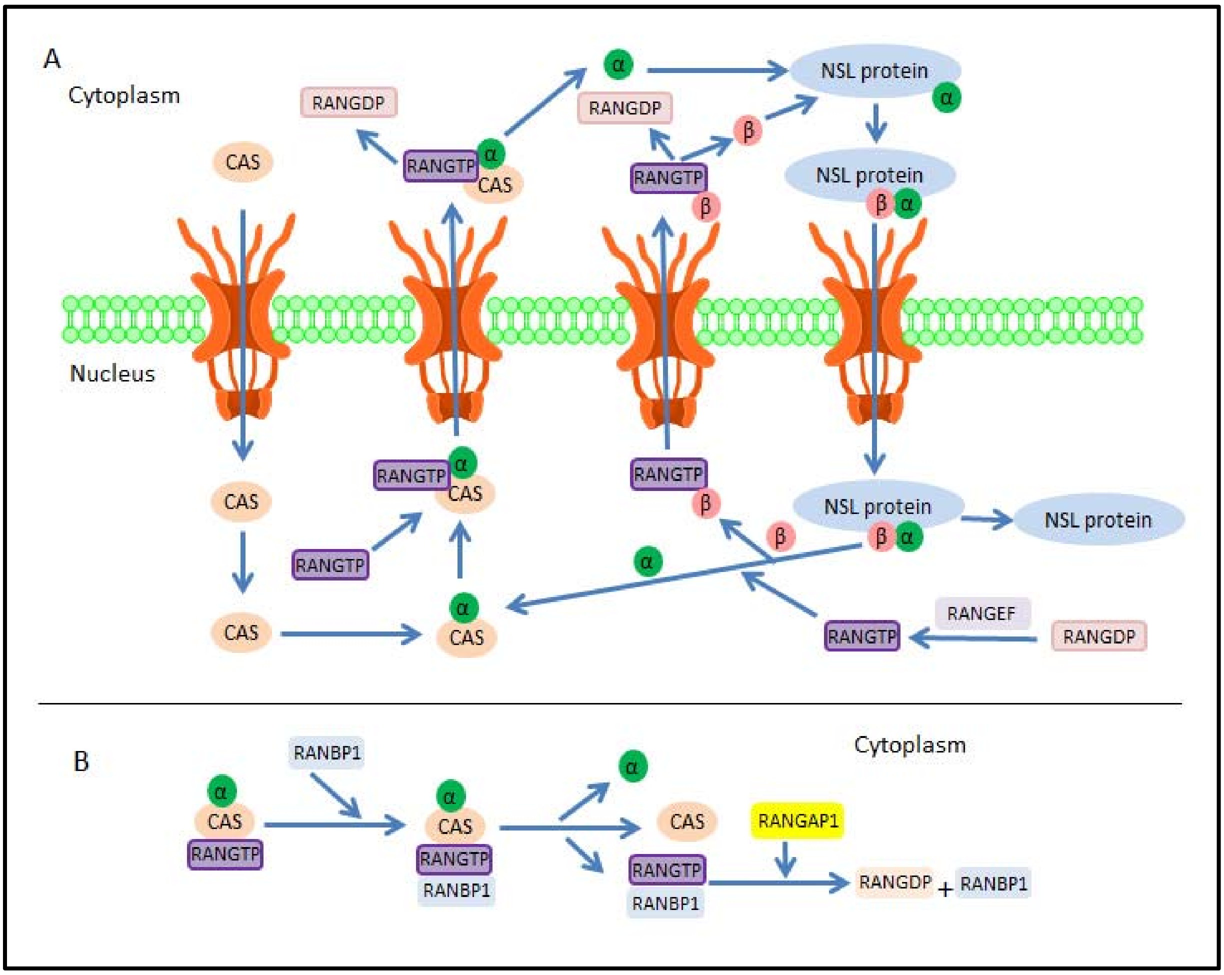

Figure 75: Nuclear-cytoplasm transport of importins and disassembly of RANGTP/CAS complex (adapted from Kau *et al.* and Bischoff *et al.*)[335,336]. **A**. Nuclear transport of importin alpha (α; green) recognizes proteins that contain a nuclear localization signal (NLS; blue) and forms a complex. This complex then binds to importin beta (β; orange), and is translocated through the nuclear pores into the nucleus. After entering the nucleus, the NLS-containing protein is dissociated by RANGTP. A high concentration of RANGTP is maintained in the nucleus by RANGEF, which converts RANGDP to RANGTP. Importin beta and RANGTP are recycled back out though the pore to the cytoplasm. Importin alpha is carried out of the nucleus by the nuclear export receptor CAS by complex formation with RANGTP, and then CAS is transported back into the nucleus through the pore.[335] **B**. Disassembly of complexes of RANGTP and CAS. In cytoplasm, RANBP1 directly promotes dissociation of RANGTP from the CAS. RAN appears to be transiently released as a RANGTP-RANBP1 complex which then can irreversibly be converted by RANGAP1 into RANGDP plus RANBP1. RANBP1 can participate in another round of disassembly.[336]

7 References

(1) Bishop, B. E. *J Hered* **1996**, *87*, 205.
(2) Passarge, E. Color Atlas of Genetics. Thieme 2013, 2
(3) Gerstein, M. B.; Bruce, C.; Rozowsky, J. S.; Zheng, D. Y.; Du, J.; Korbel, J. O.; Emanuelsson, O.; Zhang, Z. D. D.; Weissman, S.; Snyder, M. *Genome Res* **2007**, *17*, 669.
(4) Passarge, E. Color Atlas of Genetics. Thieme 2013, 48
(5) Brenner, S, & Miller, F. H., Encycolepedia of Genetics, Academic Press, 2001, 4.
(6) Passarge, E. Color Atlas of Genetics. Thieme 2013, 58
(7) Passarge, E. Color Atlas of Genetics. Thieme 2013, 58
(8) *Nature* **2004**, *431*, 931.
(9) Passarge, E. Color Atlas of Genetics. Thieme 2013, 2
(10) Nagy, A.; Perrimon, N.; Sandmeyer, S.; Plasterk, R. *Nat Genet* **2003**, *33*, 276.
(11) Stockwell, B. R. *Nat Rev Genet* **2000**, *1*, 116.
(12) Tierney, M.B. and Lamour, K.H. 2005. The Plant Health Instructor
(13) Qiu, L.; Xu, Z.; CRC Press: 2009, p 317.
(14) Kawasumi, M.; Nghiem, P. *The Journal of investigative dermatology* **2007**, *127*, 1577.
(15) Waldman, H & Janning, P, chemical biology, Wiley-VCH, 2004.
(16) Miller, A. D & Tanner, J. Essentials of Chemical Biology: Structure and Dynamics of Biological Macromolecules, Wiley, 2008.
(17) Nagendrappa, G. *Resonance* **2011**, *16*, 606.
(18) Koshland, D. E. *Proceedings of the National Academy of Sciences of the United States of America* **1958**, *44*, 98.
(19) Koshland, D. E. *Angew Chem Int Edit* **1994**, *33*, 2375.
(20) Darvas, F.; Dorman, G.; Krajcsi, P.; Puskas, L. G.; Kovari, Z.; Loerincz, Z.; Uerge, L. *Curr. Med. Chem.* **2004**, *11*, 3119.
(21) Waldmann, H and Janning, P. Willey-VCH, 2009.
(22) Spring, D. R. *Chem. Soc. Rev.* **2005**, *34*, 472.
(23) Lokey, R. S. *Curr Opin Chem Biol* **2003**, *7*, 91.
(24) Hutten, S.; Kehlenbach, R. H. *Trends Cell Biol* **2007**, *17*, 193.
(25) Duckert, H.; Pries, V.; Khedkar, V.; Menninger, S.; Bruss, H.; Bird, A. W.; Maliga, Z.; Brockmeyer, A.; Janning, P.; Hyman, A.; Grimme, S.; Schurmann, M.; Preut, H.; Hubel, K.; Ziegler, S.; Kumar, K.; Waldmann, H. *Nature chemical biology* **2012**, *8*, 179.
(26) Knoth, T.; Warburg, K.; Katzka, C.; Rai, A.; Wolf, A.; Brockmeyer, A.; Janning, P.; Reubold, T. F.; Eschenburg, S.; Manstein, D. J.; Hubel, K.; Kaiser, M.; Waldmann, H. *Angew Chem Int Ed Engl* **2009**, *48*, 7240.
(27) Mayer, T. U.; Kapoor, T. M.; Haggarty, S. J.; King, R. W.; Schreiber, S. L.; Mitchison, T. J. *Science* **1999**, *286*, 971.
(28) Torres, B. G.; Uchoa, F. D.; Pigatto, M. C.; Azeredo, F. J.; Haas, S. E.; Dallegrave, E.; Canto, R. F.; Eifler-Lima, V. L.; Dalla Costa, T. *Xenobiotica; the fate of foreign compounds in biological systems* **2013**.
(29) Osterloh, I. H.; Birkhaeuser Verlag: 2004, p 1.
(30) Francis, S. H.; Busch, J. L.; Corbin, J. D. *Pharmacol Rev* **2010**, *62*, 525.
(31) Terrett, N. K.; Bell, A. S.; Brown, D.; Ellis, P. *Bioorg Med Chem Lett* **1996**, *6*, 1819.
(32) Terrett, N. K. *Abstr Pap Am Chem S* **1998**, *216*, U256.
(33) Dale, D. J.; Dunn, P. J.; Golightly, C.; Hughes, M. L.; Levett, P. C.; Pearce, A. K.; Searle, P. M.; Ward, G.; Wood, A. S. *Org Process Res Dev* **2000**, *4*, 17.
(34) Kawasumi, M.; Nghiem, P. *The Journal of investigative dermatology* **2007**, *127*, 1577.

(35) Haggarty, S. J.; Koeller, K. M.; Wong, J. C.; Butcher, R. A.; Schreiber, S. L. *Chemistry & biology* **2003**, *10*, 383.

(36) Westwood, N. J. *Philos T Roy Soc A* **2004**, *362*, 2761.

(37) Walsh, D. P.; Chang, Y. T. *Chemical reviews* **2006**, *106*, 2476.

(38) Stockwell, B. R. *Nature* **2004**, *432*, 846.

(39) Reddy, A. S.; Zhang, S. *Expert review of clinical pharmacology* **2013**, *6*, 41.

(40) Nacher, J. C.; Schwartz, J. M. *Plos One* **2012**, *7*.

(41) Bolognesi, M. L. *Current medicinal chemistry* **2013**, *20*, 1639.

(42) Bajaj, V. K.; Gupta, R. S. *Nat Prod Commun* **2013**, *8*, 1183.

(43) Beretz, A.; Cazenave, J. P. *Planta Med* **1991**, *57*, S68.

(44) Cragg, G. M.; Newman, D. J. *Bba-Gen Subjects* **2013**, *1830*, 3670.

(45) Gullo, V. P.; McAlpine, J.; Lam, K. S.; Baker, D.; Petersen, F. *Journal of industrial microbiology & biotechnology* **2006**, *33*, 523.

(46) Campos, H. C.; da Rocha, M. D.; Viegas, F. P.; Nicastro, P. C.; Fossaluzza, P. C.; Fraga, C. A.; Barreiro, E. J.; Viegas, C., Jr. *CNS & neurological disorders drug targets* **2011**, *10*, 239.

(47) Williams, P.; Sorribas, A.; Howes, M. J. *Natural product reports* **2011**, *28*, 48.

(48) Molinari, G. *Adv Exp Med Biol* **2009**, *655*, 13.

(49) Seabra, R.; Valentao, P.; Ferreres, F.; Andrade, P. *Pr Phyt Soc* **2002**, *47*, 183.

(50) Cragg, G. M.; Newman, D. J.; Snader, K. M. *Journal of natural products* **1997**, *60*, 52.

(51) Wetzel, S.; Bon, R. S.; Kumar, K.; Waldmann, H. *Angew Chem Int Edit* **2011**, *50*, 10800.

(52) Harvey, A. L. *Drug Discov Today* **2008**, *13*, 894.

(53) Bhutani, K. K.; Gohil, V. M. *Indian journal of experimental biology* **2010**, *48*, 199.

(54) Over, B.; Wetzel, S.; Grutter, C.; Nakai, Y.; Renner, S.; Rauh, D.; Waldmann, H. *Nat Chem* **2013**, *5*, 21.

(55) Bohacek, R. S.; McMartin, C.; Guida, W. C. *Med Res Rev* **1996**, *16*, 3.

(56) Dobson, C. M. *Nature* **2004**, *432*, 824.

(57) Lipkin, M. J.; Stevens, A. P.; Livingstone, D. J.; Harris, C. J. *Comb Chem High T Scr* **2008**, *11*, 482.

(58) Kaiser, M.; Wetzel, S.; Kumar, K.; Waldmann, H. *Cellular and molecular life sciences : CMLS* **2008**, *65*, 1186.

(59) Schreiber, S. L. *Science* **2000**, *287*, 1964.

(60) Basu, S.; Ellinger, B.; Rizzo, S.; Deraeve, C.; Schurmann, M.; Preut, H.; Arndt, H. D.; Waldmann, H. *Proceedings of the National Academy of Sciences of the United States of America* **2011**, *108*, 6805.

(61) Correa, I. R.; Noren-Muller, A.; Ambrosi, H. D.; Jakupovic, S.; Saxena, K.; Schwalbe, H.; Kaiser, M.; Waldmann, H. *Chem-Asian J* **2007**, *2*, 1109.

(62) Mamane, V.; Garcia, A. B.; Umarye, J. D.; Lessmann, T.; Sommer, S.; Waldmann, H. *Tetrahedron* **2007**, *63*, 5754.

(63) Noren-Muller, A.; Reis-Correa, I.; Prinz, H.; Rosenbaum, C.; Saxena, K.; Schwalbe, H. J.; Vestweber, D.; Cagna, G.; Schunk, S.; Schwarz, O.; Schiewe, H.; Waldmann, H. *Proceedings of the National Academy of Sciences of the United States of America* **2006**, *103*, 10606.

(64) Noren-Muller, A.; Wilk, W.; Saxena, K.; Schwalbe, H.; Kaiser, M.; Waldmann, H. *Angew Chem Int Edit* **2008**, *47*, 5973.

(65) Umarye, J. D.; Lessmann, T.; Garcia, A. B.; Mamane, V.; Sommer, S.; Waldmann, H. *Chem-Eur J* **2007**, *13*, 3305.

(66) Waldmann, H. *Drug Future* **2009**, *34*, 24.

(67) Wilk, W.; Noren-Muller, A.; Kaiser, M.; Waldmann, H. *Chem-Eur J* **2009**, *15*, 11976.

(68) Wilk, W.; Zimmermann, T. J.; Kaiser, M.; Waldmann, H. *Biol Chem* **2010**, *391*, 491.

(69) Zimmermann, T. J.; Roy, S.; Martinez, N. E.; Ziegler, S.; Hedberg, C.; Waldmann, H. *Chembiochem : a European journal of chemical biology* **2013**, *14*, 295.

(70) Koch, M. A.; Schuffenhauer, A.; Scheck, M.; Wetzel, S.; Casaulta, M.; Odermatt, A.; Ertl, P.; Waldmann, H. *Proceedings of the National Academy of Sciences of the United States of America* **2005**, *102*, 17272.

(71) Noren-Muller, A.; Reis-Correa, I., Jr.; Prinz, H.; Rosenbaum, C.; Saxena, K.; Schwalbe, H. J.; Vestweber, D.; Cagna, G.; Schunk, S.; Schwarz, O.; Schiewe, H.; Waldmann, H. *Proceedings of the National Academy of Sciences of the United States of America* **2006**, *103*, 10606.

(72) Koch, M. A.; Schuffenhauer, A.; Scheck, M.; Wetzel, S.; Casaulta, M.; Odermatt, A.; Ertl, P.; Waldmann, H. *Proceedings of the National Academy of Sciences of the United States of America* **2005**, *102*, 17272.

(73) Barun, O.; Kumar, K.; Sommer, S.; Langerak, A.; Mayer, T. U.; Muller, O.; Waldmann, H. *Eur J Org Chem* **2005**, 4773.

(74) Umarye, J. D.; Lessmann, T.; Garcia, A. B.; Mamane, V.; Sommer, S.; Waldmann, H. *Chemistry* **2007**, *13*, 3305.

(75) Sanz, M. A.; Voigt, T.; Waldmann, H. *Adv Synth Catal* **2006**, *348*, 1511.

(76) Brohm, D.; Metzger, S.; Bhargava, A.; Muller, O.; Lieb, F.; Waldmann, H. *Angew Chem Int Ed Engl* **2002**, *41*, 307.

(77) Correa, I. R., Jr.; Noren-Muller, A.; Ambrosi, H. D.; Jakupovic, S.; Saxena, K.; Schwalbe, H.; Kaiser, M.; Waldmann, H. *Chemistry, an Asian journal* **2007**, *2*, 1109.

(78) Voigt, T.; Gerding-Reimers, C.; Ngoc Tran, T. T.; Bergmann, S.; Lachance, H.; Scholermann, B.; Brockmeyer, A.; Janning, P.; Ziegler, S.; Waldmann, H. *Angew Chem Int Ed Engl* **2013**, *52*, 410.

(79) Koch, M. A.; Wittenberg, L. O.; Basu, S.; Jeyaraj, D. A.; Gourzoulidou, E.; Reinecke, K.; Odermatt, A.; Waldmann, H. *Proceedings of the National Academy of Sciences of the United States of America* **2004**, *101*, 16721.

(80) Koch, M. A.; Breinbauer, R.; Waldmann, H. *Biol Chem* **2003**, *384*, 1265.

(81) Sundberg, S. A. *Curr Opin Biotech* **2000**, *11*, 47.

(82) Gilbert, I. H.; Leroy, D.; Frearson, J. A. *Current topics in medicinal chemistry* **2011**, *11*, 1284.

(83) Norcliffe, J. L.; Alvarez-Ruiz, E.; Martin-Plaza, J. J.; Steel, P. G.; Denny, P. W. *Parasitology* **2013**, 1.

(84) Bedard, J.; May, S.; Barbeau, D.; Yuen, L.; Rando, R. F.; Bowlin, T. L. *Antivir Res* **1999**, *41*, 35.

(85) Haberman, A. B. *Genet Eng News* **2005**, *25*, 36.

(86) Blackwell, H. E.; Zhao, Y. D. *Plant Physiol* **2003**, *133*, 448.

(87) Campo, D.; Lehmann, K.; Fjeldsted, C.; Souaiaia, T.; Kao, J.; Nuzhdin, S. V. *Mol Ecol* **2013**, *22*, 5084.

(88) Lieschke, G. J.; Currie, P. D. *Nature Reviews Genetics* **2007**, *8*, 353.

(89) Tissenbaum, H. A. *The journals of gerontology. Series A, Biological sciences and medical sciences* **2012**, *67*, 503.

(90) Bargmann, C. I. *Genome biology* **2001**, *2*, REVIEWS1005.

(91) Kwok, T. C.; Ricker, N.; Fraser, R.; Chan, A. W.; Burns, A.; Stanley, E. F.; McCourt, P.; Cutler, S. R.; Roy, P. J. *Nature* **2006**, *441*, 91.

(92) Rao, M.; Sockanathan, S. *Birth defects research. Part C, Embryo today : reviews* **2005**, *75*, 28.

(93) Terstappen, G. C.; Giacometti, A.; Ballini, E.; Aldegheri, L. *J Biomol Screen* **2000**, *5*, 255.

(94) Mendoza, L. G.; McQuary, P.; Mongan, A.; Gangadharan, R.; Brignac, S.; Eggers, M. *BioTechniques* **1999**, *27*, 778.

(95) Haney, S. A.; LaPan, P.; Pan, J.; Zhang, A. *Drug Discovery Today* **2006**, *11*, 889.

(96) Abraham, V. C.; Taylor, D. L.; Haskins, J. R. *Trends Biotechnol* **2004**, *22*, 15.

(97) Sklar, L. A.; Carter, M. B.; Edwards, B. S. *Curr Opin Pharmacol* **2007**, *7*, 527.

(98) Vidal-Aroca, F.; Giannattasio, M.; Brunelli, E.; Vezzoli, A.; Plevani, P.; Muzi-Falconi, M.; Bertoni, G. *Biotechniques* **2006**, *40*, 433.

(99) MacBeath, G.; Koehler, A. N.; Schreiber, S. L. *J Am Chem Soc* **1999**, *121*, 7967.

(100) Osada, H. *Biosci Biotech Bioch* **2010**, *74*, 1135.

(101) Kanoh, N.; Kumashiro, S.; Simizu, S.; Kondoh, Y.; Hatakeyama, S.; Tashiro, H.; Osada, H. *Angew Chem Int Ed Engl* **2003**, *42*, 5584.

(102) Kanoh, N.; Honda, K.; Simizu, S.; Muroi, M.; Osada, H. *Angew Chem Int Ed Engl* **2005**, *44*, 3559.

(103) Kanoh, N.; Asami, A.; Kawatani, M.; Honda, K.; Kumashiro, S.; Takayama, H.; Simizu, S.; Amemiya, T.; Kondoh, Y.; Hatakeyama, S.; Tsuganezawa, K.; Utata, R.; Tanaka, A.; Yokoyama, S.; Tashiro, H.; Osada, H. *Chemistry, an Asian journal* **2006**, *1*, 789.

(104) Kanoh, N.; Kyo, M.; Inamori, K.; Ando, A.; Asami, A.; Nakao, A.; Osada, H. *Analytical chemistry* **2006**, *78*, 2226.

(105) Miyazaki, I.; Simizu, S.; Okumura, H.; Takagi, S.; Osada, H. *Nature chemical biology* **2010**, *6*, 667.

(106) Burger, M.; Zimmermann, T. J.; Kondoh, Y.; Stege, P.; Watanabe, N.; Osada, H.; Waldmann, H.; Vetter, I. R. *Journal of lipid research* **2012**, *53*, 43.

(107) Zimmermann, T. J.; Burger, M.; Tashiro, E.; Kondoh, Y.; Martinez, N. E.; Gormer, K.; Rosin-Steiner, S.; Shimizu, T.; Ozaki, S.; Mikoshiba, K.; Watanabe, N.; Hall, D.; Vetter, I. R.; Osada, H.; Hedberg, C.; Waldmann, H. *Chembiochem : a European journal of chemical biology* **2013**, *14*, 115.

(108) Schena, M.; Shalon, D.; Davis, R. W.; Brown, P. O. *Science* **1995**, *270*, 467.

(109) Lockhart, D. J.; Dong, H.; Byrne, M. C.; Follettie, M. T.; Gallo, M. V.; Chee, M. S.; Mittmann, M.; Wang, C.; Kobayashi, M.; Horton, H.; Brown, E. L. *Nature biotechnology* **1996**, *14*, 1675.

(110) Debouck, C.; Goodfellow, P. N. *Nat Genet* **1999**, *21*, 48.

(111) Jayapal, M.; Melendez, A. J. *Clin Exp Pharmacol P* **2006**, *33*, 496.

(112) Zhu, Q.; Miecznikowski, J. C.; Halfon, M. S. *Bioinformatics* **2011**, *27*, 1284.

(113) Hughes, T. R.; Roberts, C. J.; Dai, H.; Jones, A. R.; Meyer, M. R.; Slade, D.; Burchard, J.; Dow, S.; Ward, T. R.; Kidd, M. J.; Friend, S. H.; Marton, M. J. *Nat Genet* **2000**, *25*, 333.

(114) Bilitewski, U. *Methods Mol Biol* **2009**, *509*, 1.

(115) MacBeath, G.; Schreiber, S. L. *Science* **2000**, *289*, 1760.

(116) Terstappen, G. C.; Schlupen, C.; Raggiaschi, R.; Gaviraghi, G. *Nature reviews. Drug discovery* **2007**, *6*, 891.

(117) Zhu, H.; Snyder, M. *Curr Opin Chem Biol* **2003**, *7*, 55.

(118) Fang, Y.; Frutos, A. G.; Lahiri, J. *Chembiochem : a European journal of chemical biology* **2002**, *3*, 987.

(119) Zhu, H.; Cox, E.; Qian, J. *Proteom Clin Appl* **2012**, *6*, 548.

(120) Ziauddin, J.; Sabatini, D. M. *Nature* **2001**, *411*, 107.

(121) Cong, F.; Cheung, A. K.; Huang, S. M. *Annual review of pharmacology and toxicology* **2012**, *52*, 57.

(122) Bach, S.; Knockaert, M.; Reinhardt, J.; Lozach, O.; Schmitt, S.; Baratte, B.; Koken, M.; Coburn, S. P.; Tang, L.; Jiang, T.; Liang, D. C.; Galons, H.; Dierick, J. F.; Pinna, L. A.; Meggio, F.; Totzke, F.; Schachtele, C.; Lerman, A. S.; Carnero, A.; Wan, Y.; Gray, N.; Meijer, L. *The Journal of biological chemistry* **2005**, *280*, 31208.

(123) Sato, S.; Kwon, Y.; Kamisuki, S.; Srivastava, N.; Mao, Q.; Kawazoe, Y.; Uesugi, M. *Journal of the American Chemical Society* **2007**, *129*, 873.

(124) Emami, K. H.; Nguyen, C.; Ma, H.; Kim, D. H.; Jeong, K. W.; Eguchi, M.; Moon, R. T.; Teo, J. L.; Kim, H. Y.; Moon, S. H.; Ha, J. R.; Kahn, M. *Proceedings of the National Academy of Sciences of the United States of America* **2004**, *101*, 12682.

(125) Snyder, J. R.; Hall, A.; Ni-Komatsu, L.; Khersonsky, S. M.; Chang, Y. T.; Orlow, S. J. *Chemistry & biology* **2005**, *12*, 477.

(126) Wang, G.; Shang, L.; Burgett, A. W.; Harran, P. G.; Wang, X. *Proceedings of the National Academy of Sciences of the United States of America* **2007**, *104*, 2068.

(127) Oda, Y.; Owa, T.; Sato, T.; Boucher, B.; Daniels, S.; Yamanaka, H.; Shinohara, Y.; Yokoi, A.; Kuromitsu, J.; Nagasu, T. *Analytical chemistry* **2003**, *75*, 2159.

(128) Laing, P. *Journal of immunological methods* **1986**, *92*, 161.

(129) Yates, J. R., 3rd *Journal of mass spectrometry : JMS* **1998**, *33*, 1.

(130) Schuchardt, S.; Sickmann, A. *Exs* **2007**, *97*, 141.

(131) Shaltiel, S. *Methods in enzymology* **1984**, *104*, 69.

(132) Hahn, R.; Berger, E.; Pflegerl, K.; Jungbauer, A. *Analytical chemistry* **2003**, *75*, 543.

(133) Shiyama, T.; Furuya, M.; Yamazaki, A.; Terada, T.; Tanaka, A. *Bioorganic & medicinal chemistry* **2004**, *12*, 2831.

(134) Schirle, M.; Heurtier, M. A.; Kuster, B. *Molecular & cellular proteomics : MCP* **2003**, *2*, 1297.

(135) Trepel, J.; Mollapour, M.; Giaccone, G.; Neckers, L. *Nature reviews. Cancer* **2010**, *10*, 537.

(136) Gygi, S. P.; Rist, B.; Gerber, S. A.; Turecek, F.; Gelb, M. H.; Aebersold, R. *Nat Biotechnol* **1999**, *17*, 994.

(137) Dunkley, T. P. J.; Dupree, P.; Watson, R. B.; Lilley, K. S. *Biochem Soc T* **2004**, *32*, 520.

(138) Katayama, H.; Oda, Y. *Journal of chromatography. B, Analytical technologies in the biomedical and life sciences* **2007**, *855*, 21.

(139) Ong, S. E.; Blagoev, B.; Kratchmarova, I.; Kristensen, D. B.; Steen, H.; Pandey, A.; Mann, M. *Molecular & cellular proteomics : MCP* **2002**, *1*, 376.

(140) Rix, U.; Superti-Furga, G. *Nature chemical biology* **2009**, *5*, 616.

(141) Ziegler, S.; Pries, V.; Hedberg, C.; Waldmann, H. *Angew Chem Int Edit* **2013**, *52*, 2744.

(142) Cong, F.; Cheung, A. K.; Huang, S. M. A. *Annu Rev Pharmacol* **2012**, *52*, 57.

(143) Urbaniak, M. D.; Mathieson, T.; Bantscheff, M.; Eberhard, D.; Grimaldi, R.; Miranda-Saavedra, D.; Wyatt, P.; Ferguson, M. A. J.; Frearson, J.; Drewes, G. *ACS chemical biology* **2012**, *7*, 1858.

(144) Rix, U.; Superti-Furga, G. *Nature chemical biology* **2009**, *5*, 616.

(145) Smith, G. P. *Science* **1985**, *228*, 1315.

(146) Gu, Y.; Zhang, J.; Wang, Y. B.; Li, S. W.; Yang, H. J.; Luo, W. X.; Xia, N. S. *Sheng wu gong cheng xue bao = Chinese journal of biotechnology* **2003**, *19*, 680.

(147) Shukla, G. S.; Krag, D. N. *Oncology reports* **2005**, *13*, 757.

(148) Yao, V. J.; Ozawa, M. G.; Trepel, M.; Arap, W.; McDonald, D. M.; Pasqualini, R. *The American journal of pathology* **2005**, *166*, 625.

(149) Nilsson, F.; Tarli, L.; Viti, F.; Neri, D. *Advanced drug delivery reviews* **2000**, *43*, 165.

(150) Van Dorst, B.; Mehta, J.; Rouah-Martin, E.; Somers, V.; De Coen, W.; Blust, R.; Robbens, J. *Toxicology in vitro : an international journal published in association with BIBRA* **2010**, *24*, 1435.

(151) Li, F.; Dluzewski, A.; Coley, A. M.; Thomas, A.; Tilley, L.; Anders, R. F.; Foley, M. *The Journal of biological chemistry* **2002**, *277*, 50303.

(152) Zhang, B.; Zhang, Y.; Wang, J.; Chen, J.; Pan, Y.; Ren, L.; Hu, Z.; Zhao, J.; Liao, M.; Wang, S. *Mol Med* **2007**, *13*, 246.

(153) Yu, L.; Yu, P. S.; Yee Yen Mui, E.; McKelvie, J. C.; Pham, T. P.; Yap, Y. W.; Wong, W. Q.; Wu, J.; Deng, W.; Orner, B. P. *Bioorganic & medicinal chemistry* **2009**, *17*, 4825.

(154) Phan, T.; Nguyen, H. D.; Goksel, H.; Mocklinghoff, S.; Brunsveld, L. *Chem Commun (Camb)* **2010**, *46*, 8207.

(155) Hu, S.; Guo, X.; Xie, H.; Du, Y.; Pan, Y.; Shi, Y.; Wang, J.; Hong, L.; Han, S.; Zhang, D.; Huang, D.; Zhang, K.; Bai, F.; Jiang, H.; Zhai, H.; Nie, Y.; Wu, K.; Fan, D. *Biochemical and biophysical research communications* **2006**, *341*, 964.

(156) Rosenberg, A. H.; Griffin, K.; Washington, M. T.; Patel, S. S.; Studier, F. W. *The Journal of biological chemistry* **1996**, *271*, 26819.

(157) Jung, H. J.; Shim, J. S.; Lee, J.; Song, Y. M.; Park, K. C.; Choi, S. H.; Kim, N. D.; Yoon, J. H.; Mungai, P. T.; Schumacker, P. T.; Kwon, H. J. *The Journal of biological chemistry* **2010**, *285*, 11584.

(158) Jensen-Jarolim, E.; Ganglberger, E.; Leitner, A.; Radauer, C.; Scheiner, O.; Breiteneder, H. *International archives of allergy and immunology* **1999**, *118*, 224.

(159) McPherson, M.; Yang, Y.; Hammond, P. W.; Kreider, B. L. *Chemistry & biology* **2002**, *9*, 691.

(160) Hammond, P. W.; Alpin, J.; Rise, C. E.; Wright, M.; Kreider, B. L. *The Journal of biological chemistry* **2001**, *276*, 20898.

(161) Zahnd, C.; Amstutz, P.; Pluckthun, A. *Nat Methods* **2007**, *4*, 269.

(162) Lipovsek, D.; Pluckthun, A. *Journal of immunological methods* **2004**, *290*, 51.

(163) Takahashi, T. T.; Austin, R. J.; Roberts, R. W. *Trends in biochemical sciences* **2003**, *28*, 159.

(164) Licitra, E. J.; Liu, J. O. *Proceedings of the National Academy of Sciences of the United States of America* **1996**, *93*, 12817.

(165) Griffith, E. C.; Licitra, E. J.; Liu, J. O. *Method Enzymol* **2000**, *328*, 89.

(166) Fields, S.; Song, O. *Nature* **1989**, *340*, 245.

(167) Becker, F.; Murthi, K.; Smith, C.; Come, J.; Costa-Roldan, N.; Kaufmann, C.; Hanke, U.; Degenhart, C.; Baumann, S.; Wallner, W.; Huber, A.; Dedier, S.; Dill, S.; Kinsman, D.; Hediger, M.; Bockovich, N.; Meier-Ewert, S.; Kluge, A. F.; Kley, N. *Chemistry & biology* **2004**, *11*, 211.

(168) Caligiuri, M.; Molz, L.; Liu, Q.; Kaplan, F.; Xu, J. P.; Majeti, J. Z.; Ramos-Kelsey, R.; Murthi, K.; Lievens, S.; Tavernier, J.; Kley, N. *Chemistry & biology* **2006**, *13*, 711.

(169) Khandelwal, A.; Bahadduri, P. M.; Chang, C.; Polli, J. E.; Swaan, P. W.; Ekins, S. *Pharmaceutical research* **2007**, *24*, 2249.

(170) Macchiarulo, A.; Costantino, G.; Meniconi, M.; Pleban, K.; Ecker, G.; Bellocchi, D.; Pellicciari, R. *Journal of chemical information and computer sciences* **2004**, *44*, 1829.

(171) Reineck, P.; Wienken, C. J.; Braun, D. *Electrophoresis* **2010**, *31*, 279.

(172) Wienken, C. J.; Baaske, P.; Rothbauer, U.; Braun, D.; Duhr, S. *Nat Commun* **2010**, *1*.

(173) Matulis, D.; Kranz, J. K.; Salemme, F. R.; Todd, M. J. *Biochemistry* **2005**, *44*, 5258.

(174) Zimmermann, G.; Papke, B.; Ismail, S.; Vartak, N.; Chandra, A.; Hoffmann, M.; Hahn, S. A.; Triola, G.; Wittinghofer, A.; Bastiaens, P. I. H.; Waldmann, H. *Nature* **2013**, *497*, 638.

(175) Lipowsky and E. Sackmann, Handbook of Biological Physics,19565 Volume 1, 895

(176) van den Ent, F.; Amos, L. A.; Lowe, J. *Nature* **2001**, *413*, 39.

(177) Mitchison, T. J. *Mol Biol Cell* **1992**, *3*, 1309.

(178) Carlsson, A. E. *Annu Rev Biophys* **2010**, *39*, 91.

(179) Heng, Y. W.; Koh, C. G. *Int J Biochem Cell B* **2010**, *42*, 1622.

(180) Rao, J.; Li, N. *Current cancer drug targets* **2004**, *4*, 345.

(181) Klymkowsky, M. W.; Bachant, J. B.; Domingo, A. *Cell Motil Cytoskel* **1989**, *14*, 309.

(182) Janmey, P. Handbook of Biological Physics, 1995, 1, 805 (edited by R. Lipowsky and E. Sackmann)

(183) Janmey, P. A.; Euteneuer, U.; Traub, P.; Schliwa, M. *J Cell Biol* **1991**, *113*, 155.

(184) Olmsted, J. B. *Annu Rev Cell Biol* **1986**, *2*, 421.

(185) Job, D.; Valiron, O.; Oakley, B. *Current opinion in cell biology* **2003**, *15*, 111.

(186) Desai, A.; Mitchison, T. J. *Annual review of cell and developmental biology* **1997**, *13*, 83.

(187) Jordan, M. A.; DeLuca, K.; Wagner, M. M.; Williams, D. C.; Wilson, L. *Annals of Oncology* **1998**, *9*, 20.

(188) Jordon, M. A.; Wilson, L. *Acs Sym Ser* **1995**, *583*, 138.

(189) Walczak, C. E.; Shaw, S. L. *Cell* **2010**, *142*, 364.

(190) Wade, R. H. *Mol Biotechnol* **2009**, *43*, 177.

(191) Jordan, A.; Hadfield, J. A.; Lawrence, N. J.; McGown, A. T. *Med Res Rev* **1998**, *18*, 259.

(192) Howard, J.; Hyman, A. A. *Nat Rev Mol Cell Bio* **2009**, *10*, 569.

(193) Brinkley, B. R. *Annu Rev Cell Biol* **1985**, *1*, 145.

(194) Nogales, E. *Annu Rev Biochem* **2000**, *69*, 277.

(195) Schwartz, E. L. *Clinical Cancer Research* **2009**, *15*, 2594.

(196) Straube, A.; Brill, M.; Oakley, B. R.; Horio, T.; Steinberg, G. *Mol Biol Cell* **2003**, *14*, 642.

(197) Lodish, H,; Berk, A.; Zipursky, S. L.; Matsudaira, P.; Baltimore, D. Darnell,J. W.H. Freeman and Company 2008, 761

(198) Lodish, H,; Berk, A.; Zipursky, S. L.; Matsudaira, P.; Baltimore, D. Darnell,J. W.H. Freeman and Company 2008, 761

(199) Lodish, H,; Berk, A.; Zipursky, S. L.; Matsudaira, P.; Baltimore, D. Darnell,J. W.H. Freeman and Company 2008, 761.

(200) Vermeulen, K.; Van Bockstaele, D. R.; Berneman, Z. N. *Cell Proliferat* **2003**, *36*, 131.

(201) Schafer, K. A. *Vet Pathol* **1998**, *35*, 461.

(202) Dehay, C.; Kennedy, H. *Nat Rev Neurosci* **2007**, *8*.

(203) Nasmyth, K. *New Biol* **1991**, *3*, 955.

(204) Deep, G.; Agarwal, R. *Curr Opin Invest Dr* **2008**, *9*, 591.

(205) Morgan, D. O. *Nature* **1995**, *374*, 131.

(206) Girard, F.; Strausfeld, U.; Fernandez, A.; Lamb, N. J. C. *Cell* **1991**, *67*, 1169.

(207) Arellano, M.; Moreno, S. *Int J Biochem Cell B* **1997**, *29*, 559.

(208) Vermeulen, K.; Van Bockstaele, D. R.; Berneman, Z. N. *Cell proliferation* **2003**, *36*, 131.

(209) Musacchio, A.; Hardwick, K. G. *Nat Rev Mol Cell Bio* **2002**, *3*, 731.

(210) Nigg, E. A. *Nat Rev Mol Cell Bio* **2001**, *2*, 21.

(211) Osborne, C.; Wilson, P.; Tripathy, D. *Oncologist* **2004**, *9*, 361.

(212) Kopnin, B. P. *Biochemistry-Moscow+* **2000**, *65*, 2.

(213) Wolfel, T.; Hauer, M.; Schneider, J.; Serrano, M.; Wolfel, C.; Klehmannhieb, E.; Deplaen, E.; Hankeln, T.; Zumbuschenfelde, K. H. M.; Beach, D. *Science* **1995**, *269*, 1281.

(214) Gillett, C.; Smith, P.; Gregory, W.; Richards, M.; Millis, R.; Peters, G.; Barnes, D. *Int J Cancer* **1996**, *69*, 92.

(215) Lawen, A. *BioEssays : news and reviews in molecular, cellular and developmental biology* **2003**, *25*, 888.

(216) Batinac, T.; Gruber, F.; Lipozencic, J.; Zamolo-Koncar, G.; Stasic, A.; Brajac, I. *Acta dermatovenerologica Croatica : ADC* **2003**, *11*, 225.

(217) Hainaut, P.; Olivier, M.; Pfeifer, G. P. *Mutagenesis* **2001**, *16*, 551.

(218) Friedl, P.; Wolf, K. *Nature Reviews Cancer* **2003**, *3*, 362.

(219) Hanahan, D.; Weinberg, R. A. *Cell* **2011**, *144*, 646.

(220) VanBuren, V.; Cassimeris, L.; Odde, D. J. *Biophys J* **2005**, *89*, 2911.

(221) Downing, K. H. *Annual review of cell and developmental biology* **2000**, *16*, 89.

(222) Nabi, I. R. *Journal of cell science* **1999**, *112 (Pt 12)*, 1803.

(223) Small, J. V.; Kaverina, I.; Krylyshkina, O.; Rottner, K. *FEBS letters* **1999**, *452*, 96.

(224) Waterman-Storer, C. M.; Salmon, E. D. *Curr Opin Cell Biol* **1999**, *11*, 61.

(225) Dumontet, C.; Jordan, M. A. *Nature Reviews Drug Discovery* **2010**, *9*, 587.

(226) Mitchison, T.; Kirschner, M. *Nature* **1984**, *312*, 237.

(227) Asako, H.; Kubes, P.; Baethge, B. A.; Wolf, R. E.; Granger, D. N. *Inflammation* **1992**, *16*, 45.

(228) Lemor, M.; Debustros, S.; Glaser, B. M. *Arch Ophthalmol-Chic* **1986**, *104*, 1223.

(229) Joseph, J. P.; Grierson, I.; Hitchings, R. A. *Curr Eye Res* **1989**, *8*, 203.

(230) Spiro, T. P.; Mundy, G. R. *Journal of the National Cancer Institute* **1980**, *65*, 463.

(231) Mareel, M. M.; Storme, G. A.; Debruyne, G. K.; Vancauwenberge, R. M. *Eur J Cancer Clin On* **1982**, *18*, 199.

(232) Macfadden, D. K.; Saito, S.; Pruzanski, W. *Journal of Clinical Oncology* **1985**, *3*, 415.

(233) Cheung, H. T.; Terry, D. S. *Cell Biol Int Rep* **1980**, *4*, 1125.

(234) Storme, G.; Mareel, M. M. *Cancer Res* **1980**, *40*, 943.

(235) Nakamura, M.; Mishima, H.; Nishida, T.; Otori, T. *Jpn J Ophthalmol* **1991**, *35*, 377.

(236) Horwitz, S. B. *Annals of oncology : official journal of the European Society for Medical Oncology / ESMO* **1994**, *5 Suppl 6*, S3.

(237) Schiff, P. B.; Fant, J.; Horwitz, S. B. *Nature* **1979**, *277*, 665.

(238) Schiff, P. B.; Horwitz, S. B. *P Natl Acad Sci-Biol* **1980**, *77*, 1561.

(239) Schiff, P. B.; Horwitz, S. B. *Biochemistry-Us* **1981**, *20*, 3247.

(240) Williams, R. C.; Rone, L. A. *Journal of Biological Chemistry* **1989**, *264*, 1663.

(241) Keller, H. U.; Zimmermann, A. *Invas Metast* **1986**, *6*, 33.

(242) Green, K. J.; Goldman, R. D. *Cell Motil Cytoskel* **1983**, *3*, 283.

(243) Deep, G.; Agarwal, R. *Curr Opin Investig Drugs* **2008**, *9*, 591.

(244) Lapenna, S.; Giordano, A. *Nature reviews. Drug discovery* **2009**, *8*, 547.

(245) Kitagawa, M.; Okabe, T.; Ogino, H.; Matsumoto, H.; Suzukitakahashi, I.; Kokubo, T.; Higashi, H.; Saitoh, S.; Taya, Y.; Yasuda, H.; Ohba, Y.; Nishimura, S.; Tanaka, N.; Okuyama, A. *Oncogene* **1993**, *8*, 2425.

(246) Kitagawa, M.; Higashi, H.; Takahashi, I. S.; Okabe, T.; Ogino, H.; Taya, Y.; Nishimura, S.; Okuyama, A. *Oncogene* **1994**, *9*, 2549.

(247) Lane, M. E.; Yu, B.; Rice, A.; Lipson, K. E.; Liang, C.; Sun, L.; Tang, C.; McMahon, G.; Pestell, R. G.; Wadler, S. *Cancer Res* **2001**, *61*, 6170.

(248) Coleman, M. L.; Marshall, C. J.; Olson, M. F. *Nature reviews. Molecular cell biology* **2004**, *5*, 355.

(249) Dekker, F. J.; Hedberg, C. *Bioorganic & medicinal chemistry* **2011**, *19*, 1376.

(250) Dekker, F. J.; Rocks, O.; Vartak, N.; Menninger, S.; Hedberg, C.; Balamurugan, R.; Wetzel, S.; Renner, S.; Gerauer, M.; Scholermann, B.; Rusch, M.; Kramer, J. W.; Rauh, D.; Coates, G. W.; Brunsveld, L.; Bastiaens, P. I.; Waldmann, H. *Nature chemical biology* **2010**, *6*, 449.

(251) Levitzki, A. *European journal of biochemistry / FEBS* **1994**, *226*, 1.

(252) Alessi, D. R.; Cuenda, A.; Cohen, P.; Dudley, D. T.; Saltiel, A. R. *The Journal of biological chemistry* **1995**, *270*, 27489.

(253) Kerr, A. H.; James, J. A.; Smith, M. A.; Willson, C.; Court, E. L.; Smith, J. G. *Annals of the New York Academy of Sciences* **2003**, *1010*, 86.

(254) Downward, J. *Nature Reviews Cancer* **2003**, *3*, 11.

(255) Li, D. W. C.; Liu, J. P.; Mao, Y. W.; Xiang, H.; Wang, J.; Ma, W. Y.; Dong, Z. G.; Pike, H. M.; Brown, R. E.; Reed, J. C. *Mol Biol Cell* **2005**, *16*, 4437.

(256) Oliner, J. D.; Kinzler, K. W.; Meltzer, P. S.; George, D. L.; Vogelstein, B. *Nature* **1992**, *358*, 80.

(257) Graves, B.; Thompson, T.; Xia, M. X.; Janson, C.; Lukacs, C.; Deo, D.; Di Lello, P.; Fry, D.; Garvie, C.; Huang, K. S.; Gao, L.; Tovar, C.; Lovey, A.; Wanner, J.; Vassilev, L. T. *Proceedings of the National Academy of Sciences of the United States of America* **2012**, *109*, 11788.

(258) Shangary, S.; Wang, S. M. *Clinical Cancer Research* **2008**, *14*, 5318.

(259) Shangary, S.; Qin, D. G.; McEachern, D.; Liu, M. L.; Miller, R. S.; Qiu, S.; Nikolovska-Coleska, Z.; Ding, K.; Wang, G. P.; Chen, J. Y.; Bernard, D.; Zhang, J.; Lu, Y. P.; Gu, Q. Y.; Shah, R. B.; Pienta, K. J.; Ling, X. L.; Kang, S. M.; Guo, M.; Sun, Y.; Yang, D. J.; Wang, S. M. *Proceedings of the National Academy of Sciences of the United States of America* **2008**, *105*, 3933.

(260) Kehlenbach, R. H.; Dickmanns, A.; Kehlenbach, A.; Guan, T.; Gerace, L. *The Journal of cell biology* **1999**, *145*, 645.

(261) Behrens, P.; Brinkmann, U.; Fogt, F.; Wernert, N.; Wellmann, A. *Anticancer research* **2001**, *21*, 2413.

(262) Alnabulsi, A.; Agouni, A.; Mitra, S.; Garcia-Murillas, I.; Carpenter, B.; Bird, S.; Murray, G. I. *J. Pathol.* **2012**, *228*, 471.

(263) Brinkmann, U.; Brinkmann, E.; Gallo, M.; Pastan, I. *Proceedings of the National Academy of Sciences of the United States of America* **1995**, *92*, 10427.

(264) Dimova, I.; Yosifova, A.; Zaharieva, B.; Raitcheva, S.; Doganov, N.; Toncheva, D. *European journal of obstetrics, gynecology, and reproductive biology* **2005**, *118*, 81.

(265) Brinkmann, U.; Gallo, M.; Polymeropoulos, M. H.; Pastan, I. *Genome Research* **1996**, *6*, 187.

(266) Brinkmann, U.; Brinkmann, E.; Bera, T. K.; Wellmann, A.; Pastan, I. *Genomics* **1999**, *58*, 41.

(267) Bera, T. K.; Bera, J.; Brinkmann, U.; Tessarollo, L.; Pastan, I. *Molecular and cellular biology* **2001**, *21*, 7020.

(268) Wellmann, A.; Flemming, P.; Behrens, P.; Wuppermann, K.; Lang, H.; Oldhafer, K.; Pastan, I.; Brinkmann, U. *International journal of molecular medicine* **2001**, *7*, 489.

(269) Brinkmann, U.; Brinkmann, E.; Gallo, M.; Scherf, U.; Pastan, I. *Biochemistry* **1996**, *35*, 6891.

(270) Behrens, P.; Brinkmann, U.; Wellmann, A. *Apoptosis : an international journal on programmed cell death* **2003**, *8*, 39.

(271) http://www.uniprot.org/uniprot/P55060

(272) Kutay, U.; Bischoff, F. R.; Kostka, S.; Kraft, R.; Gorlich, D. *Cell* **1997**, *90*, 1061.

(273) Peiro, G.; Diebold, J.; Lohrs, U. *Am J Clin Pathol* **2002**, *118*, 922.

(274) Brustmann, H. *Gynecol Oncol* **2004**, *92*, 268.

(275) Tai, C. J.; Hsu, C. H.; Shen, S. C.; Lee, W. R.; Jiang, M. C. *J Exp Clin Canc Res* **2010**, *29*.

(276) Uen, W. C.; Tai, C. J.; Shen, S. C.; Lee, W. R.; Tsao, T. Y.; Deng, W. P.; Chiou, H. Y.; Hsu, C. H.; Hsieh, C. I.; Liao, C. F.; Jiang, M. C. *Journal of molecular histology* **2010**, *41*, 259.

(277) Tsao, T. Y.; Tsai, C. S. S.; Tung, J. N.; Chen, S. L.; Yue, C. H.; Liao, C. F.; Wang, C. C.; Jiang, M. C. *Molecular and cellular biochemistry* **2009**, *327*, 163.

(278) Tung, M. C.; Tsai, C. S. S.; Tung, J. N.; Tsao, T. Y.; Chen, H. C.; Yeh, K. T.; Liao, C. F.; Jiang, M. C. *Cancer Epidemiology Biomarkers & Prevention* **2009**, *18*, 1570.

(279) Stella, T. C.-S.; Chen, H.-C.; Tung, J.-N.; Tsou, S.-S.; Tsao, T.-Y.; Liao, C.-F.; Chen, Y.-C.; Yeh, C.-Y.; Yeh, K.-T.; Jiang, M.-C. *Am J Pathol* **2010**, *176*, 1619.

(280) Chang, C. C.; Tai, C. J.; Su, T. C.; Shen, K. H.; Lin, S. H.; Yeh, C. M.; Yeh, K. T.; Lin, Y. M.; Jiang, M. C. *Annals of diagnostic pathology* **2012**, *16*, 362.

(281) Kubinyi, H.; Elsevier Ltd.: 2006; Vol. 3, p 921.

(282) Tai, C. J.; Shen, S. C.; Lee, W. R.; Liao, C. F.; Deng, W. P.; Chiou, H. Y.; Hsieh, C. I.; Tung, J. N.; Chen, C. S.; Chiou, J. F.; Li, L. T.; Lin, C. Y.; Hsu, C. H.; Jiang, M. C. *Experimental cell research* **2010**, *316*, 2969.

(283) Ogryzko, V. V.; Brinkmann, E.; Howard, B. H.; Pastan, I.; Brinkmann, U. *Biochemistry* **1997**, *36*, 9493.

(284) Ewings, K. E.; Ryan, K. M. *Cell research* **2007**, *17*, 829.

(285) Wijnhoven, B. P. L.; Dinjens, W. N. M.; Pignatelli, M. *Brit J Surg* **2000**, *87*, 992.

(286) Jiang, M. C.; Liao, C. F.; Tai, C. C. *Biochemical and biophysical research communications* **2002**, *294*, 900.

(287) Liao, C. F.; Luo, S. F.; Tsai, C. S.; Tsao, T. Y.; Chen, S. L.; Jiang, M. C. *Toxicol Mech Methods* **2008**, *18*, 771.

(288) Liao, C. F.; Luo, S. F.; Shen, T. Y.; Lin, C. H.; Chien, J. T.; Du, S. Y.; Jiang, M. C. *BMB reports* **2008**, *41*, 210.

(289) Klebe, C.; Nishimoto, T.; Wittinghofer, F. *Biochemistry* **1993**, *32*, 11923.

(290) Shen, D. W.; Fojo, A.; Roninson, I. B.; Chin, J. E.; Soffir, R.; Pastan, I.; Gottesman, M. M. *Molecular and cellular biology* **1986**, *6*, 4039.

(291) Sakaue-Sawano, A.; Kurokawa, H.; Morimura, T.; Hanyu, A.; Hama, H.; Osawa, H.; Kashiwagi, S.; Fukami, K.; Miyata, T.; Miyoshi, H.; Imamura, T.; Ogawa, M.; Masai, H.; Miyawaki, A. *Cell* **2008**, *132*, 487.
(292) Inoue, H.; Nojima, H.; Okayama, H. *Gene* **1990**, *96*, 23.
(293) Bonne, D.; Heusele, C.; Simon, C.; Pantaloni, D. *J Biol Chem* **1985**, *260*, 2819.
(294) Heusele, C.; Bonne, D. *Biochemical and biophysical research communications* **1985**, *133*, 662.
(295) Williams, A. K.; Dasilva, S. C.; Bhatta, A.; Rawal, B.; Liu, M.; Korobkova, E. A. *Analytical biochemistry* **2012**, *422*, 66.
(296) Jerabek-Willemsen, M.; Wienken, C. J.; Braun, D.; Baaske, P.; Duhr, S. *Assay Drug Dev Techn* **2011**, *9*, 342.
(297) Schenborn, E. T.; Goiffon, V. Methods Mol Biol 2000, 130, 147.
(298) Aoki, S.; Higuchi, K.; Ye, Y.; Satari, R.; Kobayashi, M. *Tetrahedron* **2000**, *56*, 1833.
(299) Knoth, T.; Warburg, K.; Katzka, C.; Rai, A.; Wolf, A.; Brockmeyer, A.; Janning, P.; Reubold, T. F.; Eschenburg, S.; Manstein, D. J.; Hubel, K.; Kaiser, M.; Waldmann, H. *Angew Chem Int Edit* **2009**, *48*, 7240.
(300) www.biocompare.com/Product-Reviews/40987-Rosetta-gami-B-Host-Strains-From-Novagen/
(301) http://www.emdmillipore.com/life-science-research/t7select-human-breast-tumor-cdna-library/EMD_BIO-70644/p_Prab.s1OPEsAAAEjNBx9.zLX
(302) Jung, H. J.; Kim, Y.; Chang, J.; Kang, S. W.; Kim, J. H.; Kwon, H. J. *J Mol Med* **2013**, *91*, 1117.
(303) Peterson, J. R.; Mitchison, T. J. *Chem Biol* **2002**, *9*, 1275.
(304) Dumontet, C.; Jordan, M. A. *Nat Rev Drug Discov* **2010**, *9*, 790.
(305) Voigt, T.; Gerding-Reimers, C.; Ngoc, T. T. T.; Bergmann, S.; Lachance, H.; Schoelermann, B.; Brockmeyer, A.; Janning, P.; Ziegler, S.; Waldmann, H. *Angew. Chem., Int. Ed.* **2013**, *52*, 410.
(306) Shen, D. W.; Cardarelli, C.; Hwang, J.; Cornwell, M.; Richert, N.; Ishii, S.; Pastan, I.; Gottesman, M. M. *J Biol Chem* **1986**, *261*, 7762.
(307) Akiyama, S. I.; Fojo, A.; Hanover, J. A.; Pastan, I.; Gottesman, M. M. *Somat Cell Molec Gen* **1985**, *11*, 117.
(308) Sega, G. A. *Mutation research* **1984**, *134*, 113.
(309) Kim, H. M.; Oh, G. T.; Hong, D. H.; Kim, M. S.; Kang, J. S.; Park, S. M.; Han, S. B. *Febs Letters* **1997**, *412*, 201.
(310) Coleman, M. L.; Sahai, E. A.; Yeo, M.; Bosch, M.; Dewar, A.; Olson, M. F. *Nat Cell Biol* **2001**, *3*, 339.
(311) Van Cruchten, S.; Van den Broeck, W. *Anat Histol Embryol* **2002**, *31*, 214.
(312) Schenborn, E. T.; Goiffon, V. *Methods Mol Biol* **2000**, *130*, 147.
(313) http://www.olink.com/products-services/duolink/situ-pla-technology
(314) Kanoh, N.; Kumashiro, S.; Simizu, S.; Kondoh, Y.; Hatakeyama, S.; Tashiro, H.; Osada, H. *Angew Chem Int Edit* **2003**, *42*, 5584.
(315) Kanoh, N.; Asami, A.; Kawatani, M.; Honda, K.; Kumashiro, S.; Takayama, H.; Simizu, S.; Amemiya, T.; Kondoh, Y.; Hatakeyama, S.; Tsuganezawa, K.; Utata, R.; Tanaka, A.; Yokoyama, S.; Tashiro, H.; Osada, H. *Chem-Asian J* **2006**, *1*, 789.
(316) Kanoh, N.; Osada, H. *J Syn Org Chem Jpn* **2006**, *64*, 639.
(317) https://scifinder.cas.org/scifinder/view/scifinder/scifinderExplore.jsf
(318) Federico Arcamone, Elsevier, 1981, 17, 326
(319) http://sea.bkslab.org/search/
(320) Johnson, I. M.; Kumar, S. G. B.; Malathi, R. J *Biomol Struct Dyn* 2**003,** 2*0,* 677.
(321) Eriksson, S.; Kim, S. K.; Kubista, M.; Norden, B. B*iochemistry* 1**993,** 3*2,* 2987.
(322) Plafker, K.; Macara, I. G. M*olecular and cellular biology* 2**000,** 2*0,* 3510.
(323) Wolff, B.; Sanglier, J. J.; Wang, Y. C*hem Biol* 1**997,** 4*,* 139.

(324) Kudo, N.; Matsumori, N.; Taoka, H.; Fujiwara, D.; Schreiner, E. P.; Wolff, B.; Yoshida, M.; Horinouchi, S. P*roceedings of the National Academy of Sciences of the United States of America* 1**999,** 9*6,* 9112.

(325) Clackson, T.; Lowman, H. B. Phage display. Oxford University Press, 2004. 20.

(326) Horowitz, P.; Prasad, V.; Luduena, R. F. J *Biol Chem* 1**984,** 2*59,* 4647.

(327) Declerck, F.; Debrabander, M. T*hromb Res* 1**977,** 1*1,* 913.

(328) Wendell, K. L.; Wilson, L.; Jordan, M. A. J *Cell Sci* 1**993,** 1*04,* 261.

(329) https://www.genscript.com/ssl-bin/site2/peptide_calculation.cgi

(330) Scherf, U.; Pastan, I.; Willingham, M. C.; Brinkmann, U. Pr*oceedings of the National Academy of Sciences of the United States of America 1*9**96,** 93*,* 2670.

(331) Shen, D. W.; Fojo, A.; Chin, J. E.; Roninson, I. B.; Richert, N.; Pastan, I.; Gottesman, M. M. Sc*ience 1*9**86,** 23*2,* 643.

(332) Kavallaris, M. Na*t Rev Cancer 2*0**10,** 10*.*

(333) Kavoi, B. M.; Makanya, A. N.; Kiama, S. G. An*at Histol Embryol 2*0**12,** 41*,* 374.

(334) Sampson, K. E.; Mccroskey, M. C.; Abraham, I. Jo*urnal of cellular biochemistry 1*9**93,** 52*,* 384.

(335) Kau, T. R.; Way, J. C.; Silver, P. A. Na*t Rev Cancer 2*0**04,** 4, 106.

(336) Bischoff, F. R.; Gorlich, D. Fe*bs Letters 1*9**97,** 41*9,* 249.

8 Summary

In this thesis, forward and reverse chemical genetics approaches from methodology study for target identification to biological study for target validation were used.

One aim of this work was to establish a protocol for the target identification of small molecules using cDNA phage display libraries. For that reason we generated a cDNA phage display library using HeLa cells, which are usually used for phenotypic studies and for target identification using affinity chromatography in our group. This approach was applied for GSH and identified one known hit of GSH. The binders identified by phage display were not identical with the binders identified using affinity purification in the case of the compounds we were interested in, melophlin A, CD 267 and tubulexin A. Therefore, this approach was not pursued further.

The second aim of this thesis is based on the previous screening results, that tetrahydropyran derivatives and the natural product podoverine A are potent inducers of a G2/M cell cycle arrest and apoptosis.
It could be shown that the most active compound from our tetrahydropyran library, tubulexin A, inhibits tubulin polymerization by targeting the vinca alkaloid binding site of tubulin and also the protein CAS. Further validation of the effects of those compounds on tubulin polymerization, the cell cycle, and their binding to CAS was done by biophysical measurements, binding assays, tubulin polymerization assays, immunofluorescence and life time imaging, binding assays, and affinity chromatographic methods. Results showed that CAS binds to tubulexin A independent from tubulin. Additionally, tubulin polymerization is inhibited in a synergistic manner in the presence of both, tubulexin A and CAS *in vitro*. Moreover, tubulexin A can overcome the resistance mechanisms of KB-V1 cancer cells based on the binding to the of the vinca alkaloid site. For the natural product podoverin A, further results showed that this compound inhibits tubulin polymerization also by binding to the vinca alkaloid site.

The third aim of this thesis is based on the results of our tubulexin A studies, we were interested in CAS as a new potential target protein for cancer research. We have extended the project to the discovery new CAS inhibitors based on a reverse chemical genetics

approach using microarrays in collaboration with the group of Prof. Osada (RIKEN-Wako-Japan). After chemical array screening of approximately 25,000 compounds, 263 potential hit compounds have been obtained. Further validation the hit compounds was based on phenotypic changes and specific function of the target using immunofluorescence and life time imaging, biophysical methods for the determination of the binding affinity, as well as studies on the interaction of the hit compounds with DNA and tubulin polymerization *in vitro*. 22 hit compounds affecting HeLa cells have been identified based on phenotypic changes and later on the binding affinities of 3 identified compounds were obtained by means of themophoresis measurements using MST. The most interesting compound R89 was further validated on HeLa cells and we found that this compound inhibited cell proliferation by affecting mitosis at low concentrations without significantly influencing tubulin dynamics or directly inducing apoptosis at higher concentrations. R89 binds to CAS and leads to chromosomal misalignment, multipolar mitotic spindles and induces nuclear accumulation of RANBP1.

9 Zusammenfassung

Ein Ziel dieser Arbeit war die Etablierung eines Phagen-Display-Protokolls zur Identifizierung der Zielproteine von niedermolekularen Verbindungen, die biologisch aktiv sind. Dazu wurde eine HeLa-cDNA-Phagen-Bibliothek generiert. Diese Zelllinie wird in unserer Arbeitsgruppe gewöhnlicherweise für phänotypische Studien und zur Identizierung von Zielproteinen biologisch aktiver Substanzen genutzt. Mithilfe diesen Ansatzes wurde ein bekannter Binder von Glutathion (GSH) identifiziert. Im Fall der chemischen Verbindungen Melophilin A, CD 267 und Tubulexin A, für die Zielproteine bereits bekannt waren, wurden mittels Phagen-Display Proteine identifiziert, die nicht identisch mit denen, die mittels Affinitätschromatographie gefunden wurden, sind. Aus diesem Grund wurde dieser Ansatz nicht weiter verfolgt.

Das zweite Ziel dieser Arbeit basierte auf den vorherigen Screeningergebnissen, dass Tetrahydropyranderivate und der Naturstoff Podoverin A potent einen Arrest des Zellzyklus in der G2/M Phase und Apoptose induzieren. Es konnte gezeigt werden, dass die potenteste Verbindung unserer Tetrahydropyranbibilothek, Tubulexin A, die Tubulinpolymerisation durch Interaktion mit der Vincabindestelle des Tubulins und dem Protein CAS inhibiert. Die weitere Validierung der Effekte dieser Verbindungen auf die Tubulinpolymerisation, den Zellzyklus und die Bindung an CAS erfolgte durch biophysikalische Messungen, Bindungsstudien, Experimente zur Tubulinpolymerisation, Affinitätschromatographie, Immunfluoreszenz- und Fluoreszenz-Echtzeitexperimente. Diese Experimente haben gezeigt, dass die Interaktion zwischen CAS und Tubulexin A unabhängig von Tubulin erfolgt. Außerdem konnte gezeigt werden, dass die Tubulinpolymerisation in Anwesenheit von Tubulexin A und CAS *in vitro* synergistisch inhibiert wird. Zusätzlich kann Tubulexin A die Resistenzmechanismen von KB-V1-Zellen überwinden. Auch für Podoverin A wurde gezeigt, dass die Inhibition der Tubulinpolymerisation durch Bindung an die Vincabindestelle erfolgt.

Das dritte Ziel dieser Arbeit war die Evaluierung von CAS als potentielles neues Zielprotein in der Krebsforschung. Dabei wurde ein rückwärtsgerichteter chemisch gnetischer Ansatz vergewendet um neue CAS Inhibitoren zu identifizieren. In Kollaboration mit Prof. Osada (RIKEN ASI in Wako, Japan) wurden mittels eines chemischen Mikroarrays etwa 25000 Verbindungen auf eine Bindung an CAS untersucht. Dadurch wurden 263 Verbindungen gefunden, die an CAS binden. Die weitere Charakterisierung dieser Verbindungen erfolgte durch die Untersuchung von phänotypischen Veränderungen von Zellen und der spezifischen Funktion des Proteins mittels Immunfluoreszenz, Fluoreszenzlebenszeitexperimenten und biophysikalischen Experimenten zur Bindungsaffinität, und zudem durch Studien zur Interaktion der Verbindungen mit DNA und die Effekte auf die Tubulinpolymerisation *in vitro*.

Bei der phänotypischen Analyse des Einflusses der Verbindungen auf HeLa-Zellen wurden 22 aktive Verbindungen gefunden. Für drei davon wurden Bindungsaffinitäten durch thermophoretische Messungen (MST) bestimmt. Die interessanteste Verbindung, R89 wurde weiter auf ihre Effekte in HeLa-Zellen untersucht. Bei niedrigen Konzentrationen hemmt R89 die Zellproliferation durch Beeinflussung der Mitose ohne die Tubulindynamik signifikant zu stören. , Bei höheren Konzentrationen dagegen wird die Apoptose eingeleitet. R89 bindet an CAS und führt zu Fehlanordung von Chromosomen, der Ausbildung multipolarer mitotischer Spindeln und induziert die Akkumulation von RANBP1 im Zellkern.

10 Appendix

Table I: NPDepo compounds that bind to CAS as identified using the chemical array approach.

Cpd	Name (ID)	Structure	Cpd	Name (ID)	Structure
R1	Gramicidin S Gramicidin S1 Gramicidin S-A Soviet gramicidin	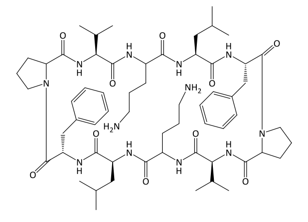	R2	1397-89-3 Amphotericin B	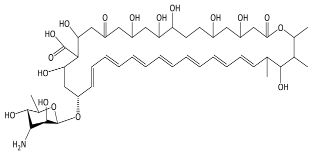
R3	41059-79-4 Timosaponin A-III	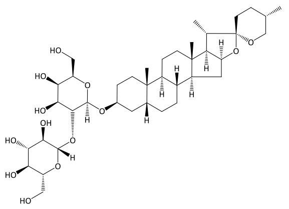	R4	357-57-3 Brucine	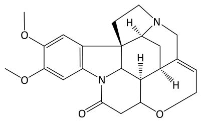
R5	145-50-6 alpha-Naphtholbenzein	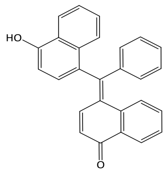	R6	41372-20-7 Apomorphine hydrochloride hemihydrate	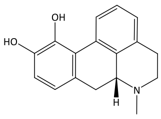
R7	115-40-2 Bromocresol purple	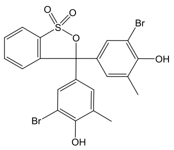	R8	17696-69-4 Hematoporphyrin dihydrochloride	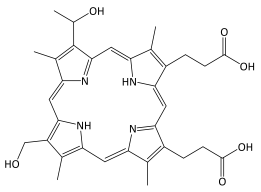
R9	50865-01-5 Protoporphyrin IX disodium salt	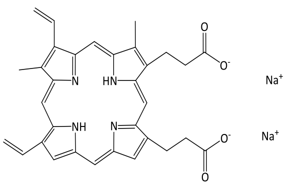	R10	-	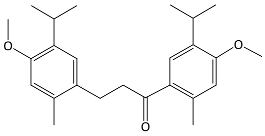
R11	Steviobioside	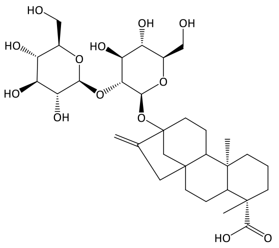	R12	-	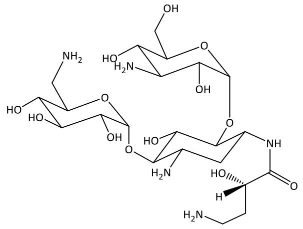

Cpd	Name (ID)	Structure		Cpd	Name (ID)	Structure
R13	-	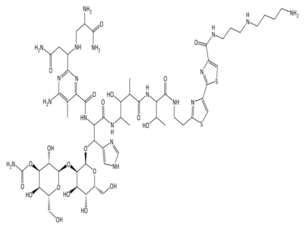		R14	Erythromycin	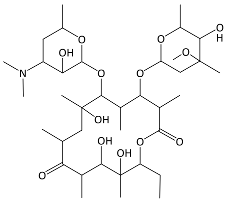
R15	Lincomycin	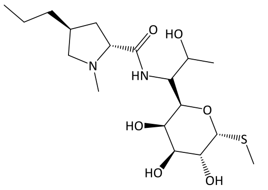		R16	16-Oxo-19-beyeranoic acid	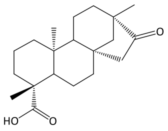
R17	-	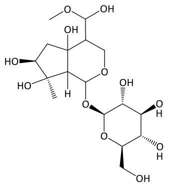		R18	Lycoctonine	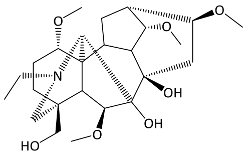
R19	-	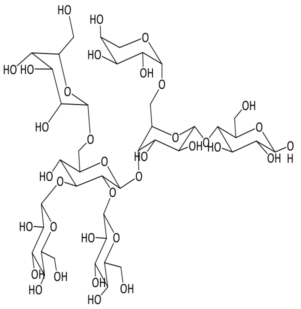		R20	-	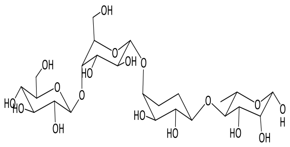
R21	Hydroxyecdysone 20,22-acetonide	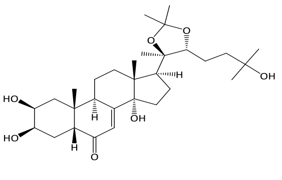		R22	Harpagoside	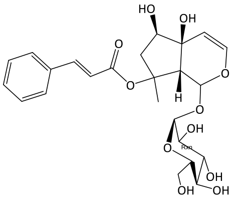
R23	-	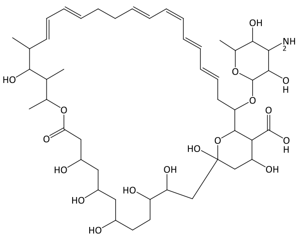		R24	Karasamine	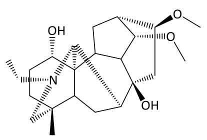

Cpd	Name (ID)	Structure	Cpd	Name (ID)	Structure
R25	Tubeimoside I	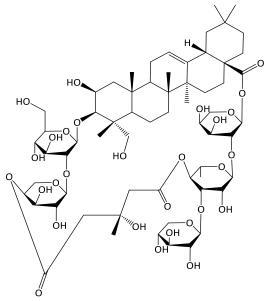	R26	T2 Toxin	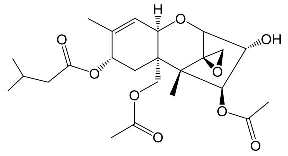
R27	Hydroxyhyoscyamine	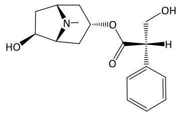	R28	3,5-bis[(3-carboxypropanoyl)amino]benzoic acid	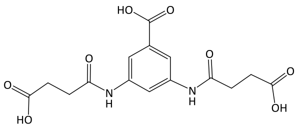
R29	2-({4-[(3-carboxypropanoyl)amino]benzoyl}amino)benzoic acid	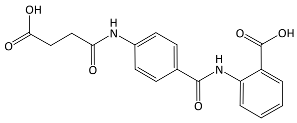	R30	-	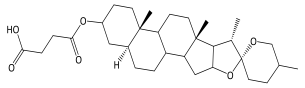
R31	-	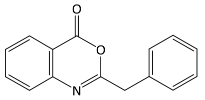	R32	-	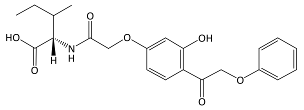
R33	-	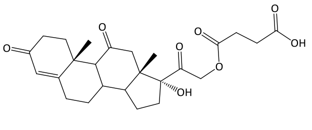	R34	-	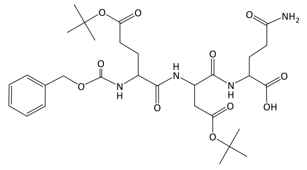
R35	-	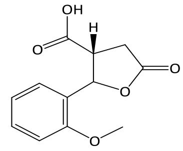	R36	-	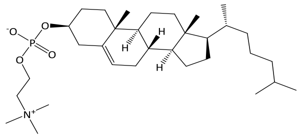
R37	-	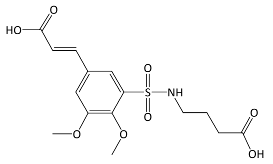	R38	-	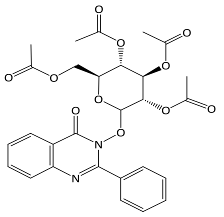
R39	-	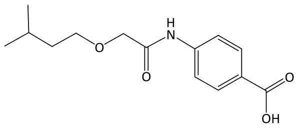	R40	-	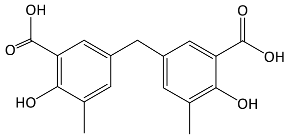
R41	-	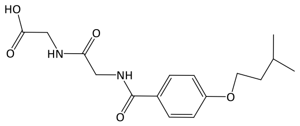	R42	-	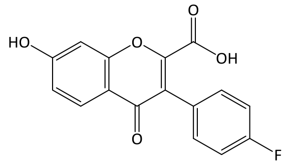

Cpd	Name (ID)	Structure	Cpd	Name (ID)	Structure
R43	-	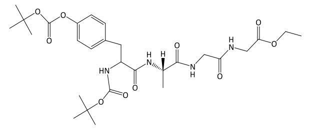	R44	-	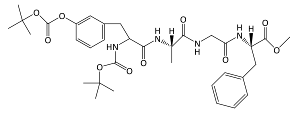
R45	-	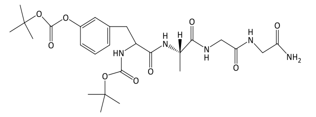	R46	-	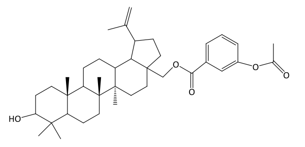
R47	-	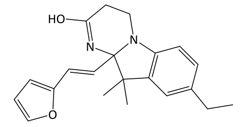	R48	-	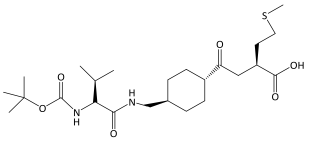
R49	-	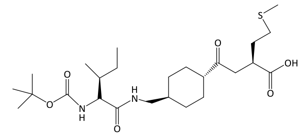	R50	-	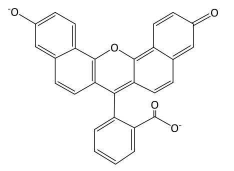
R51	-	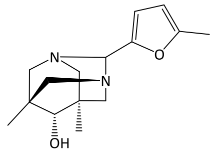	R52	-	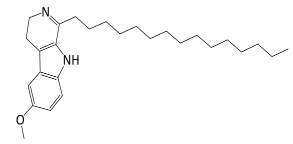
R53	-	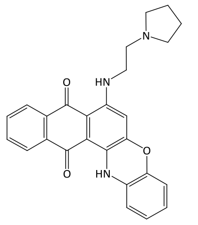	R54	-	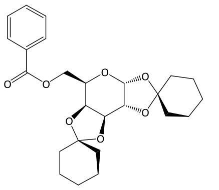
R55	-	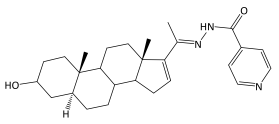	R56	-	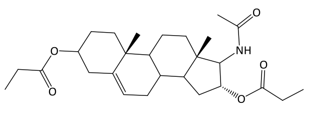
R57	-	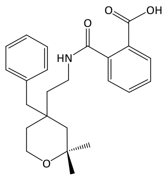	R58	-	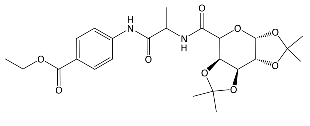
R59	-	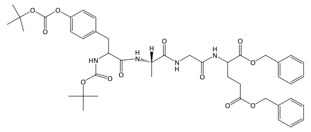	R60	-	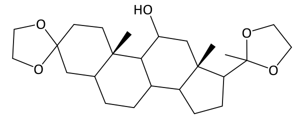
R61	-	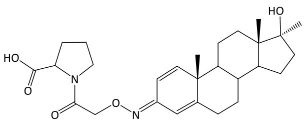	R62	-	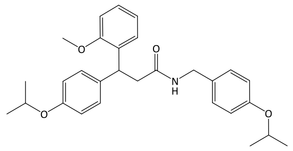

Cpd	Name (ID)	Structure		Cpd	Name (ID)	Structure
R63	-	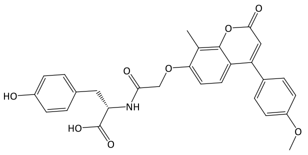		R64	-	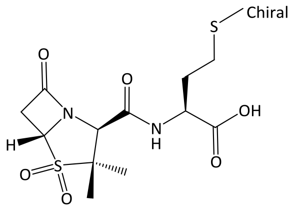
R65	-	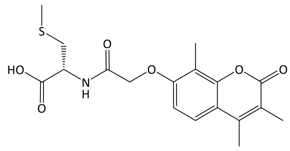		R66	-	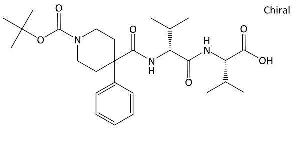
R67	-	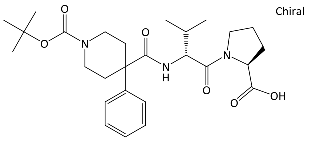		R68	-	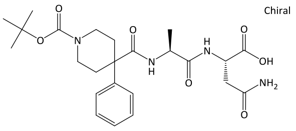
R69	-	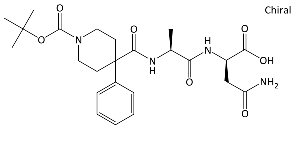		R70	-	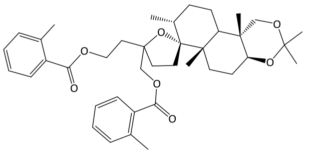
R71	MS0A0293 303-81-1 Novobiocin Cathomycin U 6391	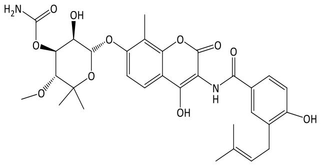		R72	Spartanamicin-B Cinerubin A Cinerubin Rhodirubin C 4915A	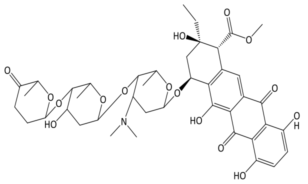
R73	Cinerubin B	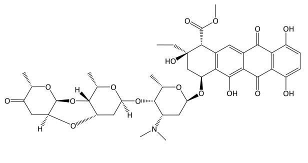		R74	Actinogan	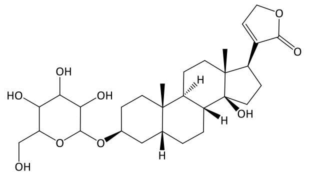
R75	(3S,5S,7R)-3,5,7-Trihydroxy-hexatriacontanoic acid methyl ester	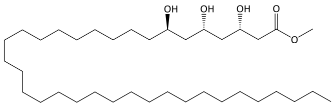		R76	(4R,4aR,7S,8aS)-2,2-Dimethyl-4-pentyl-7-trityloxymethyl-tetrahydro-pyrano[4,3-d][1,3]dioxin-5-one	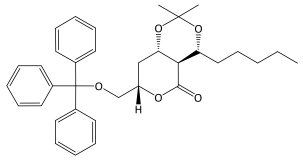
R77	(4S,6S)-4-Hydroxy-6-triphenylsilanyloxymethyl-tetrahydro-pyran-2-one	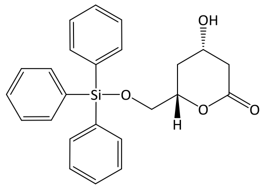		R78	-	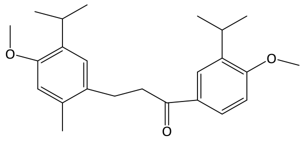

Cpd	Name (ID)	Structure	Cpd	Name (ID)	Structure
R79	-	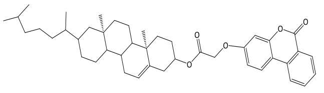	R80	-	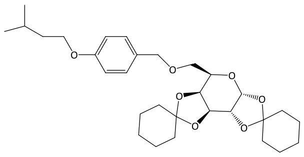
R81	-	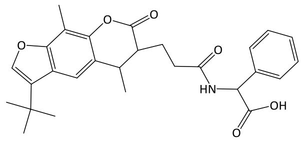	R82	-	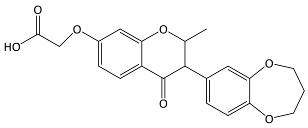
R83	-	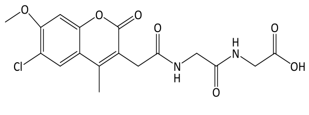	R84	-	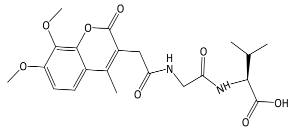
R85	-	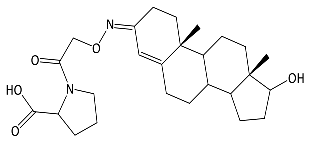	R86	-	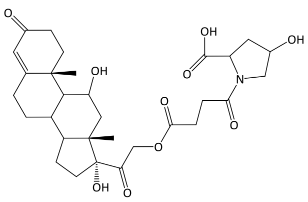
R87	-	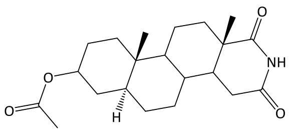	R88	-	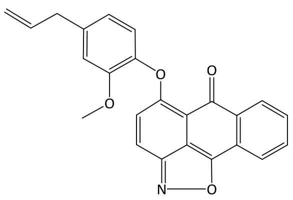
R89	-	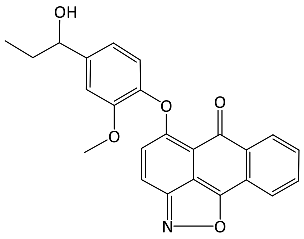	R90	-	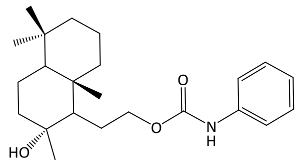
R91	-	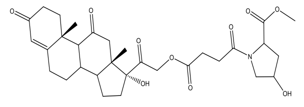	R92	-	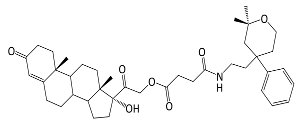
R93	-	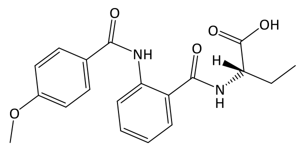	R94	-	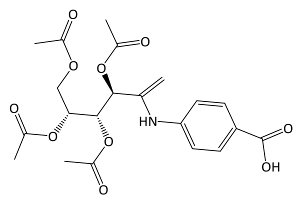
R95	-	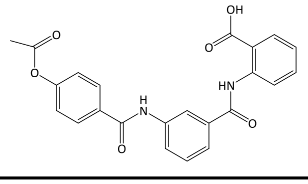	R96	-	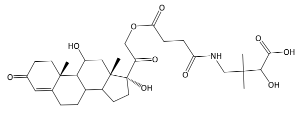

Cpd	Name (ID)	Structure	Cpd	Name (ID)	Structure
R97	-	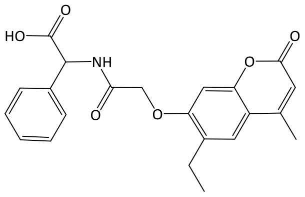	R98	-	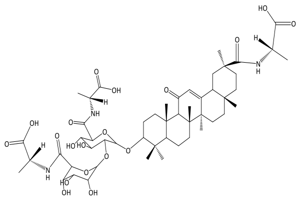
R99	-	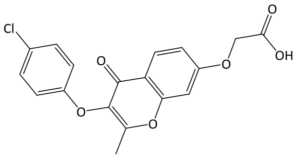	R100	-	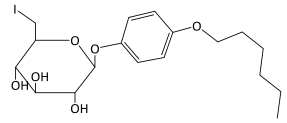
R101	-	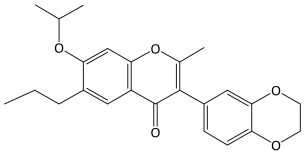	R102	-	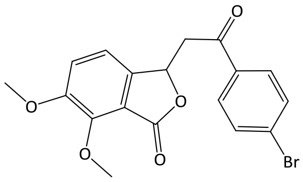
R103	-	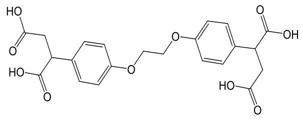	R104	-	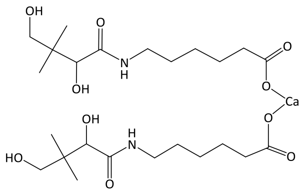
R105	-	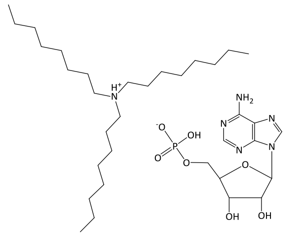	R106	-	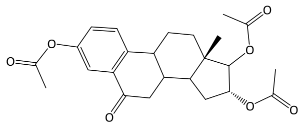
R107	-	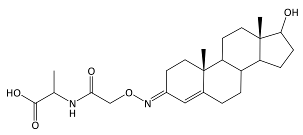	R108	-	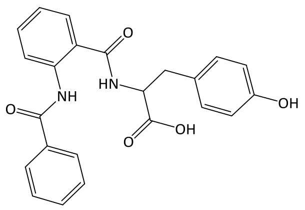
R109	-	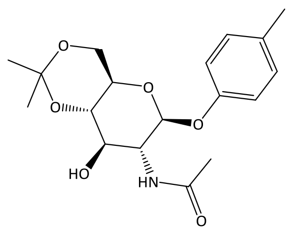	R110	-	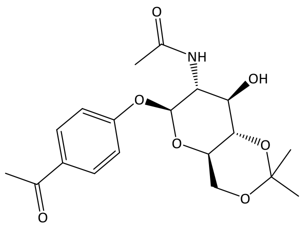

Cpd	Name (ID)	Structure	Cpd	Name (ID)	Structure
R111	-	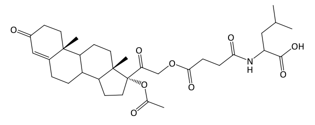	R112	-	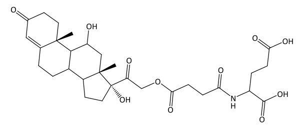
R113	-	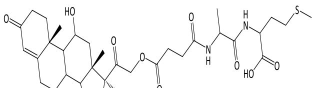	R114	-	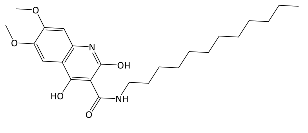
R115	-	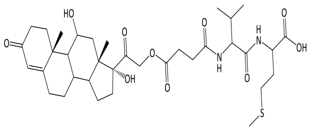	R116	-	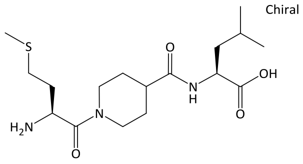
R117	-	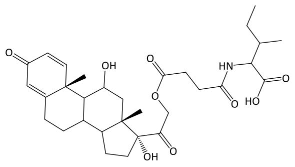	R118	-	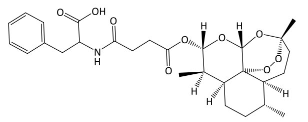
R119	-	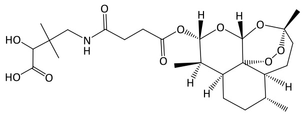	R120	-	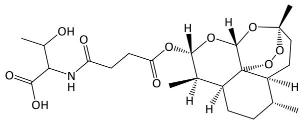
R121	-	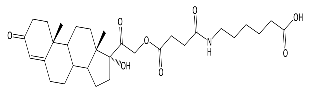	R122	-	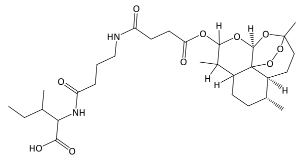
R123	DS287ll-7	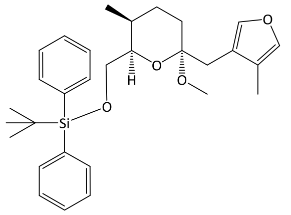	R124	MK538-21	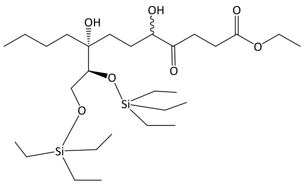
R125	MF164-69	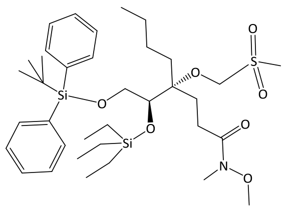	R126	MF175-10815	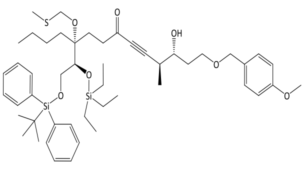

Cpd	Name (ID)	Structure	Cpd	Name (ID)	Structure
R127	DS256-H1	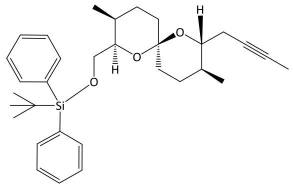	R128	TM185-2	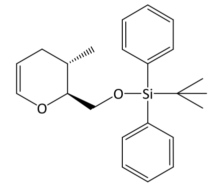
R129	TM323-2	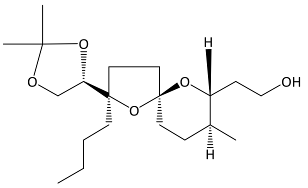	R130	O4-4	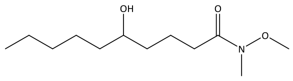
R131	KH580-12	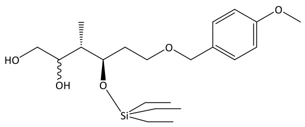	R132	S55-33,79-43	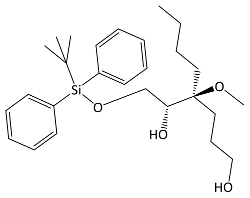
R133	A642-69	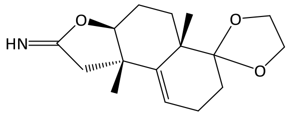	R134	B8-25	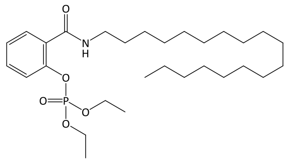
R135	B133l	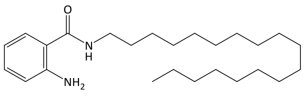	R136	B161ll-ll	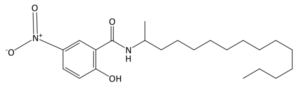
R137	B195-4	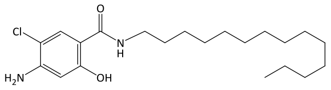	R138	B216-6	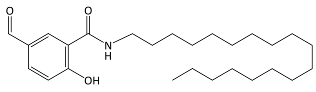
R139	K11ll-A	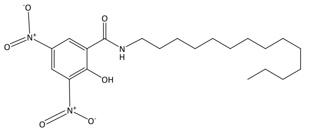	R140	Y73PA+PB	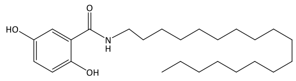
R141	Imidapril Hydrochloride(IMD)	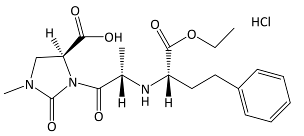	R142	Trandolapril(TRN)	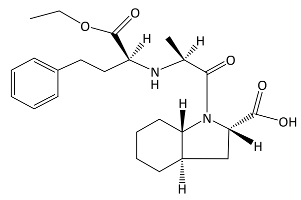

Cpd	Name (ID)	Structure		Cpd	Name (ID)	Structure
R143	Enalapril maleate(EPM)	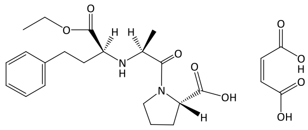		R144	RBSI-F5759	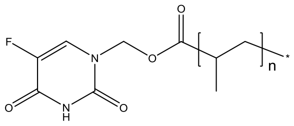
R145	16-epi-Voacarpine	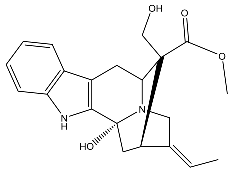		R146	Narciclasine	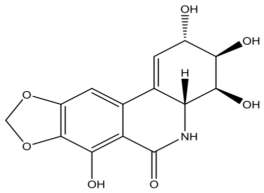
R147	MT-19	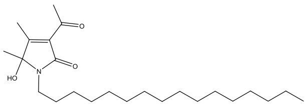				

Table II: Compounds of the COMAS library that bind to CAS as identified using the chemical array approach.

Cpd	Name (ID)	Structure		Cpd	Name (ID)	Structure
M1	SBO21-1	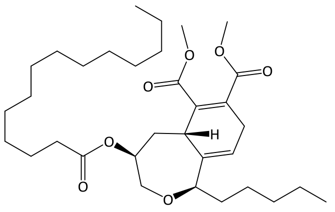		M2	SBO29-1	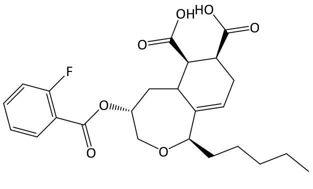
M3	TK203A-2	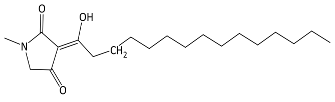		M4	MV261B-1	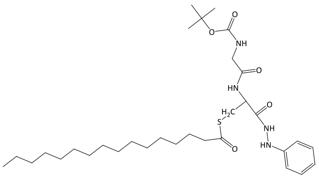
M5	AGWI000522-1	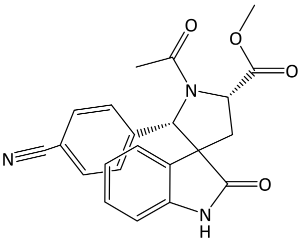		M6	PD697-1	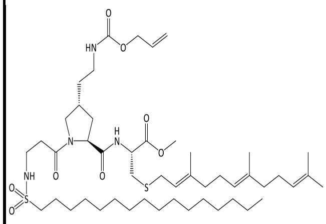
M7	MHA-128-1	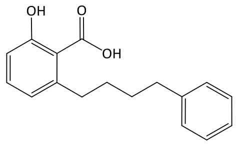		M8	KMD1CsF-1	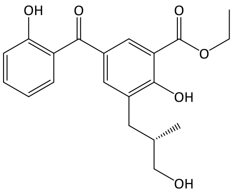
M9	KMG3NH4HH-1	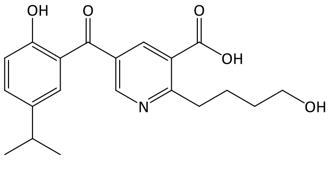		M10	LBD418-1	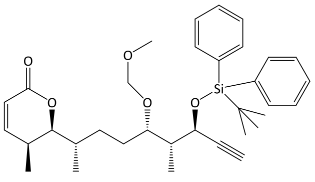
M11	LBD389-1	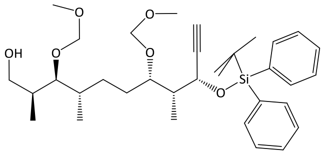		M12	LBD342-1	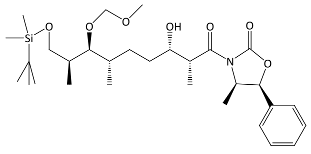

Cpd	Name (ID)	Structure	Cpd	Name (ID)	Structure
M13	RR526E-1	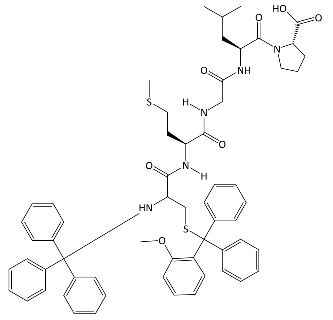	M14	PD749-1	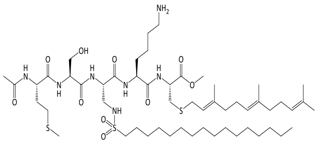
M15	LW145-1	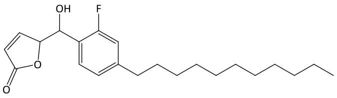	M16	LW148-1	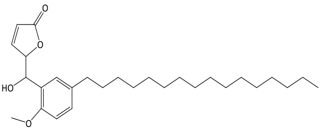
M17	EE1584I-1	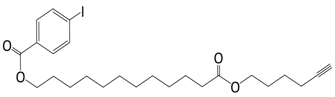	M18	EF28H4-1	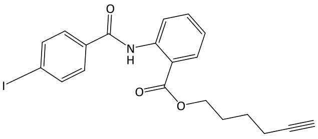
M19	LW104-1	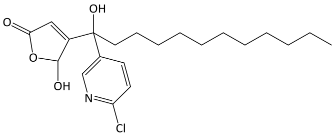	M20	RH12-1	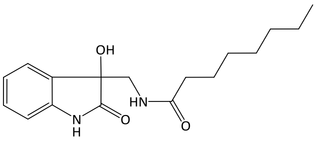
M21	RH15-1	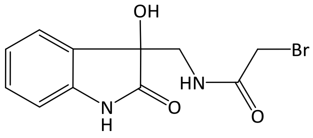	M22	RH21-1	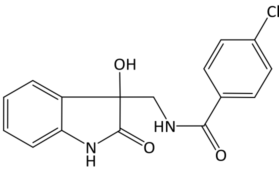
M23	KT3006-1	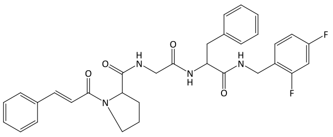	M24	KT30822-1	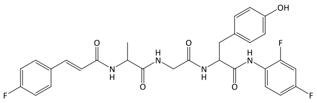
M25	KT4096-1	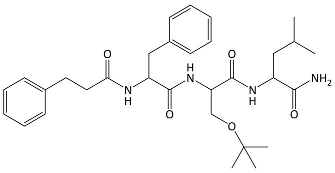	M26	KT4130-1	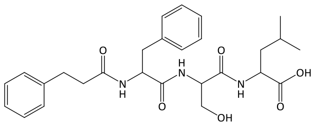

Cpd	Name (ID)	Structure	Cpd	Name (ID)	Structure
M27	KT80782-1	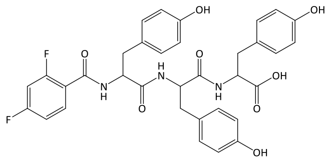	M28	KT81262-1	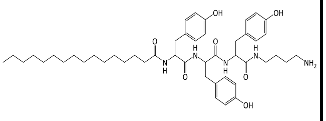
M29	KT80262-1	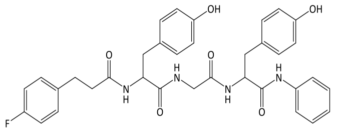	M30	TV_AKT-1	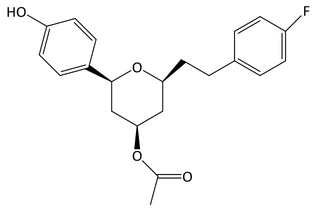
M31	SBO40-1	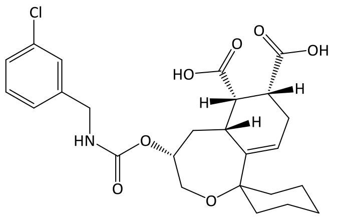	M32	SBO46-1	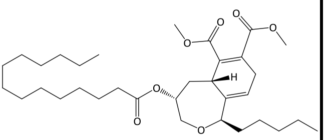
M33	SBO54-1	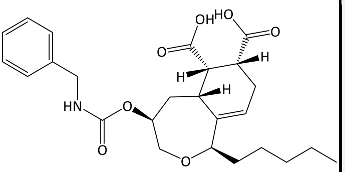	M34	SBO82-1	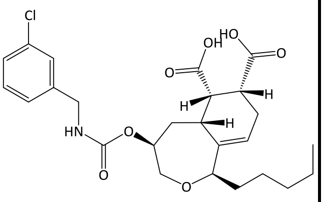
M35	SBO97-1	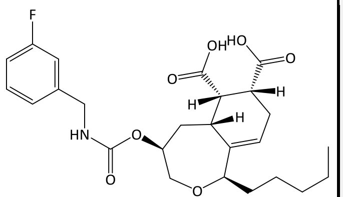	M36	MHA-126-1	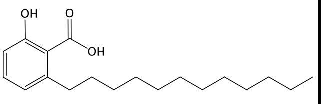
M37	AGWI000165-1	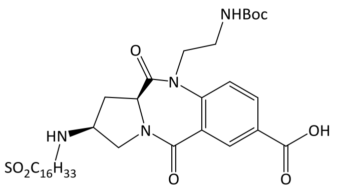	M38	LBD374-1	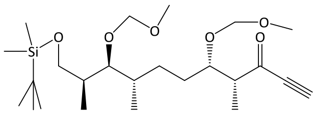
M39	AGWI000207-1	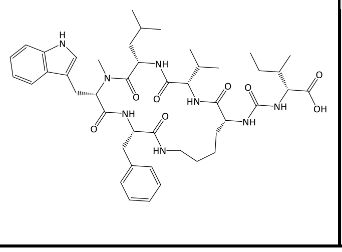	M40	KT91003-1	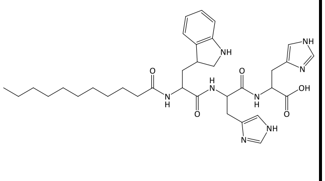

Cpd	Name (ID)	Structure	Cpd	Name (ID)	Structure
M41	KT90402-1	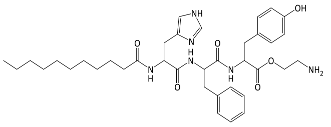	M42	KT80362-1	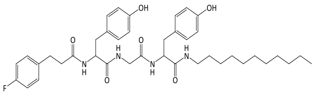
M43	AGWI000697-1	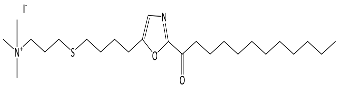	M44	LW200-1	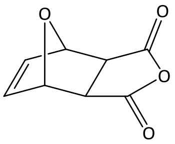
M45	KT81302-1	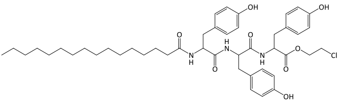	M46	KT82742-1	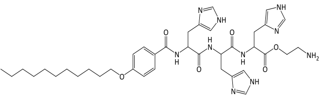
M47	KT82282-1	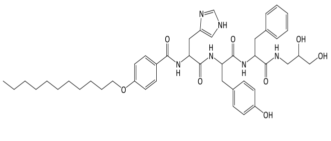	M48	AGWI000166-1	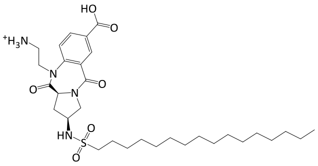
M49	AGWI000167-1	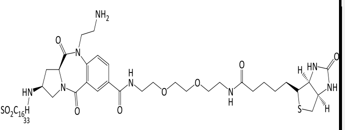	M50	KT81282-1	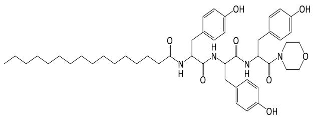
M51	KT81622-1	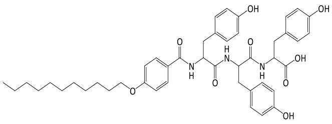	M52	BL192-3-1	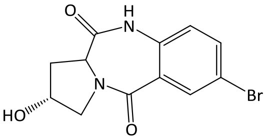
M53	PD699-1	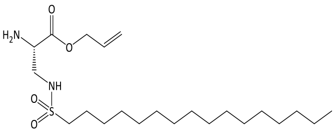	M54	KT2182-1	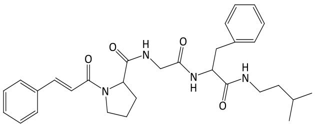
M55	KT4092-1	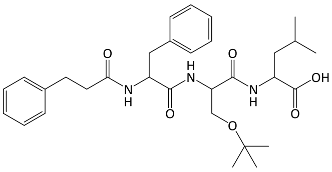	M56	MV105B-1	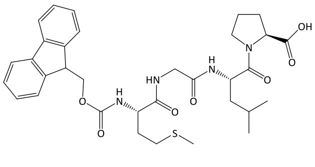
M57	LW79-1	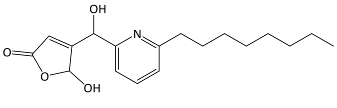	M58	STF0123-1	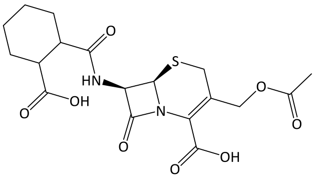

Cpd	Name (ID)	Structure		Cpd	Name (ID)	Structure
M59	STF0225-1	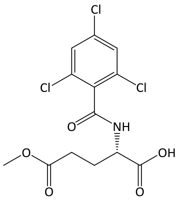		M60	ANM3305-1	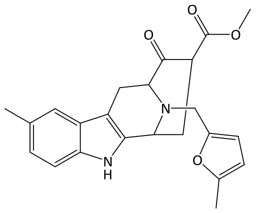
M61	MHA-25-1	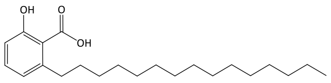		M62	KT82722-77-1	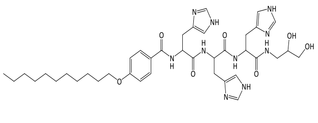
M63	KT81722-1	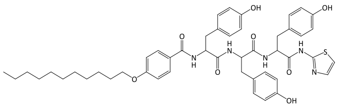		M64	MiL-367-1	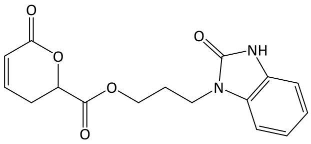
M65	KT82782-1	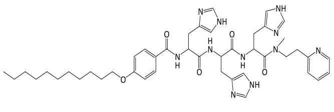		M66	EGR931-1	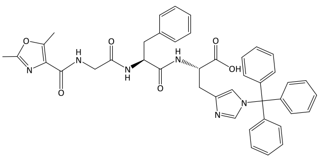
M67	SBO60-1	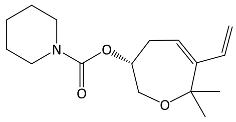		M68	KT90862-1	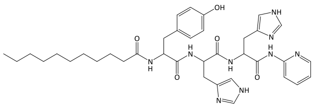
M69	SBO41-1	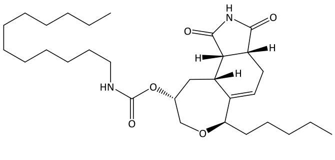		M70	SBO87-1	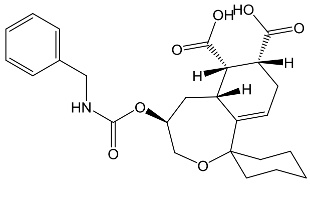
M71	SBO95-1	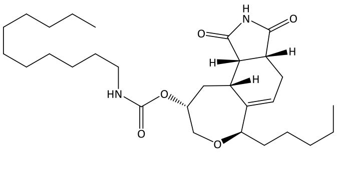		M72	AGWI000161-1	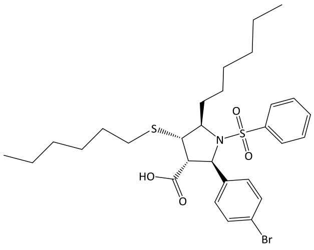
M73	AGWI000162-1	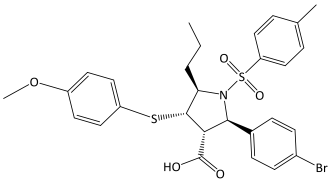		M74	EG433-1	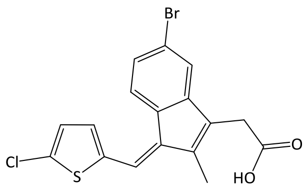

Cpd	Name (ID)	Structure		Cpd	Name (ID)	Structure
M75	AGWI000193-1	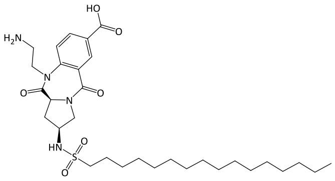		M76	MHA-38-1	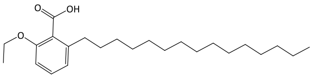
M77	MHA-66b-1	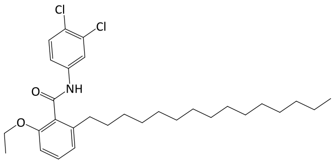		M78	MHA-78c-1	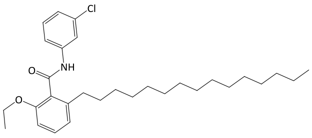
M79	MHA-69a-1	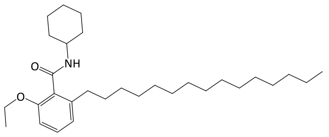		M80	MHA-107-1	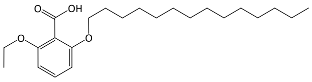
M81	AGWI000671-1	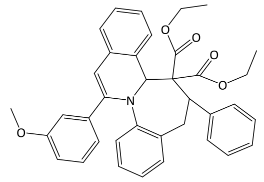		M82	KT81102-1	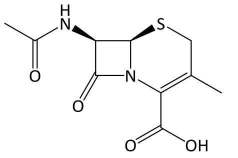
M83	LW286-1	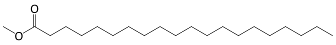		M84	LW78-1	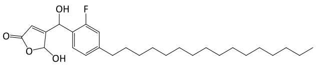
M85	LW225-1	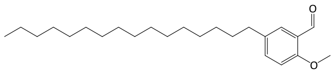		M86	LW69-1	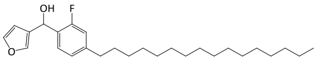
M87	AGWI000649-1	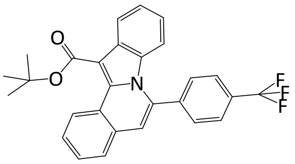		M88	PD207-1	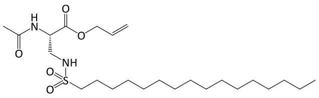
M89	MT818-1	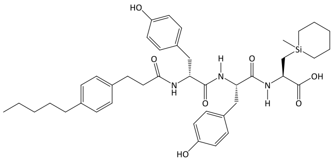		M90	CP189-1	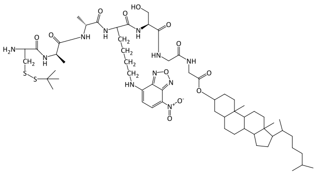
M91	LW118-1	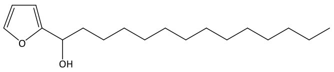		M92	LW139-1	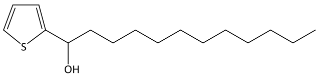

Cpd	Name (ID)	Structure	Cpd	Name (ID)	Structure
M93	KMG5PPTSH-1	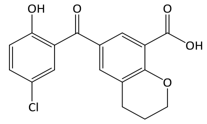	M94	KMI1PPTSH-1	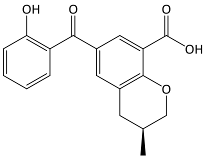
M95	STF0276a-1	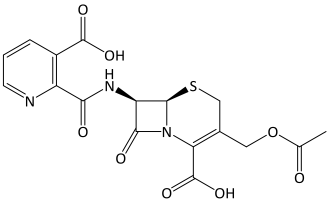	M96	TK253B-1	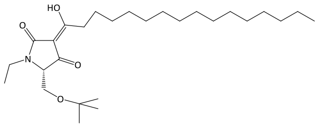
M97	STF0459-1	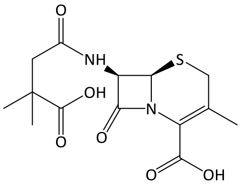	M98	LW91-1	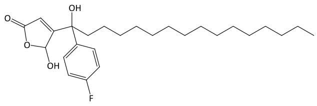
M99	LW86-1	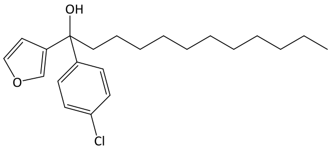	M100	LW121-1	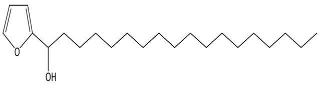
M101	LW7-1	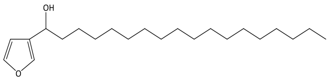	M102	LW127-1	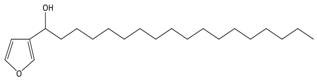
M103	LW6-1	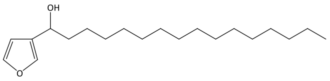	M104	LW12-1	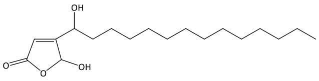
M105	SP5711-1	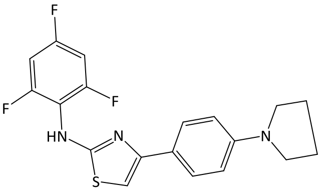	M106	STF0165-1	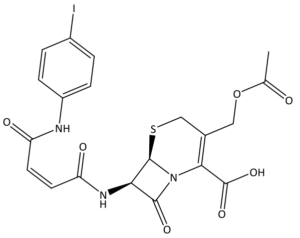
M107	STF0110-1	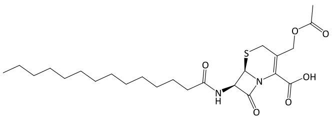	M108	STF0395-1	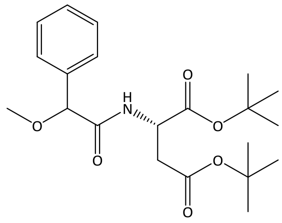

Cpd	Name (ID)	Structure	Cpd	Name (ID)	Structure
M109	STF0221-1	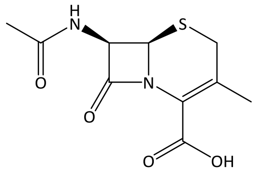	M110	SP5345-1	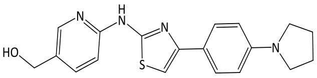
M111	STF0813-1	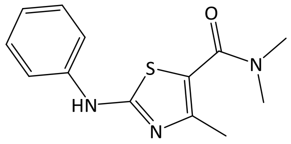	M112	STF0087-1	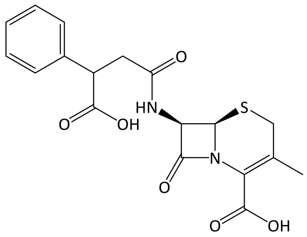
M113	MHA-27a-1	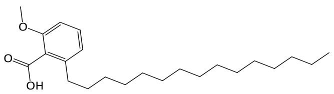	M114	PD655-1	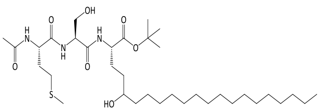
M115	GVK_108-1	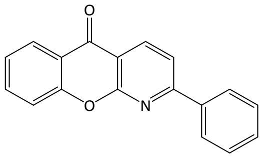	M116	PD683-1	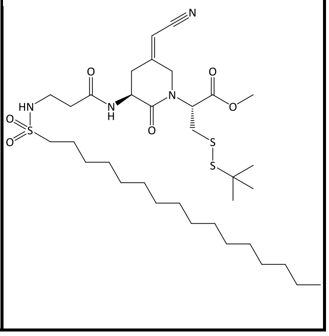

11 Abbreviations and symbols

DAPI	4’,6-Diamidino-2-phenylindole
DMSO	Dimethylsulfoxide
FITC	Fluorescein Isothiocyanate
GDP	Guanosine 5’-diphosphate
GTP	Guanosine 5’-triphosphate
GTPase	Guanosine 5’-triphosphatase
His	Histidine
HPLC	High Performance Liquid Chromatography
IC_{50}	Half maximal inhibitory concentration
EC_{50}	Half maximal effect concentration
PEG	Polyethylene Glycol
UV	Ultraviolet
PBS	Phosphate buffered saline
TBS	*Tris-buffered saline*
SDS	*Sodium dodecyl sulfate*
PIPES	Piperazine-N,N’-bis(2-ethanesulfonic acid),
TMB	3,3',5,5'-*Tetramethylbenzidine*RT
h	Hour
Sec	Second
Min	Minute(s)
MST	Microscale thermophoresis
1,8-ANS	1,8-anilinonaphthalenesulfonate
Bis-ANS	Bis(1,8-anilinonaphthalenesulfonate)
PTM	Post-translational modifications
HRP	Horseradish peroxidase
OD_{600}	*Optical Density at* a wavelength of *600 nm*
bp	Base pair
Kb	Kilobase
ELISA	Enzyme-linked immunosorbent assay
dNTP	Deoxynucleotide
BSA	Bovine serum albumin

TE	Tris-EDTA
PCA	Phenol:chloroform:isoamyl alcohol
CA	Chloroform:isoamyl alcohol
ErBr	Ethidium bromide
GPPNHP	Nonhydrolyzable GTP analogue guanosine 5'-O-(beta, gamma-imidotriphosphate)
APS	Ammonium peroxodisulfate
TEMED	N,N,N`,N`-tetramethylenethylendiamide
PVDF	Polyvinylidene difluoride
GFP	Green fluorescent protein
RT	Room temperature
Ig	Immunoglobulin
IPTG	Isopropyl-β-D-thiogalactoside
GST	Glutathione S-transferase
RNA	Ribonucleic acid
DNA	Deoxyribonucleic acid
RNAi	RNA interference
DTT	1,4-Dithiothreito
KDa	KiloDalton
LC-MS	Liquid chromatography-mass spectrometry
RAS	Rat adeno sarcoma
RAN	RAS-related nuclear *protein*
CAS	Cellular apoptosis susceptibility
CSE1L	CSE1 chromosome segregation 1-like (yeast)
aa	Amino acid
Amp^{R}	Resistant to ampicillin
Cm^{R}	Resistant to chloramphenicol
Tris	Tri-(hydroxymethyl)-aminomethane
Tween-20	Polyoxyethylensorbitane monlaurate
U	Units (enzyme activity)
v/v	Volume/volume
w/v	Weight/volume
pmol	Picromole
µL	Microliter

11 Abbreviations and symbols

mL	Mililiter
µg	Microgram
MCS	Multiple cloning sites
HCl	Hydrocloride acid
LB	Luria-Bertani
SB	Super Broth
SOB	Super Optimal Broth
SOC	Super Optimal broth with Catabolic repressor (SOB + 20mM glucose)
E. coli	*Escherichia coli*
^{o}C	Degrees centigrade
α	Alpha
β	Beta
WB	Western Blot
IP	Immunoprecipitation
IF	Immunofluorescence
PMT	Photomultiplier
BLAST	Basic Local Alignment Search Tool
et al.	et alia (and others)

12 Curriculum vitae

Name	Tran, Thi Ngoc Tuyen
Date of Birth	22/11/1980
Nationality	Vietnamese

EDUCATION

08/2009-present	**Doctoral Studies** Max Planck Institute of Molecular Physiology, Dortmund, Germany Supervisor: Prof. Dr. Herbert Waldmann
10/2011-01/2012	**Research Visit** RIKEN Advanced Science Institute, Tokyo, Japan Supervisor: Prof. Dr. Hiroyuki Osada
02/2009-07/2009	**Research Visit** Chemical Genomics Centre of Max Planck Society, Dortmund, Germany Supervisor: Prof. Dr. Luc Brunsveld
10/2003-12/2006	**Master in Molecular Microbiology** University of Natural Sciences, Hochiminh, Vietnam Supervisor: Prof. Dr. Tran, Linh Thuoc
09/1998-09/2002	**Bachelor in Molecular Microbiology** University of Natural Sciences, Hochiminh, Vietnam Supervisor: Prof. Dr. Tran, Linh Thuoc

SCHOLARSHIPS AND AWARDS

08/2009-present	PhD fellowship of International Max Planck Research School in Dortmund-Germany
12/2006	The 2nd Award for the First Competition of High Technology, Vietnam
	Award for young scientist, Vietnam

PUBLICATIONS

- B. W. Lee, H. Y. Chae, **T. T. N. Tran**, D. Kang, H. A. Kim, M. Lee, and S. H. Ihm. (2009). **A comparison of non-viral vectors for gene delivery to pancreatic beta-cells: Delivering a hypoxia-inducible vascular endothelial growth factor gene to rat islets.** *Int J Mol Med* 23(6):757-62.

- T. Voigt, C*. Gerding-Reimers*, **T. T. N. Tran***, S. Bergmann, H. Lachance, B. Schçlermann, A. Brockmeyer, P. Janning, S. Ziegler, and H. Waldmann. (2013). **A Natural Product Inspired Tetrahydropyran Collection Yields Mitosis Modulators that Synergistically Target CSE1L and Tubulin**, *Angew. Chem. Int. Ed,* 52, 410 –414**.** **equal contribution*.

- **T. T. N. Tran***, C. Gerding-Reimers*, B. Schölermann, B. Stanitzki, T. Henkel, H. Waldmann, S. Ziegler. (2014) **Podoverine A – a novel microtubule destabilizing natural product from the Podophyllum species**, *Bioorgan Med Chem*. (accepted). **equal contribution*.